Developmental regulation of Hand1 via nucleolar sequestration

David Michael John Martindill

Molecular Medicine Unit
Institute of Child Health
University College London

A thesis submitted for the degree of Doctor of Philosophy
in the subject of developmental molecular biology
to University College London (UCL).

April 2008

ProQuest LLC
789 East Eisenhower Parkway
P.O. Box 1346
Ann Arbor, MI 48106-1346

DECLARATION

I, David Michael John Martindill, confirm that the work presented in this thesis is my own. Where information has been derived from other sources, I confirm that this has been indicated in the thesis.

Signed ..

.....

11th April 2008.

ABSTRACT

The bHLH transcription factor Hand1 is essential for placentation and cardiac morphogenesis in the developing embryo. However, how the activity of Hand1 is regulated in either lineage remains largely unknown. Here we demonstrate that Hand1 is anchored in the nucleolus and negatively-regulated by the murine orthologue of the human I-mfa domain-containing protein (HIC). Nucleolar sequestration controls Hand1 activity during the differentiation of rat choriocarcinoma-1 (Rcho-1) trophoblast cells. Hand1 is sequestered in the nucleoli of Rcho-1 stem cells but is released into the nucleoplasm at the onset of their differentiation into trophoblast giant cells.

Site-specific phosphorylation of Hand1 was previously shown to modulate the affinity of Hand1 for its nucleoplasmic E-factor binding partners. We demonstrate that Hand1 phosphorylation is required for its nucleolar release, as a pre-requisite for dimerisation and biological function. Moreover, the polo-like kinase Plk4 (Sak) is responsible for this phosphorylation event. Plk4 localises to the nucleolus of Rcho-1 stem cells at phase G2 and interacts with Hand1 *in vitro* and *in vivo* to promote mitotic cell cycle exit and entry into the endocycle. We also demonstrate that the B56δ subunit of the PP2A phosphatase, shown previously to target Hand1 for dephosphorylation, is exported from the nucleus during Rcho-1 differentiation.

In this thesis we present findings that describe a novel mode of Hand1 regulation that is a crucial step in trophoblast stem cell differentiation and placentation and support previous studies that implicate the nucleolus as a molecular 'sink'. We suggest that nucleolar sequestration is an important mode of protein regulation and this may impact on a broad range of transcription factors.

CONTENTS

LIST OF FIGURES

LIST OF TABLES

GLOSSARY OF ABBREVIATIONS

- **β-Gal** ---------- beta-galactosidase
- **Act-D** ---------- actinomycin-D
- **SHF** ---------- secondary heart field
- **Amps** ---------- ammonium persulphate
- **ANF/ ANP** ---------- Atrial natriuretic factor/ atrial natriuretic peptide
- **AP** ---------- anterior-to-posterior
- **Ap-2γ** ---------- Activating protein 2 gamma
- **APC/C** ---------- anaphase-promoting complex/ cyclosome
- **ATP** ---------- adenosine 5' triphosphate
- **AV** ---------- atrioventricular
- **AVC** ---------- atrioventricular canal
- **BAC** ---------- bacterial artificial chromosome
- **bHLH** ---------- basic helix-loop-helix
- **BMP** ---------- Bone morphogenetic protein
- **bp** ---------- base pair
- **BSA** ---------- bovine serum albumin
- **CBF** ---------- CREB-binding factor
- **Cdc14** --------- Cell division cycle homologue 14
- **Cdc5** ---------- Cell division cycle homologue 5
- **CDK** ---------- Cyclin-dependent kinase
- **cDNA** ---------- complimentary deoxyribonucleic acid
- **CHD** ---------- congenital heart disease
- **CM** ---------- conditioned medium
- **CMV** ---------- cytomegalovirus
- **CNS** ---------- central nervous system
- **$CoCl_2$** ---------- cobalt chloride
- **CPC** ---------- cardiac precursor cell
- **Da** ---------- Daughterless
- **DAPI** ---------- 4',6-diamidino-2-phenylindole
- **DEPC** ---------- diethyl pyrocarbonate
- **DES** ---------- diethylstilbestrol

- **DFC** ---------- dense fibrillar component
- **dH_20** ---------- distilled water
- **DMEM** ---------- Dulbecco's modified eagle medium
- **DMSO** --------- dimethyl sulphoxide
- **DNA** ---------- deoxyribonucleic acid
- **DORV** ---------- double outlet right ventricle
- **dNTP** ---------- deoxyribonucleoside triphosphate
- **DPX** ---------- dibutyl phthalate xylene
- **DTT** ---------- dithiothreitol
- **DV** ---------- dorsal-to-ventral
- **E** ---------- embryonic day
- **E(Spl)** ---------- Enhancer of split
- **EB** ---------- embryoid body
- **EC** ---------- embryonic carcinoma
- **ECM** ---------- extracellular matrix
- **EDTA** ---------- ethylene diamine tetra-acetate
- **EGFP** ---------- Enhanced green fluorescent protein
- **EGTA** ---------- ethyleneglycol-bis(β-aminoethyl ether)-N,N,N',N'-tetra-acetic acid
- **EMSA** ---------- electrophoretic mobility shift assay
- **EPC** ---------- ectoplacental cone
- **ES (cells)** ---------- embryonic stem (cells)
- **ET-1** ---------- Endothelin-1
- **EVT** ---------- extravillous trophoblast
- **FACS** ---------- fluorescence-activated cell sorting
- **FAK** ---------- Focal adhesion kinase
- **FBS** ---------- fetal bovine serum
- **FC** ---------- fibrillar component
- **FEAR (network)** ---------- Cdc fourteen early anaphase release (network)
- **FGF** ---------- fibroblast growth factor
- **FITC** ---------- fluorescein isothiocyanate
- **FLIP** ---------- fluorescence loss in photobleaching
- **FRAP** ---------- fluorescence recovery after photobleaching

- **Fzr** ---------- Fizzy-related
- **G0** ---------- quiescent phase (of cell cycle)
- **G1** ---------- first gap phase (of cell cycle)
- **G2** ---------- second gap phase (of cell cycle)
- **GAPDH** ---------- Glucose-6-phosphate dehydrogenase
- **GC** ---------- granular compartment
- **GFP** ---------- Green fluorescent protein
- **GlyT** ---------- glycogen trophoblast
- **GST** ---------- glutathione-S-transferase
- **H** ---------- hairy
- **Hand1** ---------- Heart and neural crest-derived 1
- **Hand2** ---------- Heart and neural crest-derived 2
- **HAT** ---------- histone acetyltransferase
- **HH (stage)** ---------- Hamburger and Hamilton (stage)
- **HICp40/ 32** --------- Human inhibitor of Myo-D domain-containing protein (40kDa/ 32kDa)
- ***HICshRNAi1*** ---------- HIC short-hairpin RNA-interference construct 1
- ***HICshRNAi2*** ---------- HIC short-hairpin RNA-interference construct 2
- **HIF** --------- Hypoxia inducible factor
- **HIV** ---------- human immunodeficiency virus
- **HRP** ---------- horseradish peroxidase
- **HRT** ---------- hairy-related transcription factor
- **HS** ---------- horse serum
- **HTLV** ---------- human T-cell leukemia virus
- **ICM** ---------- inner cell mass
- **IF** ---------- immunofluorescence
- **I-mfa** --------- Inhibitor of Myo-D family A
- **ISH** ---------- *in situ* hybridisation
- **IUGR** ---------- intra-uterine growth retardation
- **IVG** ---------- interventricular groove
- **IVS** ---------- interventricular septum
- **kb** ---------- kilobase
- **kDa** ---------- kilo-Dalton
- **LIF** ---------- Leukemia inhibitory factor

- **LV** ---------- left ventricle
- **M** ---------- mitosis (of cell cycle)
- **Mash-2** ---------- Mammalian achaete-scute homologue 2
- **MCS** ---------- multi-cloning site
- **MEMα** ---------- minimum essential medium α
- **MEN** ---------- mitotic exit network
- **Mlc2v** ---------- Myosin light chain 2 ventricular isoform
- **MMP9** ---------- Matrix metalloproteinase-9
- **MPF** ---------- mitosis-promoting factor
- **mRNA** ---------- messenger RNA
- **NB** ---------- nuclear body
- **NDF** ---------- nucleolus-derived focus
- **NFκB** ---------- Nuclear factor-κB
- **NLS** ---------- nuclear localisation signal
- **NoLS** --------- nucleolar localisation signal
- **NOPdb** ---------- nucleolar proteome database
- **NOR** ---------- nucleolar organiser region
- **NP-40** ---------- nonidet P-40
- **OD_n** ---------- optical density (at n nm)
- **OFT** ---------- outflow tract
- **ORF** ---------- open reading frame
- **ORC** ---------- origin recognition complex
- **PBS** ---------- phosphate buffered saline
- **NCBI** ---------- National Centre for Biotechnology Information
- **PCAF** ---------- p300/CBP-associated factor
- **PCR** --------- polymerase chain reaction
- **PECAM** ---------- platelet endothelial cell adhesion molecule
- **PHF** ---------- primary heart field
- **PI3K** ---------- Phosphatidylinositol 3-kinase
- **PKA** --------- Protein kinase A
- **PKC** --------- Protein kinase C
- **PL-1** ---------- Placental lactogen-1
- **PL-2** ---------- Placental lactogen-2

- **Plk4** --------- Polo-like kinase 4
- ***Plk4shRNAi1*** ---------- Plk4 short-hairpin RNA-interference construct 1
- ***Plk4shRNAi2*** ---------- Plk4 short-hairpin RNA-interference construct 2
- **PLP-A** --------- Prolactin-like protein A
- **PML (bodies)** --------- promyelocytic leukemia (bodies)
- **PMSF** ---------- phenylmethylsulphonyl fluoride
- **PNB** ---------- pre-nucleolar body
- **PolI** ---------- RNA polymerase I
- **PolII** ---------- RNA polymerase II
- **snoRNP** ---------- small nucleolar ribonucleoprotein
- **SRP** ---------- signal recognition particle
- **PP2A** ---------- Protein phosphatase 2A
- **PRL** ---------- Pituitary hormone prolactin
- **RA** ---------- retinoic acid
- **Rcho-1** --------- rat choriocarcinoma-1
- **RDA** ---------- representational differential analysis
- **rDNA** ---------- ribosomal DNA
- **RENT (complex)** ---------- regulator of nucleolar silencing and telophase (complex)
- **RISC** ---------- RNA-induced silencing complex
- **RLU** ---------- relative light units
- **RNA** ---------- ribonucleic acid
- **RNAi** ---------- RNA-interference
- **RNP** ---------- ribonucleoprotein
- **rpm** ---------- revolutions per minute
- **rRNA** ---------- ribosomal RNA
- **RT-PCR** ---------- reverse transcriptase PCR
- **RV** ---------- right ventricle
- **S** ---------- DNA synthesis phase (of cell cycle)
- **S109** ---------- serine-109
- **Sak** --------- Snk/ Plk-akin kinase
- **SDS(-PAGE)** ---------- sodium dodecyl sulphate(-polyacrylamide gel electrophoresis)
- **SER5** ---------- shared enhancer region 5

- **shRNA** ---------- short hairpin RNA
- **siRNA** ---------- small interfering RNA
- **SMC** ---------- smooth muscle cell
- **SpT** ---------- spongiotrophoblast (layer)
- **Stra13** ---------- stimulated-by-retinoic-acid 13
- **SynT** ---------- syncytiotrophoblast (layer)
- **T107** ---------- threonine-107
- **TBS** ---------- tris-buffered saline
- **TBST** ---------- TBS with Tween-20
- **TE** ---------- trophectoderm
- **TEMED** ---------- N, N, N', N'-tetramethyl-ethylene diamine
- **Tet** ---------- tetracycline
- **TG (cells)** ---------- trophoblast giant (cells)
- **TGFβ** ---------- Transforming growth factor beta
- **TRITC** ---------- tetramethylrhodamine isothiocyanate
- **tRNA** ---------- transfer RNA
- **TS (cells)** --------- trophoblast stem (cells)
- **Tween-20** --------- polyoxyethylenesorbitan monolaurate
- **UV** ---------- ultraviolet light
- **VHL** --------- von Hippel-Lindau
- **VSD** ---------- ventricular septal defect
- **X-Gal** ---------- 5-bromo-4-chloro-3-indoyl-β-D-galactopyranoside
- **Y2H** --------- yeast two-hybrid
- **ZPA** ---------- zone of polarizing activity

ACKNOWLEDGEMENTS

I would firstly and especially like to thank my PhD supervisor, Paul Riley. Despite his ever-increasing workload, Paul has been a first-class teacher and guide, and has always found time to oversee my studies with unending patience and care.

This research was supported by the British Heart Foundation. We gratefully acknowledge Anthony Firulli, Vivek Mittal, Frank Sicheri and Sabine Thebault for kindly providing constructs, Michael Soares, Satoshi Tanaka, John Pizzey and Sean Wu for generously supplying the Rcho-1, trophoblast stem, P19-CL6 and transgenic ES stem cell lines respectively, and Jean-Paul Mesnard for the anti-HIC antibody. We are indebted also to Carla Rosario, Carol Swallow and James Dennis for providing the *Plk4*-null concepti and for insightful discussion regarding our manuscript prior to its submission to *Nature Cell Biology*.

I am grateful for the day-to-day help and light-heartedness provided by members of the lab, past and present, namely Nicola Smart, Catherine Risebro, Maria del mar Franco-Viseras, Athalie Melville, Richelle Searles and Alex Rossdeutsch. My thanks also extend to the rest of the Molecular Medicine Unit at the ICH, a group of people with whom it has been a pleasure to study. I have also appreciated the valuable discussions regarding this work with my postgraduate tutor Andrew Stoker, PhD upgrade examiner John Achermann and, particularly, my secondary supervisor Peter Scambler. Paul Rutland also deserves a mention for regularly chasing up my lab orders. Lastly, thank you, Maruschka, for all of those welcome snacks!

I have appreciated the support and encouragement afforded to me by my family, especially my parents and grandparents, and for the respite provided by my good friend Adam. Finally, I would like to end by acknowledging my partner Jen, a very special person with whom I have shared many happy times during the last three years.

Chapter 1

General introduction

1.1. Overview of the bHLH transcription factor, Hand1

1.1.1. Hand1 structure and evolution

Hand1, previously termed *Thing1*, *eHand* or *Hxt*, encodes the heart and neural crest-derived factor 1. The *Hand1* gene was cloned independently more than ten years ago by three different groups (Cross *et al.*, 1995; Hollenberg *et al.*, 1995; Cserjesi *et al.*, 1995). *Hand1* is located on human chromosome 5q33 and mouse chromosome 11p, and in both mammals comprises two exons separated by a single 1.5kb intron that generates a 1.9kb transcript (Figure 1.1a). The encoded Hand1 protein is 216 residues in length (Figure 1.1b).

Hand1 belongs to a large super-family of transcription factors that are characterised by a conserved, N-terminal basic helix-loop-helix (bHLH) DNA-binding/ dimerisation domain (reviewed by Massari and Murre, 2000). This domain consists of a basic region comprising a cluster of positively-charged amino acids, which precedes a HLH motif of two amphipathic α-helices linked by a loop of variable length. Transcription factors containing the bHLH domain play critical roles in cell lineage determination, for instance the founding myogenic members of the family, MyoD, Myogenin, Mrf4 and Myf5 (reviewed by Weintraub, 1993). Hand2 is the most closely-related bHLH family member to Hand1 and, in addition to Twist1, Twist2, Dermo1, Scleraxis and Tcf15, the Hand factors belong to the Twist subfamily of bHLH factors (Figure 1.2). Members of this bHLH factor subclass have roles in the development of tissues deriving from the mesoderm and neural crest. The latter cell population represents a transient and pluripotent population of migratory cells that emerge from the dorsal tip of the neural tube as a result of inductive interactions between the neural plate and the surface ectoderm.

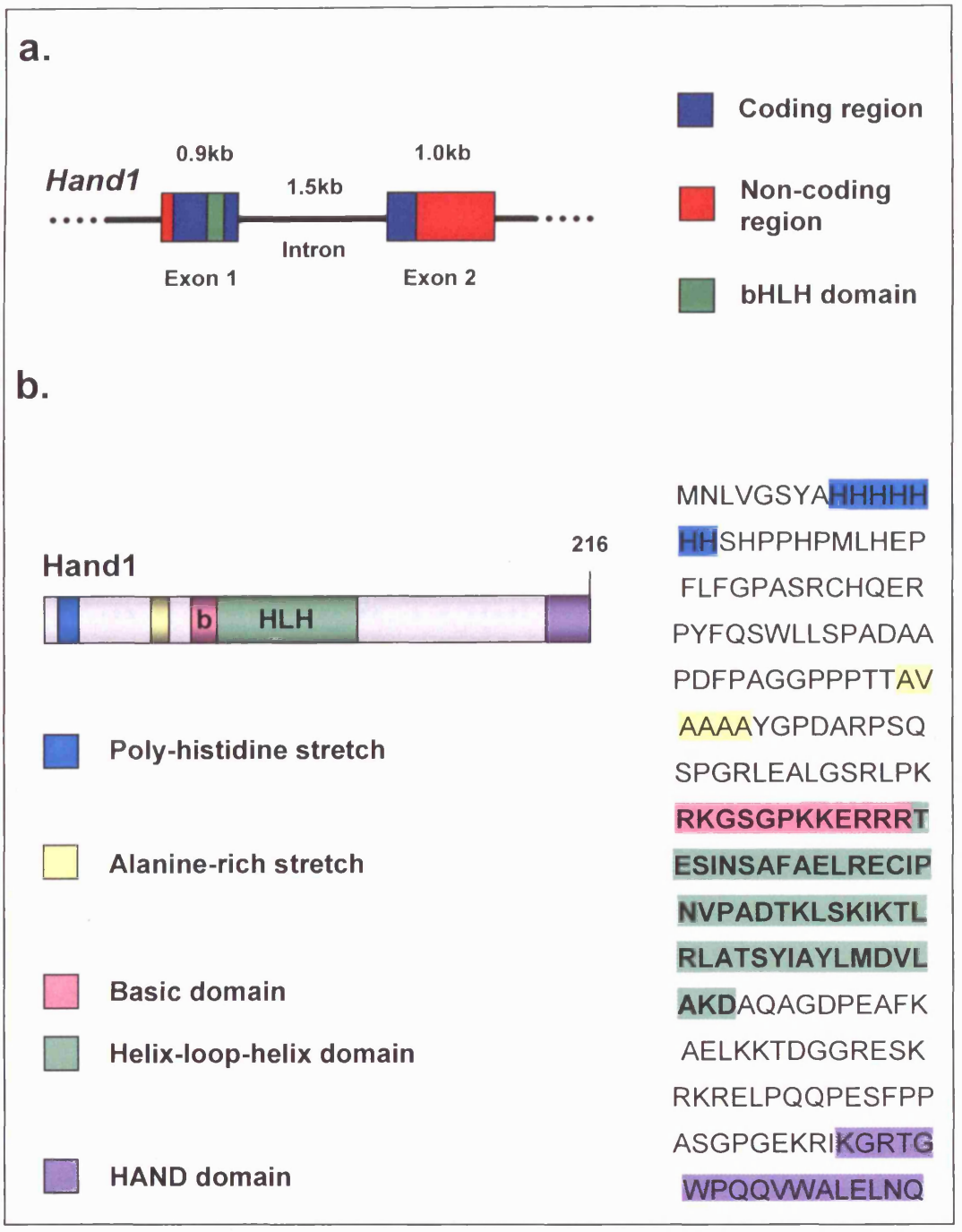

Figure 1.1. The structure of the murine Hand1 gene (a) and encoded protein (b).

Murine *Hand1* comprises two exons of 0.9kb and 1.0kb in length, separated by a 1.5kb intron (see key for details; **a**). The encoded Hand1 protein, of 216 residues and whose sequence is listed, contains several motifs including the bHLH domain (shown in bold; see key for details; **b**).

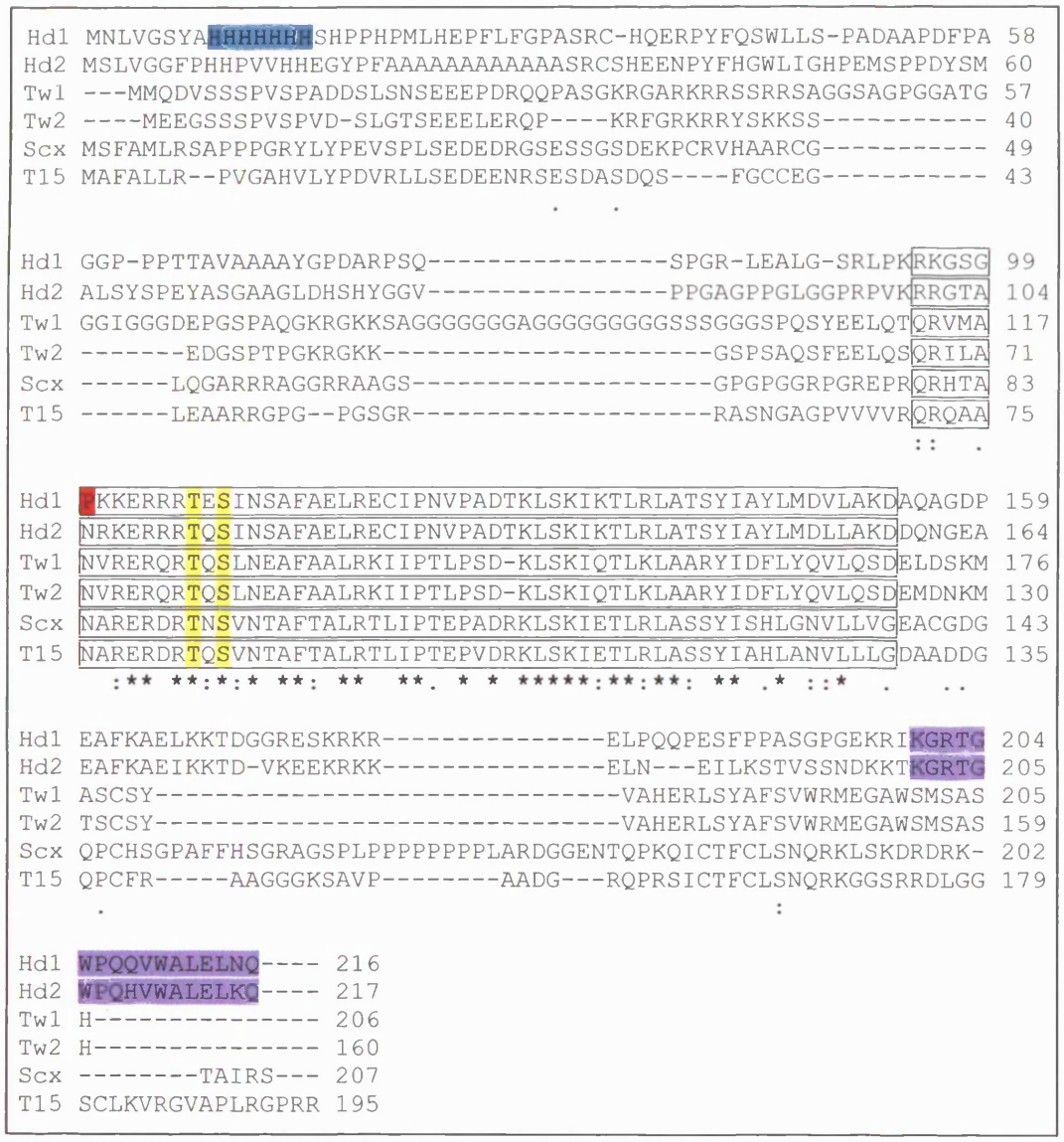

Figure 1.2. Hand1 belongs to the Twist subfamily of bHLH transcription factors.

The mouse Hand1 protein sequence was aligned with Hand2 and selected members of the Twist subfamily of bHLH transcription factors (Twist1, Twist2 (formerly known as Paraxis), Scleraxis (Scx) and Transcription Factor 15 (Tcf15; formerly known as Dermo-1). Conservation, which is particularly striking in the bHLH domain (boxed), is as follows: * absolutely conserved between sequences, : conserved amino acid substitutions, . semi-conserved amino acid substitutions. Note the asparagine-to-proline substitution in the Hand1 basic domain (highlighted in red), the conserved serine and threonine residues in the bHLH domains of all Twist subfamily members (highlighted in yellow) and that the closely-related Hand2 protein lacks the N-terminal poly-histidine stretch present in Hand1 (highlighted in blue). The C-terminal HAND domain, present in Hand1 and Hand2, is also indicated (highlighted in purple). These alignments were produced using the Clustal W program version 1.82 (www.ebi.ac.uk/clustalw/). **Hd1**: Hand1, **Hd2**: Hand2, **Tw1**: Twist1, **Tw2**: Twist2, **Scx**: Scleraxis, **T15**: Tcf15.

The primary sequence of the Hand1 bHLH domain is 47% identical to that in Twist1 and 87% identical to that in another Hand factor, Hand2 (reviewed by Firulli, 2003). Hand1 has a low sequence identity outside of the bHLH domain, being most closely-related to the neurogenic bHLH factor Hen1 (Brown and Baer, 1994). Hand1 notably contains several other unique domains (Figure 1.1b), including a 7-residue poly-histidine stretch and regions rich in alanine and proline residues. These are in addition to the highly-conserved, hydrophobic 'Hand domain' at its C-terminus that it shares with Hand2. However the roles of these motifs are largely uncharacterised.

The structure of the Hand1 protein differs markedly between species (Figure 1.3). The oldest definitive orthologue is in *Drosophila*, which possesses only a single *Hand* gene and which is equally divergent from murine *Hand1* and *Hand2*. However, the *Drosophila Hand* gene differs in structure to the *Hand* genes of higher organisms in that it possesses 4 exons and has a highly-divergent N-terminus (Kolsch and Paululat, 2002). The N-terminus shows no amino acid identity with the equivalent region of vertebrate *Hand1* or *Hand2*, and as such is unlikely to be crucial for biological function having been lost during evolution through genetic drift (reviewed by Firulli, 2003). Furthermore, *Drosophila Hand*, unlike mammalian *Hand1*, neither encodes the N-terminal poly-histidine stretch nor the alanine-rich motif. This suggests that Hand1 has acquired novel function(s) since the divergence of invertebrates and vertebrates.

The single zebrafish *Hand* gene is most closely-related to mammalian *Hand2* (Angelo *et al.*, 2000; Yelon *et al.*, 2000). This suggests that *Hand2* is the ancestral gene of the subclass from which *Hand1* was derived. Indeed, *Hand1* and *Hand2* map to human chromosomes 5q33 and 4q33 respectively, regions that possess at least 13 pairs of paralogous genes (reviewed by Lundin, 1993). This suggests that part of 5q containing Hand1 likely arose from the portion of 4q containing Hand2 in a tetraploidisation event (Knofler *et al.*, 1998). This probably occurred some time between the divergence of fish and amphibians, since the latter possess two *Hand* genes. Notably, the cardiac phenotype of $Hand1^{KO/KO}$ (cardiac); $Hand2^{KO/KO}$ mice is less severe than that of the zebrafish *hands off* mutant (McFadden *et al.*, 2005). This suggests that mammalian *Hand* genes have acquired further functions during the evolution of the four-chambered heart from the ancestral two-chambered fish heart.

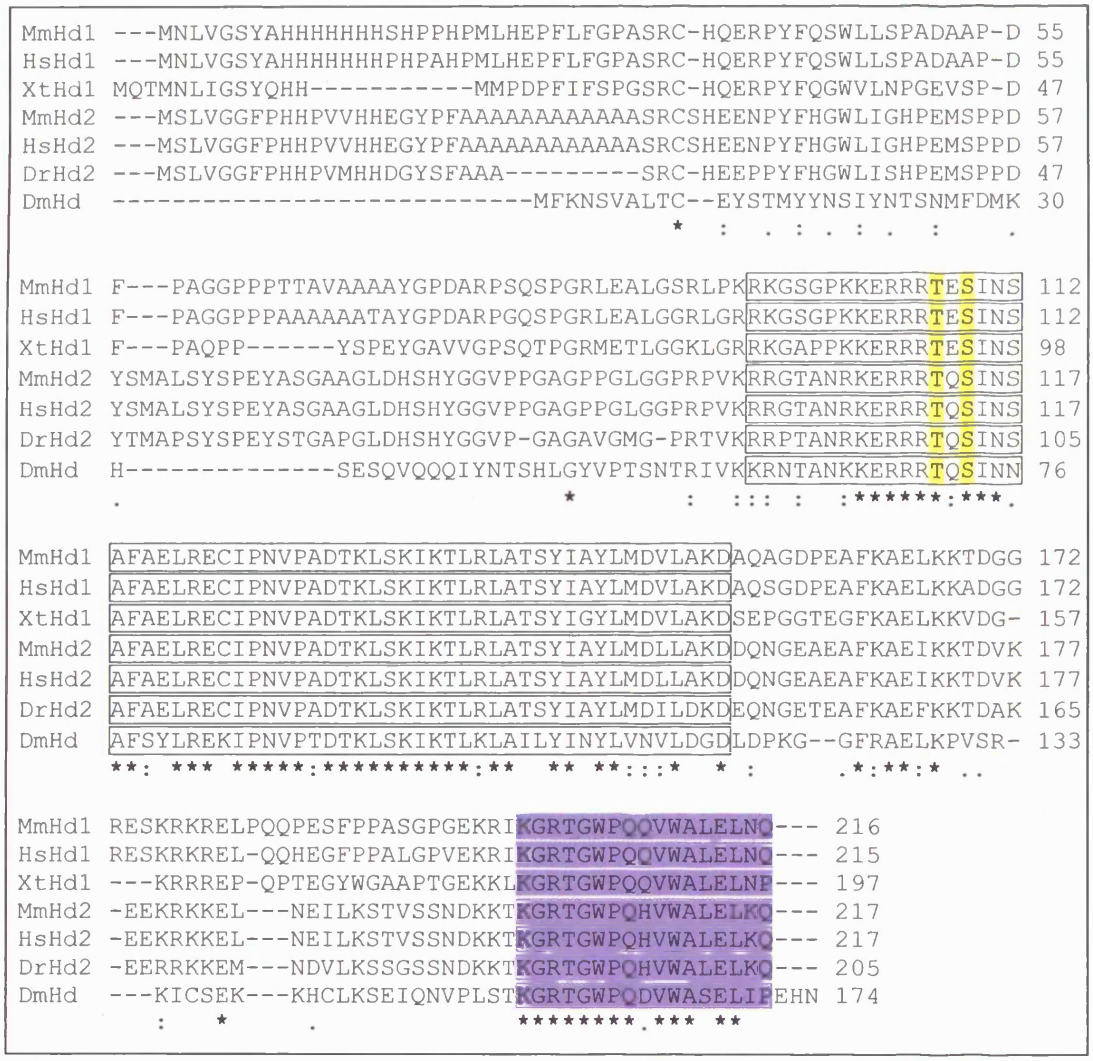

Figure 1.3. Hand protein sequence is conserved between diverse species.

Hand1, Hand2 or Hand protein sequences from mouse, human, frog, zebrafish and fruit fly were aligned as in Figure 1.2. Conservation, which is particularly striking in the bHLH domain (boxed) as well as in the so-called C-terminal Hand domain (highlighted in purple), is as follows: * absolutely conserved between sequences, : conserved amino acid substitutions, . semi-conserved amino acid substitutions. The conserved serine and threonine residues in the bHLH domains of all Hand factors are also highlighted, in yellow. **Mm**: *Mus musculus*, **Hs**: *Homo sapiens*, **Xt**: *Xenopus tropicalis*, **Dr**: *Danio rerio*, **Dm**: *Drosophila melanogaster*; **Hd1**: Hand1, **Hd2**: Hand2; **Hd**: Hand.

1.1.2. Overview of Hand1 function

The first insights into Hand1 function were gained by over-expressing *Hand1* in mouse blastomeres (Cross *et al.*, 1995) and via antisense experiments in chicks

(Srivastava *et al.*, 1995). These respectively suggested an involvement of Hand1 in placentation (this chapter, section 1.2) and cardiac morphogenesis (section 1.3). More recent studies have also implicated a role for Hand1 in the adult heart (section 1.3.3) and in the development of other tissues, particularly those with a neural crest contribution (section 1.4).

1.1.3. Hand1 regulation

Despite the cloning of the *Hand1* gene over a decade ago, the mechanisms that regulate its activity during embryogenesis remain largely unknown. Investigating how the developmental activity of Hand1 is regulated has proven difficult *in vivo* due to early embryonic lethality following loss-of-function (Riley *et al.*, 1998; Firulli *et al.*, 1998). *In vitro* analyses using cell lines in which *Hand1* is endogenously expressed has also been difficult. Few cardiac cell lines exist and trophoblast stem (TS) cells are difficult to maintain and manipulate in culture (S. Tanaka, *personal communication*). A better understanding of the mechanisms of Hand1 regulation could nevertheless provide valuable insight into the underlying cellular causes of defective placentation and idiopathic congenital heart disease (CHD). Moreover, neither mutations in human *Hand1*, nor chromosomal rearrangements involving the *Hand1* gene, have been identified in a disease setting. This implicates *Hand1* as an excellent candidate for mutations in *cis*-acting sequences or defects in its upstream regulation that could lead to placental failure or CHD in humans.

1.1.3.1. Transcriptional regulation of Hand1

A region of the human *HAND1* promoter, spanning 274bp of sequence upstream of the transcriptional start site, has been defined (Vasicek *et al.*, 2003). This contains several *cis*-acting elements that convey both positive and negative transcriptional effects on the downstream gene. These include four GC-rich sequences, which are bound by members of the specificity protein (Sp) transcription factor family, a CCAAT box, bound by the alpha-CAAT binding factor (α-Cbf), and several CG-rich recognition sequences for Egr transcription factors. Interestingly, Sp family transcription factors have recently been implicated in controlling *Hand1*

expression in rodent trophoblast (Takeda *et al.*, 2007). Alignment studies performed by another group have identified a highly-conserved 119bp enhancer element 63.7kb upstream of the *HAND1* start codon, termed the shared enhancer region 5 (SER5) (P. Riley, unpublished data). SER5 fused to GFP directed reporter gene expression predominantly in the zebrafish heart. This suggested that this enhancer may be bound by as-yet unidentified proteins to regulate the *HAND1* gene during cardiac morphogenesis. This is reminiscent of a right ventricle- (RV-) specific enhancer upstream of *Hand2*, shown to be bound by Gata factors (McFadden *et al.*, 2000), and of a branchial arch-specific *Hand2* enhancer, which is responsive to Endothelin-1-dependent signalling (Charite *et al.*, 2001).

Notably, unlike some other bHLH factors such as MyoD, *HAND1* expression is thought to not be subject to auto-regulation, as HAND1-binding sites are not present within the *HAND1* promoter (Vasicek *et al.*, 2003). As further confirmation of this, *Hand1* promoter activity is not affected by disruption of the murine *Hand1* coding region (Firulli *et al.*, 1998; Riley *et al.*, 2000). Namely, the expression of a *lacZ* or *luciferase* reporter gene, knocked into the *Hand1* locus in a targeted ES cell line, recapitulates that of endogenous *Hand1*.

Several studies suggest that signalling molecules modulate *Hand1* expression *in vivo*. This presumably occurs via their ultimate activation of transcription factors whose target genes include *Hand1*. One study used animal cap explants to show that the bone morphogenetic proteins 2 and 4 (Bmp2 and Bmp4) can induce *Hand1* expression in the developing *Xenopus* heart (Sparrow *et al.*, 1998). Importantly, this effect was blocked by the co-expression of a dominant-negative Bmp receptor. Related to this finding, ectopic Bmp4 signalling induced the expression of Hand1 in non-neural crest-derived cells in the chick oesophagus and gizzard (Wu and Howard, 2002). Furthermore, implantation of beads soaked in Bmp2 into the chick limb mesoderm up-regulated *Hand1* (Fernandez-Teran *et al.*, 2003). Thus Bmps, which generally act to ventralise tissue, may be general regulators of *Hand1* expression.

In *Xenopus* embryos treated with a retinoic acid (RA) antagonist the domain of *Hand1* expression is restricted, and may in part underlie the defective cardiac development of these embryos (Collop *et al.*, 2006). Additionally, *Et-1*- (*endothelin-*

1)-null embryos have fewer *Hand1* transcripts in the neural crest-derived pharyngeal arch mesenchyme than wild-type embryos (Thomas *et al.*, 1998a). Related to this, $G\alpha_q/G\alpha_{11}$-null embryos, which lack a pair of G-protein coupled receptors that transduce Endothelin-1 signalling, are similarly down-regulated for *Hand1* in the pharyngeal arches (Ivey *et al.*, 2003). Additionally, signalling cascades downstream of leukemia inhibitory factor (Lif) have been suggested to up-regulate genes whose products promote rodent trophoblast giant cell differentiation, including *I-mfa* and *Hand1* (Takahashi *et al.*, 2003). Finally, the study by Sparrow and colleagues also showed that high levels of Hand1 expression were detected in animal cap explants treated with high doses of the TGF-β family member, Activin A (Sparrow *et al.*, 1998).

It is also possible that *Hand1* is regulated by Notch signalling. The expression of the three hairy-related bHLH transcription (Hrt) factors, also known as hairy and enhancer-of-split related with YRPW motif (Hey) factors, is dependent on Notch signalling (Steidl *et al.*, 2000). Interestingly Hrt1, Hrt2 and Hrt3 share with Hand1 several structural and functional features, can interact with Hand1 and are co-expressed with *Hand1* in the developing heart (Firulli *et al.*, 2000). Related to this, Hand1 interacts with the factor Mastermind-like 2 (Maml2), a trans-activator of the Notch signalling pathway (P. Riley, unpublished data). Maml2 associates with Notch ligands and functions to activate transcription of the genes encoding the Hand1-related Hrt bHLH factors including Hrt1 (Wu *et al.*, 2002). However, the functional significance of Hand1 involvement in Notch signalling to date remains unknown.

No transcription factor has yet been shown to directly activate vertebrate *Hand1* transcription, either in the heart or the other tissues in which it is expressed. The expression of the *Drosophila Hand* gene is regulated by three major transcription factors that control cardiogenesis and haematopoiesis, namely the Nkx-like factor Tinman and the Gata factors Pannier and Serpent (Han and Olson, 2005). Interestingly these act through a cardiac- and haematopoietic-specific enhancer upstream of the gene. The regulation of *Drosophila Hand* by Gata factors is reminiscent of the regulation of murine *Hand2* in the developing mouse heart from a right ventricle-specific enhancer (McFadden *et al.*, 2000). However, to date, Gata factors have not been implicated in the regulation of *Hand1*.

Circumstantial evidence suggests that the transcription factors Nkx2.5 and Mash1, and the co-activators Fog-2 and Clp-1, may directly or indirectly regulate the cardiac expression of *Hand1* in vertebrates. In several cases *Hand1* is down-regulated in its native tissues in mice lacking these factors and/ or these animals exhibit cardiac phenotypes and modified gene expression profiles reminiscent of those in tetraploid-rescued *Hand1*-null mouse hearts (Biben and Harvey, 1997; Ma *et al.*, 1997; Riley *et al.*, 1998; Tanaka *et al.*, 1999; Tevosian *et al.*, 2000; Bruneau *et al.*, 2001; Huang *et al.*, 2004). Other transcription factors have also been inferred to regulate *Hand1* expression. For example, ectopic expression of normally left ventricular-restricted *Tbx5* in the right ventricle induces ectopic *Hand1* expression in the right ventricle (Takeuchi *et al.*, 2003).

The *Nkx2.5*-null mouse is a good example of a mutant whose cardiac phenotype and gene expression pattern bears similarity to those of the tetraploid-rescued *Hand1*-null mouse (Lyons *et al.*, 1995; Biben and Harvey, 1997; Tanaka *et al.*, 1999). Mice lacking *Nkx2.5* exhibit defective heart tube looping, impaired ventricular myocardial trabeculation and are down-regulated for *Mlc2v* expression in their hypoplastic left ventricle. Importantly, *Hand1* transcripts are lacking on the left side of the primitive heart tube in these embryos, implicating Nkx2.5 in the regulation of *Hand1* expression. As further evidence for a functional link between *Nkx2.5* and *Hand1*, mice lacking cardiac expression of both *Hand1* and *Hand2* exhibit severe cardiac deformities reminiscent of an *Nkx2.5*-/ *Hand2*-double knockout mouse (Yamagishi *et al.*, 2001; McFadden *et al.*, 2005). Interestingly, the expression of *Nkx2.5* is repressed in response to *Hand1* over-expression *in vivo* (McFadden *et al.*, 2005). In contrast, *Hand1*-null embryoid bodies (EBs), three-dimensional aggregates of cardiomyocytes generated by differentiating embryonic stem (ES) cells in culture, have a significantly elevated level of *Nkx2.5* transcripts (Riley *et al.*, 2000). These observations suggest that, although *Nkx2.5* expression precedes that of *Hand1 in vivo* and in differentiating EBs, Hand1 may regulate *Nkx2.5* transcription in a feedback loop.

1.1.3.2. Interaction of Hand1 with other factors

The activity of a transcription factor is commonly modulated by its interaction with other proteins and Hand1 is no exception. As a lineage-restricted (class B) bHLH transcription factor, Hand1, at least *in vitro*, conforms to the classic bHLH transcription factor paradigm (Hollenberg *et al.*, 1995; reviewed by Massari and Murre, 2000). This states that to become transcriptionally-competent, Hand1 must heterodimerise with a near-ubiquitous (class A) bHLH factor. These factors can be either the E-factor products of the *E2A* gene (E12 and E47), or the ubiquitous proteins Alf1 or Itf2. Indeed, *Hand1* was originally cloned by way of a yeast two-hybrid (Y2H) assay in which the *Drosophila* Daughterless (Da) bHLH protein, the fly counterpart of mammalian E-proteins, was used as bait (Hollenberg *et al.*, 1995). The bHLH heterodimerisation paradigm is reliant on an interaction between the HLH domains of Hand1 and its partner. This event juxtaposes the two adjacent basic domains to form a dimeric DNA-binding motif (Figure 1.4).

Hand1 does not wholly conform to the classic bHLH paradigm, however. *In vitro* a heterodimer of Hand1 and an E-factor can bind a so-called bipartite Thing1-(Th1-) or D-box site (CGTCTG), upstream of its target genes (Hollenberg *et al.*, 1995; Knofler *et al.*, 2002). Notably the Thing1-box consensus sequence is a degenerate version of the canonical E-box sequence (CANNTG), bound by most other class B-class A heterodimers and by E-factor homodimers (Chiaramello *et al.*, 1995; Hollenberg *et al.*, 1995; Sigvardsson *et al.*, 1997). The binding of Hand1 to a degenerate E-box may be due to two unusual features of the Hand1 DNA-binding domain. Firstly, the Hand1 basic domain is more positively-charged (contains more lysine (K) and arginine (R) residues) than those in other, even closely-related, bHLH proteins (for example in Hand1, K_{101}KERRR$_{106}$, but in Twist1, V_{119}RERQR$_{124}$). Secondly, the basic domain of Hand1 contains an atypical proline residue, which is an asparagine in most bHLH factors, including other members of the Twist subfamily (Figure 1.2). This unusual feature has been associated with bHLH factors that similarly bind DNA through non-canonical E-boxes such as the N-box. For example, it is also present in the *Drosophila* bHLH factors enhancer-of-split (E(Spl)) and hairy (h) (Garrell and Campuzano, 1991) as well as the mammalian Scleraxis (Atchley and Fitch, 1997), Stra13 (Boudjelal *et al.*, 1997), and hairy-related transcription (Hrt)

factors (Ishibashi *et al.*, 1993). Indeed, the substitution of a proline for the asparagine in the basic domain of MyoD disrupts its binding to E-boxes (Davis *et al.*, 1990).

Most class B bHLH proteins, particularly those expressed in a single cell type such as the myogenic factors, are unable to homodimerise. These factors either heterodimerise with E-factors to enhance transcription (Massari and Murre, 2000) or form heterodimers with Id and Mist1 factors to repress transcription (Jen *et al.*, 1997; Lemercier *et al.*, 1998). However *Hand1* is expressed in a broad range of tissues, with the potential for more complex, post-translational control mechanisms to determine its target genes in a given cell type. Consistent with this, Hand1 is known to interact with a wide range of class B bHLH factors (Table 1.1).

The interaction of Hand1 with partners beyond class A bHLH factors, in contrast to the classic bHLH factor paradigm, was first inferred over a decade ago. For example, whilst the *Placental Lactogen-I* (*PL-I*) promoter was activated by Hand1 over-expression in transfection assays *in vitro*, this effect was abolished upon *Id-1* co-expression (Cross *et al.*, 1995). *Id-1*, which encodes a HLH factor lacking the basic domain and which can therefore inactivate bHLH factors by forming a complex unable to bind DNA, is expressed at high levels in Rcho-1 stem cells but is down-regulated during TG cell differentiation (Cross *et al.*, 1995; Takeda *et al.*, 2007). Thus it is possible that Hand1 and Id-1 interact during the early stages of trophoblast differentiation and that this negatively-regulates Hand1 activity.

By conducting a yeast two-hybrid (Y2H) screen with Hand1 as bait, Firulli and colleagues confirmed that the Hand factors have 'promiscuous' dimerisation properties (Firulli *et al.*, 2000). This and a later study by the same authors identified interactions between Hand1 and the Hrt (Hey) factors (Firulli *et al.*, 2000) and the closely-related Twist1 factor (Firulli *et al.*, 2005). Hand1 also binds Mash1, forming a heterodimer that may exist *in vivo* as the two bHLH factors are co-expressed in the autonomic nervous system (Bounpheng *et al.*, 2000). However, no functional effect was attributed to this interaction. Hand1 can also form a heterodimer with MyoD (Bounpheng *et al.*, 2000; Firulli *et al.*, 2000), although this is likely biologically-irrelevant as the factors are not co-expressed *in vivo*. The bHLH factors with which Hand1 has been shown to interact are summarised in Table 1.1a.

Some studies suggest that Hand1 can also interact with non-bHLH factors in a tertiary fashion (Hill and Riley, 2004, Yamada *et al.*, 2005). That is, such an interaction can occur concomitantly with the obligate binding of Hand1 to a bHLH partner. As such, tertiary interactions are likely to involve regions outside of the Hand1 HLH motif. Although the biological significances of most of these interactions are unclear, an exception is the interaction of Hand1 with the LIM domain-containing protein Fhl2. This factor has been shown to differentially regulate the trans-activational activity of Hand1 depending on its dimerisation status (Hill and Riley, 2004). Specifically, whilst Fhl2 represses Hand1-E-factor-dependent transcriptional activity of a mock Hand1 target gene, it had no effect on Hand1-Hand1 homodimer-induced transcription. However, the mechanism by which Fhl2 interferes with Hand1-E-factor activity is currently unclear as the factor did not impact on heterodimer formation or DNA binding (Hill and Riley, 2004). Non-bHLH factors with which Hand1 interacts are summarised in Table 1.1b.

The Y2H screen conducted by Firulli and colleagues also identified several Hand1-interacting proteins with high sequence identity to Hand1 itself, suggesting that the transcription factor can function as a homodimer *in vitro* (Firulli *et al.*, 2000). Hand1 homodimers were later shown to be transcriptionally-competent by co-immunoprecipitation and mammalian two-hybrid studies (Scott *et al.*, 2000). However the DNA binding affinity of Hand1 homodimers was an order of magnitude lower than that of Hand1-E-factor heterodimers. This suggests that these homodimers must be associated with other proteins in a higher-order complex to sufficiently enhance their DNA-binding affinity. Nevertheless, tethered Hand1 homodimers can drive the differentiation of trophoblast stem (TS) cells into trophoblast giant (TG) cells in culture to a degree similar to that of the Hand1 monomer (Hu *et al.*, 2006). Furthermore, *Hand1* homodimer knock-in mice develop normally until E14.5, suggesting that Hand1 can act exclusively as a homodimer to regulate early developmental processes (Hu *et al.*, 2006).

Based upon the high degree of amino acid identity between Hand1 and Hand2 (87% amino acid identity between the bHLH regions), and the fact that Hand1 can homodimerise, it was not surprising to find that these factors can interact (Firulli *et al.*, 2000). Hand1-Hand2 heterodimers have been hypothesised to play a role in the

formation of the interventricular septum (IVS) of the heart, based on their complementary expression domains in ventricular chambers that intersect at the interventricular groove (Firulli *et al.*, 2001; reviewed by Firulli, 2003). Collectively, these findings reveal that Hand1 has a broad dimerisation profile. This may explain how this widely-expressed factor regulates discrete cohorts of genes in different tissues. For example, Hand1 may bind a trophoblast giant (TG) cell-specific bHLH factor during TG cell differentiation that directs Hand1 binding to the promoters of TG cell-specific genes. Crucially, these genes would not be regulated by Hand1 in the other lineages in which it is expressed during embryogenesis, by virtue of their lacking expression of the TG cell-specific factors to which Hand1 binds.

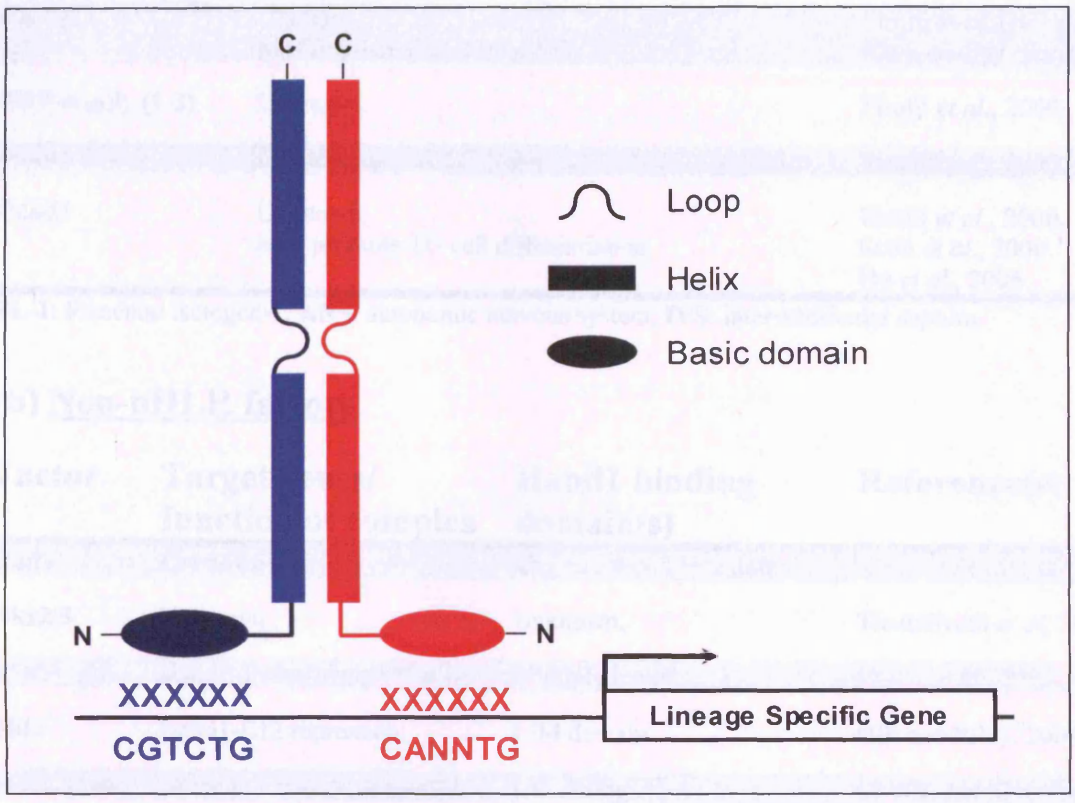

Figure 1.4. The bHLH factor heterodimerisation paradigm.

As a lineage-restricted (class B) bHLH transcription factor, Hand1 conforms to the classic bHLH transcription factor heterodimerisation paradigm. This states that to become transcriptionally-competent, Hand1 (blue protein) must bind a near-ubiquitous (class A) bHLH factor (red protein). The paradigm is reliant on an interaction between the HLH domains of Hand1 and its partner. This juxtaposes the two basic domains from each factor to form a dimeric DNA-binding motif, such that the E-factor recognises the E-box CANNTG and Hand1 the degenerate Thing1-box CGTCTG.

Table 1.1. Factors known to interact with murine Hand1.

(a) bHLH factors

Factor	Target genes/ function of complex	Reference(s)
E-factors (E12/ E47/ ALF1)	Unknown. May activate the *PL-1* promoter.	Cross *et al.*, 1995. Hollenberg *et al.*, 1995.
Id-1	Hand1 repression.	Cross *et al.*, 1995.
MyoD	Hand1 repression.	Bounpheng *et al.*, 2000. Firulli *et al.*, 2000.
Mash1	Hand1 repression. May regulate ANS development.	Bounpheng *et al.*, 2000. Firulli *et al.*, 2000.
Hand2	Unknown. May regulate IVS formation.	Firulli *et al.*, 2000. Reviewed by Firulli (2003).
HRT family (1-3)	Unknown.	Firulli *et al.*, 2000.
Twist1	Unknown.	Firulli *et al.*, 2005.
Hand1	Unknown. May promote TG cell differentiation.	Firulli *et al.*, 2000. Scott *et al.*, 2000. Hu *et al.*, 2006.

PL-1: Placental lactogen-1, **ANS**: autonomic nervous system, **IVS**: interventricular septum.

(b) Non-bHLH factors

Factor	Target genes/ function of complex	Hand1 binding domain(s)	Reference(s)
I-mfa	Unknown.	Cysteine-rich I-mfa domain.	Kraut *et al.*, 1998.
Nkx2.5	Unknown.	Unknown.	Thattaliyath *et al*, 2002b.
B56δ*	Hand1 dephosphorylation.	Multiple regions.	Firulli *et al.*, 2003.
Fhl2	Hand1-E12 repression.	LIM domain.	Hill and Riley, 2004.
Mef2, Gata	Activate *Nppa* expression**.	Unknown.	Morin *et al.*, 2005.
Sox15	Unknown.	HMG box domain.	Yamada *et al.*, 2006.
Maml2	Unknown.	Unknown.	P. Riley, unpublished data.

*As part of the Protein Phosphatase 2A (PP2A) enzyme.
***Nppa* encodes the Atrial Natriuretic Factor/ Peptide (Anf/ Anp).

1.1.3.3. Post-translational modification of Hand1

Covalent modification is a cellular mechanism that is widely-used to modulate the activity of transcription factors, including members of the bHLH super-family. For example, homo-cysteine disulphide linkage of E-protein homodimers stabilises these complexes during haematopoiesis (Benezra, 1994; Markus and Benezra, 1999). However, by far the most prolific post-translational modification is phosphorylation. Indeed, during myogenesis, phosphorylation of the basic domain of myogenic bHLH factors enhances their DNA binding affinity (Li *et al.*, 1992; Zhou and Olson, 1994). Additionally, phosphorylation of MyoD facilitates its heterodimerisation with E12 (Lenormand *et al.*, 1997). It is likely that post-translational modification acts as a molecular 'switch' that dictates the target genes of a bHLH factor. That is, phosphorylation modulates the DNA recognition sequence of a bHLH factor either directly (modification of residues in the basic domain) or indirectly (modification of residues in the HLH domain, which ultimately affects its dimerisation choice).

Through Y2H and GST-pull down assays, Firulli and co-workers identified an interaction between Hand1 and the regulatory B56δ subunit of protein phosphatase 2A (PP2A) (Firulli *et al.*, 2003). The identification of this Hand1 interactor ultimately led to the discovery that Hand1 can be site-specifically phosphorylated and dephosphorylated at two residues in helix 1. These covalent modifications were furthermore shown to be biologically relevant. Hand1 phosphorylation at these two residues increases during the differentiation of rat choriocarcinoma-1 (Rcho-1) trophoblast stem cells into trophoblast giant cells, in part due to the down-regulation of *B56δ* expression during this process. The authors subsequently showed that Hand1 mutants that could not be phosphorylated at these residues had different dimerisation affinities and biological activity to wild-type Hand1 (Firulli *et al.*, 2003). Since phosphorylation of Hand1 in the HLH domain alters its dimerisation affinity, and this bipartite DNA sequence to which it binds, changing the binding partner of Hand1 may thus be an important step in the TG cell differentiation program. Of note, the two helix 1 residues phosphorylated in murine Hand1 (T107 and S109) are conserved in murine Hand2 (T112 and S114) and murine Twist1 (T125 and S127; Figure 1.2). They are also targeted for dephosphorylation by PP2A complexes containing B56δ

(Firulli *et al.*, 2005). Moreover, the same study showed that mutation of these residues in Twist1 affects the affinity of the factor for Hand2 and this underlies some cases of Saethre-Chotzen syndrome, characterised by limb defects (Firulli *et al.*, 2005). Thus, control of bHLH activity by the modulation of phosphorylation is evolutionarily-conserved within the Twist subfamily of bHLH factors and may explain how they regulate different sets of target genes in distinct tissues.

1.1.4. Modes of Hand1 activity

As described, Hand1 can act as a transcriptional activator, for example when bound to the E-factors E12/ E47 (Hollenberg *et al.*, 1995). However, Hand1 has also been shown to function as a repressor at both the transcriptional and post-translational levels *in vitro* (Hollenberg *et al.*, 1995; Knofler *et al.*, 2002). This repressive activity may in part be underpinned by the atypical proline residue in the Hand1 basic domain. As discussed, this unusual feature has been associated with bHLH factors such as *Drosophila* enhancer-of-split (E(Spl)) and hairy (h), and mammalian Scleraxis, Stra13, and hairy-related transcription (Hrt) factors, which have also been shown to repress transcription. In this regard Hand2, which has not to date been observed to repress gene transcription, possesses an asparagine in its basic domain (reviewed by Firulli, 2003; Figure 1.2). Whether Hand1 acts as a transcription activator or repressor is likely dependent on cell type and cofactor availability, bHLH protein partner and DNA-binding sequence.

1.1.4.1. Transcriptional repression by Hand1

That Hand1 can repress transcription was first suggested by reporter assays in which a GAL4-Hand1 fusion protein repressed a reporter gene downstream of GAL4 DNA-binding sites (Hollenberg *et al.*, 1995). Other findings also support a role for Hand1 in negative gene control. Hand1 may repress *Hand2* expression in the developing yolk sac (Bounpheng *et al.*, 2000), and has been shown to repress Sox15-dependent transcription during TG cell differentiation (Yamada *et al.*, 2006). Furthermore, several genes are up-regulated in a *Hand1*-null background, implicating Hand1 in their repression (Smart *et al.*, 2002; Morikawa and Cserjesi, 2004).

The domain(s) responsible for conferring a transcriptional repressive activity to Hand1 are under debate. The original report of Hand1-dependent transcriptional repression suggested that the HLH dimerisation domain was responsible for repression of a reporter gene, suggesting that Hand1 may bind a factor, bHLH or possibly otherwise, that conveys repressive activity (Hollenberg *et al.*, 1995). Morin and colleagues showed that deletion of the Hand1 N-terminus produced a hyperactive deletion mutant that activated a reporter gene to a greater extent than wild-type Hand1 (Morin *et al.*, 2005). This supports the observation of Knofler and colleagues, who suggested the presence of a repressive domain in the Hand1 N-terminus (Knofler *et al.*, 2002). The N-terminal poly-histidine stretch and/ or a nearby alanine-rich region may be candidates and indeed similar motifs are thought to confer repressive activities to other transcription factors (Licht *et al.*, 1990; Shi *et al.*, 1991; Han and Manley, 1993). Alternatively, Hand1-mediated transcriptional repression may be a function of the C-terminal tryptophan-rich 'Hand domain'. This has homology to hydrophobic domains in the highly-related Hrt factors that recruit the co-repressor protein Groucho (Fisher *et al.*, 1996) and to motifs in hairy-related transcription factors that are known to confer a repressive activity (Steidl *et al.*, 2000). Finally, the asparagine-to-proline substitution in the basic domain of Hand1 has been associated with transcriptional repression in the bHLH family. Notably Stra13, one of the bHLH factors that share this characteristic, blocks the assembly of the basal transcription complex at gene promoters to achieve its repressive effect (Boudjelal *et al.*, 1997). However, it is unclear at present whether Hand1 is able to act in this fashion to repress its target genes.

As a final consideration, bHLH factors closely related to Hand1 interact with and modulate the function of transcriptional modifiers. For example, Twist1 inhibits chromatin remodelling and thus transcription by displacing histone acetyltransferases (HATs) such as p300 (Creb-binding protein, CBP) and p300/CBP-associated factor (PCAF) from promoters of its target genes (Hamamori *et al.*, 1999). Furthermore, Hand2, as a component of a complex with Gata4, physically interacts with CBP to synergistically activate the *Nppa* promoter (Dai *et al.*, 2002). It is thus plausible that Hand1 also recruits co-repressors to, or displaces co-activators from, the promoters of target genes. Indeed, such a function for Hand1 was proposed on the basis of its interaction with Mef2 in a transcriptional complex bound to DNA at Mef2 binding

sites (Morin *et al.*, 2005). In this regard, Hill and Riley proposed that the mechanism of action of the Fhl2 cofactor may be to displace histone acetyl-transferases from the Hand1-E-factor heterodimer-DNA complex, but not the Hand1-Hand1 homodimer transcriptional complex (Hill and Riley, 2004).

1.1.4.2. Post-translational repression by Hand1

Hand1 can also repress the activity of other transcription factors at the protein level. This was first suggested by mammalian one-hybrid experiments in which Hand1 suppressed GAL4-E47-dependent transcription from consensus E-box sequences (Knofler *et al.*, 2002). This post-translational repressive function of Hand1 is thought to occur via three mechanisms. Firstly, Hand1 can compete for the obligate class A bHLH binding partners of other class B bHLH factors, a mode of action not without precedent within the Twist bHLH factor subfamily (Spicer *et al.*, 1996). For example, Hand1 sequesters E-factors from Mash2 during TG cell differentiation to repress Mash2-dependent trans-activation (Scott *et al.*, 2000). Secondly, Hand1 may bind and inactivate other class B bHLH factors to alter the bHLH dimer pool in a similar way to the inhibitory Id and Mist1 factors during myogenesis (Jen *et al.*, 1997; Lemercier *et al.*, 1998). For example, Hand1 inhibits the DNA binding of MyoD-E12 heterodimers (Bounpheng *et al.*, 2000; Firulli *et al.*, 2000) and Alf1 homodimers (Bounpheng *et al.*, 2000) in competition EMSAs and reporter assays. Hand1 achieves this by forming heterodimers with E12, MyoD and ALF1. Finally, Hand1 can inhibit MyoD-E47 tethered heterodimers, stable complexes resistant to dimerisation competition from other bHLH factors or HLH factors such as the Id proteins (Bounpheng *et al.*, 2000). This mechanism suggests that Hand1-mediated repression does not require its interaction with another bHLH factor. Hand1-mediated post-translational repression in this case may depend on competition for common target gene promoters or cofactors, possibly including those involved in chromatin remodelling, such as histone acetyl-transferases (HATs; Morin *et al.*, 2005).

1.1.4.3. Does Hand1 function as a component of a multi-subunit protein complex?

Studies employing Hand1 deletion mutants have revealed that the Hand1 basic domain, and thus the ability of Hand1 to bind DNA, is required for Hand1 function in Rcho-1 cells (Scott *et al.*, 2000). However, some evidence suggests that Hand1 may activate its target genes as a component of a multi-subunit complex, often containing non-bHLH transcription factors.

The possibility of Hand1 belonging to a higher-order transcriptional complex was first inferred from the observation that the DNA binding affinity of Hand1 homodimers is significantly lower than that of Hand1-E-factor heterodimers (Scott *et al.*, 2000). This suggested that Hand1 associates with other proteins to enhance its DNA-binding and/ or trans-activational affinity. For example, the Hand1-interactor Fhl2 is thought to act as a scaffold around which a multi-subunit complex can assemble to enhance downstream transcriptional events (Hill and Riley, 2004). Thus Hand1 may activate genes in a DNA binding-independent fashion. Indeed, the closely-related Hand2 has been shown to operate via such a mechanism with Gata factors and the isolated HLH domain of Hand1 can drive the formation of ectopic digits in the developing limb bud (Dai *et al.*, 2002; McFadden *et al.*, 2002). This suggests that regions outside this protein-protein interaction domain are not required in some settings for Hand1 activity and that DNA-binding and trans-activation domains may be provided by other factors in a Hand1-containing multi-protein complex.

Morin and colleagues later showed that, whilst wild-type Hand1 is able to up-regulate *Nppa* expression, neither a tethered Hand1-Hand1 homodimer nor a tethered Hand1-Itf2 heterodimer could do the same (Morin *et al.*, 2005). Moreover, mutation of a Mef2-responsive element in the *Nppa* promoter drastically reduced wild-type Hand1-mediated activation (Morin *et al.*, 2005). These observations suggest that a complex containing Hand1 and Mef2 may activate *Nppa* expression. This is particularly supported by the fact that the DNA-binding domain of Mef2 was sufficient for synergy with Hand1 at the *Nppa* promoter, suggesting that Hand1 can support transcriptional activation. It was further suggested that Hand1 may represent

a stage-specific Mef2 cofactor. This was based on the observation that the Mef2 binding site in the *Nppa* promoter contributes differentially to gene activity in embryonic and postnatal cardiomyocytes (Naya *et al.*, 1999). Notably, the Hand1-dependent activation of *Nppa* was similarly abrogated when a *Gata* element was mutated (Morin *et al.*, 2005). Thus complex interactions between Hand1 and the non-bHLH transcription factors Mef2 and Gata may activate the *Nppa* promoter.

1.2. The role of Hand1 in extra-embryonic tissues

Hand1 plays a crucial role during the formation of the rodent placenta. The haemochorial placenta is the first organ to develop during embryogenesis and brings maternal and fetal vascular systems together to allow fetal intrauterine development. It is responsible for nutrient, oxygen and waste transport and also has endocrine functions.

Placental defects in humans give rise to a range of complications, including spontaneous abortion, intrauterine growth retardation (IUGR), choriocarcinoma and pre-eclampsia (reviewed in Redman and Sargeant, 2005; Sibai *et al.*, 2005). Pre-eclampsia occurs in up to 10% of all human pregnancies and is characterised by inadequate invasion of trophoblast, the fetal component of the placenta, into the maternal decidua. This in turn results in aberrant remodelling of the uterine spiral arterioles, which leads to IUGR and oedema in the fetus and hypertension and proteinuria in the mother. Investigating the role and regulation of Hand1 during placentation may thus shed some light on the molecular bases for these placental deficiencies. Additionally placental development is an attractive model system for investigating the molecular bases of stem cell maintenance and differentiation. This is in part because TS cells are extremely well-characterised in terms of stem cell potency and differentiation derivatives (Carney *et al.*, 1993; reviewed by Rossant and Cross, 2001).

1.2.1. Overview of rodent placentation

The following overview will focus on stages of murine placentation unless otherwise stated. The haemochorial placenta of rodents and primates is evolutionarily the most advanced. The distance between the maternal and fetal blood spaces is very small (~100-300μm) by virtue of the fact that the fetal trophoblast cells are in direct contact with the maternal blood.

The placenta in rodents is derived from two major cell lineages. The first, the cell lineage which contributes chiefly to the placenta, is the trophectoderm (TE). This is composed of pluripotent trophoblast stem (TS) cells and forms the epithelial portions of the placenta (Carney *et al.*, 1993; reviewed by Rossant and Cross, 2001). The second cell lineage that contributes to the rodent placenta is the extra-embryonic mesoderm, derived from the ICM, which forms the yolk sac and related structures, and the blood vessels of the placenta. The emergence of the TE during mouse development occurs when cells of the morula separate into the inner cell mass (ICM) and the epithelial TE population at the point of blastocyst formation (at embryonic day (E) 3.5). This represents the first differentiation event in the pre-implantation mammalian embryo. Studies have suggested that the segregation of ICM and TE cells is dependent on the down-regulation of *Oct-4* and *Nanog* in blastomeres destined to become the TE (Nichols *et al.*, 1998; Mitsui *et al.*, 2003; Hough *et al.*, 2006).

By the time the murine blastocyst implants into the uterus at E4.5, two separate TE populations have formed. These are the mural and polar TE. TS cells of the mural TE, which surround the blastocoel cavity and lack contact with the ICM, form a limited number (approximately 50-60) of primary TG cells (PGCs). These are the first differentiated cell type to arise during development. PGCs surround the blastocyst and facilitate the initial implantation of the blastocyst into the uterine tissue. This establishes the interface for subsequent formation of a network of blood sinuses at the periphery of the embryo, which allows the growth of the embryo prior to the formation of the definitive chorio-allantoic placenta. Meanwhile, TS cells of the polar TE, which overlie the ICM, continue to proliferate. This is likely in response to mitogenic fibroblast growth factors (Fgfs), particularly Fgf4, from the

ICM-derived epiblast of the early post-implantation embryo (Gardner and Beddington, 1988; Tanaka *et al.*, 1998; Zhong *et al.*, 2006). Fgf-dependent paracrine signalling via Fgf2r on the surface of the polar TS cells promotes their proliferation and this forms the chorion, also called the extra-embryonic ectoderm (ExE; Arman *et al.*, 1998). By E5.5, the chorion matures into the ectoplacental cone (EPC), also known as the implanting pole. The EPC subsequently flattens and expands by the primitive streak stage (E7.5) into the spongiotrophoblast (SpT) layer or 'junctional zone'. Both the EPC and SpT are progress zones that serve as reservoirs of diploid cells which progressively lose their stem cell potential. These structures ultimately spawn secondary TG cells (SGCs) from their outer reaches (reviewed by Rossant and Cross, 2001). Thus, in an E7.5 conceptus, PGCs can be found lining the implantation chamber at the more distal anti-mesometrial region of the conceptus up to the level of the EPC. In contrast, SGCs are located at the more proximal mesometrial end of the conceptus arising adjacent to the EPC.

SGCs are inherently invasive and phagocytic. These are characteristics that are underpinned by their secretion of proteases (Peters *et al.*, 1999; Nie *et al.*, 2005; Hassanein *et al.*, 2007) and their up-regulation of certain extracellular matrix protein receptors such as Alpha-7 Integrin (Sutherland *et al.*, 1993; Damsky *et al.*, 1994; Klaffky *et al.*, 2001). This facilitates the digestion of the extracellular matrix surrounding the uterine epithelial cells, so enabling SGCs to invade the maternal deciduum. The invasive capacity of SGCs has also been recapitulated in Matrigel, a uterine-like synthetic basement membrane matrix (Hemberger *et al.*, 2004). The ultimate purpose of decidual invasion is to establish intimate contact with the maternal decidua cells and to contact maternal blood sinuses by displacing maternal endothelial cells from vessels in the implantation site. As such, SGCs secrete angiogenic, vasodilatory and anti-coagulatory factors to promote maternal blood flow into the implantation site (Jackson *et al.*, 1994; Weiler-Guettler *et al.*, 1996; Achen *et al.*, 1997; Yotsumoto *et al.*, 1998). Furthermore, these cells also have endocrine functions. They secrete leutotrophic and lactogenic hormones such as prolactins and placental lactogens, which promote local and systemic adaptations in the mother that are necessary for embryonic growth and survival. For example, SGCs secrete Placental lactogen-1 (PL-1), also known as Chorionic somatomammotrophin-1 (Csh-1), which targets the ovary to maintain the corpus luteum and stimulate progesterone

production, and promotes mammary gland development and lactation (Nieder and Jennes, 1990; Faria and Soares, 1991; Hamlin *et al.*, 1994). The process of SGC differentiation is described in more detail later in this chapter (section 1.2.2).

In parallel with the process of SGC invasion, formation of the syncytiotrophoblast (SynT), also known as the labyrinth, takes place. This layer consists of villi lined with a multinucleated syncytium and is bathed in maternal blood. The SynT arises at approximately E8.5-9.0 when the allantois (extra-embryonic mesoderm-derived) fuses with the chorion (TE-derived; the process of chorio-allantoic fusion; Anson-Cartwright *et al.*, 2000). Molecular signals from the allantois may initiate the process, supported by the fact that isolated TS cells in culture, which readily differentiate into TG cells in culture after Fgf4 removal, very rarely differentiate into SynT (Hughes *et al.*, 2004). Although the SynT component of the placenta secretes hormones such as the aromatase Cyp19 (Anson-Cartwright *et al.*, 2000), it is folded and branched to provide a large surface area for nutrient, oxygen and waste exchange. As such, fetal blood vessels from the SynT layer occupy the spaces in the maternal decidua left by the invading TG cells (reviewed by Rinkenberger and Werb, 2000). Thus by E10.5, the mature chorionic placenta has formed and this is composed of three layers. The outermost layer of the placenta, that is the layer closest to the deciduum, is composed of SGCs. The SynT represents the innermost layer of the placenta, namely that closest to the embryo. Between these layers resides the SpT. Figure 1.5 summarises the process of murine placentation.

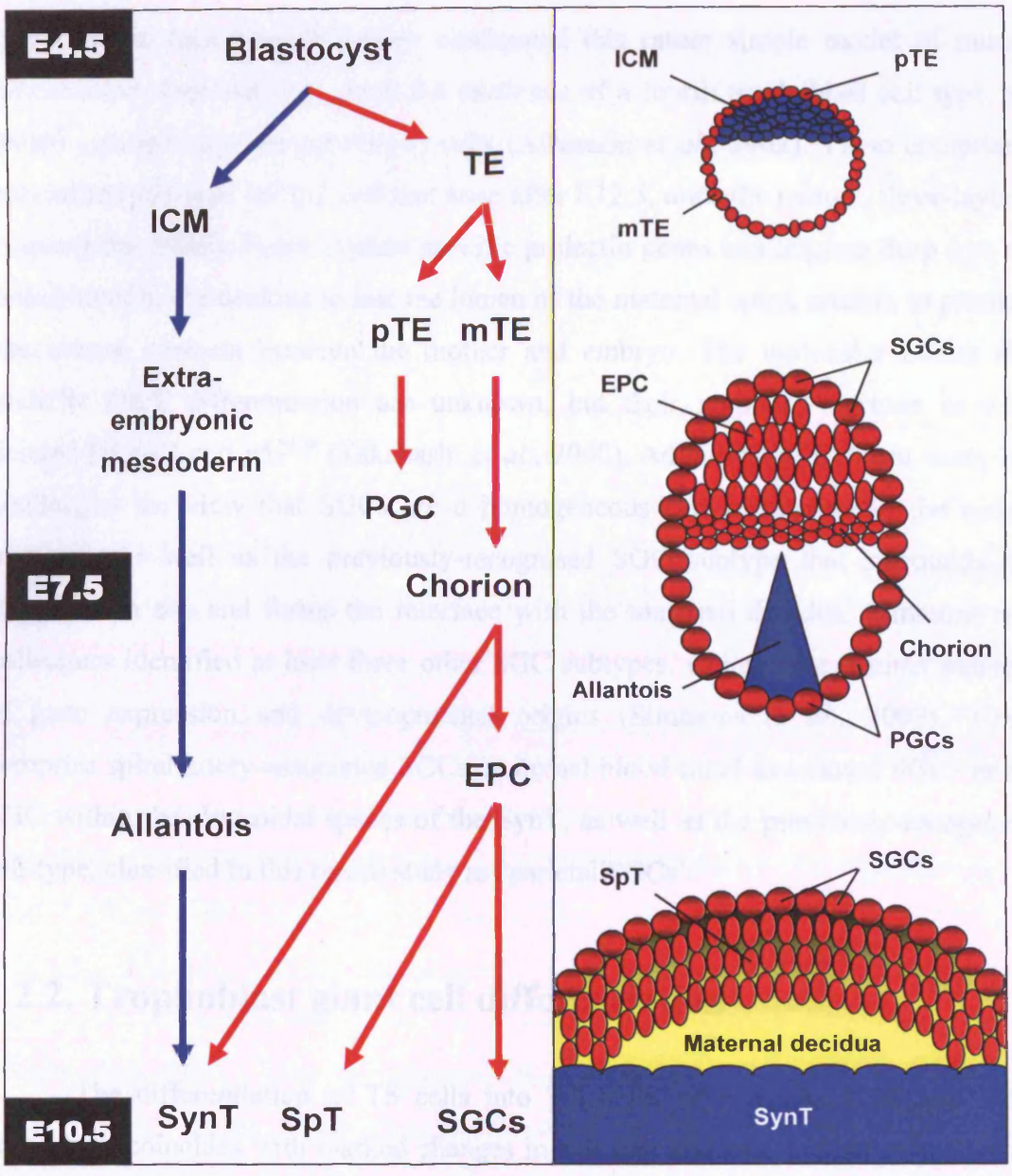

Figure 1.5. Overview of murine placentation.

At E4.5 the murine blastocyst, consisting of the mural and polar trophectoderm (mTE and pTE) and inner cell mass (ICM), implants into the maternal decidua. By E5.5 the mTE has differentiated into a limited population of primary trophoblast giant cells (PGCs), which facilitate implantation into the decidual wall. The pTE meanwhile proliferates to form the chorion. By E7.5 the ectoplacental cone (EPC) has formed from chorionic trophoblast and secondary trophoblast giant cells (SGCs) arise from this to invade the maternal decidua. By E10.5 the mature three-layered placenta has formed. SGCs comprise the outer layer and represent an interface with the maternal tissue, and the EPC has flattened to form the spongiotrophoblast (SpT), a reserve of diploid trophoblast destined to form SGCs. The innermost layer, the syncytiotrophoblast (SynT), arises when the chorionic trophoblast fuses with the allantois, and this establishes contacts with maternal blood vessels.

Some data have, however, challenged this rather simple model of murine placentation. One study suggests the existence of a fourth trophoblast cell type, so-called glycogen trophoblast (GlyT) cells (Adamson *et al.*, 2002). These comprise a specialised sub-type of SpT cell that arise after E12.5, once the mature, three-layered placenta has arisen. These express specific prolactin genes and migrate deep into the interstitium of the decidua to line the lumen of the maternal spiral arteries to promote vasculature contacts between the mother and embryo. The molecular events that underlie GlyT differentiation are unknown, but their numbers increase in mice deleted for *Igf2* and $p57^{Kip}$ (Takahashi *et al.*, 2000). Additionally, a recent study has challenged the view that SGCs are a homogeneous cell population in the rodent placenta. As well as the previously-recognised SGC subtype that surrounds the implantation site and forms the interface with the maternal decidua, Simmons and colleagues identified at least three other SGC subtypes, which have distinct patterns of gene expression and developmental origins (Simmons *et al.*, 2007). These comprise spiral artery-associated SGCs, maternal blood canal-associated SGCs and a SGC within the sinusoidal spaces of the SynT, as well as the previously-recognised sub-type, classified in this recent study as 'parietal SGCs'.

1.2.2. Trophoblast giant cell differentiation

The differentiation of TS cells into TG cells, of both the PGC and SGC subclasses, coincides with marked changes in cell size and cytoskeletal organisation (this chapter, section 1.2.2.1), the onset of endoreduplication and changes to the cell cycle machinery (section 1.2.2.2) and the elimination of endoreduplication inhibitors (section 1.2.2.3). Furthermore, there is some evidence that the process of SGC differentiation is modified by oxygen tension (section 1.2.2.4).

1.2.2.1. Cytoskeletal re-organisation

TG cell differentiation is accompanied by a dramatic increase in cell size, cytoskeletal actin re-organisation, stabilisation of cell-cell interactions and changes in focal adhesion formation (Parast *et al.*, 2001; Figure 1.6). These changes are thought to occur in three distinct stages. Firstly, an epithelial-mesenchymal transition gives

rise to a proliferative population of cells with strong cell-cell contacts. This is followed by a re-epithelialisation stage, which forms an intermediate trophoblast cell population that have destabilised cell-cell and cell-matrix interactions and decreased motility. The final phase of TG cell differentiation involves a specialised type of re-epithelialisation. This stabilises the cell-cell contacts and reorganises the actin cytoskeleton, enabling TG cells to form anchoring contacts with the decidual matrix (Parast *et al.*, 2001).

Studies by Parast and colleagues characterised in detail the cytoskeletal changes that occur during TG cell differentiation of rat choriocarcinoma-1 (Rcho-1) cells, a faithful model of TS cells in culture, and freshly-explanted E7.5 EPC-derived trophoblast (Parast *et al.*, 2001). Rcho-1 stem cells are small, highly-motile cells with patches of filamentous actin at their periphery. They also possess few, small peripheral focal complexes of Vinculin responsible for cell-cell interactions. Rcho-1 TG cells are larger, immotile cells with prominent actin stress fiber bundles and many, large internal focal Vinculin complexes (Figure 1.6). The reorganisation of the cytoskeleton correlates with changes in the activity of members of the Rho family of small GTPases including RhoA, Rac1 and Cdc42. Rcho-1 stem cells have low RhoA but high Rac1 and Cdc42 activity compared to TG cells. These GTPases are thought to regulate cytoskeletal re-organisation through phosphorylation of EphB2/EphrinB (Parast *et al.*, 2001). These cytoskeletal changes also coincide with a decrease in focal adhesion kinase (Fak) activity. Fak enhances integrin- and growth factor-mediated cell migration by turning over focal adhesions between cells and mediates coincident changes in E-Cadherin and specific Connexin expression (Reuss *et al.*, 1996). Another study reveled that the $p53/56^{lyn}$ kinases, which regulate cytoskeletal re-organisation through a phosphatidylinositol-3-kinase (PI3-K)- and protein kinase B (PKB)-dependent signalling cascade, are up-regulated during TG cell differentiation (Kamei *et al.*, 1997; Kamei *et al.*, 2002).

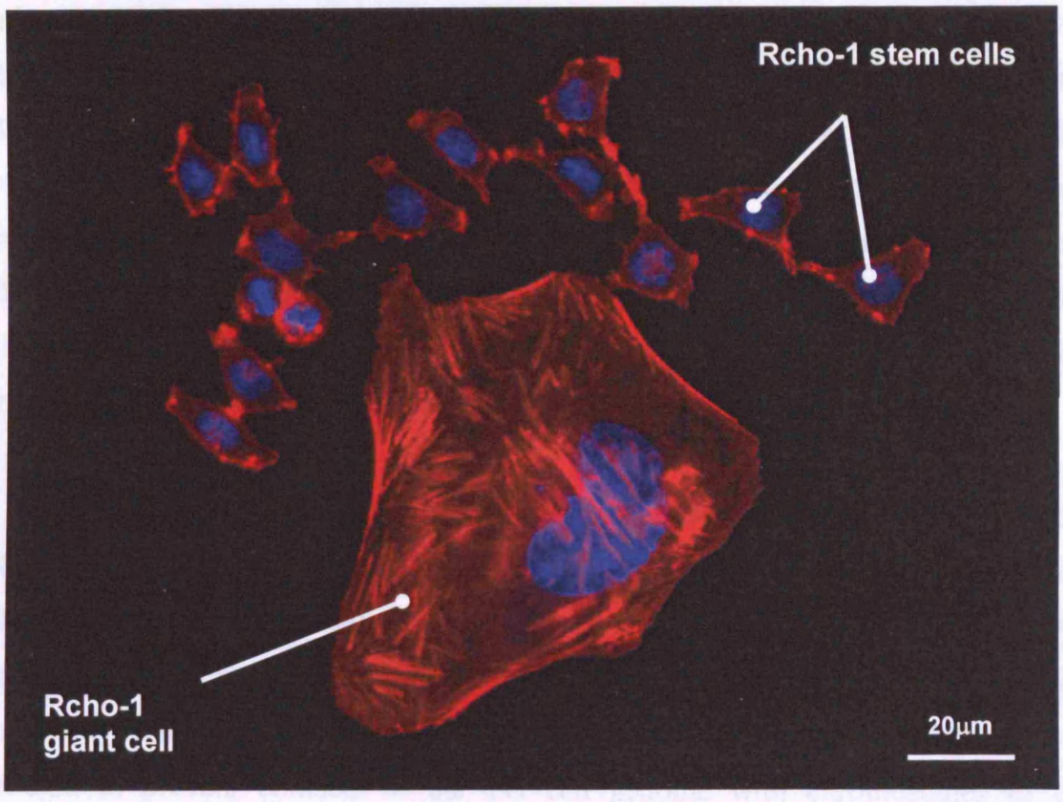

Figure 1.6. Rcho-1 trophoblast stem and trophoblast giant cells differ dramatically in terms of size and cytoskeletal organisation.

Rcho-1 trophoblast stem (TS) cells have a diameter of approximately 20μm and have patches of filamentous actin at their periphery. Rcho-1 trophoblast giant (TG) cells are larger (>100μm in diameter) and have prominent actin stress fiber bundles.

1.2.2.2. Endoreduplication and associated changes to the cell cycle machinery

Both PGCs and SGCs are polyploid, possessing DNA contents of up to a thousand times the haploid content (Varmuza *et al.*, 1988). This remarkable feature arises because progenitor TS cells exit the mitotic cell cycle and commence endoreduplication (enter the endocycle) at the point of committing to differentiate (reviewed by Rossant and Cross, 2001; Cross, 2002; Figure 1.7).

Post-mitotic endoreduplication in trophoblast, which also occurs in mammalian hepatocytes and megakaryocytes as well as in *Drosophila* salivary glands, consists of repeated rounds of DNA synthesis in the absence of intervening

mitoses. Such endoreduplication-based differentiation is initiated during the second gap phase (G2) of the final mitotic cell cycle (MacAuley *et al.*, 1998), and is thus distinct from terminal differentiation and entry into the quiescent state (G0) that occurs during phase G1. The length of an individual endocycle in trophoblast giant cells *in vivo* has been estimated as fourteen hours by pulse-chase experiments (Nakayama *et al.*, 1998). Furthermore [^{3}H]-thymidine incorporation experiments show that the rate of DNA synthesis declines during differentiation to 25% of the rate in proliferating TS cells (Hamlin and Soares, 1995).

Endocycling, in which the chromosomes do not condensate, likely enables the bulk transcription of genes whose products are crucial for uterine invasion. It may also allow the growth of cells beyond the limit defined by the nuclear/ cytoplasmic ratio that normally restricts the size of diploid cells, so permitting substantial size increases (MacAuley *et al.*, 1998). Furthermore endoreduplication in trophoblast is thought to prevent contacts of the TG cell genome with chromosomes of the phagocytosed allogenic maternal tissue. This serves to prevent an adverse immune response during embryogenesis (reviewed by Zybina and Zybina, 2005).

Endoreduplication in trophoblast is underpinned by marked modifications to the cell cycle regulation machinery (MacAuley *et al.*, 1998; Palazon *et al.*, 1998). These serve to prevent the cell from entering mitosis and so shunt it into the endocycle. For a cell to enter mitosis, mitotic (B-type, B1 and B2) cyclins bind cyclin-dependent kinases such as Cdk1 to form the mitotis-promoting factor (MPF; reviewed by Sullivan and Morgan, 2007). For a TS cell to exit the mitotic cell cycle, these mitotic cyclins must therefore be completely destroyed. This is a process which begins in phase G2 of the final mitotic cell cycle and is normally complete by the end of the first endocycle (MacAuley *et al.*, 1998; Figure 1.7).

Mitotic cyclin destruction is mediated in rodent trophoblast by the anaphase-promoting complex/ cyclosome (APC/C), which possesses E3 ubiquitin ligase activity. This complex ubiquitinates the destruction (D)-box in mitotic cyclins to target them for proteasomal degradation (Sudakin *et al.*, 1995). Other events also block the activity of the MPF. Palazon and coworkers showed that the onset of TG cell differentiation coincides with translational inhibition of Cyclin B1, resulting in

elimination of the protein, but not the transcript (Palazon *et al.*, 1998). Furthermore, the activity of Cdk1, namely the most prominent cyclin B-associated kinase, is reduced at the onset TG cell differentiation (MacAuley *et al.*, 1998). These observations may also explain why the trophoblast cell does not initiate mitosis during the first endocycle, despite the persistence of cyclin B protein. Additionally Rcho-1 TS cells switch cyclin D isoform expression from D3 to D1 during TG cell differentiation (MacAuley *et al.*, 1998). However, the reason for this is currently unclear.

The existence of defined endocyle S phases separated by gap phases suggests that endoreduplication is as carefully regulated as progression through the mitotic cell cycle (Sauer *et al.*, 1995). The initiation of, and progression through, endocyclic S-phases involves the synthesis, degradation and subcellular trafficking of cyclins E and A (Palazon *et al.*, 1998; MacAuley *et al.*, 1998). This was confirmed by the phenotype of *cyclin E1*$^{-/-}$; *cyclin E2*$^{-/-}$ TS cells, which are unable to undergo multiple rounds of DNA synthesis during endoreduplication (Geng *et al.*, 2003; Parisi *et al.*, 2003). In rodent trophoblast, the endocycle-specific cyclin A- and E-associated kinase inhibitor p57^{Kip2} was subsequently shown to halt DNA replication at the end of endocyclic S-phases as a pre-requisite for resetting origins of replication (Hattori *et al.*, 2000). This is a function that has also been attributed to the transcription factor Dp1 (Kohn *et al.*, 2003).

Several checkpoints are also altered coincident with the onset of TG cell differentiation, which is likely a consequence of the cell cycle reprogramming. For example, TG cells acquire insensitivity to DNA-damaging agents and do not arrest at the G1/S phase checkpoint upon DNA damage (MacAuley *et al.*, 1998). This is in accordance with the observed down-regulation of p53 during TG cell differentiation (Soloveva *et al.*, 2004). This is also consistent with the observation of increased numbers of TG cells in *p53*-null placentae (Komatsu *et al.*, 2007) and the fact that loss of *p53* induces mammalian cells to endoreduplicate (Cross *et al.*, 1995b; Peled *et al.*, 1996). Furthermore, in Rcho-1 stem cells, but not Rcho-1-derived TG cells, the G1-S phase transition is sensitive to the presence of growth factors. This likely underlies the ability of cultured TG cells to grow in the absence of serum (Hamlin *et al.*, 1994; Cross *et al.*, 1995; MacAuley *et al.*, 1998).

1.2.2.3. Elimination of endoreduplication inhibitors

To commence TG cell differentiation TS cells must inactivate so-called 'endoreduplication inhibitors'. These factors maintain TS cell proliferation and diploidy. They include Snail, previously called mSna (Nakayama *et al.*, 1998), and Geminin (Gonzalez *et al.*, 2006). However, how these endoreduplication inhibitors are inactivated at the onset of TG cell differentiation is currently unknown (Figure 1.7).

One of the ways in which Geminin is thought to prevent hyper-amplification of DNA is by blocking the assembly of the pre-replication complex. Accordingly, genetic ablation of *Geminin* promotes endoreduplication in murine blastomeres prior to the establishment of the TE. This has the effect of committing all cells of the blastocyst to the TG cell lineage (Gonzalez *et al.*, 2006). More is known about the activity and mechanism of action of Snail, the mammalian homologue of the *Drosophila* Snail family member Escargot. The loss of Escargot in *Drosophila* leads to abnormal development whereby ordinarily mitotic imaginal disc cells undergo endoreduplication (Hayashi *et al.*, 1993; Roark *et al.*, 1995). Conversely, ectopic expression of *Escargot* suppresses endoreduplication in *Drosophila* salivary glands (Fuse *et al.*, 1994). *Snail* expression is restricted to the proliferating TG cell precursors within the core of the EPC and later the SpT layer, but down-regulated upon SGC differentiation (Nakayama *et al.*, 1998). This was confirmed by transfection experiments in Rcho-1 cells. These showed that *Snail* over-expression blocked, whilst its antisense-mediated knock-down promoted, TG cell differentiation (Nakayama *et al.*, 1998). Furthermore, stable Rcho-1 cell transfectants for *Snail* underwent TG cell differentiation at a markedly-reduced level (Nakayama *et al.*, 1998).

Snail is a zinc finger transcriptional repressor that is thought to directly repress transcription, perhaps of pro-endoreduplicative genes (Nakayama *et al.*, 1998). Indeed, Snail possesses an N-terminal seven-amino-acid SNAG domain, which likely recruits co-repressor complexes to the promoter of the gene(s) to be repressed (Grimes *et al.*, 1996; Cano *et al.*, 2000). Otherwise Snail may compete with and/ or displace pro-endoreduplicative bHLH factors from E-box DNA elements

(Fuse *et al.*, 1994; Nakayama *et al.*, 1998). Although it was suggested that Hand1 may be one of these bHLH factors (Nakayama *et al.*, 1998), Hand1 is known to bind the degenerate E-box Thing-1 site *in vivo* (Hollenberg *et al.*, 1995). Additionally, Snai1 also promotes the expression of mitotic cyclins, via an as-yet unidentified mechanism. Over-expression of *Snail* in Rcho-1 stem cells results in markedly-increased levels of *cyclin A* and *cyclin B* transcripts, which would be inferred to drive mitotic entry at G2 in preference to the initiation of endoreduplication (Nakayama *et al.*, 1998).

1.2.2.4. Modification of trophoblast giant cell differentiation by oxygen tension

Implantation of the murine blastocyst at E4.5 occurs in hypoxic conditions (3-5% oxygen) because maternal blood flow to the implantation site is low. However, when the chorio-allantoic placenta develops and establishes connections with the maternal vasculature at E9.0-E10.0 in mice, the placental environment becomes relatively oxygen-rich (8.6% oxygen; Rodesch *et al.*, 1992).

Hypoxia is thought to promote the rapid proliferation of diploid trophoblast cells needed to amass the quantity of cells required for formation of the placenta, at least in humans (Genbacev *et al.*, 1997; Caniggia *et al.*, 2000). Ectopically increasing oxygen tension inhibits diploid trophoblast renewal and promotes precocious invasive trophoblast differentiation (Genbacev *et al.*, 1997; Caniggia *et al.*, 2000). Interestingly, the heterodimeric hypoxia-inducible factor (HIF), up-regulated by low oxygen tension, is a negative regulator of TG cell differentiation (reviewed by Fryer and Simon, 2006). Predictably, therefore, mice lacking HIF-1 subunits are embryonic lethal due to placental defects characterised by precocious TG cell differentiation at the expense of the formation of other placental layers (Kozak *et al.*, 1997; Adelman *et al.*, 2000; Cowden-Dahl *et al.*, 2005). These observations are in agreement with the hypothesis that *Mash2*, which encodes a bHLH factor required for TS cell maintenance, is up-regulated either directly or indirectly by HIF *in vitro* (Cowden-Dahl *et al.*, 2005). Interestingly, HIF-1 is thought to regulate genes that may play a role in the development of pre-eclampsia. These include the gene encoding TGF-β3,

an inhibitor of TG cell invasion, whose expression persists beyond the first trimester in pre-eclampsia and may underlie the failure of TG cell invasion (Cannigia *et al.*, 2000).

Interestingly, aspects of invasive trophoblast differentiation are compromised in Rcho-1 cells and other trophoblast stem cell models induced to differentiate under low oxygen tension (Gultice *et al.*, 2006; Lash *et al.*, 2007; Takeda *et al.*, 2007). Molecularly, Rcho-1 cells cultured under hypoxia maintained the TS cell-specific expression of *Id-1* and *Id-2*, which are down-regulated during Rcho-1 TG cell differentiation in normoxic conditions (Cross *et al.*, 1995). This is in agreement with a study that demonstrated that hypoxia prevents the down-regulation of *ID-2* during human invasive trophoblast differentiation (Janatpour *et al.*, 2000). The Id factors may thus persist to inhibit Hand1 or other bHLH factor activity, which may be responsible for a block to TG cell differentiation. Furthermore, despite retaining their characteristic gene expression profile, low oxygen correlated with reduced PL-I and Palladin protein production. The lack of Palladin, normally expressed at high levels in TG cells and which is required for the formation of focal adhesions, cell-cell junctions and stress fibres (Parast and Otey, 2000), resulted in cytoskeletal disorganisation.

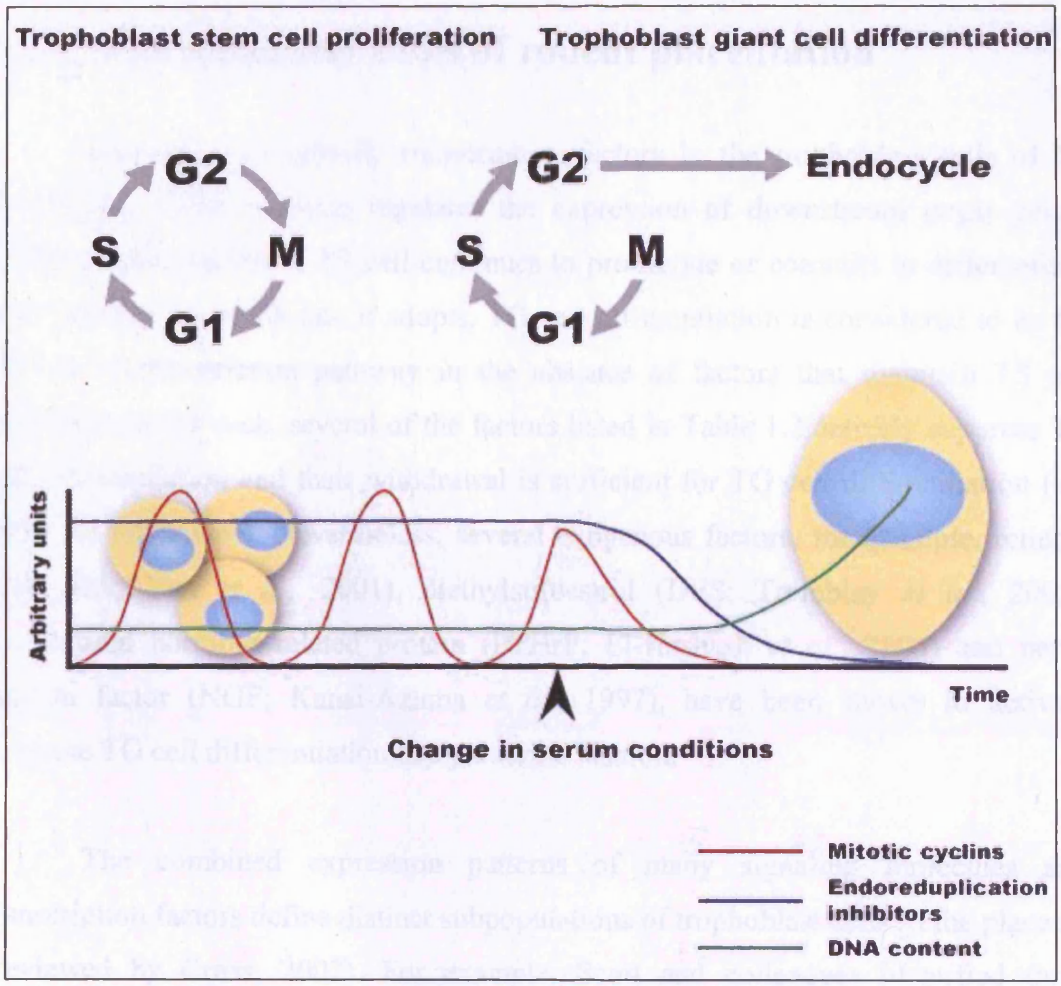

Figure 1.7. The molecular basis of trophoblast giant cell differentiation.

The commitment of trophoblast stem (TS) cells to trophoblast giant (TG) cell differentiation occurs during phase G2 of the final mitotic cell cycle. This is concomitant with cells initiating endoreduplication, the replication of genomic DNA in the absence of intervening mitoses to produce polyploid cells. As a pre-requisite for endocycle entry, the anaphase-promoting complex/ cyclosome (APC/C) must target mitotic cyclins and possibly endoreduplication inhibitors such as Snai1 and Geminin for terminal destruction. Until now the G2-specific event(s) that promote TG cell differentiation have been unclear.

M: mitosis, **G1**: first gap phase, **G2**: second gap phase, **S**: DNA synthesis phase.

1.2.3. The molecular basis of rodent placentation

Expression of specific transcription factors in the trophoblast cells of the developing rodent placenta regulates the expression of downstream target genes. These control whether a TS cell continues to proliferate or commits to differentiate, and furthermore which fate it adopts. TG cell differentiation is considered to be the 'default' differentiation pathway in the absence of factors that maintain TS cell proliferation. As such, several of the factors listed in Table 1.2 actively suppress TG cell differentiation and their withdrawal is sufficient for TG cell differentiation (see table for references). Nevertheless, several exogenous factors, for example, retinoic acid (RA; Yan *et al.*, 2001), diethylstilbestrol (DES; Tremblay *et al.*, 2001), parathyroid hormone-related protein (PTHrP; El-Hashash *et al.*, 2005) and nerve growth factor (NGF; Kanai-Azuma *et al.*, 1997), have been shown to actively promote TG cell differentiation in a paracrine fashion.

The combined expression patterns of many signaling molecules and transcription factors define distinct subpopulations of trophoblast cells in the placenta (reviewed by Cross, 2002). For example, Scott and colleagues identified three functionally-distinct trophoblast subpopulations in the E7.5-8.5 murine placenta based simply on the expression domains of *Hand1* and *Mash2*. These are the TS cells of the chorion (*Mash2* only), cells in the core of EPC or SpT (both Hand1 and Mash2) and the TG cells forming at the periphery of the EPC or SpT (*Hand1* only) (Scott *et al.*, 2000). It is clear, however, that there are many more transcriptional domains in the developing murine placenta involving other factors and that there is considerable overlap between them. A selection of the molecules that control murine placentation are summarised in Table 1.2. The role of Hand1 in regulating SGC differentiation will be described in detail in the next section (1.2.4) of this chapter.

Table 1.2. A selection of factors involved in murine placentation.

Factors required for TS cell renewal (**a**) are expressed at high levels in TS cells or promote TS cell proliferation in a paracrine fashion, but are down-regulated upon TG cell differentiation. If the genes encoding these factors have been deleted in mice, placental defects characterised by precocious TG cell differentiation generally result. Conversely, factors required for TG cell differentiation (**b**) are absent from TS cells but are up-regulated during their differentiation into TG cells. If the genes encoding these factors have been deleted in mice, placental defects characterised by a lack of TG cells generally result. Factors required for SynT differentiation and for formation of extra-embryonic mesoderm are not listed.

Factor	Function	Reference(s)
(a) Factors required for trophoblast stem (TS) cell renewal		
Fgf4, Fgf18	Act in a paracrine fashion through Fibroblast growth factor receptor-2 (Fgf2r) on the TS cell surface to activate *Cdx2* and *Eomes* expression.	Arman *et al.*, 1998. Tanaka *et al.*, 1998. Zhong *et al.*, 2006.
TGFβ family members (e.g. Nodal, Activin)	Act in a paracrine fashion to inhibit *JunB* but promote *Mash2* and *Snai1* expression.	Ma *et al.*, 2001. Guzman-Ayala *et al.*, 2004.
Cdx2	Controls trophoblast versus ICM cell fate.	Strumpf *et al.*, 2005.
Eomes	Controls polar versus mural trophectoderm fate.	Russ *et al.*, 2000.
Errβ	Unknown.	Luo *et al.*, 1997. Tremblay *et al.*, 2001.
Ap-2γ	Couples Fgf signalling to *Cdx2* and *Eomes* expression.	Auman *et al.*, 2002.
Elf5	Controls chorionic versus EPC cell fate.	Donnison *et al.*, 2005.

Factor	Function	Reference(s)
Sp1	Activates *Id-1* expression.	Takeda *et al.*, 2007.
Foxd3	Unknown.	Tompers *et al.*, 2005.
Id-1 and Id-2	May inhibit Hand1, Stra2 and Stra13 activity.	Cross *et al.*, 1995. Jen *et al.*, 1997. Takeda *et al.*, 2007.
Socs3	Suppresses Lif signalling.	Takahashi *et al.*, 2003. Isobe *et al.*, 2006.
(b) Factors required for trophoblast giant (TG) cell differentiation		
Hand1	Activates *PL-I* expression. Promotes mitotic cell cycle exit at the onset of endoreduplication.	Cross *et al.*, 1995. Hughes *et al.*, 2004.
Ap-2γ (Stra2)	Activates *PL-II* and *PTHrP* expression. Transduces retinoic acid (RA) secreted by the decidua, which promotes TG cell differentiation.	Yan *et al.*, 2001. Auman *et al.*, 2002. Ozturk *et al.*, 2006.
Stra13	Promotes mitotic cell cycle exit at the onset of endoreduplication. Transduces RA secreted by the decidua.	Yan *et al.*, 2001. Hughes *et al.*, 2004.
Gata2/3	Activates *PL-I* expression. Restricts the expression of PLP-A to secondary, rather than primary, TG cells.	Ng *et al.*, 1994. Ma and Linzer, 2000.
c-Jun	Activates expression of *PL-I* and the matrix metalloproteinase genes *Mmp2* and *Mmp9*.	Bamberger *et al.*, 2004.
JunB	Unknown.	Schorpp-Kistner *et al.*, 1999.

Factor	Function	Reference(s)
I-mfa	Inhibits Mash2 activity in diploid TG cell precursors.	Kraut et al., 1998.
Sox15	Enhances Hand1-dependent transcription.	Yamada *et al.*, 2006.
Ets family	Activate genes encoding various members of the placental lactogen family.	Yamamoto *et al.*, 1998. Sun and Duckworth, 1999.
Ngf	Unknown.	Kanai-Azuma *et al.*, 1997.
PTHrP	Maternal PTHrP stimulates PGC differentiation. PTHrP-dependent signalling in SGCs promotes entry into the endocycle. Up-regulates *Stra2* and *Stra13* but down-regulates *Mash2* and *Snail* expression.	El-Hashash *et al.*, 2005. El-Hashash and Kimber, 2006.
Pparβ	Up-regulates *I-mfa* expression but down-regulates *Id-2* expression.	Nadra *et al.*, 2006.

1.2.4. Hand1 is required for rodent placentation

The expression of murine *Hand1* in trophoblast was first demonstrated by injecting a *Hand1*-encoding plasmid into an individual blastomere of a morula (Cross *et al.*, 1995). After culturing this morula to later stages and allowing for blastocyst outgrowth, whole-mount RNA *in situ* hybridisation analyses were performed to map *Hand1* expression. This revealed an absence of *Hand1* transcripts in TS cells of the chorion layer, an up-regulation of *Hand1* in the EPC, particularly in the more differentiated cells at its periphery, and the strongest expression in the TG cell layer surrounding the implanted conceptus. Weaker and more transient *Hand1* expression was observed in the extra-embryonic mesoderm cells that form the developing yolk sac, amnion and allantois (Cross *et al.*, 1995).

This *Hand1* expression pattern was subsequently confirmed by *in vivo* studies. In one study, *Hand1* was targeted in ES cells via the insertion of a *LacZ* (*β-galactosidase*) expression cassette to create a loss-of-function *Hand1* allele (Firulli *et al.*, 1998). In E7.5 mouse embryos heterozygous for this allele, β-galactosidase staining revealed *Hand1* promoter activity in the trophectoderm of the EPC and extra-embryonic mesodermal components of the primitive placenta, namely the amnion, allantois and yolk sac, as well as in the extra-embryonic mesoderm-derived umbilical and vitelline vessels. Whilst the previous *in situ* hybridisation study failed to show *Hand1* expression in the chorion (Cross *et al.*, 1995), chorionic *LacZ* expression was detectable in these embryos (Firulli *et al.*, 1998). This implies that *Hand1* is either very weakly expressed or its transcript is unstable in chorionic TS cells.

1.2.4.1. Hand1 is required for trophectoderm specification

Hand1 mRNA was detected at the two-cell embryo prior to blastocyst formation, suggesting a role in early lineage specification (Cross *et al.*, 1995). Indeed, *Hand1* over-expression in mouse blastomeres promotes their differentiation into trophectoderm whilst in ES cells ectopic *Hand1* activity arrests cell proliferation (Cross *et al.*, 1995). The bias of blastomeres towards the trophectoderm lineage at the

expense of ICM formation resulted in blastocysts with fewer cells than wild-type blastocysts due to premature TG cell differentiation. Occasionally 'trophoblastic vesicles' arose, which resembled blastocysts but which lacked an ICM (Cross *et al.*, 1995). These observations implicate *Hand1* in the specification of trophoblast cell fate at the morula-to-blastocyst transition.

1.2.4.2. Hand1 is required for trophoblast giant cell differentiation

Reporter assays using the Rcho-1 cell line, a faithful model of TS cells, revealed that endogenous *Hand1* expression is up-regulated coincident with TG cell differentiation following serum withdrawal (Cross *et al.*, 1995). Furthermore, ectopic expression of *Hand1* drives precocious TG cell differentiation in Rcho-1 cells (Cross *et al.*, 1995). Later experiments showed that the suppression of Rcho-1 TG cell differentiation by dimethyl sulphoxide (DMSO) correlates with a down-regulation of *Hand1* expression (Sahgal *et al.*, 2005). Another group later generated *Hand1*-null TS cells from *Hand1*-null blastocysts (Hemberger *et al.*, 2004). Such cells appropriately have an impaired ability to undergo TG cell differentiation, as indicated by the down-regulation of the TG cell marker *Placental lactogen-1* (*PL-1*), upon the withdrawal of proliferation-inducing molecules such as Fgf4, its cofactor Heparin and those secreted by feeder cells. These cells also exhibit an approximately 50% decrease in invasion rates in comparison with *Hand1*-heterozygous TS cells, as assessed by Matrigel assays (Hemberger *et al.*, 2004). These and other studies (Kraut *et al.*, 1998; Scott *et al.*, 2000) imply that Hand1 is both necessary and sufficient for TG cell differentiation of Rcho-1 and trophoblast stem cells.

Two research groups independently generated a knock-out mouse model for *Hand1* by gene targeting to analyse Hand1 function *in vivo* (Riley *et al.*, 1998; Firulli *et al.*, 1998). Mice heterozygous for *Hand1* had no apparent phenotypic defects and were fertile. However, *Hand1*-null mice arrested at E7.5 and were embryonic lethal at E8.0-E9.0. This was primarily due to combined failure of EPC cells, which are reduced in number, to properly differentiate into SGCs (Riley *et al.*, 1998), and as a result of defects of the extra-embryonic mesoderm, which ultimately resulted in a hemorrhaging of the yolk sac (Firulli *et al.*, 1998). The reduced number of SGCs

resulted in a smaller implantation chamber and a failure to invade the maternal decidua to establish a maternal-fetal interface (Riley *et al.*, 1998; Figure 1.8). Indeed, the number of TG cells surrounding *Hand1*-null implantation sites at E8.5 (~80) was not significantly different from the number of mural trophectoderm cells present at the blastocyst (E3.5) stage in wild-type concepti.

These studies collectively implied that Hand1 regulates cell commitment to the trophoblast lineage and subsequent SGC differentiation in rodents. Notably the number of SGC precursors in the EPC or its derivative SpT layer is not increased in *Hand1*-null embryos, as might be expected in the absence of their differentiation, but is in fact reduced. This suggests that TS cells are able to exit the mitotic cell cycle normally in the absence of Hand1 and that the absence of Hand1 prevents their subsequent differentiation. Nevertheless, if *Hand1*-null TS cells, induced to differentiate by withdrawal of Fgf4, are transfected with a *Hand1* expression construct, their rate of differentiation is not further increased (Hughes *et al.*, 2004). Indeed, in the same study, *Hand1* over-expression was shown to promote exit from the mitotic cell cycle in TS cells concomitant with TG cell differentiation. This occurred even in culture conditions that normally maintain TS cell proliferation (Hughes *et al.*, 2004). This dominant effect of Hand1 and its ability to override factors that maintain TS cell diploidy suggests that Hand1 activity is sufficient for mitotic cell cycle exit and the onset of endoreduplication, albeit via an uncharacterised mechanism.

It is also of note that *Hand1*-null mutant blastocysts were able to implant, hatch and outgrow normally into maternal decidua (Riley *et al.*, 1998). This suggests that *Hand1*-null PGCs, responsible for blastocyst implantation, form and function normally. Despite the similarity in morphology of PGCs and SGCs, several molecules have been identified in either one or the other (Rebstock *et al.*, 1993; Ma and Linzer, 2000). This suggests that the molecular events underlying their formation probably differ and that PGC differentiation may not require Hand1. Nevertheless, maternal *Hand1* transcripts have been identified in the oocyte and cleavage-stage embryos (Cross *et al.*, 1995), which could support PGC formation in *Hand1*-null embryos. However, this is unlikely to feature at later stages (E7.5-8.0) coincident with SGC differentiation.

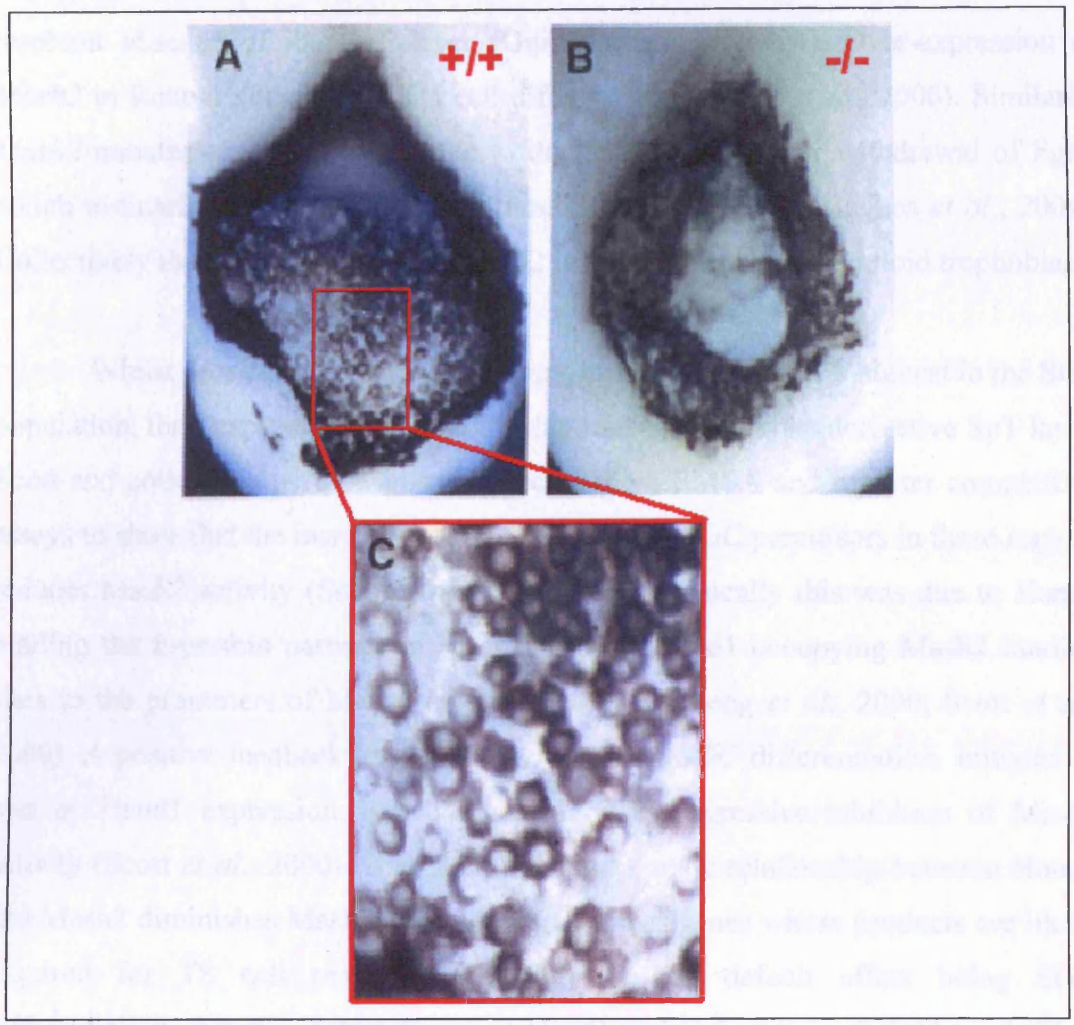

Figure 1.8. Hand1 is essential for secondary trophoblast giant cell differentiation *in vivo*.

In wild-type embryos, TS cells of the ectoplacental cone differentiate into secondary giant cells (SGCs) that invade the maternal decidua to generate a maternal-fetal interface (**a**; enlarged section shows SGCs in (**c**)). However, *Hand1*-null mice arrest at E7.5 due to a failure of SGC differentiation and SGC invasion of the maternal decidua (**b**). Adapted from Scott *et al.*, 2000.

The exact mechanism by which Hand1 drives SGC differentiation is poorly understood. A possible mechanism was suggested based on the findings of RNA *in situ* hybridisation experiments on E8.5 mouse embryos (Scott *et al.*, 2000). These showed that *Hand1* and *Mash2* expression domains overlap in the EPC and its derivative SpT layer. Mash2 is the predominant bHLH transcription factor in diploid trophoblast but is absent in SGCs. *Mash2* deficiency in mice causes embryonic lethality at E10.5 due to excessive and precocious TG cell differentiation and a

resultant absence of the SpT layer (Guillemot *et al.*, 1994). Over-expression of *Mash2* in Rcho-1 cells blocks TG cell differentiation (Scott *et al.*, 2000). Similarly, *Mash2*-transfected TS cells continue to divide for longer after withdrawal of Fgf4, which ordinarily results in TG cell differentiation by default (Hughes *et al.*, 2004). Collectively these studies implicate Mash2 in the maintenance of diploid trophoblast.

Whilst *Mash2* expression is chorionic and that of *Hand1* is highest in the SGC population, their expression domains overlap in the EPC and its derivative SpT layer. Scott and colleagues used co-immunoprecipitation, EMSA and reporter competition assays to show that the increasing levels of Hand1 in SGC precursors in these regions reduces Mash2 activity (Scott *et al.*, 2000). Mechanistically this was due to Hand1 binding the E-protein partners of Mash2, and/ or Hand1 occupying Mash2 binding sites in the promoters of Mash2 target genes (Bounpheng *et al.*, 2000; Scott *et al.*, 2000). A positive-feedback loop thus likely ensues. SGC differentiation, initiated in part by Hand1 expression, is accompanied by a progressive inhibition of Mash2 activity (Scott *et al.*, 2000). Ultimately the antagonistic relationship between Hand1 and Mash2 diminishes Mash2-induced expression of genes whose products are likely required for TS cell renewal, with the net and default effect being SGC differentiation. Whether heterodimers of Hand1 and E-factors in diploid trophoblast activate genes whose products promote TG cell differentiation, or otherwise, is presently unknown.

However, a wholly passive role for Hand1 during TG differentiation is disputed by the results of functional studies analysing Hand1 deletion mutants (Scott *et al.*, 2000). Over-expression of a Hand1 deletion mutant lacking the basic domain, which is thus unable to bind DNA but can still compete for the E-factor binding partners of Mash2, had no significant effect on TG cell differentiation. This suggests that Hand1 has a more active role during TG differentiation, namely that it regulates its own target genes. The fact that *Hand1*-null placental defects are retained in a *Hand1/ Mash2* double-null mutant mouse further supports this idea (Scott *et al.*, 2000). Thus Hand1 function is not restricted to inhibiting Mash2-dependent transcription and moreover the phenotype of *Hand1*-null embryos is not simply due to ectopic Mash2 activity.

E-factors are down-regulated during differentiation in several cell types and indeed are detectable neither in SGCs (Cross *et al.*, 1995; Scott *et al.*, 2000) nor cardiomyocytes (Riley *et al.*, 2000). Thus, although Hand1 likely titrates E-factors from Mash2 during SGC differentiation, Hand1 must itself bind different bHLH partners during later stages of this process. Possible bHLH binding partners of Hand1 in SGCs include Hand1 itself, Stra13, and/ or the Hrt (Hey) factors (Firulli *et al.*, 2000; Hughes *et al.*, 2004; Hu *et al.*, 2006). Interestingly the bHLH factors NEUROD1 and D2 are expressed during human extravillous trophoblast invasion, although it is currently unknown whether this is the case in rodents and whether Hand1 interacts with these (Westerman *et al.*, 2002). Recent studies argue against the possibility of Stra13 being a Hand1 binding partner, however. An interaction between Hand1 and Stra13 was neither detected in mammalian two-hybrid nor in co-transfection experiments and Stra13 and Hand1 did not synergistically promote SGC differentiation (Hughes *et al.*, 2004). The Hrt factors are particularly strong candidates for Hand1 interaction in both trophoblast and cardiomyocytes; *Hrt1*$^{-/-}$/ *Hrt2*$^{-/-}$ double knockout mice are embryonic lethal due to cardiac and placental defects (M. Gessler, personal communication). Notably, tethered Hand1 homodimers can drive TG cell differentiation in cultured TS cells to a degree similar to that of the Hand1 monomer (Hu *et al.*, 2006). This suggests that Hand1 may act as a homodimer to actively promote TG cell differentiation, but would require further investigation to corroborate.

Hand1 activity in TG cells may depend also on tertiary interactions, namely with non-bHLH factors. Hand1 interacts with the non-bHLH, HMG-box transcription factor Sox15 in SGCs cells (Yamada *et al.*, 2006). Sox15 is up-regulated during TG cell differentiation *in vivo* and ectopic expression of *Sox15* promotes precocious Rcho-1 TG cell differentiation in a Hand1-dependent fashion. Whilst Sox15 interaction with Hand1 enhanced Hand1-dependent transcription in reporter assays, the Hand1-Sox15 interaction had the opposite effect at Sox15-dependent promoters (Yamada *et al.*, 2006). However, the biological relevance of these observations *in vivo* is currently unclear.

Hand1, in combination with as-yet unidentified factors, likely activates genes whose products contribute to the process of SGC differentiation. Otherwise, Hand1

may repress genes whose products maintain the proliferative trophoblast population. However, few Hand1 target genes in the trophoblast lineage have been identified. This may be because Hand1 heterodimerisation partners are largely unknown and possibly since Hand1 activity, like that of Hand2, may not require the basic domain and is independent of DNA binding (McFadden *et al.*, 2002). Hand1, in combination with Gata2/3 and Ap-1 (Shida *et al.*, 1993; Ng *et al.*, 1994), regulates the gene encoding the hormone Placental Lactogen-1 (PL-1) (Cross *et al.*, 1995). This gene is down-regulated in trophoblast of *Hand1*-null mice (Riley *et al.*, 1998; Firulli *et al.*, 1998). Appropriately the mouse *PL-1* promoter contains a Thing1-box (CTGCTG) which conforms to the consensus site to which Hand1-E47 heterodimers bind (Hollenberg *et al.*, 1995). Deletion of an 86bp region of the promoter (between -274 and -188 relative to the *Hand1* transcription start site) that encompasses this element furthermore results in diminished *PL-1* promoter activity in Rcho-1 cells co-transfected with *Hand1* (Cross *et al.*, 1995; Scott *et al.*, 2000). Notably Smart and co-workers identified *Wnt2* as a putative target gene of Hand1, albeit in a cardiac cell model (Smart *et al.*, 2002). Specifically, *Wnt2* is up-regulated in a *Hand1*-null background, implicating Hand1 in its repression. This is particularly interesting in light of the fact that deletion of the *Wnt2* gene in mice is associated with defective placentation characterised by ectopic TG cells (Monkley *et al.*, 1996). Notably, the expression domain of *Hand1* in the developing mouse heart overlaps with that of the transcriptional co-activator *Cited1*, and its expression is down-regulated in the hearts of conditional *Hand1*-null embryos (Dunwoodie *et al.*, 1998; McFadden *et al.*, 2005). *Cited1* expression is furthermore required for proper placentation (Rodriguez *et al.*, 2004), suggestive of its regulation by Hand1 in trophoblast. Finally, Hughes and colleagues demonstrated that Stra13 was co-expressed in a subset of Hand1-positive TG cells (Hughes *et al.*, 2004). This implies that Hand1 may activate *Stra13* expression during TG cell differentiation.

1.2.4.3. Hand1 is required for formation of the yolk sac vasculature

During murine placentation, the yolk sac does not develop from TE (TS cells). Instead, the yolk sac is formed from two populations of cells derived from the ICM in two stages (reviewed by Rossant and Cross, 2001). Firstly, just after

blastocyst implantation, endoderm cells migrate onto the basal surface of the PGC layer and form the parietal yolk sac. This absorbs nutrients from the maternal blood via capillaries in the decidua. It is not known whether Hand1 is required for this process. Subsequently, by E8.0, extra-embryonic mesoderm cells migrate to the inner surface of the parietal yolk sac. This generates the visceral yolk sac, composed of primitive vitelline vessels and haematopoietic cells, which facilitate more efficient exchange of materials between embryo and mother until formation of the definitive chorio-allantoic placenta. Hand1 is specifically expressed in this mesodermal yolk sac component (Firulli *et al.*, 1998).

Hand1-null embryos do not display reduced numbers of extra-embryonic mesodermal cells, suggesting that the gene is not required for their differentiation. However, such embryos have a visceral yolk sac that is rough and disorganised in appearance, particularly in the area in contact with the EPC (Firulli *et al.*, 1998). In addition, their yolk sac vasculature is abnormal, which results in extensive leakage of haematopoietic cells into the space between the yolk sac and the amnion (yolk sac hemorrhaging; Firulli *et al.*, 1998; Riley *et al.*, 1998). Many of the features of *Hand1*-null embryos, such as a failure to undergo turning and the formation of a crooked neural tube, may in this respect be consequences of a defective extra-embryonic blood supply.

A recent study cast some light on the function of Hand1 in the visceral yolk sac vasculature (Morikawa and Cserjesi, 2004). This reported that Hand1 is required for the remodelling and maturation of the visceral yolk sac blood vessels, including the recruitment of smooth muscle cells (SMCs) to the endothelial network. Endothelial cells exist in the *Hand1*-null visceral yolk sac, as indicated by immunofluorescence for platelet endothelial cell adhesion molecule (PECAM). Thus early vasculogenesis, namely the formation and clustering of endothelial cells, is not dependent on Hand1. However, the PECAM-positive endothelial cells of *Hand1*-null visceral yolk sacs were distributed in a honeycomb-like structure. This was characteristic of an immature vascular plexus, similar to the yolk sac phenotype of mice deleted for angiogenic genes such as *Tie1*, *Tie2* and *Vegf* (Sato *et al.*, 1995; Carmeliet *et al.*, 1996). Recruitment of SMCs to the endothelial network was also defective in *Hand1*-null visceral yolk sacs. This was demonstrated by reduced

immunofluorescence for the early SMC marker smooth muscle alpha-actin (SMαA). Loss of smooth muscle support results in vessels that lack the strength to carry blood under pressure, and moreover may underlie the leakage of haematopoietic cells from the visceral yolk sac into the yolk sac-amniotic space. Thus vasculogenesis, the process by which angioblasts differentiate into endothelial cells to form the vascular primordium, occurs in *Hand1*-null visceral yolk sacs. However, Hand1 is required for angiogenesis, namely the maturation of the primitive endothelial plexus to refine into a functional vascular system.

In the same study, several angiogenic genes were shown by RT-PCR analysis to be up-regulated in *Hand1*-null extra-embryonic membranes, implicating Hand1 in their repression. The mis-expression of these genes may account for the observed visceral yolk sac vasculature defects. These genes include the signalling molecules *vascular endothelial growth factor* (*Vegf*), *angiopoetin 1* (*Ang1*) and the *ephrin B ligand Efnb2*. Furthermore, the expression of genes encoding the Vegf receptors Flk1, Flt1 and Nrp1, and that encoding the Ang1 receptor Tie1, are all up-regulated in *Hand1*-null yolk sacs. Additionally, *Notch1/4* expression, also implicated in vasculogenesis, is enhanced in *Hand1*-null yolk sacs. This occurs together with an up-regulation of the Notch-dependent gene *Hey1* (Morikawa and Cserjesi, 2004). This implies a direct role for Hand1 in Notch signaling, which attaches functional significance to our observed interaction of Hand1 with the placenta-expressed Notch regulator Maml2 (P. Riley, unpublished data; Appendix 8).

1.2.5. Human placentation and the role of HAND1 in human extra-embryonic tissues

The process of human placentation is markedly different to that in rodents (reviewed by Georgiades *et al.*, 2002; Malassine *et al.*, 2003). This is perhaps explained by the fact that the placenta is a relatively young organ in evolutionary terms. In humans, proliferation and differentiation of pluripotent, trophectodermal cytotrophoblasts, the equivalent cell population to rodent TS cells, gives rise to three placental layers. These are the syncytial chorionic villi (equivalent to the rodent SynT), cytotrophoblast cell columns (also called anchoring villi; equivalent to the

rodent SpT) and the extravillous cytotrophoblast (EVT; equivalent to the outermost rodent SGC layer). These layers are thought to be in place by the third week of pregnancy (reviewed by Loregger *et al.*, 2003), which is much earlier, relative to the length of gestation, than the time taken for the three-layered murine placenta to form (E10.5).

Reminiscent of the emergence of TG cells from the periphery of the rodent EPC, cytotrophoblast cell columns, bound to the uterine wall, give rise to EVT cells. EVT cells are known to up-regulate MMP9, which facilitates digestion of the uterine matrix (Librach *et al.*, 1991), and have evolved mechanisms, such as the secretion of immuno-suppressors, to evade maternal immune responses (Roth *et al.*, 1996). The EVT cells therefore invade the uterine endometrium to attain contacts with the maternal spiral blood vessels and also serve an endocrine function by secreting hormones such as human chorionic gonadotrophin (hCG) and human placental lactogen (hPL) (reviewed by Loregger *et al.*, 2003). However, unlike the process of rodent TG cell differentiation and invasion, little is known about the mechanisms of EVT formation. Strikingly, human EVT cells do not undergo endoreduplication, but may instead fuse to produce multinucleate cells (al-Lamki *et al.*, 1999). Notably, based on patterns of gene expression, it has been suggested that human EVT cells are more analogous to murine glycogen trophoblast (GlyT) cells (Giorgiades *et al.*, 2002).

Despite the morphological differences between rodent and human placentation, several factors that function in rodent placentation are also expressed in the developing human placenta. For example, the human *MASH2* (*HASH2*), *STRA13* and *I-MFA* genes are expressed, in varying degrees, in both isolated cytotrophoblasts and the EVT invading the maternal decidua (Janatpour *et al.*, 1999; Meinhardt *et al.*, 2005). Moreover, *HASH2* is down-regulated during EVT differentiation, but *STRA13* and *I-MFA* are up-regulated, which is reminiscent of the molecular changes during rodent placentation (Table 1.2). Additionally, a later study by the same authors showed that *ID-2*, expressed at high levels in cytotrophoblast stem cells, is down-regulated during EVT differentiation. Moreover, *ID-2* over-expression inhibits EVT differentiation and trophoblast invasion of a Matrigel matrix substance *in vitro* (Janatpour *et al.*, 2000).

However, most importantly for our study, a role for human HAND1 in placentation has yet to be demonstrated. Neither RT-PCR, RNase protection assays nor RNA *in situ* hybridisation could detect *HAND1* expression in human cytotrophoblasts or the invasive EVT layer (Russell *et al.*, 1997; Knofler *et al.*, 1998; Janatpour *et al.*, 1999; Meinhardt *et al.*, 2005). *HAND1* mRNA and protein are, however, abundantly expressed in the JEG-3 and BeWo human choriocarcinoma cell lines (Knofler *et al.*, 2002). Furthermore, RT-PCR analysis and immuno-histochemical staining of blastocysts has revealed *HAND1* mRNA and protein within the trophectodermal cell layer of the blastocyst (Knofler *et al.*, 2002). These findings suggest that the transcription factor could be required for early trophoblast specification and/ or differentiation (Knofler *et al.*, 2002). Moreover, *HAND1* expression is detectable in the mesodermal components of the human placenta, for example purified amnion cells (*in vitro*) and amniotic epithelium (*in vivo*; Knofler *et al.*, 2002) at different stages of gestation. This suggests that HAND1 may be required for differentiation and/ or function of the early amnion during human placentation.

1.3. The role of Hand1 in the developing heart

Hand1 has been shown to play a crucial role during the formation of the rodent heart. The heart is the first organ to develop and function in the vertebrate embryo proper. The complexity of cardiac morphogenesis is underlined by the fact that congenital heart disease (CHD), the physical manifestation of defects in this process, occurs in 8 of 1000 (~1%) of live births in humans. The importance of normal cardiac morphogenesis is also underlined by the multitude of lethal phenotypes in animal models carrying null mutations in genes critical for cardiovascular development. CHD is also the most prevalent cause of miscarriage (Hoffman, 1995). CHDs tend to affect segments of the heart, rather than the whole organ, reflecting the modular fashion of heart development (reviewed by Fishman and Olson, 1997).

Several genes have been shown to play a role in cardiac morphogenesis in the mouse and have been linked to specific CHDs in humans. Their encoded transcription

factors belong to a wide range of families. These include basic helix-loop-helix (bHLH), homeobox, T-box, zinc finger and MADS domain classes (reviewed by Harvey, 1999; Risebro and Riley, 2006). Hand1 has a crucial role in cardiac morphogenesis, as discussed below, but no mutations in this gene have been identified in human patients to date. Nevertheless, delineating how Hand1 is involved in heart development may provide valuable insight into the underlying molecular and cellular causes of a subset of patients with idiopathic CHD.

1.3.1. Overview of cardiac morphogenesis

1.3.1.1. Formation of the linear heart tube

The following overview will focus on stages of murine cardiac morphogenesis unless otherwise stated. The heart is the first organ to form and function in the vertebrate embryo proper. Heart morphogenesis initiates soon after gastrulation, at around E7.0 in the developing mouse embryo. The process begins with the specification of cardiac precursor cells (CPCs) in the anterior portion of the lateral plate mesoderm, partly in response to molecular signals from the underlying endoderm (reviewed by Chen and Fishman, 2000). This region is termed the pre-cardiac mesoderm, cardiac crescent, cardiac primordia or primary heart field (PHF) (reviewed by Harvey, 1999). PHF CPCs are arranged in two bilaterally-symmetrical populations located in the anterior region of the primitive streak on either side of the embryonic midline. Subsequently, several cardiac transcription factors are induced in these cells. These include the homeobox factor Nkx2.5, the earliest known marker of the cardiomyocyte lineage (Lints *et al.*, 1993).

At E7.5 in the mouse, the paired CPC populations that comprise the PHF migrate medially to the anterior of the embryo and by E8.0 fuse at the ventral embryonic midline to form the so-called linear heart tube. This structure is composed of an inner endocardium and an outer myocardial layer, which are separated by an extracellular matrix called 'cardiac jelly'. This is attached to the body wall by the dorsal mesocardium and begins to pump blood rhythmically through its posterior end by E8.5 in the mouse, 29 hours in the chick and by day 23 in humans (reviewed by

Risebro and Riley, 2006). The formation of the linear heart tube is summarised in Figure 1.9.

Recently, data have emerged that suggest that the heart is actually formed from two distinct CPC populations. In addition to the PHF, a more anterior and dorsal population of CPCs arise in the so-called second lineage, or secondary (anterior) heart field (SHF; Kelly and Buckingham, 2002; Zaffran *et al.*, 2004). This is located in the splanchnic mesoderm and may be specified by the transcription factor Islet1 (Isl1). This population is therefore distinct from the PHF that contributes to the linear heart tube. Between E8.5 and E10.5, namely during cardiac looping, CPCs of the SHF contribute to the arterial pole myocardium of the developing outflow tract (OFT), as well as to the myocardium of the right ventricle (RV). In addition, CPCs of the SHF contribute to the endothelium of the aortic arch arteries (Kelly and Buckingham, 2002; Zaffran *et al.*, 2004).

Lineage tracing analyses of the Islet-1 factor and retrospective clonal analyses were recently used to show that the PHF and the SHF are both derived from an ancestral population of cardiac progenitors, formed at around E6.5 (Meilhac *et al.*, 2004). This has been interpreted that the two heart fields actually represent a single heart-forming region (van den Hoff *et al.*, 2004). Moreover, whilst this study agreed with the model that two separate cardiac lineages contribute to heart formation, it revealed that each contributes slightly differently to the developing heart than the previously-defined PHF and SHF. Namely, the left ventricle (LV) was derived entirely from the PHF and the OFT from the SHF, yet both lineages were shown to contribute to all other regions of the heart (Meilhac *et al.*, 2004).

1.3.1.2. Heart tube looping and the ballooning model

At E8.0-8.5 during mouse development, the linear heart tube undergoes a morphological transition. This is termed rightward (dextral) cardiac looping (reviewed by Harvey, 1999). During this process, which is conserved among all vertebrates, the original anterior-posterior polarity of the linear heart tube is converted into a left-right asymmetry, the first manifestation of this in the developing

embryo. This ensures that the presumptive chambers are aligned with the presumptive great vessels of the heart. During looping, the linear heart tube detaches from the dorsal mesocardium and substantially elongates via the contribution of cells from the SHF (Kelly and Buckingham, 2002; Zaffran *et al.*, 2004). The process of murine heart tube looping is summarised in Figure 1.9.

Cardiac looping may be driven by asymmetric expression of extracellular matrix (ECM) molecules, for example Flectin, that differentially modulate the rate of cardiomyocyte migration (Tsuda *et al.*, 1996; Linask *et al.*, 2002). Otherwise the process may rely on shear forces of blood flow (Hove *et al.*, 2003), and/ or the external forces of surface tension imposed by other embryonic or extra-embryonic structures (Voronov, 2004). Ultimately, the looping process creates a structure with a single ventricle, which has an inflow and an outflow region that connect to a single atrium via the atrioventricular canal (AVC) and the outflow tract respectively. Abnormalities in cardiac looping can cause defective OFT alignment, resulting in the aorta and the pulmonary artery arising from the right ventricle (double outlet right ventricle (DORV); reviewed by Risebro and Riley, 2006).

Early cell fate analyses in the mouse suggested that the linear and early-looping heart tube is patterned molecularly along the anterior-to-posterior (A/P) axis into the presumptive segments of the heart (Yutzey *et al.*, 1995). However, the recent discovery of the SHF has led to the conclusion that the linear heart tube mainly contributes to the LV (Kelly and Buckingham, 2002; Zaffran *et al.*, 2004). Moreover, this early model has been succeeded by the 'ballooning model' of chamber development (Christoffels *et al.*, 2000). This is based on extensive gene expression studies and proposes that chamber formation occurs in two steps. The first step involves the formation of the linear heart tube, composed of 'primary' myocardium. This has molecular polarity along the anterior-to-posterior and dorsal-to-ventral axes. This is followed by the specification of 'secondary' (working, chamber) myocardium at the ventral surface of the heart tube, which has a distinct molecular profile to that of the primary myocardium. As the heart tube loops, cells of the outer curvature of the primitive chambers proliferate and so 'balloon' out from the heart tube to generate the four chambers of the heart. Genes are activated in the outer curvature demarcating the future working myocardium of the atria and ventricles including

Nppa, *Chisel* and *Connexin 40* (*Cx40*). The myocardium of the inner curvature, inflow tract, atrioventricular canal and OFT retains the gene expression profile it exhibited in the linear heart tube and thus remains as primary myocardium (Christoffels *et al.*, 2000).

Notably, the myocardium of the OFT, derived from the SHF, also receives a significant contribution from the cardiac neural crest during cardiac looping. This is also true of the aortic arch arteries and the interventricular septum. The cardiac neural crest population arises from rhombomeres 6-8, and migrates through pharyngeal arches 3, 4 and 6 (reviewed by Kirby and Waldo, 1995; Srivastava *et al.*, 1997; Waldo *et al.*, 1999; Waldo *et al.*, 2005). As such, ablating the cardiac neural crest in chicks causes cardiac defects, particularly affecting the OFT, as well as aortic arch anomalies (Kirby and Waldo, 1995).

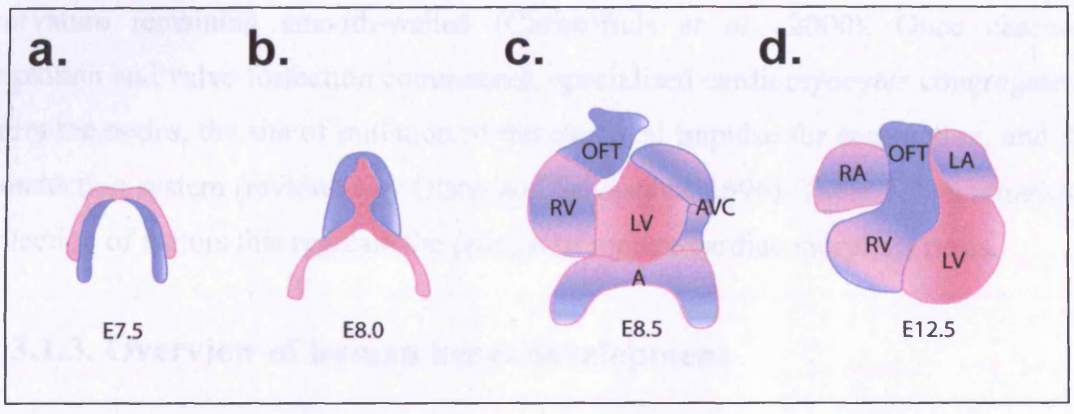

Figure 1.9. Overview of murine cardiac morphogenesis.

Vertebrate cardiac morphogenesis begins when the primary heart field (PHF) progenitors are specified in the lateral plate mesoderm at E7.5, in the so-called cardiac crescent (purple). The second cardiac lineage (blue) is located in the splanchnic mesoderm, in the so-called secondary heart field (SHF) (**a**). The PHF progenitors migrate and fuse at the ventral midline of the embryo, forming the linear heart tube at E8.0 (**b**). Between E8.5-10.5 the linear heart tube undergoes rightward cardiac looping and the SHF progenitors migrate to this structure and contribute to the arterial and venous poles (**c**). All regions of the heart tube are colonised by progenitors from both fields with the exceptions of the LV (derived entirely from PHF) and the OFT (derived entirely from SHF). Following cardiac looping, the heart undergoes maturation and the chambers septate, forming the mature four-chambered organ by E12.5 (**d**; adapted from Risebro and Riley, 2006).

LA: left atrium, **RA**: right atrium, **LV**: left ventricle, **RV**: right ventricle, **OFT**: outflow tract, **A**: atria.

Following murine heart tube looping and the expansion of the chambers, namely beyond E12.5, there is a requirement for heart remodeling and separation of the chambers to ensure uni-directional blood flow. The murine heart assumes its four-chambered structure coincident with the formation of endocardial cushions, the precursors of the cardiac valves and the membranous septae (reviewed by Eisenberg and Markwald, 1995). This occurs at two regions of the heart tube, namely at the position of the atrioventricular canal (AVC) and outflow tract (OFT). In parallel with endocardial cushion formation, the ventricular myocardium grows out from the ventral surface of the heart tube. This results in the formation of finger-like projections of myocardium surrounded by endocardium, called trabeculae. These are thought to provide contractive force to the beating heart during murine embryogenesis (reviewed by Harvey, 1999). Thus the primitive ventricles exhibit dorso-ventral (DV) asymmetry: trabeculae only form at the outer curvature, the inner curvature remaining smooth-walled (Christoffels *et al.*, 2000). Once chamber septation and valve formation commences, specialised cardiomyocytes congregate to form the nodes, the site of initiation of the electrical impulse for contraction, and the conduction system (reviewed by Olson and Srivastava, 1996). Table 1.3 summaries a selection of factors that regulate the process of murine cardiac morphogenesis.

1.3.1.3. Overview of human heart development

Heart development in humans is similar to that described in the mouse, both in terms of morphological changes and the relative time-points during development at which they occur (reviewed by Harvey, 1999). During human embryogenesis, the cardiogenic plate, the equivalent progenitor population to the murine PHF at E7.5, is specified at day 15. This population gives rise to two endocardial tubes on either side of the embryo. These fuse at the midline and form a linear, contractile heart tube by day 21 (equivalent to the E8.0 linear heart tube in mice). Next, the heart tube loops at around day 28 (E8.5-E9.5 in mice), and the atria separate before the ventricles, resulting temporarily in a three-chambered heart, similar to that observed in the frog. By day 50 the four chambers and the OFT have completely septated, and the valves and conduction system have been established. Despite the subtle differences during cardiac morphogenesis between the mouse and human, the transcription factors that regulate this process are largely comparable.

Table 1.3. A selection of factors involved in murine cardiac morphogenesis.

Note that Hand1 is involved in multiple processes during murine cardiac morphogenesis. The factors listed are not exhaustive. Adapted from the review by Risebro and Riley (2006); references therein.

E	Stage of cardiac morphogenesis	Factors
7.0	Specification of the PHF CPCs	Bmp ligands, Fgf ligands, Wnt11, Mesp1
7.5-8.0	Migration and fusion of PHF CPCs at the embryonic midline to form the linear heart tube	Nkx2.5, Gata factors, Mef2, Myocardin, Tbx20, Foxp4
8.0-10.5	Cardiac looping	Hand1, Nodal, Pitx2
8.0-10.5	Specification of the SHF CPCs and their migration to the looping heart tube	Isl1, Mef2c, Tbx1, FoxH1, Bmp ligands, Fgf8, Fgf10
10.5-12.5	Ventricular chamber formation and expansion	
	LV formation and expansion	Hand1, Tbx5, Irx4
	RV formation and expansion	Hand2, Irx4
13.5	Septation	Hand1, Cited2
14.5	Valvulogenesis	Hand1, Smad6, TGFβ, Notch

E: embryonic day, **PHF**: primary heart field, **SHF**: secondary heart field, **LV**: left ventricle, **RV**: right ventricle, **CPC**: cardiac precursor cell.

1.3.2. Hand1 is essential for cardiac morphogenesis

A significant proportion of the murine cardiovascular system is derived from lateral plate mesoderm and cardiac neural crest, and *Hand1* is strongly expressed in both lineages. The Hand proteins of all species play highly-conserved roles in cardiac morphogenesis, with an emphasis on regulating differentiation of CPC into cardiomyocytes rather than the initial specification of CPCs (reviewed by Firulli, 2003).

1.3.2.1. Hand/ Hand1 cardiac expression and role(s) in non-mammalian cardiac morphogenesis

Invertebrates and fish possess only a single *Hand* gene. *C. elegans* has a gene with homology to *Hand1*, *hnd-1*, which is initially broadly expressed in the mesodermal precursors that generate striated muscles, but subsequently becomes restricted to the somatic gonadal precursor (SGP) cells (Mathies *et al.*, 2003). Thus *hnd-1* may have roles in both myogenesis and gonadogenesis. *Ciona intestinalis* is also thought to possess a *Hand* gene, which is expressed in its primitive heart, but its precise roles during development are unknown (Davidson and Levine, 2003).

The oldest definitive version of a *Hand* gene is present in *Drosophila*. *Drosophila Hand*, which is equally divergent from mammalian *Hand1* and *Hand2*, is expressed in both cardioblast and pericardial cells of the developing dorsal vessel, the fly equivalent of the vertebrate heart (Kolsch and Paululat, 2002; Han *et al.*, 2006). This is unusual as all other cardiac-specific transcription factors in *Drosophila* are expressed in only one of these cell types. This suggests that *Drosophila* Hand may be a master regulator of heart-specific genes (Kolsch and Paululat, 2002). However, expression of *Drosophila Hand* is initiated after that of the early regulators Tinman and Bagpipe (Yelon *et al.*, 2000), which implicates *Drosophila* Hand in the subsequent differentiation of dorsal vessel cell types rather than in their initial specification. A more recent study suggested that *Drosophila* Hand is also involved in haematopoiesis, as disruption of *Hand* by homologous recombination results in a deficiency of pericardial and lymph gland haematopoietic cells (Han *et al.*, 2006).

This phenotype is accompanied by profound cardiac defects, including hypoplastic myocardium, a deficiency of pericardial cells and abnormal cardiac morphology.

In zebrafish, which possess a primitive heart composed of a single atrium and a single ventricle, mutation of the single *Hand* gene (*han*) results in the formation of the *hands off* mutant (Angelo *et al.*, 2000; Yelon *et al.*, 2000). In addition to deformations of the pectoral fin, the *hands off* phenotype is characterised by an ablation of the single ventricular chamber. This is caused by impaired CPC specification and an inability to form a linear heart tube. Moreover, there is a marked lack of ventricular *myosin heavy chain* and *tbx5* expression in these mutants, which results in the primitive heart tissue being molecularly of atrial identity (Angelo *et al.*, 2000; Yelon *et al.*, 2000). Thus pre-cardiac, *Nkx2.5*-expressing lateral plate mesoderm is specified to the cardiac lineage but continued differentiation and development is impaired. Notably the primordial *han* gene in zebrafish is most closely-related to higher vertebrate *Hand2*, suggesting that there is no *Hand1* gene in fish and that *Hand2* is the ancestral member of the *Hand* gene family (reviewed by Firulli, 2003).

In *Xenopus*, which possesses a three-chambered heart with two atria and a single ventricle, both *Hand1* and *Hand2* exist. However, there has until recently been some controversy regarding the cardiac expression pattern of *Xenopus Hand1*. Sparrow and colleagues concluded that *Hand1* expression in the primitive heart tube is asymmetric, at least in the lateral plate mesoderm, exhibiting randomness as to its expression on the left or right side (Sparrow *et al.*, 1998). In the myocardium and pericardium, transcripts are also asymmetrically distributed, but in these tissues they are specifically restricted to the left side. Moreover, the authors could not detect *Hand1* expression in the neural crest-derived pharyngeal (branchial) arches. However, a later study showed a uniformly-symmetric expression of *Hand1*, that is, without left-right asymmetry, throughout all tissues of the developing heart (Angelo *et al.*, 2000). Furthermore, these authors were able to detect *Hand1* transcripts in the pharyngeal arches.

A subsequent study employed three-dimensional reconstruction techniques to derive accurate models from digital images of serial histological sections to analyse the morphological changes that accompany heart formation in *Xenopus* in more detail (Mohun *et al.*, 2000). These revealed that *Hand1* expression is dynamic in the *Xenopus* myocardium during cardiac morphogenesis. Specifically, *Hand1* transcripts are initially restricted to the left side of the linear heart tube myocardium but become more symmetrical just before the onset of heart tube looping. After the onset of looping, *Hand1* expression localises to the ventral portion of the myocardium that will develop into the single *Xenopus* ventricle (Mohun *et al.*, 2000). To date, however, functional insight into the *Xenopus* Hand proteins in the developing heart is lacking.

Chick *Hand1* is co-expressed with *Hand2* throughout the heart tube (Srivastava *et al.*, 1995; Srivastava *et al.*, 1997). *Hand1* transcripts in the chick are first detected at HH stage 8 in the cardiac crescent, and in the paired heart primordia as they fuse at HH stage 9. *Hand1* is expressed throughout the cardiac tube and the inflow region at HH stage 10. At HH stage 15, after cardiac looping, *Hand1* is expressed in the atria, the future LV, bulbus cordis, truncus arteriosus and throughout the branchial arches (Srivastava *et al.*, 1995; Srivastava *et al.*, 1997).

Antisense experiments first implied a role for Hand1 in chick heart development (Srivastava *et al.*, 1995). Hamburger and Hamilton (HH) stage 8 chick embryos were treated with antisense oligonucleotides specific to *Hand1* and *Hand2* transcripts, both singly and in combination, to knock-down their expression during development. Applied alone, the antisense oligonucleotides had no effect on cardiac development. However, in combination they arrested cardiac morphogenesis at the cardiac looping stage (stage 11-12). This has led to speculation that the Hand genes may be functionally-redundant, as discussed further in this chapter (section 1.5). Like frog Hand1, however, little is known at present regarding the function of chick Hand1 during cardiac morphogenesis.

1.3.2.2. Hand1 cardiac expression and role(s) in mammalian cardiac morphogenesis

Hand1 expression and function during mammalian cardiac morphogenesis has been chiefly studied in the mouse (Figure 1.10). Cardiac expression of murine *Hand1* is first detected throughout the PHF at E7.0 (Firulli *et al.*, 1998; Riley *et al.*, 1998). Previous studies suggested that, at the onset of heart tube looping, *Hand1* is expressed at the anterior and posterior termini of the linear heart tube (Yutzey *et al.*, 1995; Biben and Harvey, 1997; Srivastava *et al.*, 1999). Early studies also reported symmetrical *Hand1* expression along the left-right axis of the heart tube during looping (Thomas *et al.*, 1998b). However, both conclusions are now considered incorrect.

More detailed analyses have revealed that by E9.5 and after cardiac looping, *Hand1* expression is actually confined to the left side of the linear heart tube myocardium (Biben and Harvey, 1997). Subsequently, after cardiac looping, *Hand1* transcripts are distributed heterogeneously along the dorso-ventral (DV) axis. *Hand1* is expressed strongly in the outer (ventral) curvature of the LV, and weakly in the outer curvature of the RV and the cardiac neural crest cells-derived of the developing OFT (Riley *et al.*, 2000; Figure 1.10a). Hand1 expression is, however, absent from the atria and the inner (dorsal) curvature of all structures. Thus Hand1 is uniquely expressed in derivatives of both the PHF (LV) and the SHF (OFT). During subsequent cardiac morphogenesis, *Hand1* expression remains high in these regions of the developing heart until E10.5, after which it declines. At E11.5 *Hand1* is still expressed in the OFT and by E13.5 expression becomes restricted to the sites of the developing valves (Cserjesi *et al.*, 1995).

The generation of mice lacking *Hand1* identified a role for the transcription factor in the formation of extra-embryonic structures (Firulli *et al.*, 1998; Riley *et al.*, 1998). However, the early embryonic lethality of these embryos originally precluded analysis of Hand1 function in the embryo proper. Thus to prove that the early developmental arrest of *Hand1*-null mutants was caused by abnormal placentation,

and to investigate embryonic roles for Hand1, tetraploid-rescue was performed (Riley *et al.*, 1998). Aggregation chimeras were generated from *Hand1* mutant and tetraploid morulae. This meant that the resulting embryo was derived from diploid *Hand1* mutant cells, whilst the extra-embryonic tissues were derived from wild-type tetraploid cells. Thus, if early lethality was primarily due to extra-embryonic defects, the embryo would be rescued and would develop further, allowing analysis of Hand1 function in the embryo proper.

Tetraploid-rescued *Hand1*-null mouse embryos arrest at around E10.0 and are embryonic lethal by E10.5 (Riley *et al.*, 1998). Specifically, the *Hand1*-null embryo possesses an un-looped, un-segmented heart tube and a malformed OFT and LV (Figure 1.10b). These phenotypes suggest that Hand1 may have a crucial role in the regulation of cardiac looping. This model is supported by the observation that *Hand1* is expressed in the outer curvature of the LV, the leading edge of the looping heart tube (Biben and Harvey, 1997; Sparrow *et al.*, 1998) and by the fact that *Hand1* is down-regulated in *Nkx2.5*-null embryos, which also fail to undergo rightward looping (Biben and Harvey, 1997; Tanaka *et al.*, 1999).

However a putative role for Hand1 in the regulation of cardiac looping cannot account for the fact that cardiac looping is initiated, albeit not completed, in tetraploid-rescued *Hand1*-null mice (Riley *et al.*, 1998). Furthermore it is not wholly compatible with the phenotype of *situs inversus* (*inv/inv*) mice, whose left-right heart asymmetry is reversed due to an atypical leftward looping. In these mice, expression of *Hand1* persists in the LV and that of *Hand2* in the RV, albeit in reversed anatomical locations (Thomas *et al.*, 1998b). This suggests that *Hand1* expression is chamber- rather than side-specific. Moreover it indicates that the *Hand* genes are involved in the development of segments of the heart tube, rather than controlling the direction of cardiac looping. Indeed, *Hand1*-null embryos undergo defective LV morphogenesis, manifesting as a LV with a thin LV wall and a lack of myocardial trabeculation (Riley *et al.*, 1998), whilst *Hand2*-null embryos have a hypoplastic RV (Srivastava *et al.*, 1997). Thus debate has surrounded whether Hand1 is involved in regulating cardiac looping as a primary function that affects ventricular

morphogenesis, or whether the role of Hand1 is restricted to ventricle specification and maturation coincident with looping.

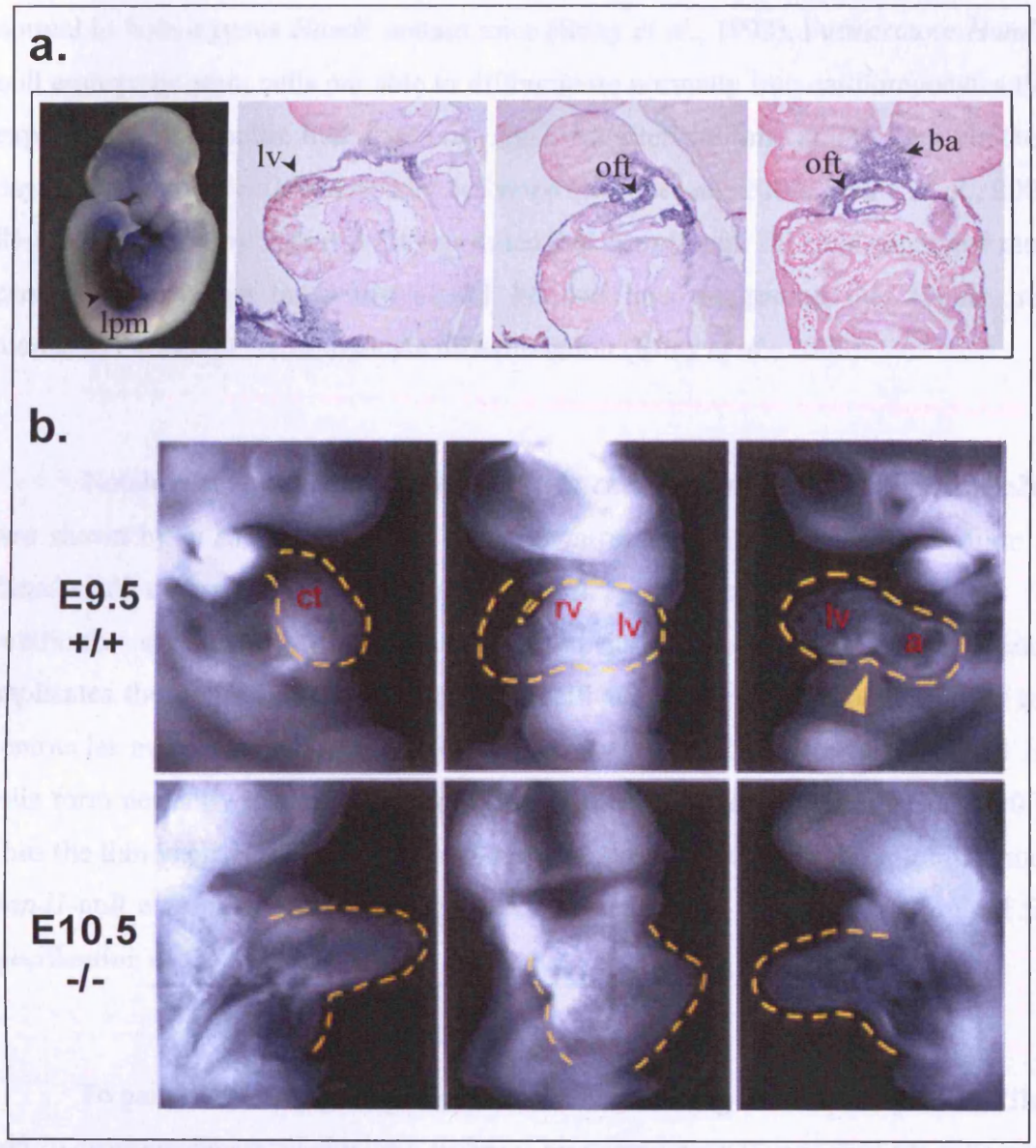

Figure 1.10. Hand1 is expressed in the developing mouse heart and is essential for murine cardiac morphogenesis.

At E9.5, subsequent to cardiac looping, Hand1 expression in the developing mouse heart becomes restricted to the outer curvature of the left ventricle (**lv**) and the outflow tract (**oft**). At this stage, Hand1 is also expressed in the lateral plate mesoderm (**lpm**) and at the midline region of the first branchial (pharyngeal) arch (**ba**) (**a**; Hand1 *in situ* hybridisation of E9.5 wild-type embryo courtesy of C. Risebro). Tetraploid-rescued *Hand1*-null embryos are embryonic lethal at E10.5 due to defects in cardiac looping and left ventricular morphogenesis (**b**; adapted from Riley *et al.*, 1998).

Despite the apparent defects in left ventricular myocardium in *Hand1*-null hearts, cardiomyocyte commitment and differentiation can occur in the absence of Hand1. The expression of cardiomyocyte marker genes, for example *Nkx2.5*, are normal in homozygous *Hand1* mutant mice (Riley *et al.*, 1998). Furthermore *Hand1*-null embryonic stem cells are able to differentiate normally into cardiomyocytes that express cardiac-specific transcripts *in vitro* even after the time point (approximately day 6) at which *Hand1* is normally activated (Riley *et al.*, 2000; Smart *et al.*, 2002; Risebro *et al.*, 2006). However, it was noted that *Hand1*-null ES cells generated more cardiomyocytes than the wild-type R1 ES cell line, suggesting that Hand1 may modulate the rate of cardiomyocyte differentiation (Riley *et al.*, 2000).

Notably, at least one gene, *myosin light chain-2 ventricular isoform* (*Mlc2v*), was shown by *in situ* hybridisation to be down-regulated in the LV myocardium of *Hand1*-null embryos (Riley *et al.*, 1998). *Mlc2v* encodes a protein required for ventricular cardiomyocyte differentiation and its putative regulation by Hand1 implicates the transcription factor in the specification and/ or differentiation of left ventricular myocardium. Despite this, cardiomyocytes derived from *Hand1*-null ES cells form normally and express *Mlc2v*, albeit at reduced levels (Riley *et al.*, 2000). Thus the thin ventricular wall and down-regulation of *Mlc2v* in the tetraploid-rescued *Hand1*-null embryos may be secondary effects and Hand1 may not be required for specification of the LV.

To gain further insight into the role of Hand1 during heart development, Riley and co-workers generated chimeric embryos by aggregating *Hand1*-null ES cells with ROSA26 embryos (Riley *et al.*, 2000). ROSA26 embryos ubiquitously express *lacZ* and so can be visualised by staining for β-galactosidase to assess cell contribution. Low-contribution chimeras, composed of 50% *Hand1*-null ES cells or less, were able to develop normally. However, in E8.0 chimeras derived from >50% *Hand1*-null ES cells, a non-random distribution of cells in the developing heart was observed. Specifically, *Hand1*-null cells were under-represented in the caudal region of the linear heart tube, fated to become the LV. This may occur because *Hand1*-null cells that initially colonised these regions failed to proliferate or underwent apoptosis. By

E9.5, after cardiac looping, mutant cells were under-represented in the outer curvature of the myocardium of the LV and the OFT. Accordingly such embryos at E10.5 were smaller than their littermates and their heart tubes were abnormal, possessing a thin, transparent wall. These chimera studies thus collectively indicate a cell-autonomous requirement for Hand1 in the expansion of the outer curvature of the LV during cardiac looping (Riley *et al.*, 2000). The described studies have implicated Hand1 in LV specification and outer curvature expansion coincident with cardiac looping. More recent functional studies have revealed a role for Hand1 in the formation of the interventricular septum (IVS), the atrioventricular (AV) valves and the outflow tract (OFT).

In a study by Togi and colleagues, the *Hand1* cDNA was targeted to the *Mlc2v* locus to force its constitutive expression in both its native left ventricular myocardium, but also the right ventricular myocardium (Togi *et al.*, 2004). Hand1 over-expression was also detected in the intervening region that forms the interventricular septum (IVS). The outer curvatures of the LV and RV, known as the interventricular boundary region or interventricular groove (IVG), does not expand during the formation of the muscular IVS during normal cardiac morphogenesis. In contrast, over-expression of *Hand1* throughout the ventricular myocardium and in septal cardiomyocytes resulted in hyper-expansion of the outer curvatures of both ventricles. This generated a single, expanded ventricle and was associated with an absence of the IVS, resulting in embryonic lethality between E12.5 and E14.5.

In order to exclude the possibility that the septal defect was a secondary or non-specific effect, the same authors also generated transgenic embryos that over-expressed *Hand1* in the ventricles alone (Togi *et al.*, 2004). This ensured that *Hand1* expression was absent from the boundary region between the ventricles. In these transgenic embryos, the IVS formed normally. These results thus suggested that Hand1 plays an important role in defining the ventricular boundary and that an absence of *Hand1* expression in the IVG may be critical for the proper positioning and formation of the IVS. This is interesting in light of the finding that over-expression of the *Tbx5* transcription factor in both ventricles, which promotes ectopic

Hand1 expression in the RV and IVG, results in failed IVS morphogenesis (Takeuchi *et al.*, 2003).

McFadden and colleagues more recently generated conditional, heart-specific *Hand1*-null (*Hand1* cardiac$^{KO/KO}$) embryos. The authors generated mice harbouring a *Hand1* allele flanked by Cre recombinase loxP recognition sites. They then crossed these with mice harbouring *Cre recombinase* downstream of a cardiac-specific *alpha-myosin heavy chain* (*αMHC*) promoter or *Nkx2.5* enhancer. The embryos thus specifically lacked *Hand1* expression in cardiac tissues. Although viable until birth, these embryos exhibited a spectrum of heart defects. These included left ventricular hypoplasia, abnormally-thickened atrioventricular (AV) valves, and ventricular septal defects (VSDs). Of particular note, these mice had a disorganised but thickened ventricular septum at all stages of development. This supports the findings of Togi and colleagues, who suggested that the absence of Hand1 in the IVG is a pre-requisite for normal growth and/ or positioning of the IVS. Thus whilst over-expression of *Hand1* abolishes septum formation (Togi *et al.*, 2004), cardiac deletion of *Hand1* causes an expansion of the septum (McFadden *et al.*, 2005). These studies also support previous findings that implicate Hand1 in (left) ventricular expansion (Riley *et al.*, 1998; Riley *et al.*, 2000).

The AV valve malformations of conditional, cardiac *Hand1*-null mutant mice are interesting because the *alpha-MHC:Cre* transgene does not direct *Cre* expression in endocardial cushions or their valve derivatives. This suggests that Hand1 may regulate an unidentified myocardium-derived signal that regulates endocardial cushion morphogenesis. However, early myocardial function has been shown to affect endocardial cushion development (Bartman *et al.*, 2004), and therefore abnormal myocardial differentiation in these embryos could have an effect on endocardial cushion development. Previous studies have also shown that regions of the AV endocardial cushions contribute to both the atrial and ventricular septa (Bartram *et al.*, 2001). This in interesting in light of the VSDs in *Hand1*-null hearts, present in 90% of the embryos (McFadden *et al.*, 2005). However, comparison of cell proliferation rates and apoptosis levels between wild-type and mutant endocardial

cushions revealed no significant differences.

OFT defects were observed in some of the conditional *Hand1* knock-out mice at postnatal day 1-2 (McFadden *et al.*, 2005). In this regard, a role for Hand1 in OFT morphogenesis has been implied by the findings of a more recent study (Risebro *et al.*, 2006). Using homologous recombination in ES cells, Risebro and colleagues inserted the *Tet-Off trans-activator* (*tTA*), responsive to the antibiotic tetracycline (Tet), into the *Hand1* locus, under the control of the *Hand1* promoter and regulatory regions. Mice derived from these cells, the *tTA* knock-in strain, were termed 'drivers', and these were crossed with 'responder' mice. In the responder mice, a tetracycline-responsive region was placed upstream of a full-length *Hand1* cDNA and randomly inserted into ES cells to establish mice harbouring a Tet-responsive *Hand1* transgene. Manipulation of *Hand1* expression during gestation with the Tet derivative doxycyline allowed the authors to force over-expression of *Hand1* in its 'native' (Hand1-expressing) tissues during embryogenesis.

In embryos over-expressing *Hand1*, the heart tube was significantly extended and underwent extraneous rightward looping. The ultimate effect of this was that the distal OFT became significantly expanded in length (Risebro *et al.*, 2006). The observed OFT expansion was not due to an enhanced migration of CPCs from the SHF, indicated by the normal expression of the SHF markers *Isl1*, *Mef2c* and *Hand2* in *Hand1*-over-expressing embryos. However, RT-PCR and *in situ* hybridisation data demonstrated down-regulation of several markers of cardiomyocyte differentiation in the OFT. These included *Nppa*, *Wnt11*, *Chisel*, *Nkx2.5* and *Gata4*. This was accompanied by an enhanced rate of cell proliferation, as assessed by enhanced levels of phospho-histone H3. Additionally, markers of cardiomyocyte differentiation were also down-regulated in the left ventricular myocardium of *Hand1* gain-of-function embryos. This was accompanied in many embryos by defective expansion of the developing LV. The authors suggested on the basis of this cardiac phenotype that Hand1 has a cell-autonomous role in promoting CPC proliferation during heart development.

In light of the findings of this study, it is likely that Hand1 promotes SHF CPC proliferation prior to their commitment to differentiate into cardiomyocytes at the site of the developing OFT. Thus in *Hand1*-over-expressing hearts, CPCs are unable to differentiate into cardiomyocytes at the time that Hand1 would normally be down-regulated, resulting in significant CPC hyperplasia in the distal OFT myocardium. The thin-walled LV in *Hand1*-over-expressing embryos may similarly be explained by CPC hyperplasia. Hyper-proliferation of CPCs may prevent the outer curvature of the LV from expanding and ballooning ventrally as secondary myocardium in accordance with the ballooning model to produce the LV chamber (Christoffels et al., 2000). This is supported by the fact that the LV myocardium of *Hand1*-over-expressing hearts is down-regulated for markers of secondary myocardium, for example *Nppa* and *Chisel*, which is suggestive of failed secondary myocardium differentiation (Risebro *et al.*, 2006). These findings agree with the Hand1 loss-of-function studies. They are consistent with the left ventricular hypoplasia and a shortening of the OFT observed in the conditional, heart-specific *Hand1* mutant embryos (McFadden *et al.*, 2005), and may suggest that the hypoplastic OFT and a thin-walled LV of *Hand1*-null tetraploid-rescued embryos are underpinned by deficiencies in CPC proliferation (Riley *et al.*, 1998).

Whilst *Hand1* over-expression in the developing heart promotes CPC proliferation, it is unclear how Hand1 regulates this activity per se. One possibility is via transcriptional modulation of the genes encoding the cell cycle regulators Cyclin D2 and Cdk4, suggested by their up-regulation in the gain-of-function embryos and embryoid bodies, but their down-regulation in *Hand1*-null embryoid bodies (Risebro *et al.*, 2006). Although it is unclear whether Hand1 directly activates the *Cyclin D2* and *Cdk4* genes, adult transgenic mice over-expressing *Cyclin D2* in the myocardium show enhanced cardiomyocyte proliferation (Pasumarthi and Field, 2002) and Cyclin D2 represses cell hypertrophy by enhancing proliferation (Busk *et al.*, 2005).

Further insights into the role of Hand1 during murine cardiac morphogenesis have been made possible by the identification of some of its target genes. An isolated study suggested that Hand1, in combination with Hand2, regulates cardiac expression of the gene encoding the striated muscle-specific metabolic enzyme adenylosuccinate

synthetase 1 (Adss1) (Lewis *et al.*, 1999). Hand1 is also thought to activate the *Nppa* gene, which encodes the Atrial Natriuretic Factor/ Peptide (ANF/ ANP). Cardiac-specific *Hand1*-null mice have a reduced level of *Nppa* transcripts in the LV (McFadden *et al.*, 2005), whilst ectopic expression of *Hand1* in the RV was sufficient to mis-express *Nppa* expression in this region (Togi *et al.*, 2004). Furthermore, Hand1 regulates the expression of *Nppa* in transfection assays *in vitro*, likely through a mechanism reliant on its interaction with other cardiac-specific transcription factors such as Mef2 (Morin *et al.*, 2005).

As described, Hand1 has been implicated in the migration of cardiomyocyte and neural crest populations during cardiac looping and OFT morphogenesis (Riley *et al.*, 2000). Another study employing representational differential analysis (RDA), which compared RNA species from *in vitro*-differentiated wild-type and *Hand1*-null ES cells, appropriately implicated cohorts of Hand1 target genes in cell movement and migration (Smart *et al.*, 2002). In *Hand1*-null EBs, *Thymosin β4* (*Tβ4*), which encodes a protein involved in actin-based cell motility (Smart *et al.*, 2007), was significantly down-regulated. Conversely, *Cystatin C*, which encodes a cysteine protease inhibitor involved in ECM degradation and remodelling (Afonso *et al.*, 1997) was up-regulated. This was also true of *α-cardiac actin*, which encodes a component of the cardiomyocyte cytoskeleton (Arber *et al.*, 1997). Using whole-mount *in situ* hybridisation, all three analysed genes were moreover shown to be temporally- and spatially-co-expressed with *Hand1* in the LV and OFT of wild-type embryos and mis-expressed in *Hand1*-null mutant hearts. Additionally *Wave3*, a member of the WASP family that functions downstream of the Rac GTPase during cell migration, is up-regulated in a *Hand1*-null background (P. Riley, unpublished data). In addition to the genes involved in cell migration, the RDA screen identified various others, including several involved in cell cycle regulation (a selection of these genes is listed in Table 1.4). Nevertheless it remains to be determined whether Hand1 directly or indirectly regulates these genes.

Table 1.4. A selection of putative cardiac target genes of Hand1, up-regulated (a) or down-regulated (b) in a *Hand1*-null background. Adapted from Smart *et al.*, 2002; references therein.

Gene	Function of Encoded Protein
(a) Genes up-regulated in a *Hand1*-null background	
Cystatin C	Cysteine protease inhibitor/ ECM remodelling
Cyclin D2	G1 phase cyclin
Wnt2	Placentation
α-cardiac actin	Component of cardiac sarcomere
HMGP2	Oct2 interactor
(b) Genes down-regulated in a *Hand1*-null background	
Thymosin β4	Regulates actin polymerisation/ cell motility
Fibronectin	Extracellular matrix (ECM) component
Lim kinase 1	Actin assembly
Wave3	Negative regulator of Ras neuroblast proliferation/ cell cycle control
Tif1β	Transcriptional co-repressor

Circumstantial evidence also implicates other genes as Hand1 targets. The expression domain of *Hand1* in the developing mouse heart overlaps with that of the transcriptional co-activator *Cited1* and its expression is down-regulated in the hearts of conditional *Hand1*-null embryos (Dunwoodie *et al.*, 1998; McFadden *et al.*, 2005). Additionally, the myocardial marker *Chisel* is up-regulated upon *Hand1* over-expression in the ventricular myocardium (Togi *et al.*, 2004). This is also true of *Cx40*, whose expression is also reduced in *Hand1* cardiac$^{KO/KO}$ embryos (McFadden *et al.*, 2005). Another putative Hand1 target is *endothelin-1* (*ET-1*) (Morin *et al.*, 2005), which has also been implicated in the regulation of *Hand1* expression (Ivey *et al.*, 2003), suggesting that these factors operate in an auto-regulatory feedback loop. Notably, despite the up-regulation of *Hand2* in a *Hand1*-null background (Morikawa

and Cserjesi, 2004), and its down-regulation upon *Hand1* over-expression in the RV (Togi *et al.*, 2004), it is unlikely that Hand1 and Hand2 regulate each other's activity, consistent with their non-overlapping respective domains of expression (Cserjesi *et al.*, 1995; Srivastava *et al.*, 1995).

1.3.3. Roles of Hand1 in the adult heart

Hand1 expression was previously undetected in the adult mouse heart (Cserjesi *et al.*, 1995; Srivastava *et al.*, 1995). However, more recent studies identified *Hand1* transcripts in adult rodent and human ventricles, but not the atria (Natarajan *et al.*, 2001; Thattaliyath et al., 2002). Moreover experiments in adult rodent hearts showed that following cardiac hypertrophy induced by pharmacological (phenylephrine treatment) and surgical (aortic constriction) manipulation, *Hand1* and *Hand2* expression were down-regulated in the LV and RV respectively (Thattaliyath *et al.*, 2002). This is in agreement with a previous study, which demonstrated a down-regulation of *HAND1*, but not *HAND2*, in the hearts of human patients suffering pathological ischemic or dilated cardiomyopathy (Natarajan *et al.*, 2001).

Supporting these observations, mouse hearts lacking cardiac lineage protein-1 (Clp-1), which exhibit a fetal form of cardiac hypertrophy characterised by a reduced left ventricular chamber with thickened myocardial walls, are down-regulated for *Hand1* (Huang *et al.*, 2004). Furthermore, *Irx4*-null mice, which have reduced *Hand1* expression in the developing LV, are prone to adult-onset, left ventricular hypertrophy (Bruneau *et al.*, 2001). Finally, some evidence implicates the Hand1 interactor Fhl2 in modulating the hypertrophic response in the heart (Kong *et al.*, 2001). Thus Hand1 appears to inhibit cardiac hypertrophy in both the adult human and rodent hearts. As such, the down-regulation of *Hand1* expression in rodent hypertrophy and human cardiomyopathy may allow cardiomyocytes to reinitiate the fetal gene program and thus promote physiological changes that allow the heart to respond to genetic insult or environmental stresses by undergoing hypertrophy.

1.4. The role of Hand1 in other developing tissues

Hand1 is expressed during the development of murine lineages that receive a significant contribution from the neural crest population. Notably Hand1 transcripts are not detectable in the developing or migrating neural crest cells, arguing against a role for the transcription factor in the formation or migration of these cells. However, *Hand1* expression is up-regulated by the time such cells have populated the pharyngeal arches and aortic arch arteries, suggesting a role in neural crest cell differentiation (Firulli *et al.*, 1998; Thomas *et al.*, 1998b).

At E10.5 *Hand1* transcripts and/ or promoter activity are detectable in the precursors of the sympathetic trunk ganglia, whilst by E11.5 expression is up-regulated in lateral mesoderm derivatives, namely the first pharyngeal arch and the developing mid- and hindgut (Cserjesi *et al.*, 1995; Firulli *et al.*, 1998). At mid-gestation *Hand1* is also expressed in the forebrain, the septal region of the tongue bud and the mandible (Cserjesi *et al.*, 1995; Hollenberg *et al.*, 1995). Riley and colleagues confirmed these findings by identifying regions of the embryo, in addition to the left ventricular myocardium, from which *Hand1*-null ES cells are excluded (Riley *et al.*, 2000). This study identified a requirement for Hand1 in the branchial arches and dorsal root ganglia, both of which are in part neural crest-derived, and in several mesoderm-derived structures such as the limb bud and gut.

1.4.1. Hand1 is required for limb morphogenesis

Whilst Hand2 activates *Sonic hedgehog* (*Shh*) as an essential step during the formation of the zone of polarising activity (ZPA) (Charite *et al.*, 2000), little is known about the precise role of Hand1 during limb morphogenesis. Early studies demonstrated low Hand1 levels in the mouse limb buds at E10.5 (Cserjesi *et al.*, 1995). Thattaliyath and colleagues showed later that mis-expression of either Hand1 or Hand2 in the developing limb bud in transgenic mice induces ectopic digits, and that this activity is dependent exclusively on the HLH region (Thattaliyath *et al.*, 2002).

Fernandez-Teran and co-workers more recently demonstrated that *Hand1* expression, initially detectable in the ventral mesoderm of the developing chick limb (Hamilton and Hamburger stages 17-20), becomes restricted to a more antero-ventral population of mesoderm cells and later to the ventral portions of the digits (Fernandez-Teran *et al.*, 2003). Importantly, a re-specification of the anterior mesoderm in the developing chick limb, in response to Shh or retinoic acid application, leads to a down-regulation of *Hand1* expression. Conversely, over-expression of *Hand1* in a low percentage of cases results in duplications of digit 2. The pattern of *Hand1* expression in two chick mutants further supports its association with the anterior identity of the mesoderm (Fernandez-Teran *et al.*, 2003). The limbs of the *talpid-2* (*ta*^{2}) mutant, which have a constitutively-active Shh pathway that results in all the limb mesoderm being posteriorised, do not express detectable levels of Hand1. Conversely, the *oligozeugodactyly* (*ozd*) chick mutant, which lacks limb-specific Shh activity, is accordingly up-regulated for *Hand1*. However, at present, the precise function(s) of Hand1 during limb development are unclear.

1.4.2. Hand1 is involved in gut formation

The expression of *Hand1* in the gut is conserved between organisms, although the specific cells in which it is expressed varies. The *Drosophila Hand* gene is expressed in circular visceral midgut muscle progenitors (Kolsch and Paululat, 2002), whilst in the chick transcripts encoding *Hand1* are observed only within the cells forming the epithelial lining of the small intestine and colon (Wu and Howard, 2002). This is the first description of *Hand* gene expression in an endoderm-derived tissue.

In the mouse, *Hand1* expression is restricted to smooth muscle cells of the embryonic gut and persists in the adult mouse intestine (Cserjesi *et al.*, 1995; Hollenberg *et al.*, 1995). A later study suggested that different lineages of cells in the developing mouse gut express *Hand1* and *Hand2*. Whilst *Hand2* is required for the neuronal differentiation of neural crest cells, *Hand1* expression is limited to mesodermal gut derivatives (D'Autreaux *et al.*, 2007). To date, neither the role of Hand1 during gut morphogenesis, nor in the adult gut, is understood.

1.4.3. Hand1 is required for the formation of the autonomic nervous system

Drosophila Hand is expressed in the developing central nervous system, but its role during this process is largely unknown (Kolsch and Paululat, 2002). In the chick, Hand1 plays a role in the development of the autonomic nervous system. Antisense knock-down of *Hand1* transcripts revealed Hand1 involvement in the differentiation of avian neural crest-derived cells into sympathetic, catecholaminergic neurones in culture (Howard *et al.*, 1999). This may be dependent on an interaction between Hand1 and the neurogenic bHLH factor Mash1 (Bounpheng *et al.*, 2000). The same factors also activate the catecholaminergic differentiation program *in vivo* and in cultured chick neural crest cells (Howard *et al.*, 1999). However, the precise function(s) of Hand1 during the formation of the autonomic nervous system, and whether this role is conserved in mammals, are currently unclear.

1.4.4. Hand1 is required for craniofacial and tooth development

Barbosa and colleagues recently identified a role for Hand1, in co-operation with Hand2, in the regulation of distal midline mesenchyme development (Barbosa *et al.*, 2007). *Hand1* is expressed in the distal (ventral) zone of the branchial arches (arches 1 and 2), an expression domain that partly overlaps with that of *Hand2* and whose derivatives include the inter-dental mesenchyme and the distal symphysis of Meckel's cartilage. The authors generated mice with neural crest-specific deletion of *Hand1*, using *Cre* recombinase controlled by the neural crest cell-specific *Wnt1* promoter, in combination with various *Hand2* mutant alleles. Whilst the loss of Hand1 activity in neural crest cells had no phenotypic effect, concurrent *Hand2* deletion led to impaired growth of the distal midline mesenchyme of the first branchial arch. Secondary to the loss of distal midline mesenchyme, both the terminal differentiation of chondrocytes in Meckel's cartilage symphysis and the membranous ossification of the mandible is aberrant, leading to impaired growth of the lower incisors. Interestingly, expression of the genes *Msx2*, *Pax9* and *Prx2* was down-regulated in the distal mesenchyme, implicating the Hand factors in their regulation.

1.5. Functional redundancy of *Hand* genes

Several studies have suggested the existence of functional redundancy between the Hand factors, that is, an ability to compensate for each other. Functional redundancy was first inferred when knock-down of *Hand1* and *Hand2* using antisense oligonucleotides in combination, but not in isolation, was shown to disrupt heart development at the cardiac looping stage in chick embryos (Srivastava *et al.*, 1995). These antisense experiments suggested that the Hand factors play redundant roles in avian cardiac development.

However, uniform overlapping expression of the *Hand* genes applies only to the chick. The distinct and only partially-overlapping expression patterns of *Hand1* and *Hand2* in mice, and the complementary phenotypes of *Hand1*-null and *Hand2*-null mice, suggest that the Hand factors have separate and independent roles in murine ventricular morphogenesis (Firulli *et al.*, 1998; Riley *et al.*, 1998). For example, *Hand1*-null mice are characterised, in part, by defective LV morphogenesis, whilst loss of *Hand2* results in the formation of a hypoplastic RV (Srivastava *et al.*, 1997). Related to this, Hand2 and Nkx2.5 synergistically regulate expression of *Nppa* in the RV, but this is not true of Hand1 and Nkx2.5, despite their ability to physically interact (Thattaliyath *et al.*, 2002b). Other data also support the idea that Hand1 and Hand2 have non-overlapping roles during embryogenesis. For example, whilst *Hand2* is up-regulated in *Hand1*-null yolk sacs, this attempted compensatory mechanism is ultimately insufficient as yolk sac defects persist (Morikawa and Cserjesi, 2004). In agreement with this, the yolk sac vasculature defects in *Hand2*-null mice are distinct from those seen in *Hand1*-null mice (Srivastava *et al.*, 1997; Firulli *et al.*, 1998).

Nevertheless, evidence does exist to support the idea that Hand factors have overlapping functions in mice. The lethality of *Drosophila Hand* mutants can be rescued by the cardiac expression of a single human *HAND* gene (Han *et al.*, 2006). The zebrafish *hands off* cardiac phenotype is caused by the loss of the *han* gene, which bears most similarity to mammalian *Hand2*. The *hands off* fish have cardia bifida, which is a is much more severe than the *Hand2*-null cardiac phenotype in the mouse (Srivastava *et al.*, 1997; Angelo *et al.*, 2000; Yelon *et al.*, 2000). This suggests

that in *Hand2*-null mutant mice, in which *Hand1* and *Hand2* cardiac expression domains partially overlap, Hand1 may somewhat compensate for the loss of *Hand2*. Since zebrafish possess only one *Hand* gene, no such compensation can occur, and the resultant phenotype is more severe (Yelon *et al.*, 2000).

Studies in mouse models have also suggested the existence of functional redundancy between the Hand factors. For example, over-expression of the HLH domain of either *Hand1* or *Hand2* in the developing limb bud induces polydactyly (McFadden et al., 2002). Additionally, a more recent study showed that when *Hand1* cardiac-specific knockout mice, which die of mild cardiac abnormalities at birth, are crossed into a *Hand2*-heterozygous background, the resulting mutants have a more severe embryonic lethal phenotype (McFadden *et al.*, 2005). Such mice are embryonic lethal at E10.5 due to a thin and poorly-trabeculated left ventricular myocardium. Similarly, the removal of one *Hand1* allele significantly exacerbated the *Hand2*-null phenotype, resulting in an earlier embryonic lethality. Furthermore, embryos lacking both *Hand* genes ($Hand1^{KO/KO}$ (cardiac); $Hand2^{KO/KO}$) displayed the most severe cardiac phenotype, an ablation of both ventricles, and were embryonic lethal at E9.0. The authors proposed that the absence of both *Hand* genes results in a loss of CPC specification at an early stage of cardiogenesis, similar in mechanism to that that is thought to underlie the lack of cardiomyocytes and failure of ventricular morphogenesis in the *hands off* zebrafish mutant, deficient for the sole *Hand* gene (Angelo *et al.*, 2000; Yelon et al., 2000). Finally, a recent study showed that distal midline mesenchyme development was only impaired when both *Hand1* and *Hand2* were deleted in the neural crest lineage (Barbosa *et al.*, 2007). Given the *Hand1* domain is completely included in the *Hand2* domain in the branchial arches, this suggests that Hand2 activity compensates for the loss of *Hand1* and that the Hand factors redundantly regulate the same sets of target genes in the pharyngeal arches.

In conclusion, in species with more than one Hand gene, the encoded Hand factors may function in a redundant fashion, but only to a degree. Some of their observed functional overlap may be due to their dimerisation with a common partner that confers a dominant function regardless of the Hand protein to which it is bound. Knock-in studies in which either *Hand* gene is replaced by the other and vice versa are required to confirm Hand factor functional redundancy *in vivo*.

1.6. The rat choriocarcinoma-1 (Rcho-1) cell line

Gain- and loss-of-function studies have provided only limited insight into the specific role(s) of Hand1 during development. A better understanding of the mechanisms of Hand1 function and regulation could nevertheless provide insight into the underlying cellular causes of defective placentation and idiopathic CHD. Indeed, no mutations in the human *Hand1* gene have been identified. This implicates *Hand1* as an excellent candidate for mutations in *cis*-acting sequences or defects in its upstream regulation that could lead to congenital heart or placental failure in humans.

Mechanisms regulating the developmental activity of Hand1 remain elusive and have been difficult to discern both *in vitro* and *in vivo*. In terms of cell culture experiments, there are no faithful models of cardiomyocytes. With respect to the *in vivo* lineages in which *Hand1* is expressed, for example cardiomyocytes and primary TS cells, they are often difficult to maintain and manipulate in culture (S. Tanaka, personal communication). ES cells have previously been employed to investigate aspects of Hand1 regulation and function in *vivo* (Riley *et al.*, 2000; Smart *et al.*, 2002; Risebro *et al.*, 2006). Several studies suggest that the process of ES cell differentiation into EBs faithfully models cardiomyocyte differentiation in the developing heart (Maltsev *et al.*, 1993; Doevendans *et al.*, 2000; Fijnvandraat *et al.*, 2003). However, the percentage of ES cells that give rise to *Hand1*-expressing cardiomyocytes can be very low and this can rule out their use in certain assays (reviewed by Boheler *et al.*, 2002).

For these reasons, we employed a trophoblast cell model, the rat choriocarcinoma-1 (Rcho-1) cell line, to investigate the mechanistic bases of Hand1 post-translational regulation *in vivo*. These cells are easy to culture and faithfully mimic many aspects of primary TS cells *in vitro*, including an ability to undergo trophoblast giant (TG) cell differentiation (Hamlin *et al.*, 1994; Sahgal *et al.*, 2006). Most importantly for our study, *Hand1* appears to be both necessary and sufficient for the process of Rcho-1 TG cell differentiation (Cross *et al.*, 1995; Scott *et al.*, 2000). This made the use of the Rcho-1 trophoblast model highly attractive for interrogating key aspects of Hand1 cellular function.

1.6.1. Overview

Rcho-1 cells were derived from a transplantable rat choriocarcinoma (Rcho), a highly-malignant trophoblast tumour, 25 years ago (Teshima *et al.*, 1983). Asynchronous Rcho-1 stem cells have a large nuclear-to-cytoplasmic ratio and comprise a morphogenetically-heterogeneous population. They consist of either mitotic, rounded cells with circularly-distributed peripheral actin, or slightly-spread, highly-motile interphase cells possessing patches of actin at the periphery (Faria and Soares, 1991; Figure 1.6). After differentiation, Rcho-1 TG cells resemble their *in vivo* counterparts by virtue of a dramatic increase in cytoskeletal complexity and immotility. Rcho-1 stem cells moreover mimic TS cells in that their differentiation into TG cells is dependent on mitotic cell cycle exit and entry into the endocycle (MacAuley *et al.*, 1998).

Importantly, the molecular mechanisms underlying Rcho-1 TG cell differentiation are largely conserved. Rcho-1-derived TG cells faithfully recapitulate the incremental changes in gene expression typical of *bona fide* TG cell differentiation. For example, they up-regulate members of the placental prolactin family related to the pituitary hormone prolactin (PRL) (Hamlin *et al.*, 1994). The changes to the cell cycle machinery that coincide with mitotic cell cycle exit and the onset of endoreduplication in Rcho-1 cells also faithfully copy those that occur in rodent trophoblast *in vivo* (MacAuley *et al.*, 1998). In this regard, numerous analyses have effectively employed Rcho-1 cells as a model system in which to investigate changes in gene expression pattern during TG cell differentiation (Yamamoto *et al.*, 1994; Grummer *et al.*, 1996; Oda *et al.*, 2001; Mehta *et al.*, 2002; Hayashi *et al.*, 2004; Morris-Buus and Boockfor, 2004; Novak *et al.*, 2004; Xu *et al.*, 2005; Hassanein *et al.*, 2007; Minekawa *et al.*, 2007). These are in addition to studies that have successfully used the Rcho-1 cell line as a tool to investigate the role of Hand1 during TG cell differentiation (Cross *et al.*, 1995; Scott *et al.*, 2000; Firulli *et al.*, 2003).

Cultured Rcho-1 stem cells can be induced to undergo TG cell differentiation by numerous methods. These include increasing the plating density, applying ectopic factors such as retinoic acid, the anti-retroviral drug PMEA or diethylstilbestrol

(DES), or simply by replacing mitogen-rich fetal bovine serum (FBS) with horse serum (HS) (Cross *et al.*, 1995; Hatse *et al.*, 1998; Yan *et al.*, 2001; Tremblay *et al.*, 2001). Rcho-1 TG cells can subsequently be separated from Rcho-1 stem cells by virtue of their increased adherence and accompanying insensitivity to trypsin (Parast *et al.*, 2001). The spontaneous differentiation rate of Rcho-1 stem cells is 5.9±0.5% per 24 hours, which represents the percentage of Rcho-1 cells cultured in FBS-supplemented medium that initiate TG cell differentiation over a 24 hour period (Nakayama *et al.*, 1998; Scott *et al.*, 2000). Consistency in cell culture practices is vital, since variations in culture densities and passaging ratios influence cell phenotype (Cross *et al.*, 1995).

Rcho-1 TG cells are specifically a model of SGCs. The ontogeny of expression of members of the PRL gene family during Rcho-1 differentiation resembles that of cells originating from the periphery of the EPC (Hamlin *et al.*, 1994). This is supported by the observation that a monoclonal antibody directed to Rcho-1 stem cells specifically recognises proliferative TG cell precursors at the periphery of the EPC (Verstuyf *et al.*, 1992). Furthermore, recent data has likened Rcho-1 cells to SGCs by virtue of their cytoskeletal organisation and gene expression profile (Parast *et al.*, 2001; Gultice *et al.*, 2006). In light of the recent findings by Simmons and co-workers, it is encouraging also that the only subtype of SGC that expresses *PL-1*, in common with Rcho-1 TG cells, is the so-called 'parietal SGC' (Simmons *et al.*, 2007). This is the cell type that forms the interface with the maternal decidua and which has traditionally been refereed to as the 'SGC'.

1.6.2. Differences between TS cells and Rcho-1 cells

The Rcho-1 cell model is not, however, perfect. These cells do differ from their *in vivo* counterparts due to phenotypic drift in culture. By flow cytometry, Rcho-1 stem cells were shown to possess up to eight times the haploid content, in contrast to diploid TS cells (MacAuley *et al.*, 1998). The underlying reason for this difference is unknown. Furthermore, pulse-chase experiments revealed that the length of an Rcho-1 endocycle is between 40-50 hours (MacAuley *et al.*, 1998), significantly longer than the 14-hour endocycle of TS cells (Nakayama *et al.*, 1998). Moreover

Rcho-1 stem cells are a transformed cell line and unlike cultured TS cells they can grow in an Fgf4-independent, un-regulated manner, without the additional factor(s) provided by conditioned medium (CM) or embryonic fibroblast feeder cells necessary for TS cell maintenance (Tanaka *et al.*, 1998; Hughes *et al.*, 2004). This may, in part, be due to the specific, as-yet unidentified, mutations that occurred during the transformation of TS cells into the choriocarcinoma cells from which Rcho-1 cells were originally derived.

Although generally conserved, certain aspects of the gene expression profile of Rcho-1 TS and TG cells differs to that of their counterparts *in vivo*. For example, Rcho-1 TG cells do not express the TS cell-specific bHLH factor *Mash2* and, unlike TS cells, cannot differentiate into syncytiotrophoblast upon *Gcm1* over-expression (Scott *et al.*, 2000; Hughes *et al.*, 2004). Rcho-1 stem cells express low levels of *Hand1*, whilst TS cells only initiate *Hand1* expression when they are positioned at the outer reaches of the EPC (Cross *et al.*, 1995; Hughes *et al.*, 2004; Gultice *et al.*, 2006). Additionally *Sox15* expression increases during TG cell differentiation *in vivo*, but is not expressed during Rcho-1 differentiation (Yamada *et al.*, 2006). Furthermore, *PL-1* is only transiently expressed in SGCs *in vivo*, and yet its expression persists during Rcho-1 cell differentiation *in vitro* (Nieder and Jennes, 1990; Faria and Soares, 1991; Hamlin *et al.*, 1994). Finally, whilst Rcho-1 cells express increasing levels of Mmp9 through 13 days of culture, *in vivo* trophoblast cells reduce *Mmp9* expression at an earlier time during differentiation (Peters *et al.*, 2000). However, these differences are subtle and do not preclude the use of Rcho-1 cells as a relatively faithful model of *in vivo* TS cells to investigate the mechanisms underlying Hand1 regulation during TG cell differentiation.

1.7. Aims of these PhD studies

A subject of long-standing interest in developmental biology centers on how the differentiation of stem cells is temporally controlled. Several studies have shown that specific transcription factors, including those of the basic helix-loop-helix (bHLH) super-family, play a major role in the commitment of certain stem cell

populations to differentiation. For example, it has been known for nearly a decade that the bHLH factor Hand1 is involved in determining trophoblast stem (TS) cell fate during rodent placentation and has been implicated in regulating cardiomyocyte differentiation during cardiac morphogenesis (Riley *et al.*, 1998; Firulli *et al.*, 1998). However, how Hand1 biological activity is regulated in either lineage remains largely unknown.

Hand1 protein-protein interactions are clearly very important for modulating Hand1 activity (Table 1.1). However, to date, Hand1 has only been shown to functionally interact with other bHLH factors *in vivo*. Given the promiscuous dimerisation properties of Hand1, we hypothesised that the transcription factor may interact with non-bHLH factors, which may play a role in regulating Hand1 function and biological activity. In this regard, we carried out a yeast two-hybrid screen to identify Hand1 interactors and isolated the murine orthologue of the nucleolar factor HICp40.

The following PhD studies examined the functional significance of the Hand1-HICp40 interaction in a model of TS cells and progressed to uncover a novel, potentially more widespread, mechanism of controlling the developmental activity of a transcription factor via its nucleolar sequestration and subsequent release. Later in the thesis we evaluate these findings in terms of the known functions of the nucleolus and of Hand1, and describe ongoing studies and areas of potential future work. A better understanding of Hand1 regulation and function during invasive trophoblast differentiation may provide insight into the underlying molecular and cellular defects resulting in common placental defects such as pre-eclampsia. This is a very common disease that occurs in up to 15-10% of all human pregnancies and is characterised by inadequate invasion of trophoblast into the maternal decidua and deficient remodelling of the uterine spiral arterioles (reviewed by Redman and Sargeant, 2005; Sibai *et al.*, 2005). Additionally, delineating the cellular mechanisms that control Hand1 activity during cardiomyocyte differentiation may suggest how signalling cascades involving the transcription factor become aberrant during a subset of idiopathic congenital heart disease.

Chapter 2

Materials and methods

Described below are the materials and methods used during the course of this work. Reagents, PCR primers, PCR programs, antibodies and *in situ* hybridisation riboprobes employed are listed in Appendices 1-7. The yeast two-hybrid analysis (this chapter, section 2.3), characterisation of the Hand1-HICp40 interaction (section 2.4) and whole-mount RNA *in situ* hybridisation of HICp40 (section 2.5) were carried out by Maria del mar Franco Viseras. The northern blot analysis (section 2.8) was carried out by Catherine Risebro.

2.1. Construction of plasmids

Several constructs used during the course of this study either existed in house or were obtained from outside sources. These included those used for:

- Yeast two-hybrid assay: pGBDU-Hand1 (provided by Stanley Hollenberg).
- *In vitro* transcription assay: pcDNA3-Hand1 and pcDNA3-E12 (existed in-house), pcDNA3-HICp40, pcDNA3-HICp32 and pcDNA3-HICΔC (provided by Sabine Thebault).
- Immunofluorescence: pCEP4.1-B56δ (provided by Anthony Firulli), pEGFP-HICp40 and pEGFP-HICp32 (provided by Sabine Thebault), pGFP-Plk4 (provided by Frank Sicheri) and pEGFP-MyoD (provided by Vivek Mittal).
- Co-immunoprecipitation: pFLAG-Hand1 (existed in-house), pHIS-HICp40 and pHIS-HICp32 (provided by Sabine Thebault) and pFLAG-Plk4 (wild-type) and pFLAG-Plk4 (T170D) (provided by Carol Swallow and James Dennis).
- Various other assays: pHand2-Neo, pFLAG-Hand1 (T107;S109A) and pFLAG-Hand1 (T107;S109D) (provided by Anthony Firulli).

The following constructs were generated for specific use in this project.

- The pHand1-EGFP construct was produced by inserting the full-length *Hand1* cDNA, generated by PCR amplification of the pcDNA3-Hand1 template, including the ATG start codon but minus the stop codon, into the pEGFP-N1 vector downstream and in frame with the *EGFP* cDNA (*Clontech*).
- The pHand1(T107;S109A)-EGFP and pHand1(T107;S109D)-EGFP constructs

were generated in a similar way, but by PCR amplification of the relevant point-mutated, full-length *Hand1* cDNAs from the pFLAG-Hand1(T107;S109A) and pFLAG-Hand1(T107;S109D) templates, and their insertion in-frame with the EGFP cDNA in the pEGFP-N1 vector.

- The pHand1-EGFP fragments (pbHLH$_{Hand1}$-EGFP and pHand1$_{His}$-EGFP; Appendix 4) were generated in a similar way, but by PCR amplification of the relevant stretch of *Hand1* cDNA from the pEGFP-Hand1 template and their insertion in-frame with the EGFP cDNA in the pEGFP-N1 vector.
- The pHand2-EGFP construct was generated in a similar way, but by PCR amplification of the full-length *Hand2* cDNA from the pHand2-Neo vector template and its insertion in-frame with the EGFP cDNA in the pEGFP-N1 vector.
- The pGST-Hand1 construct was generated by PCR amplification of the full-length *Hand1* cDNA from the pFLAG-Hand1 template and its insertion in-frame with the GST cDNA in the pGEX4.1 (*Promega*) vector.
- The pKS$^+$-MICp40 and pcDNA3-MICp40 constructs were generated by PCR amplification of the *MICp32* cDNA using a specific IMAGE clone as a template (#12645-K05). This cDNA, inserted into the pKS$^+$ vector, was then extended by the upstream ligation of a PCR product amplified from a template consisting of a BAC containing mouse genomic sequence (#RP24-350N23). This generated pKS$^+$-MICp40. pcDNA3-MICp40 was produced by simply excising the full-length *MICp40* cDNA from pKS$^+$-MICp40 and inserting it into the pcDNA3 vector.
- The RNAi constructs (*HICshRNAi1*, *HICshRNAi2*, *Plk4shRNAi1* and *Plk4shRNAi2*) were generated by inserting annealed 21bp or 22bp sense and antisense *HICp40* and *Plk4* oligonucleotides downstream of the H1 RNA polymerase III promoter in a modified pcDNA3 vector (Kunath *et al.*, 2003). The oligonucleotide design is predicted to generate a transcript with a hairpin structure containing a 9 base-pair loop. The sequences were designed in accordance with published guidelines (Cui *et al.*, 2004; www.bioit.dbi.udel.edu/rnai/). This involved employing sequences of the form 5'-AA(N$_{17-19}$)TT-3' or 5'-AA(N$_{19-21}$), where N is any nucleotide, starting at least 100 nucleotides downstream from the start codon. This pattern is optimal because siRNAs with 3' overhanging UU

dinucleotides are the most effective. Sequences with GC content below 30% or above 79% were also excluded due to considerations relating to thermo-stability and the formation of secondary structure. Sequences containing AAAA or TTTT were also excluded since they are inappropriate for siRNA generation via RNA polymerase III-mediated promoters due to the tendency of RNA polymerase III transcription to terminate at these sequences. In addition, sequences containing CCCC or GGGG are excluded from consideration as they are known to form a nucleotide quartet and may affect RNAi function. The annealing reaction was carried out in a total volume of 10µl with 1× annealing buffer and was left to proceed at an initial temperature of 95°C that gradually cooled to room temperature.

With the exception of the RNAi constructs, these constructs were generated as follows. *Pfu* DNA polymerase-based PCR was used to amplify the relevant cDNA from 10ng plasmid or 100ng BAC template. Each of the primers used for the PCR contained recognition sites for specific restriction enzymes at their 5' end (see below), such that the generated PCR products could be cut and ligated into the relevant vector, generally within the polylinker region (multi-cloning site (MCS)). Notably, each primer contained a recognition site for a different restriction enzyme, to exclude the possibility of incorrect orientation of the insert in the vector plasmid after ligation. After the PCR, the reaction mix was supplemented with $1/6^{th}$ of its volume of gel loading solution, loaded onto a 1% agarose gel (in 1×TBE) and run through the gel for 90 minutes at 100V. The amplified DNA was visualised by way of an ultra-violet illuminometer and excised from the gel using a scalpel. It was then purified by way of the QIAquick™ Gel Extraction Kit (*Qiagen*) according to the manufacturer's protocol. Each end of the amplified PCR product was subsequently digested using the relevant restriction enzymes (*New England Biosciences*). The digestions were performed separately for each enzyme at 37°C, in a total volume of 10µl for the first digest and then 20µl for the second, with 1× reaction buffer and 10× BSA. Between the two digests, the first enzyme was denatured by heating the mixture to 65°C for ten minutes. Concurrently, 1µg of each vector into which the cDNAs were to be inserted were also cut with the same enzymes. The enzymes used to cut the various DNAs were as follows:

- Wild-type and mutant *Hand1* cDNAs, *Hand1* cDNA fragments and *Hand2* cDNA, were restricted with *Eco*RI (5' end) and *Bam*HI (3' end) for insertion into pEGFP-N1.
- *MICp32* cDNA was restricted with *Dra*II (5' end) and *Bam*HI (3' end) for insertion into pKS^+. A 510bp region of the mouse BAC upstream of the *MICp32* start codon was inserted upstream of *MICp32* using the *Kpn*I (5') and *Dra*II (3') enzymes.
- The annealed 21bp or 22bp oligonucleotides were designed such that their overhangs were complementary to the Asp718 (5' end) and XbaI (3' end) sites downstream of the H1 RNA polymerase III promoter in the modified pcDNA3 vector.

After another round of agarose gel electrophoresis and gel purification to purify restricted insert and linearised vector DNA, DNA ligation was carried out. An appropriate amount of insert and vector, estimated by assessing the relative molar ratios of the two species by agarose gel electrophoresis, were mixed in the presence of 2μl ligase buffer and 1U T4 DNA Ligase (both from *Promega*) in a total volume of 20μl. Generally, insert was incubated at a three-fold molar excess with vector. The reaction was left to proceed overnight at an initial temperature of 30°C that gradually cooled to 4°C. In control ligations, vector and insert were incubated individually and a mix lacking T4 DNA ligase was also included. The following day, 5μl of the ligation mixture was added to 50μl of DH5α subcloning efficiency competent *E. coli* cells (*Invitrogen*), which were subsequently incubated on ice for 20 minutes to promote plasmid uptake. Cells were then incubated at 42°C for one minute ('heat shock'), which induced expression of the antibiotic resistance marker on the transformed construct, and returned to ice for another five minutes. Next, 1ml of antibiotic-free Luria broth (LB) was added to the cells, which were then incubated at 37°C for 60-90 minutes to allow for expression of the gene whose encoded enzyme confers antibiotic resistance. After centrifugation and re-suspension of the cells in a smaller volume of LB, the cells were then plated on LB-agar plates containing the appropriate antibiotic, using a flamed, glass spreader, carried out in such a way as to ensure single colony growth. Plates were then incubated at 37°C overnight to select for transformants.

The following day, colonies were picked from these plates and grown in 2-3ml LB containing the appropriate antibiotic over 8 hours in a shaking incubator at 37°C. 1.5ml of each culture was then centrifuged at 12,000rpm for 2 minutes and the supernatant discarded. Next, 200µl TELT solution A was added to the pellet, which was then vortexed and placed on ice for 20 minutes to lyse the cells. Subsequently, protein was removed from the preparation by extraction in 200µl phenol:chloroform:isoamyl alcohol (24:24:1). The mixture was vortexed before spinning at 12,000rpm for 2 minutes. The upper, aqueous phase was removed and added to 200µl isopropanol, and this mixture was then placed on a rotating platform for one hour at room temperature to precipitate DNA. After centrifugation for 30 minutes at 12,000rpm and removing the supernatant, the remaining DNA pellet was washed with 70% ethanol and re-suspended in TE (pH8.0) supplemented with RNAse A. An aliquot of this DNA (5µl) was then digested with the appropriate enzymes as before, and the size of the respective fragments ascertained by agarose gel electrophoresis in the presence of a HindIII/λ DNA size ladder. In the case of the RNAi constructs, whose oligonucleotide insert was too small to resolve by agarose gel electrophoresis, the presence of the correct insert was determined by colony PCR. This was carried out using one primer specific to the insert and one to the vector backbone and involved transferring a sample of the colony grown in LB to the PCR reaction tube using a 10µl pipette tip. If the DNA was correct, 10ng was re-transformed into competent cells, and the *Qiagen* Maxiprep Kit™ was used to generate sizeable quantities of the DNA from a larger bacterial culture according to the manufacturer's instructions. After suspending the DNA in TE (pH8.0), its concentration was assessed using a spectrophotometer set at OD_{260}.

2.2. Cell culture

Rcho-1 cells were a kind gift from Michael Soares, trophoblast stem cells were obtained from Satoshi Tanaka, P19-CL6 embryonic carcinoma (EC) cells were generously provided by John Pizzey and the transgenic embryonic stem (ES) cell line was a kind gift from Sean Wu. The H9c2 and NIH-3T3 cell lines existed in house and their ATCC catalogue numbers are CRL-1446 and CRL-1658 respectively.

Cells were cultured in $75cm^3$ flasks containing 15ml of relevant medium in a humidity-controlled chamber at 37°C and 5% CO_2. Cells were passaged by washing with 10ml of sterile PBS, applying 1ml of pre-warmed 0.05% trypsin/ 0.02% EDTA for 5 minutes at 37°C until the cells were lifted off the plate, spinning down the cells at 7,000rpm for 10 minutes and plating down 10-30% of the flask contents in fresh 15ml of appropriate medium. This was carried out at each 48 hour period, which was particularly necessary in the case of NIH-3T3, P19, P19-CL6 and Rcho-1 cells, which divide particularly rapidly and can reach confluence in a short period of time.

Certain cell lines and assays required specific culturing conditions. Prior to seeding ES cells, plates were coated with 0.1% gelatin to ensure proper cell adhesion. To culture trophoblast stem (TS) cells, a 'feeder' layer of primary mouse embryonic fibroblast (MEF) cells, pre-treated with the antibiotic mitomycin-C, were first grown to 70% confluence. At this point, TS cells were plated on top and the conditions changed to TS cell-specific medium. Synchronising cells at the G2/M phase checkpoint was achieved by application of 400ng/ml nocodazole, a drug that promotes Tubulin depolymerisation and which therefore blocks mitosis. Culturing cells in hypoxic conditions was carried out by one of two methods. The first method involved culturing cells in a humidified, normoxic (ambient air, supplemented with 5% carbon dioxide/ 21% oxygen) chamber at 37°C in medium supplemented with 250μM cobalt chloride, which has previously been shown, in cell types including Rcho-1 cells, to initiate intracellular signalling cascades triggered ordinarily by low oxygen (Hayashi *et al.*, 2004). Otherwise, cells were incubated in a humidified, hypoxic chamber (*Coy Laboratory Products*), maintained at 1% oxygen/ 5% carbon dioxide/ 94% nitrogen at 37°C. In order to decrease cellular exposure to oxygen, reagents used in hypoxic experiments were pre-equilibrated in the chamber for a minimum of 30 minutes prior to use. In both cases, an appropriate cellular response to hypoxic conditions was assessed by western blot analysis to assess an up-regulation of the hypoxic inducible factor-1 alpha (HIF1α) subunit.

Several cell lines were induced to undergo differentiation *in vitro* by modifying culture conditions. To induce Rcho-1 trophoblast giant (TG) cell differentiation, freshly-passaged Rcho-1 stem cells were washed with 10ml PBS and

then treated with 15ml differentiation-inducing medium. The medium was completely replaced at 48 hour intervals throughout the differentiation process. By 48-72 hours after the initiation of differentiation, trophoblast giant cells were observed in the cultures. Of note, a relatively homogeneous population of Rcho-1 stem cells could be obtained, in common with previous studies (Cross *et al.*, 1995; MacAuley *et al.*, 1998), by trypsinising freshly-plated Rcho-1 cells, by virtue of the fact that TG cells are trypsin-resistant. To induce P19-CL6 embryonic carcinoma (EC) cell differentiation into cardiomyocytes, cells were grown to confluence and re-suspended in bacteriological-grade dishes in medium supplemented with 0.8% DMSO. After two days of incubation, medium was replenished with fresh DMSO-containing medium, and after 4 days in suspension aggregates were plated in medium lacking DMSO. By 5-6 days after the initiation of aggregate formation, rhythmically-contracting cardiomyocytes were observed in the cultures. To induce transgenic embryonic stem (ES) cell differentiation into cardiomyocytes, cells were trypsinised at approximately 80% confluency and were re-suspended in ES medium minus ESGRO. Cells were transferred to 10cm non-gelatin coated bacteriological dishes at low density. Cells were maintained in floating culture for 14 days and their medium partially replaced daily, with care taken not to remove the embryoid bodies (EBs). By 10-14 days after the initiation of differentiation, rhythmically-contracting, fluorescent cardiomyocytes (within the EBs) were observed in the cultures.

Although most cell types used in this study could be transfected at a high efficiency with Effectene^{TM} (*Qiagen*), we found that the transfection efficiency of Rcho-1 and trophoblast stem cells transfected with Lipofectamine^{TM} 2000 (*Invitrogen*) was significantly higher. Transfection with Effectene^{TM} was carried out as per the manufacturer's instructions. Briefly, cells were plated 16 hours before transfection into 6-well plates such that they had reached approximately 70% confluency by the time of transfection. 100µl DNA condensation buffer (EC buffer) and 8µl Enhancer were added to 1-1.5µg total plasmid DNA, and mixed by vortexing for 1 second. The total amount of transfected DNA per well was kept constant by adding an appropriate amount of empty expression vector or pcDNA3. The DNA-Enhancer mix was incubated at room temperature for 5 minutes to allow condensation of the DNA. 15µl Effectene^{TM} was then added to this mix and vortexed

for 10 seconds. The samples were then incubated at room temperature to allow Effectene™-DNA complex formation. During this incubation time, cells were washed with sterile PBS and 1.2ml fresh medium was added to each well. 800µl fresh medium was then added to the transfection complexes, mixed by pipetting up and down, and added drop-wise to the cells. Swirling the dish gently attained uniform distribution of the complexes. The cells were then incubated for 48 hours in normal culture conditions, although the medium was changed completely 24 hours post-transfection. Transfection with Lipofectamine 2000™ was carried out again as per the manufacturer's instructions. Briefly, cells were plated 16 hours before transfection into 6-well plates such that they had reached approximately 80% confluency by the time of transfection. In two separate tubes, 2-2.5µg total plasmid DNA was added to 100µl serum- and antibiotic-free medium, and 5µl of Lipofectamine™ 2000 was added to another 100µl of such medium. The two mixtures were mixed thoroughly by pipetting up and down, and were subsequently incubated at room temperature for 30 minutes to allow for complex formation. During this time, cells were washed with sterile PBS and 1.8ml fresh, serum- and antibiotic-free medium was added to each well. The mixture (about 200µl) was then added to each well in a drop-wise fashion, and the plates were then swirled to attain a uniform distribution of complex. Cells were then incubated at 37°C for 5-8 hours in normal culture conditions. After this time, cells were washed with PBS and treated with normal, serum- and antibiotic-added medium and incubated for 48 hours in normal culture conditions.

For the generation of *Hand1-dsRed* knock-in ES cells, transgenic ES cells (generously provided by Sean Wu) were co-transfected with the Hand1-dsRed construct and a pTK-Neo selection plasmid (*Clontech*) using Effectene™ (*Qiagen*). Initially, a killing curve was determined with concentrations of neomycin (G418; from 50-200µg/ml), applied 48 hours post-transfection, to determine the optimum concentration of antibiotic. After 14 days' culture at the optimum concentration of neomycin, resistant clones were picked into 96-well plates and the cultures expanded in media containing a maintenance concentration of neomycin (50µg/ml). Once the stable clones had expanded sufficiently, samples were taken for DNA extraction and aliquots were frozen down. For genomic DNA extraction from selected cells, cells

were lysed, using 0.5% SDS and 0.25μg/μl proteinase K, at 55°C for three hours. The DNA was extracted in one volume of 1:1 phenol:chloroform on a nutator, for a minimum of 30 minutes. The extraction mix was centrifuged at 12,000rpm for 10 minutes at 4°C and the upper, aqueous phase then transferred to a fresh Eppendorf. The DNA was then precipitated with 0.6 volumes of isopropanol, on a nutator, for a minimum of 30 minutes. The mixture was then spun down at 12,000rpm for 10 minutes at 4°C and the remaining pellet washed in 70% ethanol and re-suspended in 50μl of TE (pH8.0). This DNA was then used as a template in a PCR reaction with relevant primers to genotype for stable *Hand1-dsRed* expression.

For RNA and protein extraction, cells were harvested in all cases by washing twice with 10ml ice-cold PBS, scraping with an elongated rubber spatula and spinning down the resultant mixture in 10ml ice-cold PBS at 7,000rpm for 10 minutes. Supernatant PBS was then removed using an aspirator. Cell pellets were then lysed by one of the following methods.

- To lyse cells for the luciferase and β-Gal assays, the cell pellet was re-suspended in 450μl 1× reporter lysis buffer (RLB; *Promega*) and vortexed for 10 seconds. The resultant mixture was then frozen and thawed rapidly twice between -70°C and 37°C to ensure complete cell lysis. Cell debris was then removed by centrifugation at 12,000rpm for 2 minutes at 4°C and the supernatant was transferred to a fresh Eppendorf.
- To lyse cells for mRNA extraction, the cell pellet was re-suspended in 1ml Micro-FastTrack^{TM} 2.0 lysis buffer (*Invitrogen*) and was incubated at 45°C for 20 minutes to allow the complete digestion of proteins and ribonucleases. The lysate was then passed through a 21-gauge needle 4 times to shear any remaining DNA. Finally, the NaCl concentration of the samples was adjusted to a final concentration of 0.5M to attain optimum salt concentration for mRNA purification.
- To lyse cells for western blotting and anti-FLAG co-immunoprecipitation, the cell pellet was treated with 800μl FLAG IP kit lysis buffer, to which 8μl of a protease inhibitor cocktail had been added. The mixture was vortexed and incubated at 4°C on a spinning wheel for 30 minutes, before being centrifuged to remove cell

debris for 10 minutes at 12,000rpm. The supernatant was then transferred to a fresh tube.

- A previously-described method was used to generate whole-cell lysates subtracted for the nucleolar fraction (Kurki *et al.*, 2004). Briefly, the cell pellet was treated with 100µl so-called 'NP-40 lysis buffer', the constituents of which are listed in Appendix 1, and was vortexed vigorously for 30 seconds before being incubated on ice for 20 minutes. After centrifugation for 10 minutes at 12,000rpm the supernatant was removed, and this represents the whole-cell lysate subtracted for the nucleolar fraction.
- To lyse cells for co-immunoprecipitation, the cell pellet was treated with 0.5ml ice-cold RIPA buffer, to which 10µl of a protease inhibitor cocktail had been added. The mixture was vortexed and incubated at 4°C on a spinning wheel for 30 minutes, before being centrifuged to remove cell debris for 10 minutes at 12,000rpm. The supernatant was then removed.

Cells to be immunostained were seeded onto glass cover slips (13mm diameter), which had been incubated for 5 minutes in 0.1% gelatin, and which were themselves placed into wells of a 6-well plate. After cells had adhered and/ or been transfected, they were washed twice with 2ml PBS. Cells were fixed with either 4% paraformaldehyde in PBS (if they were to be probed with anti-C23) or ice-cold 100% methanol (used in all other cases) and incubated for 10 minutes at room temperature. Cells were then washed twice with PBS and then permeabilised with 0.5% Triton X-100 in PBS and incubated for a further 5 minutes. Cells were then washed once more with PBS, and then blocked with 1% Bovine Serum Albumin (BSA) in PBS for 2 hours at 4°C. Next, cover slips were removed from the plates, attached to glass slides using DPX cover mount and encircled with a ring of wax using an *Immedge* Pen. The slides were housed in a dark (aluminum foil-covered), humidity-controlled chamber. Cells were then washed twice with 1% BSA in PBS by applying drop-wise and aspirating the liquid. The relevant primary antibody, diluted in 1% BSA-PBS, was then added drop-wise to the cells, which were then incubated overnight. A secondary antibody-only coverslip was included as a control and was left overnight in 1% BSA-PBS alone.

The following morning, after washing cells three times for 5 minutes with PBS, the relevant fluorescin isothiocyanate (FITC)- or tetramethyl rhodamine isocyanate (TRITC)-labelled secondary antibody, diluted in 1% BSA-PBS, was applied to cells and incubated for 1 hour. Cells were then washed with PBS twice, and 5μg/ml of the DNA stain bis-benzamide (Hoechst 33342) was applied in PBS for 10 minutes at room temperature. Cells were again washed twice with PBS, and were mounted with cover-slips secured in 50% glycerol-PBS.

Fluorescent images were obtained, and cell counts conducted, using a *Zeiss Axio Imager M1* fluorescent microscope with 10×, 20× and 40× *Zeiss Plan-Neofluar* objectives and FITC, TRITC and DAPI filters. Images were captured with a *Zeiss Axiocam* CCD-videocamera followed by image processing and multiplayer analysis using *AxioVision*™ 3.0. Time-lapse movies were recorded using a *Zeiss Axiovert 135* fluorescent microscope with the program *Openlab*™ *4.0.*

For long-term storage, cells were frozen to -70°C in medium containing 45% DMEM, MEMα or NCTC-135 (as appropriate), 45% serum and 10% DMSO. This was carried out in an isopropanol bath (*Coy Laboratory Products*; isopropanol added fresh) to ensure gradual cooling. After 72 hours cells were transferred to liquid nitrogen.

2.3. Yeast two hybrid assay

The Y2H screen was carried out as described previously using a mouse E9.5/10.5 library (Hollenberg *et al.*, 1995). Bait (Hand1) was cloned into the DNA-binding domain vector (pGBDU-C3), which was expressed as a fusion protein to amino acids 1-147 of the yeast Gal4 protein. The cDNA library was cloned into the activation domain vector, which was expressed as a fusion protein to amino acids 768-881 of Gal4. pGBDU-C3 contains the URA-3 (Uracil) selectable marker.

One litre of the yeast strain PJ69-4A* was transformed with 500μg of a mixture of the mouse embryo library and 10mg of salmon sperm carrier DNA by the lithium acetate method with 10% DMSO. Briefly, this involved preparing a carrier

mix of sheared salmon sperm carrier DNA (10mg/ml) by boiling 5µl of carrier mix for 5 minutes, followed by rapid chilling on ice. 100ng of DNA was then added to the carrier mix. 100µl of competent yeast cells was also added, together with 300µl of 1×lithium acetate/ 1×TE/ 40% PEG, and the cell/ DNA mixture incubated at 30°C for 30 minutes. 70µl of DMSO was added to the cell/ DNA mixture, and this was followed by a heat shock at 42°C for 15 minutes. Cells were harvested (10,000rpm, 10 seconds at room temperature), re-suspended in 500µl of dH_20 and plated onto minimal media plates with the appropriate selection (histidine-deficiency) and incubated at 30°C for 2-3 days. Histidine-synthesising clones were lysed in liquid nitrogen and assayed for β-Gal activity on filters. Library DNA from colonies which were positive with pGBDU-Hand1 was sequenced, and the sequences were tested against the National Centre for Biotechnology Information (NCBI) database using the BLAST search program.

* The genotype of the yeast strain PJ69-4A is gal4, gal80, his3-200, trp1-901, ura3-52, leu2-3, 112, + GAL2→ADE2, LYS2::GAL1→HIS3, met2::GAL7→LacZ.

2.4. *In vitro*-translation and GST-pull down assay

The pGEX4.1-Hand1, pcDNA3-HICp40, pcDNA3-HICp32 and pcDNA3-HICΔC plasmids were processed for *in vitro* transcription and translation using a TNT™ kit (*Promega*), as per the manufacturer's instructions. Briefly, 1µg of supercoiled DNA was combined with 25µl TNT rabbit reticulocyte lysate, 2µl reaction buffer and 1µl amino acid mixture (minus methionine). 3µl ^{35}S-methionine (*Amersham Pharmacia*), 1U of RNAsin (RNAse inhibitor) and 1U of RNA polymerase (T7) was added and the volume made up to 50µl with dH_20. The reaction was incubated for 60-120 minutes at 30°C.

For the GST pull-down assay, 2µg GST-Hand1 was captured on glutathione-Sepharose beads and 0.5µg radio-labelled HICp40, HICp32 and HICΔC were then added. Binding was performed in 150ml binding buffer overnight on a rotating wheel at 4°C. The next morning, the beads were washed four times with binding buffer. The

beads were eluted in 20µl of 2× Laemmli buffer (+5% beta-mercaptoethanol) and boiled for ten minutes. Protein interactions were then analysed by SDS-PAGE, followed by western blot, with 5% of the input crude extract being used for the determination of protein expression levels (see section 2.9).

2.5. Whole-mount *in situ* hybridisation

The whole-mount *in situ* protocol was carried out in RNAse-free conditions. Thus, prior to use, all equipment was rinsed once with *RNAseZap* (*Ambion*) and twice with dH_20 to remove RNAse activity. Embryos were extracted and fixed in 4% paraformaldehyde (in PBS) overnight at room temperature, then transferred to 100% methanol. Embryos were then re-hydrated through 75%, 50% and 25% methanol in PBS for five minutes each, and then washed twice in PBS for 10 minutes each. The embryos were then digested with 10µg/ml proteinase-K in PBS for 15 minutes at room temperature, rinsed once in PBS and post-fixed for 30 minutes in 4% formaldehyde in PBS and 0.1% gluteraledhyde. Following post-fixing, the embryos were washed twice in PBS, for five minutes, and then pre-hybridised in hybridisation solution overnight at 68°C in a humidity-controlled chamber.

The riboprobe was denatured at 95°C for three minutes and cooled immediately on ice. The following day, the riboprobe was applied to the embryos at an approximate concentration of 400ng/ml in fresh hybridisation solution, and this was left to incubate overnight at 68°C. After hybridisation with the riboprobe, the embryos were rinsed twice for five minutes, and washed three times for 30 minutes in hybridisation solution at 68°C. Next, the embryos were washed three times for 30 minutes in TBST at room temperature on a nutator. The embryos were subsequently blocked in TBST with 10% sheep serum and 1% BSA for a minimum of three hours at room temperature on a nutator.

The antisense RNA probe was labeled with digoxigenin (*Roche*), and this was then incubated with the samples at a concentration of 1:2000 on a nutator at 4°C overnight. Following this, the embryos were washed at room temperature on a nutator three times for one hour in TBST and washed twice for 10 minutes in PBS. After

washing, the embryos were developed in Nitro Blue Tetrazolium and 5-bromo-4-chloro-3-indolyl-phosphate (NBT/BCIP) solution (one tablet in 10ml dH_20; *Amersham Pharmacia*) in the dark (aluminum foil-covered) at room temperature on a nutator. Once the signal strength was sufficient, the embryos were washed in PBS with 0.1% Triton X-100 to stop the reaction and were fixed overnight at room temperature in 4% paraformaldehyde in PBS. To reduce background, embryos were cleared in 100% methanol for 10 minutes on a nutator and re-hydrated through a methanol-PBS gradient. Embryos were then imaged using a *Nikon* SMZ-U microscope, and photographed using a *FujiFilm* FinePix S2 Pro digital camera and Hyper-Utility Software HS-S2.

2.6. Luciferase assay

100µl of luciferase assay buffer (*Promega*) was added to 20µl of cell lysate (transfected with appropriate vector(s) and the *pCMV-βgal* plasmid 48 hours before) in a *Turner Designs* TD-20/20 illuminometer. Luminescence was measured at room temperature for 10 seconds. A concurrent β-Gal assay was performed by adding 50µl 1× Reporter Lysis Buffer (*Promega*) and 150µl 2×β-Gal assay buffer to 100µl cell lysate. The mixture was vortexed and incubated at 37°C until the reaction turned yellow (indicating the presence of O-nitrophenyl, which was usually between 30 minutes and 2 hours). To stop the reaction, 300µl of 1M Na_2CO_3 was added and the samples vortexed. The A_{420} was measured for each sample and was in the linear range between 0.2 and 0.8.

2.7. RNA extraction and RT-PCR analysis

Cells were lysed as described earlier, and mRNA was extracted using *Invitrogen*'s Micro FastTrack^{TM} 2.0 kit, as per the manufacturer's instructions. Briefly, the cell lysate was added to an oligo(dT) cellulose column and placed on a nutator at room temperature for an hour. The oligo(dT) cellulose was then pelleted by centrifugation at 6000rpm for 2 minutes and then washed 3 times in Binding Buffer. Next, the oligo(dT) cellulose was re-suspended in Binding Buffer and transferred to a

spin column. The spin column was subsequently washed 3 times with Binding Buffer, and a further 2 times with Low Salt Wash Buffer. The mRNA was eluted from the spin column with Elution Buffer. 20µl glycogen carrier, 70mM (pH5.2) sodium acetate and 100% ethanol were then added to this solution, and the mixture was frozen on dry ice to precipitate the mRNA as a pellet. The mRNA pellet was then re-suspended in 10µl of Elution Buffer, assessed for concentration using a nanodrop spectrophotometer, and stored at -70°C.

Prior to the RT-PCR reaction, 100ng purified RNA was incubated with 1× RQ1 RNase-free DNase (*Promega*) in 1× RQ1 RNase-free DNase reaction buffer in dH_20 at a final volume of 10µl for 30 minutes at 37°C. After this time, 1µl of RQ1 DNase Stop Solution was added to the mixture to terminate the reaction, and this total mixture was then incubated at 65°C for 10 minutes to inactivate DNase activity. The mixture (11µl) was then split into two tubes of 5.5µl each, which each contained 1mM dNTP mix in dH_20, 300ng random primers and were made up to 10µl with dH_2O. These mixtures were then incubated at 65°C for five minutes.

The reverse transcription reaction was then carried out. Each tube was treated with a mixture containing 1× first strand buffer (*Invitrogen*), 5mM $MgCl_2$, 0.01M DTT and 40 units RNAsin (*Promega*), but only one set were also treated with 50 units of Superscript II RT (*Invitrogen*). This meant that one set of tubes acted as a control for genomic DNA contamination. Both sets of tubes were then subject to a pre-programmed RT-PCR reaction to produce first-strand cDNA (using a *PE Applied Biosystems* GeneAmp® PCR System 9700 PCR machine). PCR was then performed using the first-strand cDNA as a template and *Taq* polymerase-containing Ready-To-Go™ beads (*Amersham Biosciences*). The PCR mix was then supplemented with $1/6^{th}$ of its volume of gel loading solution, loaded onto a 1% agarose gel (in 1× TBE) and run for an hour at 100V. DNA was then visualised by way of an ultra-violet illuminometer and photographed.

2.8. Northern blot analysis

Northern blot analysis was carried out in RNAse-free conditions. Thus, prior to use, all glassware and electrophoresis equipment was rinsed once with *RNAseZap* (*Ambion*) and twice with dH_20 to remove RNAse activity. Northern blots were carried out using the *NorthernMax*^{TM} formaldehyde-based system (*Ambion*). Briefly, 2μg of sample RNA, extracted from cells as described earlier, was mixed with 3 volumes of formaldehyde/ ethidium bromide (provided in the kit) to a final concentration of 10μg/ml. The samples were denatured for 15 minutes at 65°C in a dry heat block, pulsed, and loaded into a 1% agarose, 1× denaturing gel buffer (RNase-free) gel (included with the kit). The gel was run in 1× MOPS gel running buffer at 5V/cm (distance between the two electrodes) until the bromophenol dye front reached the bottom of the gel. The mRNA on the gel was then visualised by way of UV light, photographed and transferred to a positively-charged nylon membrane (Hybond^{TM}-N^+; *Amersham*) by the downward-capillary method for 2 hours in MOPS gel transfer buffer (included with the kit). Following transfer, the membrane was rinsed in 1×MOPS gel running buffer and the mRNA was cross-linked by baking at 80°C for 20 minutes. Next, the membrane was pre-hybridised at 42°C for 1 hour in ULTRAhyb^{TM} (*Ambion*) in a bottle rotator hybridisation oven. The RNA probe was radio-labeled by the random primer labeling method and was then denatured and added immediately to the pre-hybridised blot. Hybridisation was carried out overnight at 42°C. The membrane was then washed twice at room temperature with agitation using low-stringency wash solution, followed by two washes at 42°C in the hybridisation oven using high-stringency wash solution. The blot was then wrapped in cling film and exposed to Kodak BioMax autoradiography film for 15 minutes to overnight, depending on the relative signal strength as determined by Geiger counter measurement.

2.9. SDS-PAGE and western blot analysis

Western blotting was performed using the *Bio-Rad Mini-Protean® III* apparatus (*Ambion*). Briefly, lysate samples were mixed with an equal volume of 2× Laemmli buffer (+5% beta-mercaptoethanol) and denatured for 10 minutes at 100°C.

The samples were loaded on an SDS-PAGE gel (approximate dimensions 65×85×1.5mm). Electrophoresis was performed in 1× TGS running buffer at a constant current of 30mA until the dye front reached the bottom of the gel. Importantly, the samples were run in parallel with 10µl of the Rainbow (full-range) protein molecular weight marker (*Amersham*), to indicate the molecular weight of sample proteins. The separated proteins were then transferred to a Hybond^{TM}-C nitrocellulose membrane (*Amersham*) by a 'wet transfer' method using an electroblotter (*Biometra*). Briefly, this involved placing the nitrocellulose membrane on top of the gel and closest to the anode, and inserting a small sheet of Whatman paper and a thin sheet of sponge on either side. A constant current of 200mA was then applied to this entire assembly, which was submerged in 1× TGS transfer buffer, for 2 hours at 4°C. Proteins on the membrane were then visualised by staining in 0.2% Ponceau S. Next, the membrane was then rinsed in 1× TBS and blocked in blocking buffer for 2 hours at room temperature on a nutator, and was then briefly rinsed with TBST. The primary antibody was then diluted in blocking buffer to the required concentration, added to the membrane in a sealed polythene bag and incubated overnight at 4°C on a nutator. The next morning, the membrane was washed 6 times for 10 minutes with wash buffer on a nutator. The secondary antibody, conjugated to horseradish peroxidase (HRP), was subsequently diluted to the required concentration in blocking buffer and incubated with the membrane in a sealed polythene bag on a nutator for 1 hour. The membrane was then washed again 6 times for 10 minutes with wash buffer. A further two, 5-minute washes were then carried out in 1× TBS. Subsequently, the membrane was developed using ECL^{TM} Western blotting detection reagents (*Amersham*). A 1:1 mix of the ECL^{TM} components was freshly made and 0.123ml/cm^2 was added to the membrane for one minute. The blot was then wrapped in cling film and exposed to autoradiography film for 5 seconds to 30 minutes, depending on the signal strength.

2.10. Co-immunoprecipitation

To purify the FLAG-Plk4 proteins for use in the kinase assay, Rcho-1 cells were transfected with either *pFLAG-Plk4* or *pFLAG-Plk4;T170D* (gain-of-function, activating mutant). After 48 hours cells, were lysed using FLAG IP kit lysis buffer as

described, and the resultant lysates were immuno-precipitated using a α-FLAG M2 antibody Kit (*Sigma*) as per the manufacturer's protocol. Briefly, 40μl of the supplied Anti-FLAG M2 affinity gel was washed three times with 0.5ml 1× Wash Buffer and once with 0.5ml 1× Elution Buffer. 1ml of cell lysate was added to this pre-washed Anti-FLAG M2 affinity gel and incubated overnight at 4°C on a rotating wheel. The next morning, the resin, now bound to the FLAG-tagged fusion protein to be purified, was centrifuged for 30 seconds and washed again three times with 0.5ml 1× Wash Buffer. 3× FLAG Elution Buffer was prepared by adding 3μl of the provided 3× FLAG peptide solution to 100μl kinase buffer. This was then added to the washed affinity gel, incubated on a rotating wheel for 30 minutes at 4°C and subsequently centrifuged. The supernatant, containing the eluted FLAG fusion protein, was then transferred to a fresh tube. An equal volume of 2× Laemmli buffer (+5% beta-mercaptoethanol) was then added to the precipitates. Protein interactions were then analysed by SDS-PAGE followed by autoradiography, and 5% percent of the input crude extract was used for determining protein expression levels by western blot analysis (see section 2.9).

To purify Hand1-Plk4 complexes formed *in vivo*, Rcho-1 cells were treated for 1 hour with medium supplemented with 10% horse serum to induce a commitment towards differentiation and then lysed in RIPA buffer as described. The control cell population was untreated, asynchronous Rcho-1 stem cells. 250μl protein sepharose A/G beads (*Amersham Pharmacia*) were pre-blocked by incubation in an equal volume of 1% BSA in PBS on a rotating wheel for one hour at 4°C. After brief centrifugation at 6,000rpm to collect the resin and after washing once with PBS, 3-4μg of α-Plk4 antibody was conjugated to the resin in the same volume of fresh 1% BSA in PBS for 2 hours under the same conditions. After centrifugation to remove the supernatant, cell lysates were added to these antibody-conjugated beads and the mixture was incubated at 4°C on a rotating wheel overnight to allow for immuno-precipitation. The following morning, the beads, to which endogenous Plk4 was now bound, were centrifuged at 6,000rpm for 1 minute and washed five times (between similar centrifugations) with ice-cold PBS. After all traces of supernatant were removed using a fine pipette, an equal volume of 1% BSA in PBS was then added to the beads. An equal volume of 2× Laemmli buffer (+5% beta-mercaptoethanol) was

then added to the precipitates. Protein interactions were then analysed by SDS-PAGE followed by autoradiography, and 5% percent of the input crude extract was used for determining protein expression levels by western blot analysis (see section 2.9).

2.11. *In vitro* phosphorylation (kinase) assay

FLAG-Plk4 (wt) and FLAG-Plk4 (T170D) were *in vivo*-translated in transfected Rcho-1 cells and purified as described (see section 2.10). The eluates were incubated with 30μg of GST-Hand1 or lysates from wild-type Hand1-EGFP or Hand1-EGFP T107;S109A/D-transfected Rcho-1 cells and 2μCi of 30 $CimM^{-1}$ ^{32}P γdATP (*Amersham*) for 30 minutes at 37°C in kinase buffer in a total volume of 30μl. In separate, parallel reactions, 2μg of α-Casein was used as a positive control, as described previously (Swallow *et al.*, 2005), and 30μg GST and 30μg BBS2-GST were used as negative controls. After the reaction, radio-labelled protein was boiled in 2× Laemmli buffer (+5% beta-mercaptoethanol) and then analysed by SDS-PAGE (western blot analysis; see section 2.9). The gel was then washed in TBS and dried on Whatman paper before exposure to Kodak BioMax autoradiography film.

2.12. *Plk4*-null embryo analysis

Genotyping of embryos by nested PCR was carried out on tissue taken from wax-embedded sections. E7.5 *Plk4*-null concepti were fixed with 4% paraformaldehyde (in PBS) for a minimum of 4 hours, but preferably overnight (especially for whole embryos). Thereafter, embryos were either dehydrated and wax-embedded or cryo-embedded.

Wax embedding was carried out by dehydrating the embryos through a graded ethanol series, two hours in each 50%, 70%, 80%, 90% and 96% ethanol/ dH_20, followed by two one-hour incubations in 100% ethanol. The embryos were then cleared in 100% butanol overnight at room temperature. Next, the embryos were transferred to a 1:1 mix of butanol:molten pastillated fibrowax (*BDH*) for 30 minutes at 60°C. The embryos were then incubated in 100% molten fibrowax at 60°C for 24

hours, with three changes of wax during this period. The embryos were then placed in individual moulds, orientated with a warm needle, and left to set. The embedded embryos were stored at 4°C until sectioning. Sections were cut at 10μm thickness in a Micro HM 330 microtome (*Microm*), and gently guided in series onto TESPA-coated slides. The embryo sections were dried on a flat bed dryer (*R.A. Lamb*) for 30-60 minutes at 50°C and stored in a dry, dust-free box at room-temperature until analysis.

Cryo-embedding was carried out using established protocols. Firstly, the embryos were cryo-protected by incubating at 4°C in 30% sucrose (in PBS) overnight, or until the samples sunk to the bottom of the vessel. Then, embryos were infiltrated by applying a 1:1 mixture of sucrose in PBS:OCT embedding medium (*Miles Inc.*) for 30 minutes. The embryos were then transferred to an embedding mould, which was filled with fresh OCT. The embryos were then oriented with a pipette tip, frozen on dry ice until solid, wrapped in aluminum foil and then stored at -70°C until ready for sectioning. Sections were cut at 10μm thickness in a Cryo-2000 cryostat (*Sakura*), and gently guided in series onto Superfrost™ glass slides (*LSL*) and allowed to dry at room temperature. Slides were carefully wrapped in aluminum foil and then stored at -70°C until analysis.

Sections were processed prior to analysis. Wax sections were de-waxed and re-hydrated, by applying 100% of the de-parafinising agent Histoclear (*R.A. Lamb*) for five minutes, carrying out serial ethanol dilutions applying 100% ethanol twice, then 95%, 80%, 70% and 50% once each, and then carrying out two 5-minute washes in dH_20. Cryosections were simply thawed to room temperature and washed twice in PBS. For histology, sections were stained with haematoxylin and eosin. This was carried out by application of 0.5% eosin (aqueous) for one minute and then by washing in dH_20. Meyer's haematoxylin solution was then applied for 5 minutes and slides were washed twice in dH_20. The slides were then visualised on an *Olympus* SZ4045TR microscope. For immunostaining, sections were firstly boiled in 0.1M citric acid (pH6.0) for five minutes (antigen retrieval), circled with an ImmEdge pen and permeabilised with 0.5% Triton X-100/PBS for five minutes. They were then blocked in 1% BSA in PBS for 30 minutes. The slides were then incubated with primary antibodies against Hand1 (*Abcam*), Nucleostemin (NS; *R&D Systems*) or

Plk4 (*Abcam*; to confirm the PCR genotyping of *Plk4*-null embryos) overnight in a humidity-controlled chamber at 4°C. A secondary antibody-only coverslip was included as a control, and was left overnight in block. The embryos were then washed three times in block solution and the relevant, fluorophore-conjugated secondary antibody was applied to samples in a humidity-controlled chamber at room temperature for one to three hours. The samples were then counterstained with the nuclear marker bis-benzamide (Hoechst 33342) at a concentration of 5μg/ml in PBS for 10 minutes. Slides were mounted with coverslips using a 1:1 mixture of PBS and glycerol and wrapped in foil until imaging.

2.13. Embryoid body (EB) dissociation

Individual cardiomyocytes were isolated from *in vitro*-differentiated embryoid bodies (EBs) using collagenase-B according to a previously-published protocol (Maltsev *et al.*, 1993). Briefly, 5-10 fluorescent, beating EBs were manually isolated using a pipette tip, and placed into an Eppendorf containing 1ml low calcium medium. The isolated cells were then spun down and re-suspended in 1ml enzyme medium (supplemented with 1mg/ml collagenase-B) for 30 minutes at 37°C in order to dissociate the individual cells. The cells were then incubated in 1ml KB medium with gentle shaking at room temperature for one hour to complete their dissociation. The dissociated cells were then completely re-suspended in an appropriate volume of normal ES culture medium and incubated overnight in 0.1% gelatin-treated flasks at 37°C under normal cell culture conditions.

Chapter 3

Nucleolar interaction with HICp40 negatively-regulates Hand1 activity

3.1. INTRODUCTION

Hand1 is essential for placentation and appropriate genesis of the heart. However, how its activity is regulated during these embryologically-distinct processes is largely unknown. Protein-protein interactions commonly regulate the activity of transcription factors and indeed numerous bHLH factors, and some non-bHLH factors, have been shown to bind to and modulate the activity of Hand1 (Chapter 1, Table 1.1). The promiscuous dimerisation properties of Hand1 led us to speculate that a wider range of non-bHLH factors may also bind the transcription factor to achieve functional effects. We thus conducted a yeast two-hybrid (Y2H) screen to identify novel Hand1 cofactors.

3.2. RESULTS

3.2.1. Hand1 interacts with the murine orthologue of HICp40

In order to identify proteins that interact with Hand1 and that may modulate its activity, we conducted a yeast two-hybrid (Y2H) screen using Hand1 as bait. This identified numerous Hand1-interacting factors from a murine E9.5/ E10.5 cDNA library (Hollenberg *et al.*, 1995; Appendix 8). The assay was validated by the identification of an interaction between Hand1 and Alf1, the murine orthologue of human E47, a class A bHLH factor previously shown to bind Hand1 (Hollenberg *et al.*, 1995).

Sequence analysis of one particular Hand1 interactor (identified by two independent clones in the Y2H screen) revealed an 89% nucleotide identity and 95% amino acid identity with the murine orthologue of the human inhibitor of MyoD family (I-mfa) domain containing protein (HIC). HIC is otherwise known as the MyoD family inhibitor containing protein (Mdfic) or as the protein derived from the

kidney-derived transcript-1 (*Kdt1*). HIC consists of two isoforms of molecular weights 32kDa and 40kDa, denoted HICp32 (of 246 amino acid residues) and HICp40 (of 355 amino acid residues), respectively. These arise from different translational initiator codons (GTG_0 for HICp40 and ATG_{591} for HICp32; Thebault *et al.*, 2000a). The structure of HIC is shown in Figure 3.1.

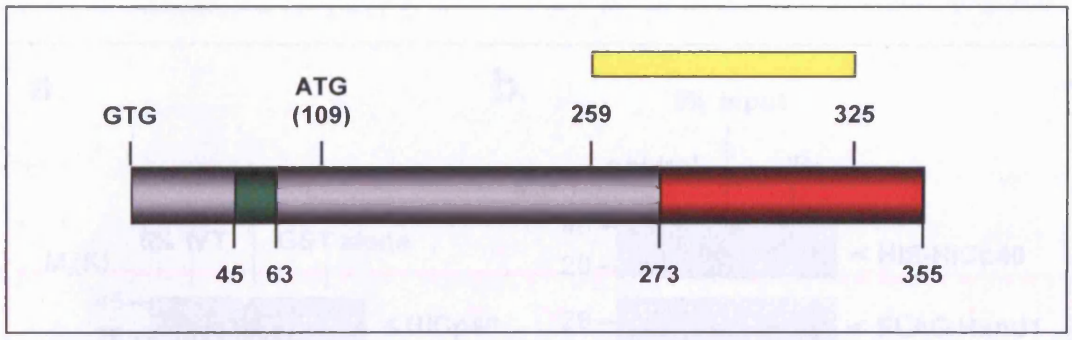

Figure 3.1. The structure of HIC, a novel Hand1 interactor identified in a yeast two-hybrid (Y2H) assay using Hand1 as bait.

HICp40, translated from an unusual GTG start codon, possesses two so-called nucleolar localisation signals (NoLS) at its N-terminus of the form R/K-R/K-X-R/K (shown in green). These are lacked by the HICp32 isoform, which is translated from a downstream ATG start codon. At the C-terminus of both HIC isoforms there is a cysteine-rich I-mfa domain (shown in red), which has significant homology to the sequence of the I-mfa domain in the ancestral I-mfa protein. The location of the Hand1-interacting clones identified by Y2H in the HIC protein sequence, which overlap with the I-mfa domain, are shown in yellow.

Our Y2H clones represent the mouse orthologue of HIC, which we term murine I-mfa domain containing protein (MIC). This cDNA is represented in the EST database (GenBank accession number BB222360) and includes a coding region with 81% amino acid identity to that of HICp32. The full-length MIC gene can be located in ENSEMBL (NM_175088), where transcript information predicts an exon/ intron structure and further 5' coding sequence with homology to the longer human isoform HICp40. Full-length HICp40 homologues in the monkey, chicken and various other species are also listed in ENSEMBL. We cloned the full-length MICp40 cDNA by extending the MICp32 cDNA (from an IMAGE clone) using a BAC sequence. By *in vitro* translation (IVT) we subsequently demonstrated that, like *HICp40*, *MICp40* encodes two proteins, of molecular weights 40kDa and 32kDa (data not shown).

We then sought to corroborate the Hand1-HICp40 interaction *in vitro* (Figure 3.2). This interaction was initially demonstrated by a pull-down assay using a GST-Hand1 fusion protein and *in vitro*-translated HICp40 (Figure 3.2a). Furthermore, a HIS-HICp40 fusion protein could be co-immunoprecipitated using a FLAG-Hand1 antibody in transfected NIH-3T3 cells (Figure 3.2b). These results therefore collectively confirm that Hand1 interacts with the HIC protein *in vitro*.

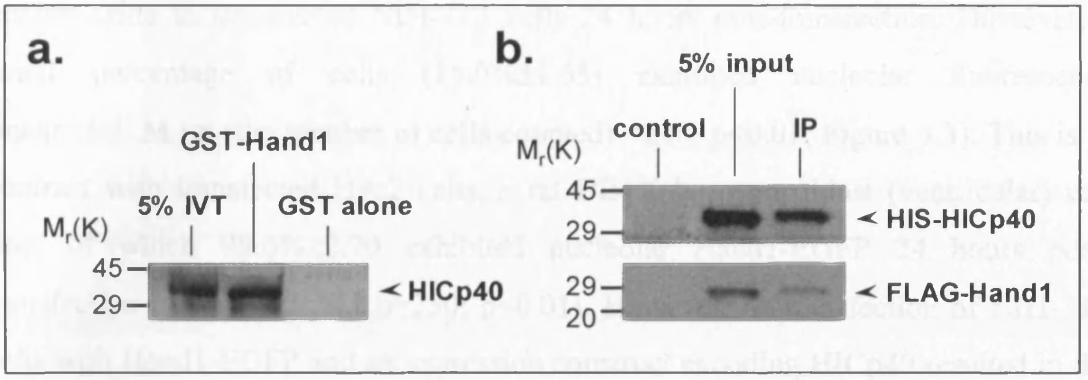

Figure 3.2. Confirmation of the Hand1-HIC interaction by GST pull-down and co-immunoprecipitation assays.

A GST pull-down assay using a GST-Hand1 fusion protein and *in vitro*-translated HICp40 confirmed the ability of Hand1 to interact with HICp40 (**a**). Co-immunoprecipitation of FLAG-Hand1 with HIS-HICp40 in transfected NIH-3T3 cells with polyclonal α-HIS antibody further corroborated the Hand1-HICp40 interaction (**b**).

3.2.2. HICp40 sequesters Hand1 in the nucleolus

By virtue of their translation via alternative initiator codons, the two HIC isoforms have a common C-terminal I-mfa domain but their N-termini significantly differ. This has implications for the sub-cellular localisations of the two isoforms. The N-terminus of HICp40 contains two highly-basic, so-called nucleolar localisation signals (NoLS) between residues 45 and 63 in its extended (109aa) N-terminus (of the form R/K-R/K-X-R/K, specifically RKRR and RRRR), which are lacking in HICp32 (Figure 3.1). The use of a secondary, upstream codon has been reported previously to generate a longer isoform of a protein that contains a NoLS, for example, in the case of PTHrP (Lam *et al.*, 2000). Thus, whilst HICp40 localises to nucleoli, with additional cytoplasmic fluorescence, HICp32 assumes a granular

cytoplasmic distribution with only weak nuclear staining (Thebault *et al.*, 2000a; Thebault *et al.*, 2000b).

In light of the differences in subcellular location of the HIC isoforms, we next sought to investigate whether interaction of Hand1 with these proteins occurs in discrete subcellular compartments. A Hand1-EGFP fusion protein was generally nuclear-wide in transfected NIH-3T3 cells 24 hours post-transfection. However, a small percentage of cells (15.0%±1.55) exhibited nucleolar fluorescence (mean±S.E.M.; n (the number of cells counted) =240; $p<0.01$; Figure 3.3). This is in contrast with transfected H9c2 cells, a rat DB1X heart myoblast (ventricular) cell line, of which 98.6%±2.70 exhibited nucleolar Hand1-EGFP 24 hours post-transfection (mean± S.E.M.; n=250; $p<0.01$). However, co-transfection of NIH-3T3 cells with Hand1-EGFP and an expression construct encoding HICp40 resulted in the restriction of the largely nuclear-wide fluorescent fusion protein almost exclusively to the nucleolar compartment (85.4%±1.24 of co-transfected cells exhibited nucleolar EGFP fluorescence 24 hours post-transfection (mean±S.E.M.; n=210; $p<0.01$; Figure 3.3). Hand1-EGFP localisation to nucleoli was independent of fixation method and was confirmed by immunostaining to illustrate co-localisation with the nucleolar protein C23 (Nucleolin), a factor involved in ribosomal biogenesis. Interestingly, co-transfection of NIH-3T3 cells with Hand1-EGFP and an expression construct encoding HICp32 did not result in the restriction of the largely nuclear-wide fluorescent fusion protein to the cytoplasm. In conclusion, these results demonstrate that the interaction of Hand1 with HICp40 results in the nucleolar sequestration of Hand1.

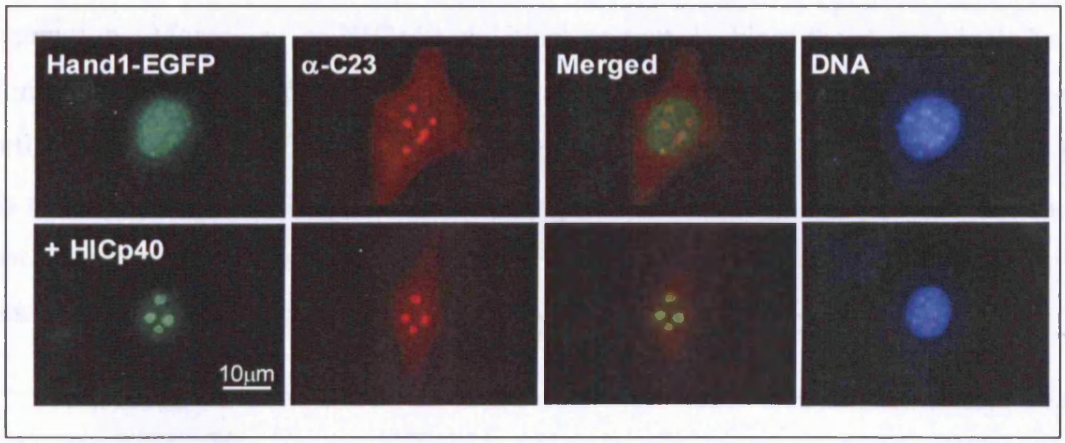

Figure 3.3. HICp40 sequesters Hand1-EGFP in the nucleolus.

Hand1-EGFP is predominantly localised throughout the nucleus in transfected NIH-3T3 cells with a small percentage (~15%) exhibiting weak staining in the nucleolus as confirmed by immunostaining for the nucleolar protein Nucleolin (C23; top row). However, upon ectopic expression of HICp40, >85% of cells exhibit nucleolar-localised Hand1-EGFP (bottom row). See text for statistical significance.

3.2.3. Nucleolar sequestration of Hand1 negatively-regulates its transcriptional activity

In light of previously-described roles for the HIC isoforms as negative regulators of specific developmental pathways (discussed later in this chapter (section 3.3.1)), we then investigated the functional consequences of their interaction with Hand1. To this end, we carried out transient transfection assays in NIH-3T3 cells (Figure 3.4). HICp40 repressed the ability of a Hand1-E-factor (E12) heterodimer to trans-activate a 'mock' Hand1 target gene. This comprised six high affinity Thing1 box (Th1) sequences upstream of a minimal *α-cardiac actin* promoter and a *luciferase* cassette (Hill and Riley, 2004). This result revealed that HICp40 negatively-regulates Hand1 activity *in vitro*.

Notably, HICp32, which lacks the N-terminal nucleolar localisation signals present in HICp40, was unable to abrogate Hand1 transcriptional activity to the extent of full-length HICp40 in the described reporter assay (Figure 3.4). Thus the HICp40 N-terminal nucleolar localisation signal is necessary for optimal Hand1

repression. Moreover, a HICp40 deletion mutant lacking the C-terminal I-mfa domain (HICΔC) could not significantly repress Hand1-E12-mediated reporter gene activity (Figure 3.4). Thus the C-terminal I-mfa domain of HICp40 is necessary for its interaction with and repression of Hand1. The fact that the HICΔC protein could not significantly sequester Hand1-EGFP to the nucleoli of NIH-3T3 cells in a similar assay to that described in Figure 3.3 adds weight to this conclusion (data not shown).

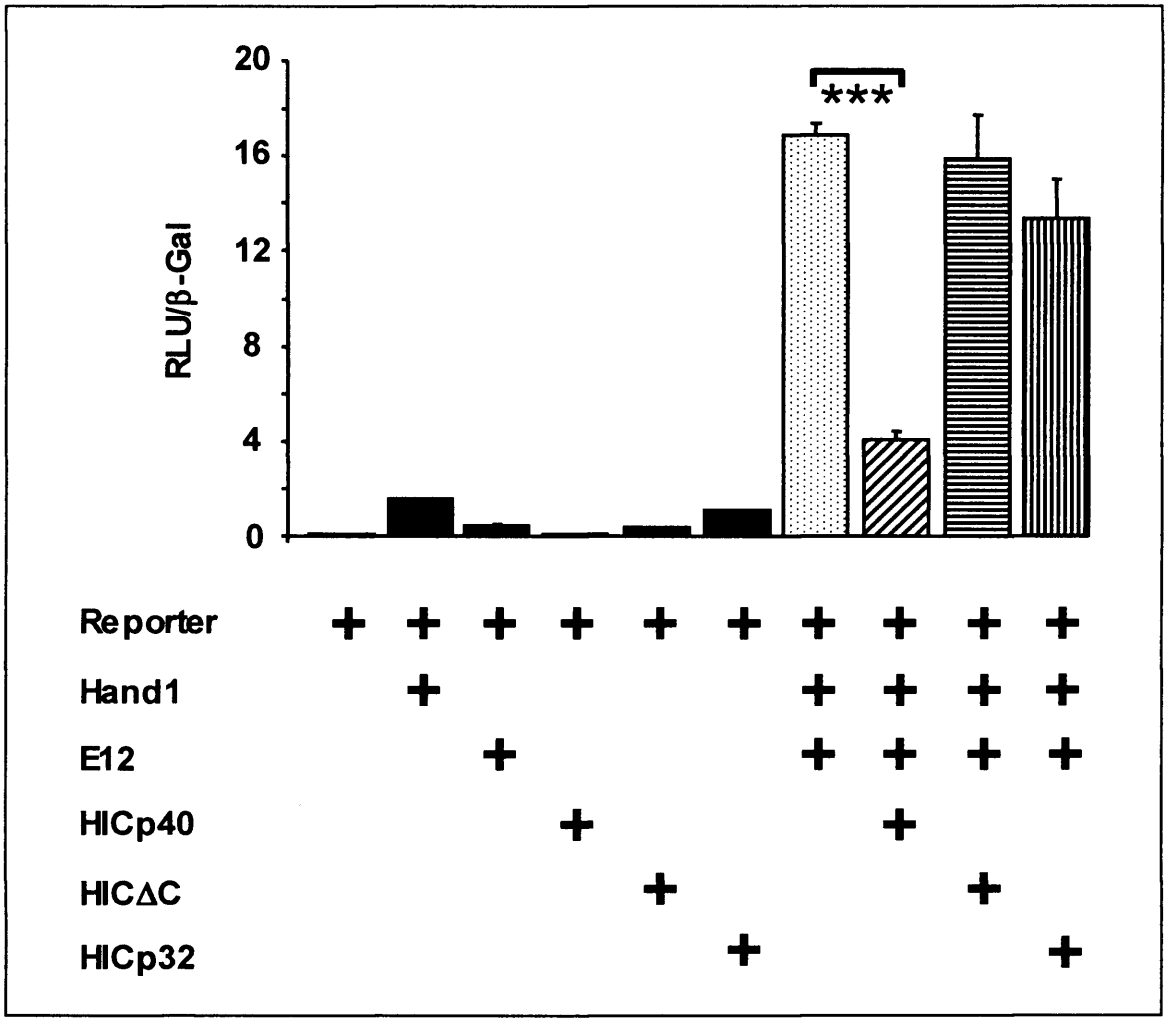

Figure 3.4. HICp40 negatively regulates Hand1 activity.

In a transient transfection reporter assay in NIH-3T3 cells, the Hand1-E12 heterodimer can activate expression of a 'mock' Hand1 target gene comprising six high-affinity Hand1-binding sites (Thing1 boxes) upstream of a minimal *α-cardiac actin* promoter and a *luciferase* cassette (dotted-bar). However, HICp40 significantly represses Hand1-E12 activity in this assay (diagonal lined-bar). HICΔC, a HICp40 deletion mutant lacking the C-terminal I-mfa domain, cannot significantly repress Hand1-E12 heterodimer activity (horizontal-lined bar). HICp32, which lacks the N-terminal nucleolar localisation signals present in the N-terminus of HICp40, can only modestly repress Hand1-E12 heterodimer activity (vertical-lined bar). Measurements are mean±S.E.M.; n=3; *** indicates $p<0.001$.

We also investigated the regions of Hand1 required for its functional interaction with HICp40 (Figure 3.5). An EGFP fusion with the isolated Hand1 bHLH domain ($bHLH_{Hand1}$-EGFP) does not localise to the nucleolus (Figure 3.5a). Furthermore an EGFP fusion with a fragment of Hand1 containing its poly-histidine stretch and flanking sequence ($Hand1_{His}$-EGFP), is nuclear-wide (Figure 3.5b). In both cases, this is true even upon HICp40 over-expression (data not shown). Both fusion proteins were expressed at detectable levels in transfected cells, as assessed by western blot analysis using an anti-EGFP antibody. In conclusion, neither the Hand1 bHLH domain nor the Hand1 poly-histidine stretch are sufficient for interaction with HICp40.

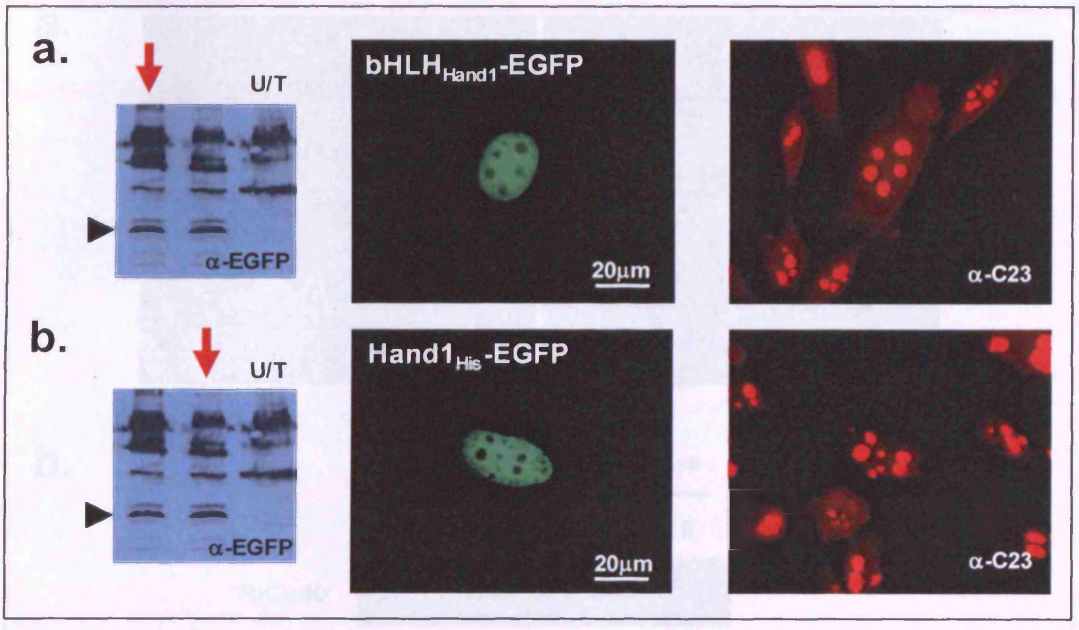

Figure 3.5. Neither the Hand1 basic domain, nor the Hand1 poly-histidine stretch, is sufficient for nucleolar interaction with HICp40.

An EGFP fusion with the isolated bHLH domain of Hand1 ($bHLH_{Hand1}$-EGFP) cannot localise to the nucleoli of transfected NIH-3T3 cells (**a**). An EGFP fusion with a fragment of Hand1 containing the N-terminal histidine-rich domain, $Hand1_{His}$-EGFP, is also nuclear-wide (**b**). Presented also are western blot analyses using an anti-EGFP antibody to illustrate expression of the EGFP fusion proteins in transfected cells. **U/T**: untransfected.

3.2.4. HICp40 is co-expressed with Hand1 in several tissues during development

We next investigated whether the Hand1-HICp40 interaction is likely to occur *in vivo* (Figures 3.6 and 3.7). In Rcho-1 cells, a rat cell line which was discussed in Chapter 1 (section 1.6), HICp40-EGFP is nucleolar (Figure 3.6a). Furthermore, the rat orthologue of *HICp40*, '*RICp40*', is endogenously expressed in both Rcho-1 stem cells and Rcho-1 cells induced to differentiate over an eight-day time-course into trophoblast giant cells, as determined by RT-PCR (Figure 3.6b).

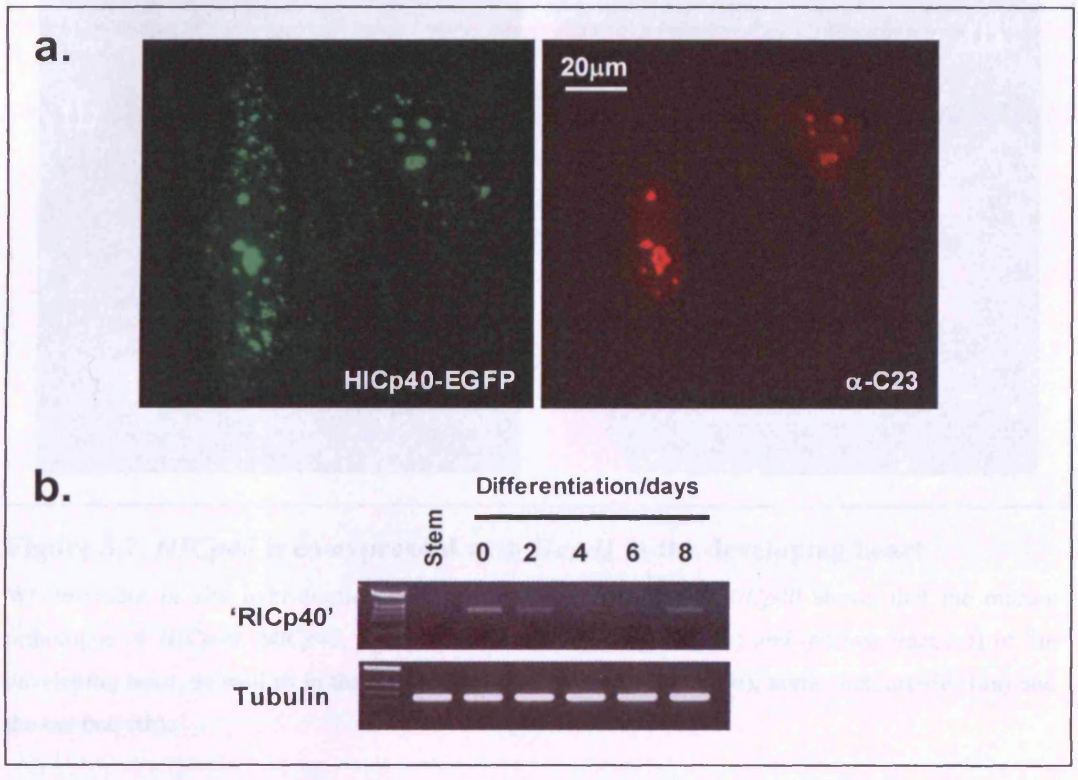

Figure 3.6. HICp40-EGFP localises to Rcho-1 stem cell nucleoli and the rat orthologue of HICp40 is endogenously expressed in Rcho-1 cells during their differentiation.

HICp40-EGFP is predominantly nucleolar, but with some cytoplasmic fluorescence, in Rcho-1 trophoblast stem cells (**a**). Rcho-1 trophoblast stem cells endogenously express weak but detectable levels of transcripts of the rat orthologue of HICp40, 'RICp40', as assessed by RT-PCR, and its expression is maintained during their differentiation into trophoblast giant cells over an eight-day time-course (**b**).

We then determined the endogenous expression pattern of *MICp40* (Figure 3.7). Whole mount *in situ* hybridisation was performed on E9.5 wild-type embryos using a probe for full length HICp40. This showed that endogenous *MICp40* is expressed in the LV and OFT of the developing heart, and as such is co-expressed with *Hand1* during embryogenesis (as reviewed in Chapter 1, section 1.3.2.2). Collectively, these findings strongly suggest that the Hand1-HICp40 interaction, resulting in Hand1 nucleolar sequestration, may regulate Hand1 activity *in vivo*.

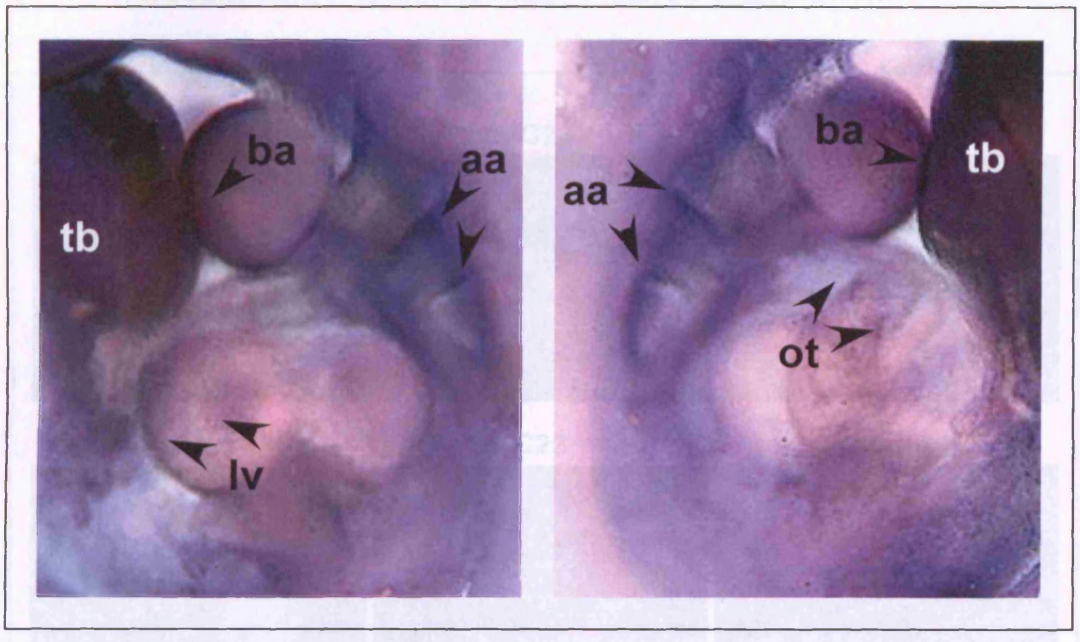

Figure 3.7. *HICp40* is co-expressed with *Hand1* in the developing heart.

Whole-mount *in situ* hybridisation using a probe for full length *HICp40* shows that the murine orthologue of *HICp40*, *MICp40*, is expressed in the left ventricle (**lv**) and outflow tract (**ot**) of the developing heart, as well as in the first branchial (pharyngeal) arch (**ba**), aortic arch arteries (**aa**) and the tail bud (**tb**).

3.2.5. Members of the bHLH family closely-related to Hand1 do not localise to the nucleolus

We finally investigated whether bHLH transcription factors closely-related to Hand1 localise to the nucleolus (Figure 3.8). EGFP fusions with both the closely-related bHLH factors Hand2 (Figure 3.8a) and MyoD (Figure 3.8b) are nuclear-wide in transfected NIH-3T3 cells. This suggests that nucleolar localisation, at least among closely-related members, is specific to Hand1 within the bHLH family.

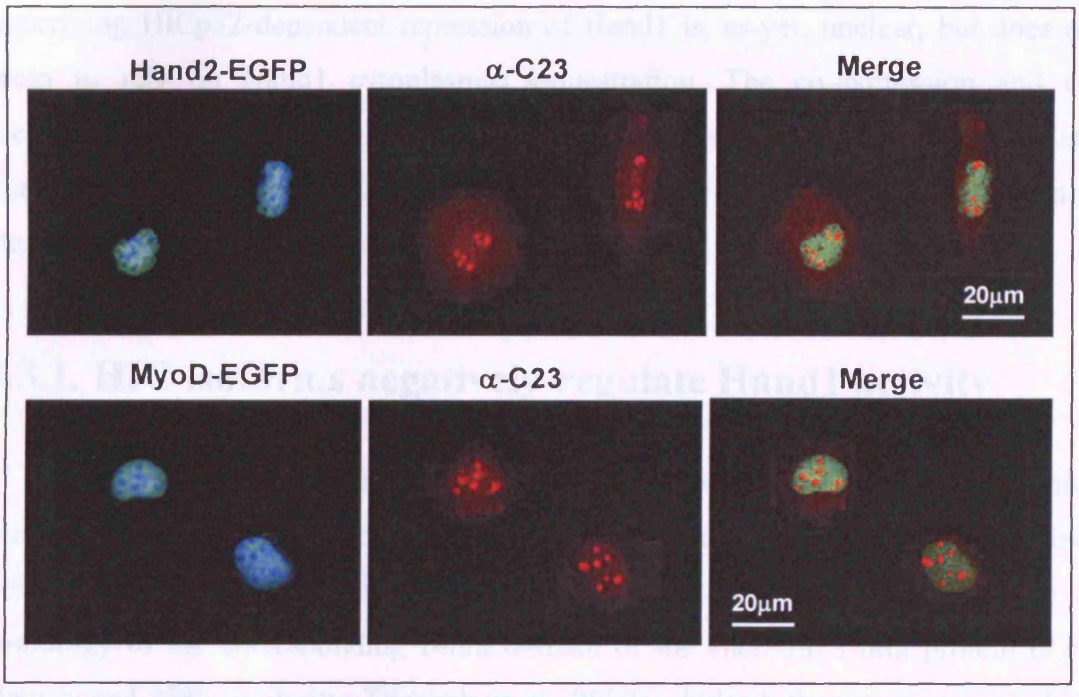

Figure 3.8. Nucleolar localisation of Hand1-EGFP is not observed with EGFP fusions of the related bHLH factors Hand2 and MyoD.

The related bHLH transcription factor-EGFP fusion proteins, Hand2-EGFP (**a**) and MyoD-EGFP (**b**), are nuclear-wide in transfected Rcho-1 stem cells.

3.3. DISCUSSION

Using a Y2H screen with Hand1 as bait, we identified a negative regulator of Hand1, the murine orthologue of the human I-mfa domain-containing protein (HIC). HIC comprises two isoforms, HICp40 and HICp32. The data presented in this chapter strongly suggest that the interaction of Hand1 with either factor, but particularly with HICp40, results in the negative-regulation of Hand1 transcriptional activity. HICp40 achieves this by sequestering Hand1 in the nucleolus. However, the mechanism underlying HICp32-dependent repression of Hand1 is, as-yet, unclear, but does not seem to rely on Hand1 cytoplasmic sequestration. The co-expression and co-localisation of Hand1 with the murine orthologue of HIC in rodent trophoblast and during cardiac morphogenesis moreover suggests that this mechanism may control Hand1 activity *in vivo*.

3.3.1. HIC isoforms negatively-regulate Hand1 activity

In our Y2H screen, the region of HIC that interacted with Hand1 and which was indispensable for its repression of Hand1 mapped to a portion of its cysteine-rich, C-terminal I-mfa-domain. The I-mfa domain of HIC has a high degree of homology to the corresponding I-mfa domain of the ancestral I-mfa protein (77% identity and 81% similarity; Thebault *et al.*, 2000a). Indeed, the two proteins, which are found in all vertebrates, are thought to have arisen by duplication, supported by their similar intron-exon structures and homologous flanking genes (Wang *et al.*, 2007). Without exception, the determined roles of both I-mfa and HIC depend absolutely on the presence of the I-mfa domain, reflecting its importance in protein-protein interactions.

During somitogenesis in the mouse, the I-mfa protein is confined to cells of the ventral somite, the sclerotome, and here it inhibits the potent myogenic bHLH factors MyoD, Myf5, Mrf4 and Myogenin to prevent myogenesis (Chen *et al.*, 1996). I-mfa is also thought to interact with and negatively-regulate the chondrogenic bHLH factor Scleraxis, and as such *I-mfa*-null embryos exhibit delayed caudal neural tube

closure and skeletal patterning defects (Kraut *et al.*, 1998). The I-mfa protein also has a crucial role during placentation. During this process it inhibits Mash2, a bHLH factor required for TS cell maintenance (reviewed in Chapter 1, section 1.2.4.2), by sequestering it in the cytoplasm. This contributes to the process of TG cell differentiation. Appropriately, I-mfa is strongly-expressed in cells at the periphery of the EPC and in SGCs, and an *I-mfa*-null mouse is embryonic lethal at E9.5 due to a significantly-reduced number of SGCs (Kraut *et al.*, 1998). Furthermore *I-mfa* over-expression induces precocious TG cell differentiation in the Rcho-1 trophoblast stem cell model, whilst conversely an *I-mfa*-null trophoblast stem cell line cannot undergo TG cell differentiation in culture (Kraut *et al.*, 1998).

Most importantly for our study, an interaction between I-mfa and Hand1, which is dependent on the I-mfa domain, has previously been reported in trophoblast cells (Kraut *et al.*, 1998). However, the functional significance of this interaction remains unknown. Thus our results are in agreement with previous studies that report a role for I-mfa-domain-containing proteins in the negative regulation of factors involved in rodent placentation. Whilst no functional consequence was previously attributed to the interaction of the I-mfa protein with Hand1, we show that the interaction of Hand1 with I-mfa domain-containing isoforms negatively-regulates the bHLH factor.

Similarly, the HIC proteins also play crucial roles in post-transcriptional repression of developmental factors. Reminiscent of I-mfa, every reported function of HIC is absolutely dependent on its interaction with other proteins via its C-terminal I-mfa domain. As such, deletion mutants lacking this portion are unable to mimic the full-length protein in relevant assays (Chen *et al.*, 1996; Kraut *et al.*, 1998). The HIC isoforms were first identified by Thebault and colleagues on the basis of their differential regulation of human retroviral promoters in the presence of viral transcriptional activators (Thebault *et al.*, 2000a). Specifically, the HIC proteins enhance transcription from the Human T-Cell Leukemia Virus-1 (HTLV-1) long terminal repeat (LTR) promoter in the presence of the HTLV-1 trans-activator Tax, but down-regulate Human Immunodeficiency Virus-1 (HIV-1) proviral transcription in the presence of the HIV-1 trans-activator Tat (Thebault *et al.*, 2000a).

Later studies implicated the *Xenopus* orthologues of the HIC proteins, XICp40 and XICp32, in embryonic axis specification (Kusano and Raab-Traub, 2002; Snider *et al.*, 2001; Snider and Tapscott, 2005). Specifically, the XIC proteins bind to and mask the DNA-binding domain of the ventralising, HMG-box transcription factor Tcf3 to repress Wnt-dependent signalling. This blocks Tcf3-dependent expression of *Wnt* target genes a pre-requisite for the activation of the dorsalising homeodomain transcription factor Siamois and formation of the dorsal (Spemann) organiser (Snider *et al.*, 2001; Snider and Tapscott, 2005). Embryos injected with a morpholino to *XIC* mRNA thus lacked head structures, a neural tube and paraxial mesoderm, and were down-regulated for several dorsal organiser factors such as *goosecoid* and *Cerberus* (Snider and Tapscott, 2005). Conversely, another study revealed that the XIC proteins have a stimulatory effect on Wnt signalling, namely by binding the glycogen synthase kinase-3β-binding site on Axin and preventing Axin-mediated phosphorylation of β-Catenin as a pre-requisite for its degradation. β-Catenin is then able to translocate to the nucleus and activate T-cell factors (Tcf) and lymphocyte enhancer factors (Lefs), which activate their *Wnt* target genes (Kusano and Raab-Traub, 2002). This study also showed that XIC binds Axin to prevent its interaction with Mekk1, so blocking downstream c-Jun N-terminal kinase (Jnk) signaling in the nucleus. However, the functional significance of these interactions and effects are currently unknown. Overall, our results are in agreement with previous studies that have reported a role for I-mfa domain-containing proteins in the negative regulation of developmental factors, including members of the bHLH transcriptional factor super-family.

In conclusion, the HIC proteins can repress the transcriptional activity of Hand1 *in vitro*. Importantly, the C-terminal I-mfa domain of HIC, a portion of which interacted with Hand1 in our Y2H assay and which is present in both HIC isoforms, was necessary for this effect. This is in agreement with previously-determined roles for HIC and the ancestral I-mfa protein in the negative regulation of developmental factors. In many cases these targets, like Hand1, are members of the bHLH family and have roles in determining cell fate.

3.3.2. HICp40 sequesters Hand1 in the nucleolus

Our results demonstrate that HICp40 sequesters Hand1 in the nucleolus and that this is specific to Hand1 amongst closely-related bHLH family members. We show that the consequence of Hand1 nucleolar sequestration is its transcriptional repression. The nucleolar sequestration of a target factor by HICp40 may not be without precedent. HICp40 activates HTLV-1 proviral transcription from the LTR promoter by blocking bHLH transcription factor activity (Thebault *et al.*, 2000a). This occurs because the HTLV-1 trans-activator Tax activates proviral transcription by binding co-activators such as CBP, which are also bound to by certain bHLH factors such as c-Myb (Colgin and Nyborg, 1998). HICp40 may repress bHLH factors by sequestering them in the nucleolus, supported by our findings regarding Hand1 presented in this chapter. Conversely, the repression of HIV-1 proviral transcription from the LTR promoter by HICp40 (Thebault *et al.*, 2000a) is thought to be underpinned by the nucleolar sequestration of the HIV-1 trans-activator Tat in the nucleolus (Young *et al.*, 2003). Of note, HICp40 also binds and inhibits, perhaps via nucleolar sequestration, the Cyclin T1 component of the positive transcription elongation factor b (pTEFb) complex (Young *et al.*, 2003). This may block pTEFb-dependent phosphorylation of the C-terminal domain of RNA Pol II, which is required for the transcriptional elongation of HIV-1 transcripts (Zhu *et al.*, 1997). Thus our findings are in agreement with several of the established roles for HICp40 in the repression of factors, often via nucleolar sequestration.

Hand1 nucleolar sequestration may occur either via active transport into the organelle in complex with HICp40, which may shuttle between the nuclear and nucleolar compartments, or via passive diffusion followed by HICp40-dependent nucleolar retention. With respect to the latter possibility, the nucleolus lacks a membrane and so any soluble protein should be able to diffuse in and out of the organelle. By the 'hit and run' model, passive diffusion of nucleoplasmic proteins into the nucleolus is thought to be followed by non-specific retention of only those proteins which possess a nucleolar localisation signal (NoLS) (van Eenennaam *et al.*, 2001; Misteli, 2000; Olson, 2002). In contrast, active transport of proteins into the nucleolus is generally considered unlikely. Although a consensus sequence has not been identified, several viral proteins, for example HIV-I Rev and Tat, contain

sequences with homology to cellular NoLS motifs and depend on these to localise to the nucleolus and hijack the host ribosome biogenesis machinery and/ or as a pre-requisite for proviral replication (reviewed by Hiscox, 2007; Sirri *et al.*, 2008). The NoLS is usually highly-basic, containing mainly arginine and lysine residues (reviewed by Thebault and Mesnard, 2001). As such, the motif is thought to form electrostatic interactions with negatively-charged nucleic acids or acidic components of the ribosome biogenesis machinery. For example, the nucleolar factors Ubf and C23 bind rDNA (Maeda *et al.*, 1992; Heine *et al.*, 1993; Schmidt-Zachmann and Nigg, 1993) and pRB binds the B23 factor, which has roles in ribosomal biogenesis (Takemura *et al.*, 2002). A ribosome biogenesis machinery-attached scaffold of protein anchors, which include HICp40, is thus formed, and these possess high-affinity binding sites for specific nucleoplasmic proteins, which have neither a NoLS nor an obvious nucleolar role. Currently, the mechanisms underlying nucleolar release are largely unknown, but, in light of the consensus view of nucleolar retention, are likely to require energy and/ or post-translational modification.

Our data thus suggest that binding of HICp40 to Hand1 is necessary and sufficient for Hand1 nucleolar sequestration. Our observation that a higher proportion of transfected H9c2 cells exhibit nucleolar-localised Hand1-EGFP than transfected NIH-3T3 cells may in this regard be due to the presence or absence of HICp40 cofactors or other proteins involved in nucleolar translocation of Hand1, or otherwise due to variations in the abundance of HICp40 between cell lines. Further work is required to investigate these possibilities, but it is interesting that a recent study indicated a variation in the abundance of *HIC* mRNA between several cell lines (Wang *et al.*, 2007). At present, the differences in Hand1-EGFP sub-cellular localisation between cell lines are unclear.

Importantly, our data rule out the putative, albeit degenerate, NoLS of the form R/K-R/K-X-R/K in the Hand1 basic domain (RKGSGPKKERRR) as being sufficient for Hand1 nucleolar localisation. A possible involvement of this sequence in the nucleolar localisation of Hand1 was suggested by two observations. Analogous sequences in the related zebrafish bHLH factor Myf5 are required for nucleolar localisation (Wang *et al.*, 2005) and Hand1-EGFP remains nucleolar in the HICp40-deficient cell line, human breast epithelial MCF-7 cells (Wang *et al.*, 2007; data not

shown). However, two pieces of data argue against HICp40-independent Hand1 nucleolar localisation. An EGFP fusion with Hand2, which also possesses a similar, putative NoLS motif in its basic domain, does not localise to the nucleolus. Furthermore, the highly-related bHLH family member Twist1 has been localised throughout the nucleus of several cell types (A. Firulli, personal communication). This suggests that HICp40 probably binds Hand1 specifically amongst members of the bHLH family. Additionally, the isolated Hand1 bHLH domain is unable to traffic to nucleoli when fused to EGFP. Nevertheless, the localisation of Hand1-EGFP to the nucleolus in a HICp40-deficient background gives some insight into the mechanistic basis of Hand1 nucleolar sequestration. Specifically, this suggests that HICp40 is not required for the active transport of Hand1 into the nucleolus. Thus Hand1 is likely to enter the nucleolus either in complex with other protein(s) or passively by diffusion and the role of HICp40 may be restricted to the subsequent retention of Hand1 in the organelle.

Despite these findings, the sequestration of some factors in the nucleolus is reliant on the nucleolar sequesteror unmasking a 'cryptic' NoLS in the nucleoplasmic target protein. This is thought to reinforce the negative regulatory mechanism. For example, Mdm2 possesses a 'quiescent' NoLS that is only activated by its binding to its nucleolar anchor, $p19^{ARF}$ (Lohrum *et al.*, 2000). Thus it cannot be ruled out that binding of HICp40 to Hand1 may unmask a cryptic NoLS in Hand1, possibly the putative signal in its basic domain. Nevertheless, contrary to this hypothesis is the fact that an EGFP fusion with the isolated Hand1 bHLH domain is unable to localise to the nucleolus. Thus, at present, it is unclear as to whether HICp40 is sufficient for Hand1 localisation to the nucleolus. Indeed, the fact that our Y2H screen identified an interaction between Hand1 and another nucleolar component (Fibrillarin-2; Appendix 8) hints that other proteins may be involved in the nucleolar sequestration and/ or retention of the transcription factor.

Our data suggest that the C-terminal I-mfa domain of HICp40 is necessary for its interaction with Hand1. However, only by carrying out assays employing the isolated I-mfa domain would we be able to investigate whether this domain is sufficient to bind Hand1, or whether Hand1 also binds other regions of HICp40. Furthermore it is currently unknown which domain(s) of Hand1 bind HICp40.

Preliminary assays show that the bHLH domain of Hand1 is not sufficient, since an EGFP fusion with this domain failed to localise to the nucleolus, even upon *HICp40* over-expression. We hypothesised that the Hand1-HICp40 interaction could be underpinned, in part, by contacts between the poly-histidine stretch in the N-terminus of Hand1 and cysteine residues in the HIC I-mfa domain. HIC and I-mfa bind histidine-rich regions in gonadotrophin-inducible transcription factor 1 (Giot1) and in the Cyclin T1 subunit of the pTEFb complex (Mizutani *et al.*, 2001; Young *et al.*, 2003; Wang *et al.*, 2007). These interactions are dependent upon the cysteine-rich I-mfa domain coordinating bivalent metal ions in combination with histidine residues in the target protein. Importantly the N-terminal poly-histidine stretch is absent in the closely-related, but non-nucleolar, Hand2 factor. However, despite these precedents, our data suggest that the Hand1 poly-histidine stretch is not sufficient for HICp40 interaction and Hand1 nucleolar localisation. Nevertheless, despite these findings, the bHLH domain and the poly-histidine stretch may still be involved in binding HICp40, that is, they may be necessary for the interaction. This could be assessed by determining whether EGFP fusions with Hand1 mutants lacking these domains localise to the nucleolus. Ultimately, GST-pull down and co-immunoprecipitation assays (as conducted to generate the data presented in Figure 3.2) employing Hand1 deletion fragments would need to be carried out to definitively map interaction domains.

Notably, the cytoplasmic HICp32 isoform is still able to moderately abrogate Hand1 activity. HICp32 is cytoplasmic, so we investigated whether it was able to restrict Hand1 to this subcellular compartment in a method similar to the negative regulation, mediated by cytoplasmic sequestration, of the Mash2 and myogenic bHLH factors by I-mfa (Chen *et al.*, 1996; Kraut *et al.*, 1998). However, this was not the case, suggesting that HICp32 may instead interfere with the DNA binding activity of Hand1, another mechanism by which I-mfa represses the activity of its bHLH targets (Chen *et al.*, 1996; Kraut *et al.*, 1998). Further investigation will, of course, be required to confirm this hypothesis, but it is interesting that I-mfa, as described, interacts with Hand1 but does not repress its activity *in vitro* (Kraut *et al.*, 1998). This implies that sequences outside of the I-mfa domain of HICp32 are required for the repression of Hand1. Despite this, it is clear that nucleolar sequestration, reliant upon the HICp40 N-terminal NoLS motifs, is required for maximal, possibly biologically-

relevant, Hand1 repression. In this regard it can be inferred that HICp32-dependent repression of Hand1, unlike its confinement to the nucleolus, cannot completely block its biological activity. It is also interesting in light of the modest negative regulation of Hand1 by HICp32 that several other nucleolar anchors also have a secondary, nucleolus-independent mode of regulating their target factor. For example, although $p19^{ARF}$ sequesters the p53 agonist Mdm2 in the nucleolus to enhance p53 stability (Tao and Levine, 1999; Weber *et al.*, 1999) and $p19^{ARF}$ isoforms lacking the signals required for nucleolar localisation are thought to bind to and stabilise p53 to enhance its activity independent of effects on Mdm2 subcellular localisation (Llanos *et al.*, 2001). Additionally, whilst Cfi1 (Net1) primarily sequesters the Cdc14 phosphatase in the nucleolus to prevent it dephosphorylating its nuclear targets and promoting exit from mitosis (Shou *et al.*, 1999; Visintin *et al.*, 1999), cells co-transfected with Cdc14 and Cfi1 exhibit a Cdc14 loss-of-function phenotype despite Cdc14 being nucleoplasmic. This suggests that Cfi1 directly affects the catalytic activity of Cdc14 independently of nucleolar sequestration (Visintin *et al.*, 1999). In conclusion, the underlying molecular basis of HICp32-dependent repression of Hand1 transcriptional activity is unknown and requires further investigation.

In conclusion, HICp40 is required for Hand1 nucleolar localisation and this has the effect of repressing Hand1 transcriptional activity. On the basis of these data, we can conclude that HIC and I-mfa repress their target transcription factors in a similar way. Both factors interact with all of their target proteins via their I-mfa domains and furthermore negatively-regulate them via subcellular confinement, either to the nucleolus by HICp40 or to the cytoplasm by I-mfa (Chen *et al.*, 1996; Kraut *et al.*, 1998; Thebault *et al.*, 2000a; reviewed by Thebault and Mesnard, 2001; Snider *et al.*, 2001; Kusano and Raab-Traub, 2002; Snider and Tapscott, 2005; data presented in this study). This may restrict the access of these target factors to their binding partners and/ or target genes and so limit their biological activity. At present, however, it is unclear which regions of Hand1 are required for HICp40 interaction and this is a subject of ongoing studies.

3.3.3. Summary and concluding remarks

The nucleolus has been traditionally viewed as a 'ribosome biogenesis factory' (reviewed by Perry, 1966). However, more recently, proteomic studies have demonstrated the nucleolar localisation of transcription factors, cell cycle regulators and tumour suppressors that are unlikely to play any part in the traditional roles of this organelle (Scherl *et al.*, 2002; Andersen *et al.*, 2002; Andersen *et al.*, 2005). This has led to the suggestion that the nucleolus also acts as a molecular 'safe' or 'sink' to retain and negatively regulate proteins, preventing them from interacting with their downstream protein partners or target genes until a specific cell cycle stage or metabolic state. Indeed, this is a mechanism not without precedent among transcription factors. For example, the activity of p53 is modulated by $p19^{ARF}$-dependent nucleolar sequestration of its negative regulator, Mdm2 (Tao and Levine, 1999; Weber *et al.*, 1999). Other examples include the inhibition of c-Myc-induced progression through the cell cycle by the sequestration of the transcription factor in the nucleolus by $p19^{ARF}$ (Datta *et al.*, 2004) and the modulation of cell proliferation by NoBP-dependent nucleolar sequestration of Fgf3 (Reimers *et al.*, 2001).

In agreement with these previous studies, we have identified an interaction between Hand1 and HICp40, a factor known to negatively-regulate several developmental factors in a post-translational fashion. The functional basis of this is the sequestration of Hand1 in the nucleolar compartment. This may occur during development to prevent Hand1 from binding its nucleoplasmic protein partners and activating its target genes until a specific cell cycle stage or metabolic state. Moreover, since the nucleolus lacks a membrane, this stockpile of pre-existing Hand1 could be instantaneously released to permit a rapid response to molecular and/ or cellular cues, which could occur without the need for transcriptional up-regulation or even nuclear import.

Importantly, HICp40-dependent nucleolar sequestration is likely to regulate the activity of Hand1 *in vivo*. Although *HIC* is chiefly expressed in lymphoid tissues, Thebault and colleagues localised embryonic murine *HIC* mRNA to organs in which Hand1 is expressed, including the developing small intestine (Thebault *et al.*, 2000a). Nevertheless, their northern blot analysis was restricted to a limited number of tissues

and there was no information on *HIC* expression in the heart. We have, however, demonstrated a co-localisation of Hand1 and the murine orthologue of HICp40 in the developing mouse heart by *in situ* hybridisation experiments. Moreover, the two mRNA species particularly overlapped in the left ventricular myocardium and outflow tract (OFT). Furthermore, we have demonstrated nucleolar localisation and endogenous expression of the rat orthologue of HICp40 in Rcho-1 trophoblast stem cells and their TG cell derivatives, coincident with Hand1.

Since Hand1 is involved in the terminal differentiation of trophoblast and cardiomyocyte cells (Riley *et al.*, 2000; Hughes *et al.*, 2004; reviewed in Chapter 1, sections 1.2.4 and 1.3.2), its nucleolar sequestration and negative-regulation by HICp40 may contribute to determining cell fate. For example, nucleolar localisation and inactivation of Hand1 may correlate with a trophoblast stem cell or cardiac precursor cell decision to proliferate. Upon Hand1 activation through its release into the nucleoplasm, these cells could then be committed to differentiation. Thus to assess the physiological significance of the findings of this chapter *in vivo*, we next investigated the biological relevance of Hand1 nucleolar anchorage in an appropriate cell model and our findings are presented in the following chapter.

Chapter 4

Nucleolar sequestration and release regulates Hand1 activity in rodent trophoblast

4.1. INTRODUCTION

Hand1 plays an essential role in the differentiation of rodent trophoblast, the first lineage to arise in the developing embryo (reviewed in Chapter 1, section 1.2.4). Study of the regulation and function of Hand1 in this lineage is difficult, however, since trophoblast stem (TS) cells are difficult to maintain and manipulate in culture (S. Tanaka, personal communication). Thus we employed the rat choriocarcinoma-1 (Rcho-1) TS cell line (reviewed in Chapter 1, section 1.6), to investigate the biological significance of Hand1 nucleolar sequestration *in vivo*.

Rcho-1 cells represent a faithful model of TS cells. They can be induced to exit the mitotic cell cycle and undergo endoreduplication concomitant with differentiation into so-called trophoblast giant (TG) cells (Kraut *et al.*, 1998; Scott *et al.*, 2000; Hughes *et al.*, 2004; Sahgal *et al.*, 2006). Importantly for our study, Rcho-1 cells endogenously express Hand1 and its expression is necessary and sufficient for TG cell differentiation (Cross *et al.*, 1995; Kraut *et al.*, 1998; Scott *et al.*, 2000). However, the precise role of Hand1 and how its activity is regulated during this process are unknown. Hand1 expression is detectable in Rcho-1 TS cells, albeit at a lower level compared to differentiated Rcho-1 TG cells (Cross *et al.*, 1995), so the activity of Hand1 in this lineage may be post-translationally regulated. In this chapter, we show that the activity of Hand1 is regulated during Rcho-1 differentiation by its nucleolar sequestration and release, and discuss the implications of this finding.

4.2. RESULTS

4.2.1 Nucleolar Hand1-EGFP relocates to the nucleoplasm during TG cell differentiation

In order to investigate whether Hand1 nucleolar localisation plays a role in its regulation in rodent trophoblast, we ectopically expressed a Hand1-EGFP fusion protein in Rcho-1 stem cells cultured in conditions favouring Rcho-1 stem cell

maintenance (20% FBS-supplemented medium). We then tracked the subcellular localisation of Hand1-EGFP over a 72 hour period post-transfection (Figure 4.1).

In proliferating Rcho-1 stem cells 24 hours post-transfection, Hand1-EGFP was almost exclusively localised to nucleoli. However, after 48 and 72 hours post-transfection, Hand1-EGFP gradually dispersed from nucleoli to assume a nuclear-wide distribution. This was coincident with the differentiation of the transfected Rcho-1 stem cells to TG cell differentiation (Figure 4.1). Additionally, the kinetics of the change in Hand1-EGFP localisation were recorded using time-lapse video-microscopy. This revealed Hand1-EGFP release from the nucleolus over a 12-hour period as individual transfected cells began to differentiate, which was coincident with decreased motility and an increase in cell size (Movie 4.1, Appendix 10).

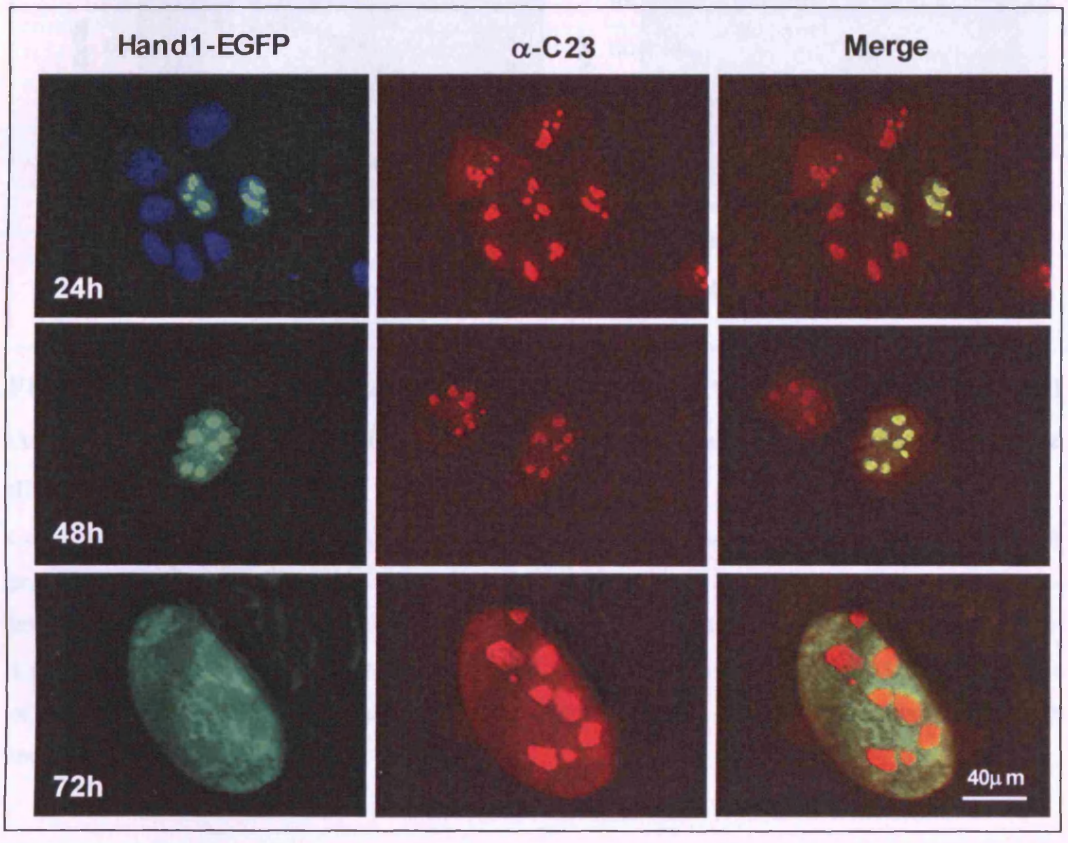

Figure 4.1. Release of nucleolar Hand1-EGFP coincides with Rcho-1 stem cell commitment to a trophoblast giant cell fate.

In Rcho-1 stem cells, Hand1-EGFP localises exclusively to the nucleoli. However, nucleolar Hand1-EGFP becomes nuclear-wide as these cells undergo trophoblast giant cell differentiation over a 72 hour period post-transfection.

Quantitatively, the relative proportions of transfected cells with nucleolar versus nuclear-wide EGFP fluorescence and the number of fluorescent TG cells were determined at each time point (Figure 4.2). These cell counts revealed that the nuclear dispersal of Hand1-EGFP during the 72-hour time course of the experiment was statistically significant (Figure 4.2a). Moreover, the number of fluorescent TG cells at the 72-hour point was significantly higher than the number of fluorescent TG cells 24 hours after transfection and statistically greater than the number of Rcho-1 stem cells at the time-point (Figure 4.2b). This confirmed that nucleolar release of Hand1-EGFP correlates with TG cell differentiation.

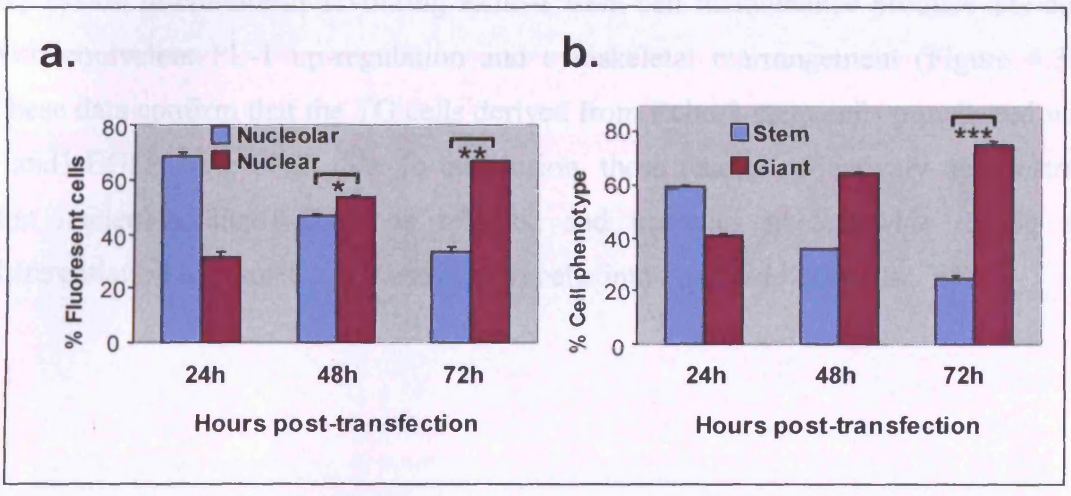

Figure 4.2. The relocation of Hand1-EGFP that coincides with Rcho-1 stem cell commitment to differentiation is statistically-significant and correlates with the differentiation process.

Cell counts of Hand1-EGFP-expressing Rcho-1 cells reveal a significant reduction in nucleolar fusion protein with a corresponding elevation in nuclear-wide localisation over a 72 hour period post-transfection (**a**). Cell counts of the same populations reveal an increasing number of fluorescent Rcho-1 giant cells during the course of the experiment (**b**). Measurements are mean±S.E.M.; n (the number of cells counted per treatment at each time point) = 450; * indicates $p<0.05$; ** indicates $p<0.01$; *** indicates $p<0.001$.

Importantly, these figures were corrected for spontaneous Rcho-1 differentiation in medium that ordinarily maintains Rcho-1 stem cell proliferation (5.9% per 24-hour period; Nakayama *et al.*, 1998; Scott *et al.*, 2000), and for an observed increase in differentiation rate due to the transfection with a construct

encoding EGFP alone (10.3% per 24-hour period; mean±S.E.M.; n=250; $P<0.01$). This applies to all cell counts in this thesis.

We next undertook experiments to confirm that Hand1-EGFP, upon its release from the nucleolus, promotes normal TG cell differentiation. TG cells derived from Rcho-1 stem cells by a change in serum conditions (20% FBS to 10% horse serum) dramatically up-regulate the TG cell marker PL-1 and undergo cytoskeletal rearrangement, as assessed by phalloidin staining for F-actin (Figure 4.3a). Importantly, Rcho-1 stem cells induced to differentiate by ectopic Hand1-EGFP expression in conditions favouring Rcho-1 stem cell maintenance produce TG cells with equivalent PL-1 up-regulation and cytoskeletal rearrangement (Figure 4.3b). These data confirm that the TG cells derived from Rcho-1 stem cells transfected with Hand1-EGFP were *bona fide*. In conclusion, these results collectively demonstrate that nucleolar Hand1-EGFP is released and becomes nuclear-wide during the differentiation of transfected Rcho-1 stem cells into *bona fide* TG cells.

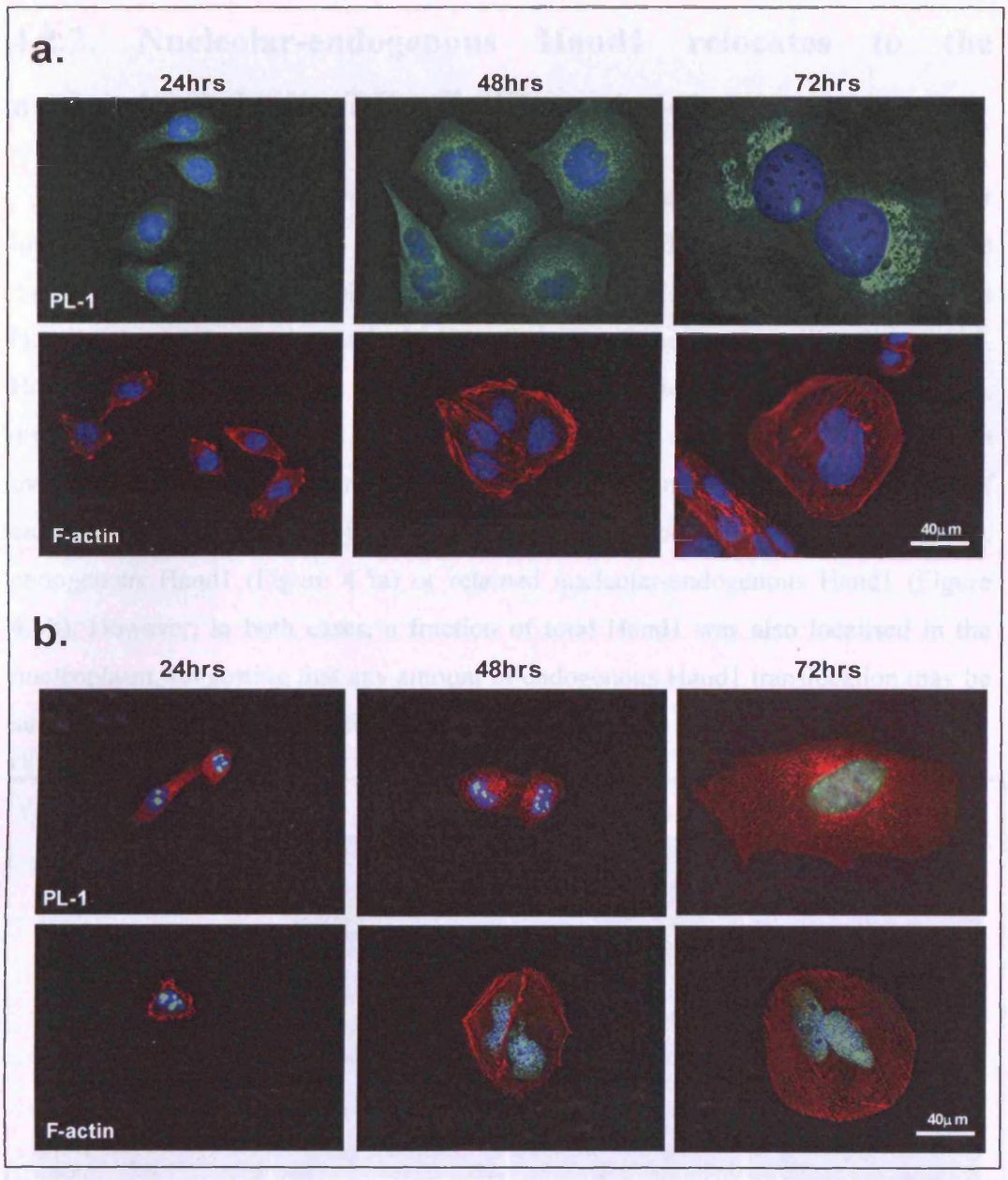

Figure 4.3. Hand1-EGFP-induced differentiation of Rcho-1 cells produces *bona fide* trophoblast giant cells.

Rcho-1 giant cells induced by a change in serum conditions (20% FBS to 10% HS) undergo a dramatic up-regulation in the TG cell-specific marker PL-1 and complex cytoskeletal rearrangement as visualised by phalloidin staining for F-actin (**a**). Rcho-1 cells induced to differentiate by over-expression of ectopic Hand1-EGFP (in medium supplemented with 20% FBS) produce giant cells with equivalent PL-1 up-regulation and cytoskeletal rearrangement (**b**).

4.2.2. Nucleolar-endogenous Hand1 relocates to the nucleoplasm during TG cell differentiation

We next sought to investigate whether the observed changes in the subcellular localisation of Hand1-EGFP during Rcho-1 TG cell differentiation applies also to endogenous Hand1. Immunostaining for Hand1 and C23 revealed that endogenous Hand1 is restricted to the nucleoli of proliferating Rcho-1 stem cells (Figure 4.4). However, upon a change in serum conditions to promote TG cell differentiation, nucleolar-endogenous Hand1 is released and assumes a nuclear-wide localisation over a 72-hour period (Figure 4.4). In addition to the nuclear-wide localisation of endogenous Hand1 in TG cells, a cohort (<5% of total cells) exhibited peri-nuclear, endogenous Hand1 (Figure 4.5a) or retained nucleolar-endogenous Hand1 (Figure 4.5b). However, in both cases, a fraction of total Hand1 was also localised in the nucleoplasm, suggesting that any amount of endogenous Hand1 translocation may be sufficient to drive TG cell differentiation.

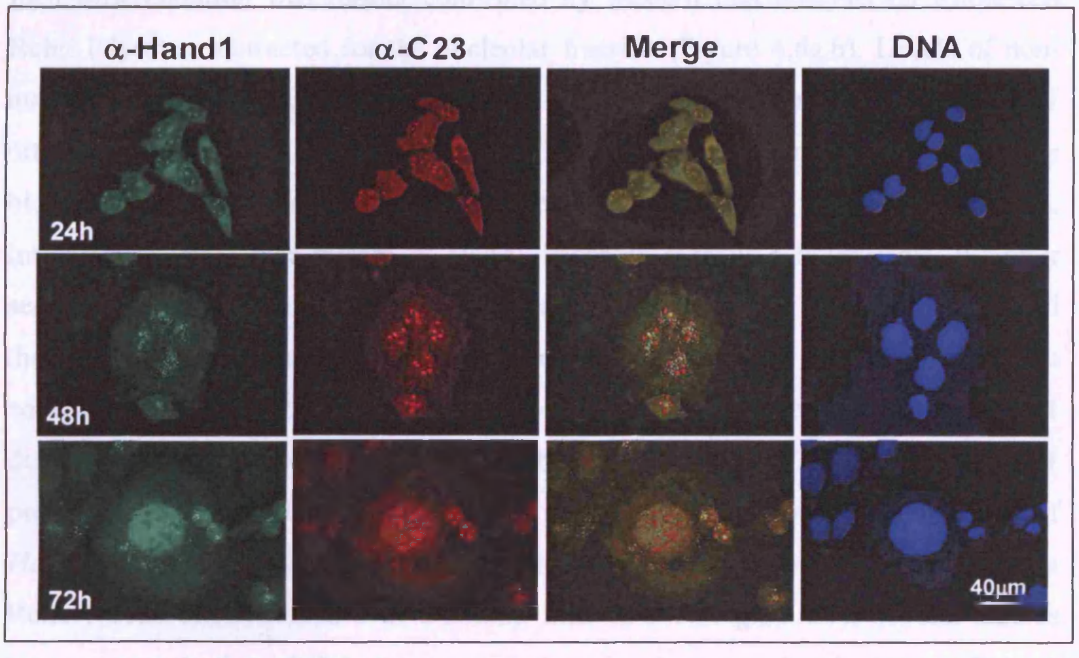

Figure 4.4. Release of nucleolar-endogenous Hand1 coincides with Rcho-1 stem cell commitment to a trophoblast giant cell fate.

Immunostaining for α-Hand1 and α-C23 over a 72 hour time-course of Rcho-1 differentiation reveals that endogenous Hand1 is predominantly localised to nucleoli in Rcho-1 stem cells (indicated as 24h). However, nucleolar-endogenous Hand1 is released to assume a nuclear-wide localisation coincident with a commitment of Rcho-1 stem cells to differentiate over a 72-hour period.

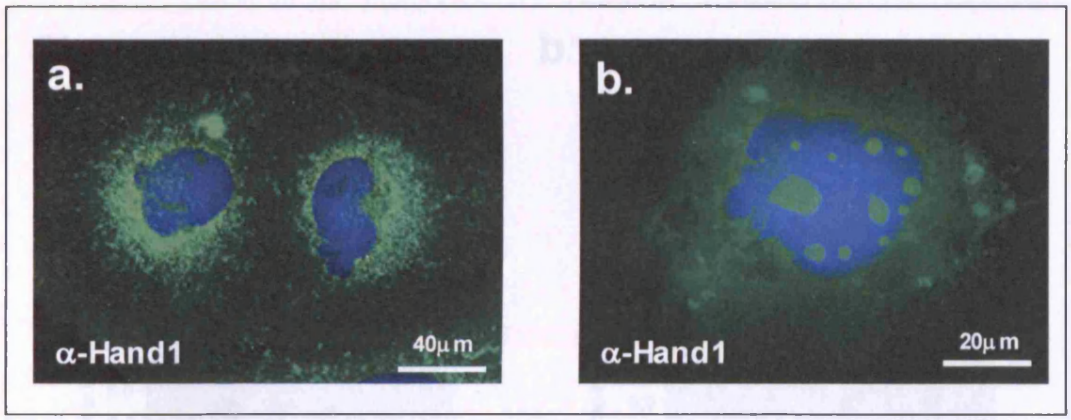

Figure 4.5. Endogenous Hand1 can occupy different subcellular localisations in trophoblast giant cells.

Endogenous Hand1 is localised to the peri-nuclear region (**a**) or occasionally retained in the nucleolus (**b**) in <5% of TG cells (induced by a change in serum conditions and differentiated for 72 hours). However, a proportion of Hand1 in both instances is nuclear-wide and induces TG cell differentiation.

Release of endogenous Hand1 from the nucleoli of Rcho-1 stem cells during their differentiation was further confirmed by western blot analysis on whole-cell Rcho-1 lysates subtracted for the nucleolar fraction (Figure 4.6a,b). Levels of non-nucleolar Hand1 protein were analysed over an 8-day time-course of Rcho-1 differentiation induced by a change in serum conditions (Figure 4.6a). The western blot data confirm the absence of nuclear-wide Hand1 in Rcho-1 stem cells. Interestingly, nucleolar release of Hand1 becomes evident 3 hours ('day 0') after serum withdrawal. Furthermore, a more detailed western blot time-course revealed that endogenous Hand1 relocates from the nucleolar to the nucleoplasmic compartment just 1.5-2 hours after serum conditions are modified to promote Rcho-1 differentiation (Figure 4.6b). Importantly, the elevated levels of non-nucleolar Hand1 protein at the onset of differentiation are not accompanied by an up-regulation of *Hand1* transcription, as revealed by a northern blot analysis on mRNA extracted from Rcho-1 cells differentiated over a similar time-course (Figure 4.7). Several studies have reported that *β-Tubulin* transcription is down-regulated during Rcho-1 differentiation (Faria and Soares, 1991; Hamlin *et al.*, 1994). This explains our preference for the GAPDH probe and antibody in these analyses. In addition, GAPDH protein was shown to localise to the nucleolus in recent nucleolar proteomic analyses, further validating its use here as a loading control (Andersen *et al.*, 2002).

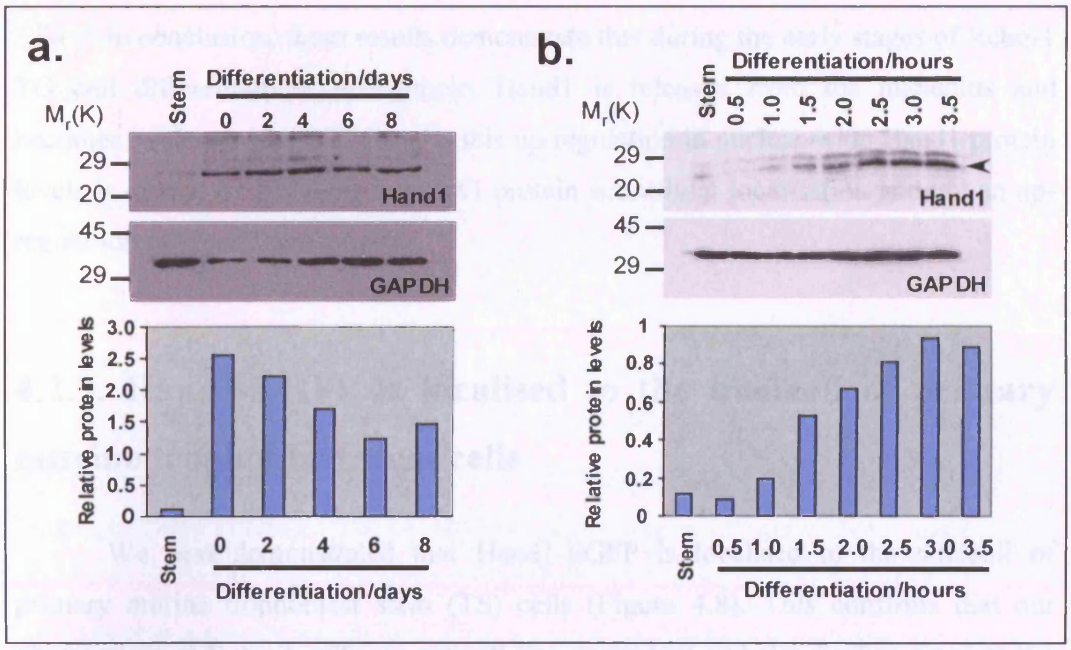

Figure 4.6. Redistribution of nucleolar-endogenous Hand1 during Rcho-1 differentiation is confirmed by western blot analysis.

Western blot analysis using whole-cell lysates of Rcho-1 cells (subtracted for the nucleolar fraction) induced to differentiate over an 8-day time course reveal that nucleolar-endogenous Hand1 becomes nuclear-wide just 3 hours ('day 0') after a change in serum conditions (20% FBS to 10% HS) (**a**). A more detailed time-course reveals that this nucleolar-to-nuclear relocation of endogenous Hand1 is initiated just 1.5 hours after this change in serum conditions (**b**).

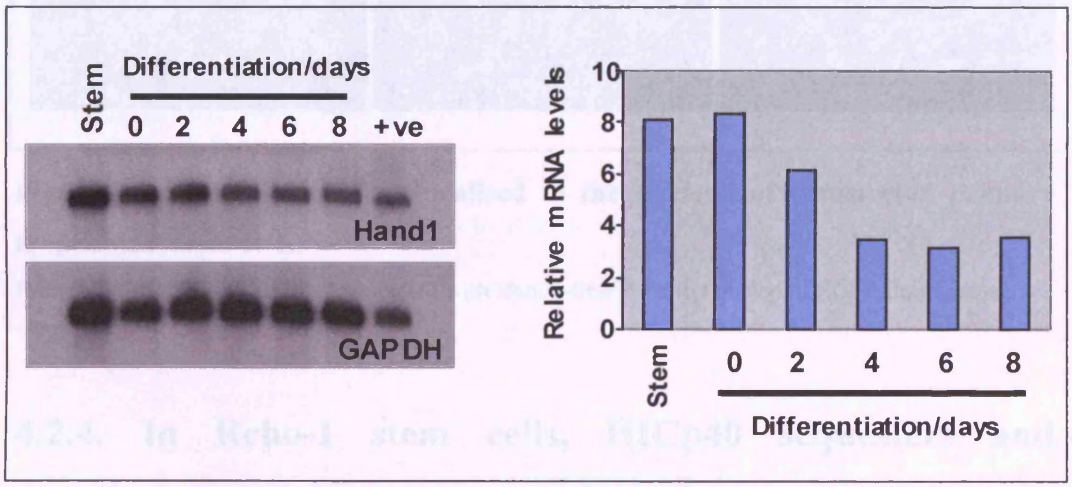

Figure 4.7. *Hand1* transcription is not up-regulated during Rcho-1 trophoblast giant cell differentiation.

Northern blot analysis reveals that *Hand1* transcription is not up-regulated at the onset of TG cell differentiation in Rcho-1 cells induced to differentiate by a change in serum (20% FBS to 10% HS).

In conclusion, these results demonstrate that during the early stages of Rcho-1 TG cell differentiation, endogenous Hand1 is released from the nucleolus and becomes nuclear-wide. Importantly, this up-regulation in nuclear-wide Hand1 protein levels is caused by a change in Hand1 protein subcellular localisation and not an up-regulation of *Hand1* transcription.

4.2.3. Hand1-EGFP is localised to the nucleoli of primary murine trophoblast stem cells

We next demonstrated that Hand1-EGFP is localised to the nucleoli of primary murine trophoblast stem (TS) cells (Figure 4.8). This confirms that our observations in Rcho-1 cells are not cell line-dependent and also further supports the authenticity of the Rcho-1 model with respect to trophoblast *in vivo*.

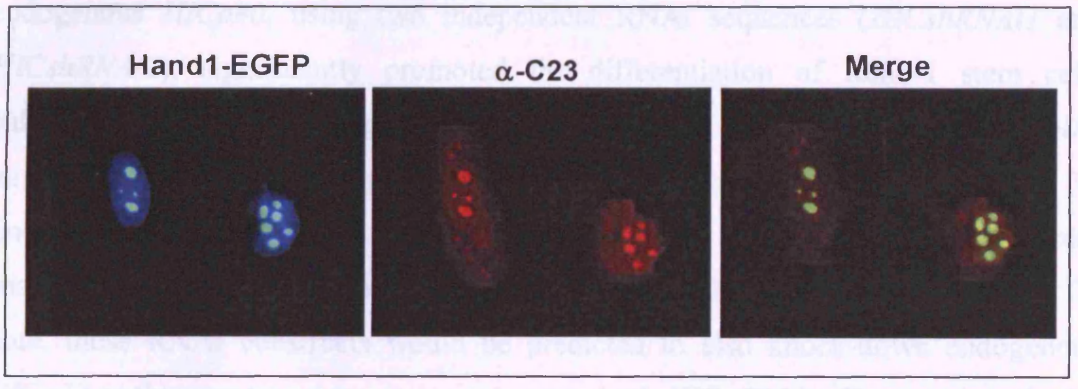

Figure 4.8. Hand1-EGFP is localised to the nucleoli of transfected primary trophoblast stem cells.

Primary trophoblast stem cells transfected with Hand1-EGFP exhibit nucleolar EGFP fluorescence.

4.2.4. In Rcho-1 stem cells, HICp40 sequesters and negatively-regulates endogenous Hand1 in the nucleolus

To investigate the functional significance of Hand1 nucleolar sequestration by HICp40 *in vivo*, we next conducted over-expression (gain-of-function) and RNA-interference (RNAi)-mediated knock-down (loss-of-function) assays involving

HICp40 in Rcho-1 stem cells (Figure 4.9). Over-expression of HICp40 as an EGFP fusion protein (HICp40-EGFP) significantly blocked the differentiation of Rcho-1 stem cells cultured in differentiation-inducing conditions, compared to untransfected Rcho-1 cells cultured in the same conditions (Figure 4.9a). Only transfected cells were counted, and these were identified by virtue of EGFP fluorescence.

We conversely used RNAi to knock-down endogenous *HICp40*. RNAi is a multi-step process involving the generation of a large double-stranded RNA (dsRNA), which is cleaved into small interfering RNAs (siRNAs) *in vivo* by an RNase III endonuclease. These siRNAs down-regulate target gene expression by forming an RNA-induced silencing complex (RISC) with cellular proteins. RISC then promotes the degradation of mRNAs containing sequences similar to the siRNA component and also may silence the target gene by recruitment of chromatin remodelling complexes (reviewed by Hannon, 2002). RNAi-mediated knock-down of endogenous *HICp40*, using two independent RNAi sequences (*HICshRNAi1* and *HICshRNAi2*), significantly promoted the differentiation of Rcho-1 stem cells cultured in non-differentiating conditions (Figure 4.9b; sequence of RNAi oligonucleotides and their position within HICp40 are shown in Appendix 3). Endogenous *HICp40* knock-down was confirmed in this study by western blot analysis using an anti-HIC antibody, a kind gift from J.-M. Mesnard (Figure 4.9c). Of note, these RNAi constructs would be predicted to also knock-down endogenous *HICp32* as they contain sequences common to both *HIC* cDNAs. However, nucleolar localisation of endogenous Hand1 was a functional read-out that applied exclusively to HICp40-dependent sequestration.

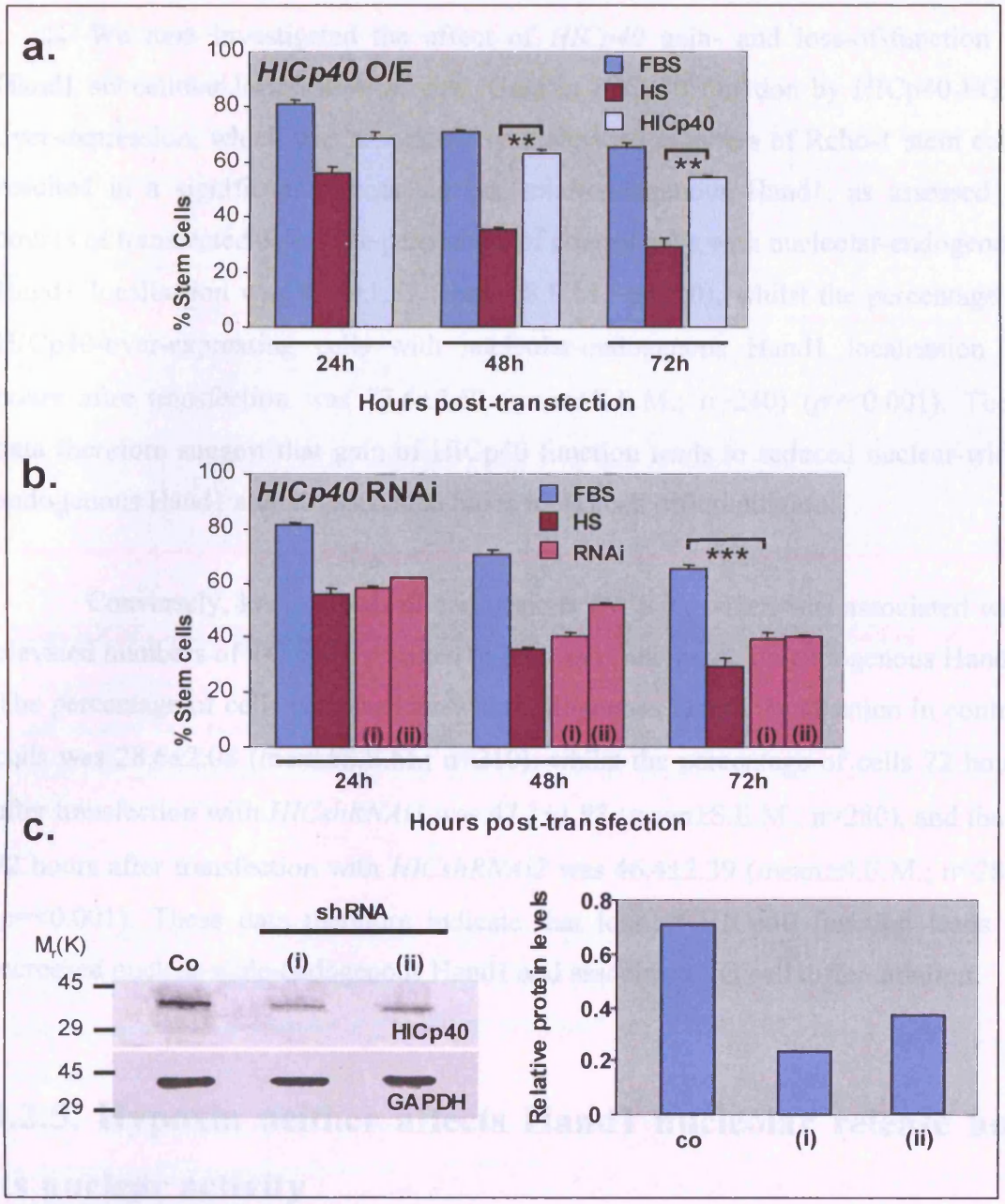

Figure 4.9. HICp40 gain- and loss-of function assays reveal that HICp40 sequesters Hand1 into the nucleolus and negatively-regulates its activity *in vivo*.

Over-expression of HICp40-EGFP in Rcho-1 stem cells cultured in differentiation-inducing conditions (shown as HS) significantly inhibits TG cell differentiation (**a**). In comparison, knock-down of endogenous *HICp40* in Rcho-1 stem cells cultured in non-differentiating conditions (shown as FBS), using two independent RNAi sequences of *HICp40* (*HICshRNAi1* (i) and *HICshRNAi2* (ii)), significantly promotes TG cell differentiation (**b**). *HICp40* knock-down was demonstrated in this assay by western blot analysis using an anti-HIC antibody and then comparing HIC levels between un-transfected (control, Co) and transfected cells by scanning densitometry (**c**). Measurements are mean±S.E.M.; n=350; ** indicates $p<0.01$; *** indicates $p<0.001$. **o/e**: over-expression.

We next investigated the effect of *HICp40* gain- and loss-of-function on Hand1 subcellular localisation *in vivo*. Gain in HICp40 function by HICp40-EGFP over-expression, which was associated with elevated numbers of Rcho-1 stem cells, resulted in a significant increase in nucleolar-endogenous Hand1, as assessed by counts of transfected cells. The percentage of control cells with nucleolar-endogenous Hand1 localisation was 43.9±1.87 (mean±S.E.M.; n=210), whilst the percentage of HICp40-over-expressing cells with nucleolar-endogenous Hand1 localisation 72 hours after transfection was 77.6±2.67 (mean±S.E.M.; n=240) (p=<0.001). These data therefore suggest that gain of HICp40 function leads to reduced nuclear-wide-endogenous Hand1 and an associated block to TG cell differentiation.

Conversely, knock-down of endogenous *HICp40*, which was associated with elevated numbers of TG cells, resulted in increased nuclear-wide-endogenous Hand1. The percentage of cells with nuclear-wide-endogenous Hand1 localisation in control cells was 28.6±2.08 (mean±S.E.M.; n=210), whilst the percentage of cells 72 hours after transfection with *HICshRNAi1* was 47.1±1.93 (mean±S.E.M.; n=280), and those 72 hours after transfection with *HICshRNAi2* was 46.4±2.39 (mean±S.E.M.; n=280) (p=<0.001). These data therefore indicate that loss of HICp40 function leads to increased nuclear-wide-endogenous Hand1 and associated TG cell differentiation.

4.2.5. Hypoxia neither affects Hand1 nucleolar release nor its nuclear activity

Previous studies have revealed that hypoxia blocks the proper differentiation of Rcho-1 stem cells and other trophoblast stem cell models *in vitro* (Gultice *et al.*, 2006; Lash *et al.*, 2007; Takeda *et al.*, 2007). Therefore, we sought to determine whether culture of Rcho-1 cells under hypoxic conditions has an effect on Hand1 nucleolar release. Hypoxic conditions were attained by either supplementing the medium with 250μM cobalt chloride, which has previously been shown, in cell lines including Rcho-1 cells, to initiate intracellular hypoxic signalling cascades (Hayashi *et al.*, 2004), or by culturing cells in a hypoxic chamber (1% oxygen, 5% carbon dioxide, 94% nitrogen). Cells cultured under hypoxic conditions were shown by

western blot analysis to have increased levels of the alpha subunit of the hypoxia inducible factor (HIF), a heterodimeric transcription factor activated by low oxygen (reviewed by Cannigia, 2000). This is consistent with an appropriate cellular response to low oxygen tension (Figure 4.10).

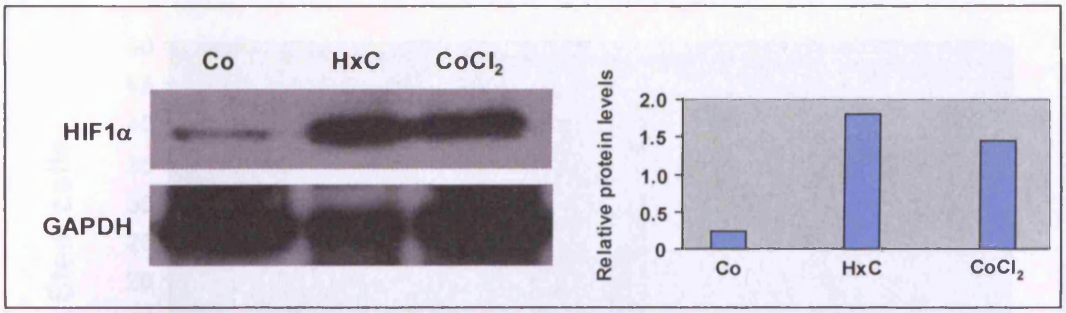

Figure 4.10. Rcho-1 cells cultured under conditions that induce a hypoxic cellular response up-regulate the hypoxia-inducible factor-1 alpha subunit.

Culture of Rcho-1 cells in a hypoxic chamber (HxC) or in medium supplemented with 250μM cobalt chloride ($CoCl_2$) induces HIF1α up-regulation. This was assessed by western blot analysis using an anti-HIF1α antibody and then comparing HIF1α levels between control (cultured in normoxic conditions; Co) and cells exhibiting a hypoxic response by scanning densitometry.

Culture of Rcho-1 stem cells in differentiation-inducing (10% HS-supplemented medium) conditions in either medium supplemented with cobalt chloride or in a hypoxic cell culture chamber resulted in a significant suppression of TG cell differentiation over 72 hour period in conditions that favour their differentiation (Figure 4.11). This is compared with Rcho-1 cells differentiated in normoxic, differentiation-inducing conditions and was assessed by PL-1 expression and changes in cytoskeletal organisation by staining for F-actin, as carried out by a previous study (Gultice *et al.*, 2006). However, the percentage of Rcho-1 stem cells cultured in normoxic, differentiation-inducing conditions for 72 hours that exhibit nucleolar-endogenous Hand1 localisation (43.9±1.87 (mean±S.E.M.; n=210)) was not significantly different to the percentage of Rcho-1 stem cells cultured in hypoxic-response-inducing, differentiation-inducing conditions for the same time period with nucleolar-endogenous Hand1 (44.6±2.01 (mean±S.E.M.; n=220) for cells cultured in a hypoxic chamber, and 45.6±1.51 (mean±S.E.M.; n=220) for cells cultured in medium supplemented with 250μM $CoCl_2$). Furthermore, hypoxia had no effect on

the ability of Hand1-EGFP to drive Rcho-1 differentiation over a 72 hour period post-transfection (Figure 4.12). These data therefore suggest that oxygen tension influences the process of TG cell differentiation, but achieves this neither by affecting the release of Hand1 from the nucleolus, nor Hand1-EGFP activity in the nucleus.

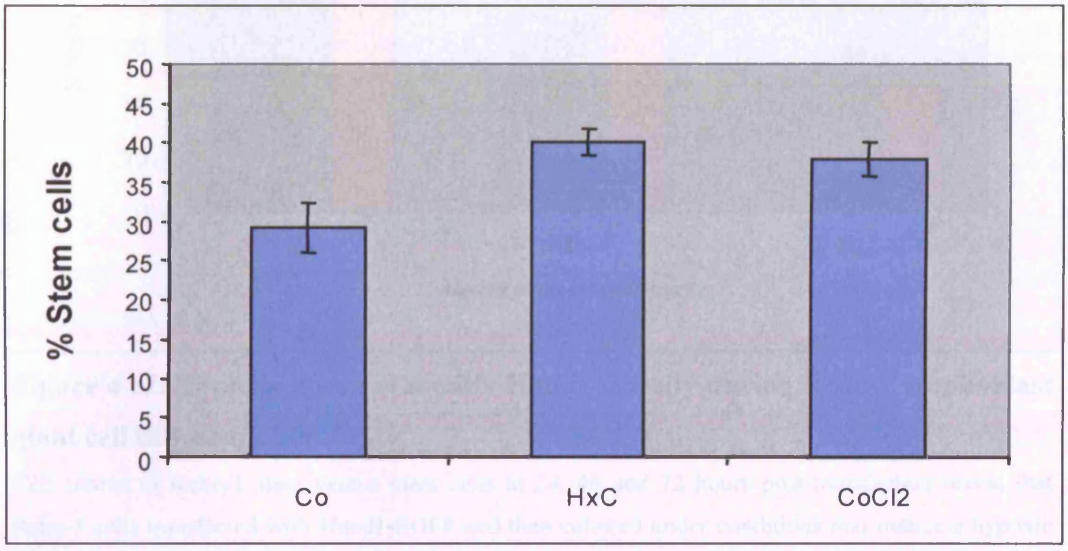

Figure 4.11. Hypoxia significantly blocks Rcho-1 TG cell differentiation.

Cell counts of Rcho-1 cells 72 hours after serum conditions were changed to promote their differentiation (20% FBS to 10% HS) revealed that cells cultured in hypoxic-response-inducing conditions (either in a hypoxic cell culture chamber (**HxC**) or in the presence of 250μM $CoCl_2$) have a reduced rate of TG cell differentiation, indicated by a reduced number of giant cells and an increased number of stem cells, than control cells cultured in normoxic conditions (**Co**). TG cells were identified by PL-I up-regulation and cytoskeletal re-organisation. Measurements are mean±S.E.M.; n=270; * indicates $p<0.05$; ** indicates $p<0.01$.

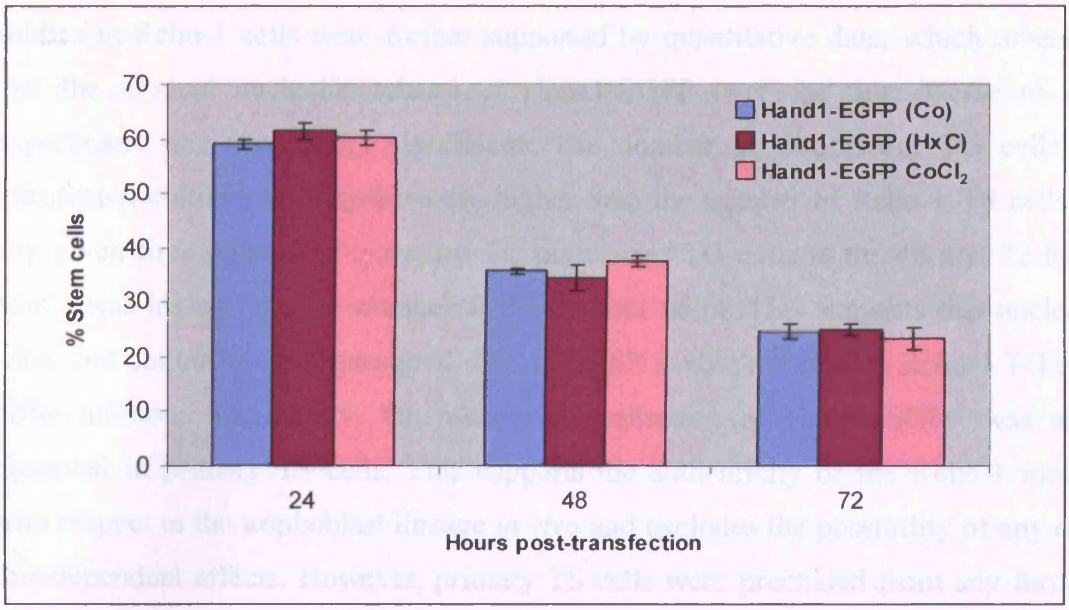

Figure 4.12. Hypoxia does not modify Hand1 activity during Rcho-1 trophoblast giant cell differentiation.

Cell counts of Rcho-1 stem versus giant cells at 24, 48 and 72 hours post-transfection reveal that Rcho-1 cells transfected with Hand1-EGFP and then cultured under conditions that induce a hypoxic response (either in a hypoxic cell culture chamber (**HxC**) or in the presence of 250μM $CoCl_2$) do not have a significantly different rate of differentiation to control cells transfected with Hand1-EGFP and then cultured under normoxic conditions (**Co**). All cells were cultured under differentiation-inducing conditions (10% HS-supplemented medium). TG cells were identified by PL-I up-regulation and cytoskeletal reorganisation. Measurements are mean±S.E.M.; n=250.

4.3. DISCUSSION

4.3.1. The activity of Hand1 is regulated by nucleolar sequestration and release in rodent trophoblast

We have demonstrated that a Hand1-EGFP fusion protein, nucleolar in Rcho-1 stem cells, gradually disperses throughout the nucleus over a time course of 72 hours as these cells undergo TG cell differentiation. TG cells exhibiting nuclear-wide Hand1-EGFP are importantly *bona fide*, as determined by a characteristic up-regulation of *PL-1* and associated changes in actin cytoskeleton and cell motility (Faria *et al.*, 1991; Parast *et al.*, 2001). The Hand1-EGFP immuno-localisation

studies in Rcho-1 cells were further supported by quantitative data, which revealed that the gradual nucleolar release of Hand1-EGFP over the time-course of the experiment was statistically significant. The number of fluorescent TG cells in transfected cultures was significantly higher than the number of Rcho-1 TS cells at any given time point, and moreover the number of TG cells at the 48 and 72 hour points was higher than the number at the 24 hour point. This suggests that nuclear-wide, but not nucleolar-sequestered, Hand1-EGFP is able to promote Rcho-1 TG cell differentiation. Importantly, the nucleolar localisation of Hand1-EGFP was also observed in primary TS cells. This supports the authenticity of the Rcho-1 model with respect to the trophoblast lineage *in vivo* and excludes the possibility of any cell line-dependent effects. However, primary TS cells were precluded from any further use in these studies due to well-characterised problems with the maintenance of primary TS cells in an undifferentiated state in culture and very low transfection efficiency (S. Tanaka, personal communication).

Immunostaining for endogenous Hand1 using an anti-Hand1 antibody revealed a similar relocation of the protein during Rcho-1 differentiation. This result was confirmed by western analysis using the same antibody on whole cell lysates, subtracted for nucleolar content, taken over a time course of Rcho-1 differentiation induced by serum withdrawal. Notably, nucleoplasmic levels of Hand1 protein were significantly elevated only 1.5-3 hours after a change in serum conditions to promote differentiation. This suggests that the release of nucleolar Hand1 into the nucleoplasm is required for the earliest stages of TG cell differentiation. This event may even be responsible for the commitment of Rcho-1 stem cells to a TG cell fate. Crucially, this rapid increase in nuclear Hand1 protein level does not appear to be due to an up-regulation of *Hand1* transcription. Northern analysis on the equivalent time-course revealed neither a change in *Hand1* mRNA levels at the onset of Rcho-1 differentiation nor during long-term differentiation. This observation of a constant level of *Hand1* transcription during differentiation, although entirely reproducible, is at odds with previous studies (Cross *et al.*, 1995; Firulli *et al.*, 2003). The reason(s) for this discrepancy remains unclear.

It is worth here speculating on the underlying basis for the protocol used in this chapter to generate sub-cellular lysates. The study by Kurki and colleagues does

not explain how the protocol operates at the molecular level (Kurki *et al.*, 2004). Nonetheless immunostaining for nucleolar and non-nucleolar proteins revealed appropriate enrichment in the two subcellular fractions (data not shown), which suggested that the lysis protocol successfully separates the two cell compartments. We presume that the lysis buffer used in our current study, sufficient to lyse the cell and nuclear membranes, cannot break up the nucleoli. As will be discussed in Chapter 6 (section 6.4.1), nucleoli are membrane-less. Nonetheless they are robust structures whose architecture is held together by the rDNA and ribosome biogenesis machinery. When mammalian nuclei are physically disrupted, nucleoli remain intact even under conditions that disintegrate most other subnuclear bodies. Crucially, HICp40 and Hand1 would remain in the nucleolar fraction as many proteins that localise to the nucleolus are thought to bind the negatively-charged rDNA and acidic nucleolar proteins. So perhaps the inherently compact, dense structure of the nucleolus is resistant to (insoluble in) the NP-40 lysis buffer and can be separated in pellet form from the remainder of the cell lysate by ultra-centrifugation. NP-40 lysis buffer may be a more 'gentle' reagent than, for example, RIPA buffer in this regard. Only upon boiling the pellet in Laemelli buffer can the nucleolar proteins be denatured and suspended in solution. Possibly, this fraction also contains other organelles, meaning that the 'nucleolar' fraction is impure. However a 'dirty' method such as this was sufficient to illustrate the bulk translocation of Hand1 from the nucleolar to the nuclear fraction for the purposes of our study. Further confirmation of the nucleolar sequestration and release of Hand1 could be attained by employing the more precise nucleolar isolation protocol of Angus Lamond's group (listed at www.lamondlab.com/pdf/noprotocol). This involves centrifugation of sonicated nuclei through sucrose solutions of graded concentration.

We have also demonstrated a functional relationship between HICp40 and Hand1, important for the control of TS cell fate, which involves the nucleolar sequestration and inactivation of Hand1 in Rcho-1 stem cells. Over-expression of HICp40 as an EGFP fusion protein in differentiation-inducing conditions significantly reduced Rcho-1 differentiation compared to untransfected Rcho-1 cells cultured in the same conditions. Conversely, RNAi-mediated knock-down of *HICp40* significantly enhanced the differentiation of Rcho-1 stem cells cultured under conditions that ordinarily maintain a proliferative Rcho-1 stem cell population.

Furthermore, this gain- or loss-of-function of HICp40 correlated with a bias towards Hand1 nucleolar- or nuclear-localisation respectively, as assessed by cell counts. This confirms that the effects of *HICp40* gain- and loss-of-function on TG cell differentiation are mediated through changing Hand1 subcellular localisation.

According to our data, the level of Hand1-EGFP nuclear translocation does not seem to correlate precisely with the increase in Rcho-1 TG cell differentiation. Similarly, although cohorts (<5%) of TG cells exhibited peri-nuclear- or nucleolar-endogenous Hand1, in both cases some fluorescence was also nuclear-localised. Although the spontaneous rate of Rcho-1 differentiation was taken into account during our quantitative analyses, the exact figure may have varied between transfected populations. Furthermore, Hand1 is clearly not the only factor that promotes TG cell differentiation and other factors that modulate this process may have affected the cell counts. For example, Ap-2γ is another transcription factor required for TG cell differentiation (Auman *et al.*, 2002) and its activity may have varied between transfected populations in our assays. Overall, however, our data indicate that the release of any amount of nucleolar Hand1-EGFP, or nucleolar-endogenous Hand1, may be sufficient to drive Rcho-1 TG cell differentiation. In summary, the data presented in this chapter are consistent with a role for HICp40-mediated nucleolar sequestration of Hand1 in governing TS cell fate.

4.3.2. Hypoxia inhibits Rcho-1 differentiation but not by modulating Hand1 nucleolar release

Mounting evidence suggests a link between protein nucleolar sequestration and the cellular response to hypoxia. Nucleolar confinement of both the alpha subunit of HIF-1 (Fatyol and Szalay, 2001) and its negative regulator, the von Hippel-Lindau (VHL) tumour suppressor (Mekhail *et al.*, 2004), modulate HIF-1 activity. Additionally, human STRA13, a bHLH factor whose mouse orthologue has been proposed to interact with Hand1 in TG cells (Hughes *et al.*, 2004), is up-regulated by hypoxia (Ivanova *et al.*, 2001). Interestingly, Stra13 also associates with Msp58, a protein that localises to the nucleolus (Lin and Shih, 1998). We thus hypothesised that Hand1 may be released from nucleolar confinement only under normoxic

conditions. Indeed, previous studies have demonstrated that aspects of Rcho-1 TG cell and other trophoblast stem cell model differentiation are blocked by low oxygen concentration (Gultice *et al.*, 2006; Lash *et al.*, 2007; Takeda *et al.*, 2007; reviewed in Chapter 1, section 1.2.2.4). A model whereby Hand1 is only released from the nucleolus under normoxic conditions would be biologically-relevant in that TG cell differentiation would be blocked until the placenta makes contacts with the maternal blood supply and cellular oxygen concentration increases. This post-translational mechanism would furthermore explain why, in the study by Gultice and colleagues, *Hand1* mRNA and protein levels were normal in Rcho-1 cells undergoing differentiation under hypoxic conditions (Gultice *et al.*, 2006).

Consistent with the previous studies, we indeed showed that hypoxia suppressed the ability of Rcho-1 cells to differentiate over a 72-hour period. This was assessed by a block to *PL-I* up-regulation and impaired cytoskeletal development. However, this block to differentiation was not due to an inability of Hand1 to escape from the nucleolus. There was no significant difference between the relative proportions of nucleolar- versus nuclear-wide-endogenous Hand1 in TG cells cultured under normoxic or hypoxic conditions for 72 hours after the culture conditions were modified to induce a hypoxic response. Thus, if impaired TG cell differentiation in hypoxic conditions is due to a deficiency of Hand1 activity, these data suggest that the factor may be negatively-regulated after its nucleolar release. However, a further assay revealed that the ability of Hand1-EGFP to drive Rcho-1 differentiation is not modified by hypoxia. On first consideration, these data suggest that the nuclear activity of Hand1 is not modified by oxygen tension. However, *Hand1* was over-expressed in this experiment, and as such any mechanism that ordinarily negatively-regulates endogenous Hand1 in trophoblast cultured under hypoxic conditions may have been squelched by ectopic Hand1-EGFP. In any case, this result serves to reiterate the fact that Hand1 is not the only factor that promotes TG cell differentiation (Chapter 1, Table 1.2b). Hypoxia may thus modify the activity of any one of a number of these TG cell differentiation-inducing factors. At present, just how hypoxia modifies the process of TG cell differentiation, through effects on Hand1 or otherwise, is unknown. What is clear, however, is that oxygen concentration does not appear to modify the nucleolar release of Hand1 during TG cell differentiation.

4.3.3. Summary and concluding remarks

In this chapter we have demonstrated that the previously-described elevation of Hand1 activity during Rcho-1 TG cell differentiation is primarily due to a relocation of pre-existing Hand1 protein rather than an up-regulation of *Hand1* expression. Hand1 is sequestered in an inactive state in the nucleoli of proliferating Rcho-1 stem cells by the rat orthologue of HICp40. However, upon commitment of these cells to a TG cell fate, Hand1 is released into the nucleoplasm, where it can drive Rcho-1 differentiation. However, we provide data that rules out the possibility that hypoxia, previously shown to impair proper Rcho-1 TG cell differentiation, modulates Hand1 nucleolar release.

Protein redistribution may be a more efficient method of regulating TG cell differentiation. Hand1 protein release into the nucleoplasm enables a rapid, likely almost instantaneous, commitment of Rcho-1 stem cells to a TG cell fate. This mechanism is probably more suited to govern TS cell fate than the relatively slow alternative of inducing an up-regulation of the *Hand1* gene, followed by protein translation, in response to serum withdrawal. In this regard, our findings support previous studies that implicate the nucleolus as a molecular 'safe' or 'sink' that temporarily stores factors in an inactive state until a specific cell cycle stage or metabolic state (Tao and Levine, 1999; Weber *et al.*, 1999; Datta *et al.*, 2004).

Our RT-PCR data, presented in Figure 3.6b, indicate a persistence of the rat orthologue of HICp40 in differentiated Rcho-1 TG cells. Thus it is likely that HICp40 and/ or Hand1 are post-translationally modified to abrogate their interaction and permit Hand1 nucleolar release. In this regard, we next investigated the mechanism underlying Hand1 nucleolar release at the point of Rcho-1 stem cell commitment to differentiate and our findings are presented in the following chapter.

Chapter 5

Phosphorylation of Hand1 underlies its release from the nucleolus

5.1. INTRODUCTION

We next investigated the molecular mechanism that underlies the release of Hand1 from the nucleolus. Post-translational modification is a quick and reversible way of modulating the activity of a transcription factor. For example, phosphorylation of residues within the basic domain of myogenic bHLH transcription factors enhances their DNA-binding efficiency (Li *et al.*, 1992; Zhou and Olson, 1994). Additionally, phosphorylation of MyoD encourages its heterodimerisation with E12 (Lenormand *et al.*, 1997). A wide range of post-translational modifications and ligands have been implicated in the nucleolar-nucleoplasmic or nucleolar-cytoplasmic shuttling of factors (Table 5.1). Despite this, phosphorylation is by far the most widely-used mechanism that underpins the nucleolar release of factors and several protein kinases and phosphatases have been localised to this organelle (Andersen *et al.*, 2005). The best-characterised example of this is the phosphorylation of the budding yeast protein phosphatase Cdc14 by the polo-like kinase Cdc5. This event promotes Cdc14 nucleolar release as an essential step towards exit from mitosis (Shou *et al.*, 1999; 2002; Visintin *et al.*, 1999; 2003; Yoshida and Toh-e, 2002).

Hand1 is phosphorylated at the helix 1 residues T107 and S109 during Rcho-1 TG cell differentiation (Firulli *et al.*, 2003). These residues are highly-conserved between bHLH factors of the Twist subfamily (Figure 1.1b). This process is enhanced by a down-regulation of the protein phosphatase 2A (PP2A) regulatory subunit B56δ, which targets Hand1 for dephosphorylation. The protein kinases PKC and PKA were suggested to site-specifically phosphorylate Hand1 during Rcho-1 differentiation. The resultant net increase in Hand1 phosphorylation at these two residues was shown to enhance the affinity of the transcription factor for its E-factor binding partners as an important step in the TG cell differentiation program (Firulli *et al.*, 2003). We hypothesised, therefore, that phosphorylation of Hand1 at these helix 1 residues underlies its nucleolar release, as a pre-requisite for its E-factor binding and biological activity in the nucleus.

Table 5.1. Post-translational modifications that underlie the nucleolar-nucleoplasmic/ cytoplasmic shuttling of factors.

Post-translational Modification	Factor	Reference(s)
Asymmetric dimethylation of arginine residues	bFGF	Xu *et al.*, 2003.
Poly(ADP-ribosyl)ation	CTCF	Torrano *et al.*, 2006.
Hydrogen ion binding	VHL	Mekhail *et al.*, 2004.
GTP binding	B23	Finch *et al.*, 1995.
	Nucleostemin	Tsai and McKay, 2005.
	Rrp22	Elam *et al.*, 2005.
	Gnl3l	Rao *et al.*, 2006.
Calcium ion binding	Calmodulin	Thorogate and Torok, 2007.
Phosphorylation	Nucleolin	Schwab and Dreyer, 1997.
	Ki-67	Endl and Gerdes, 2000.
	Cdc14	Shou *et al.*, 2002.
	pRB	Takemura *et al.*, 2002.
	TIF-IA	Mayer *et al.*, 2005.
	Limk2	Goyal *et al.*, 2006.
	B23	Negi and Olson, 2006.

5.2. RESULTS

5.2.1. Phosphorylation of nucleoplasmic Hand1 increases during Rcho-1 differentiation

We first sought to investigate whether the nucleolar release of Hand1 coincides with increased Hand1 phosphorylation. To this end, we conducted western blot analysis using an anti-phosphoserine antibody on whole-cell Rcho-1 lysates subtracted for the nucleolar fraction over a time course of differentiation induced by a change in serum conditions (from 20% fetal bovine serum (FBS) to 10% horse serum (HS); stem, 0-8 days; Figure 5.1). This assay revealed that phosphorylation of non-

nucleolar-endogenous Hand1 increased during this time-course, particularly between the stem cell stage and 'day 0' (3 hours after a commitment to differentiate), relative to total cellular-endogenous (i.e. including nucleolar) Hand1. This suggests that Hand1 is phosphorylated coincident with its release from the nucleolus.

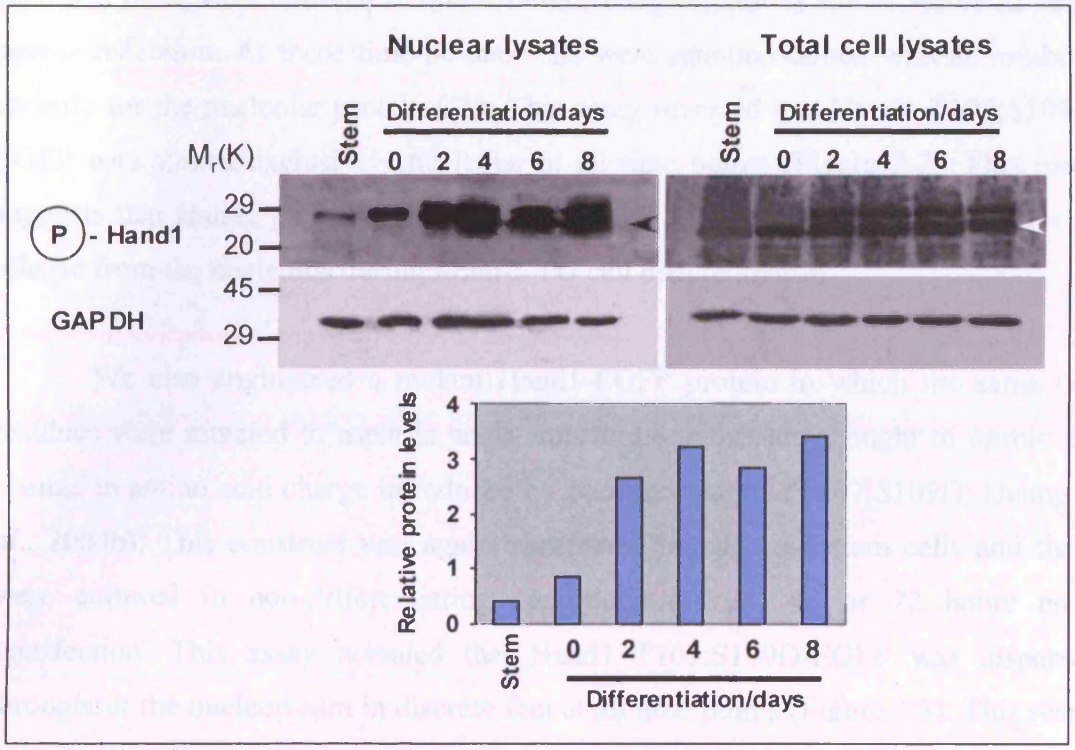

Figure 5.1. Non-nucleolar, endogenous Hand1 is phosphorylated during Rcho-1 differentiation.

Phosphoserine western (lysates subtracted for the nucleolar fraction and total cell, including nucleolar) on Rcho-1 cells over a time-course of differentiation in 10% horse serum (HS; stem, 0-8 days). Elevated non-nucleolar-endogenous, phosphorylated Hand1 at the onset of differentiation ('day 0'; 3 hours' exposure to HS) suggests nucleolar-to-nuclear re-distribution of phosphorylated Hand1.

5.2.2. A Hand1 mutant that cannot be phosphorylated cannot escape from the nucleolus, whilst a Hand1 phosphorylation mimic is nuclear-wide

We next investigated whether the phosphorylation of Hand1 is required for its nucleolar release and moreover which residues are phosphorylated. To this end, we

fused the EGFP cDNA to a Hand1 mutant generously provided by Anthony Firulli in which the two residues previously shown to be phosphorylated during Rcho-1 differentiation were mutated to alanines and, therefore, cannot be phosphorylated (T107;S109A) (Firulli *et al.*, 2003). This construct was transfected into Rcho-1 stem cells and these were cultured in non-differentiating conditions for 24, 48 or 72 hours post-transfection. At these time-points, cells were immunostained with an antibody specific for the nucleolar protein C23. This assay revealed that Hand1 T107;S109A-EGFP was almost exclusively nucleolar at all time points (Figure 5.2). This result suggests that Hand1 phosphorylation at residues T107 and S109 is necessary for its release from the nucleolus during Rcho-1 TG cell differentiation.

We also engineered a mutant Hand1-EGFP protein in which the same two residues were mutated to aspartic acids, substitutions that are thought to mimic the change in amino acid charge introduced by phosphorylation (T107;S109D; Huang *et al.*, 2004b). This construct was again transfected into Rcho-1 stem cells and these were cultured in non-differentiating conditions for 24, 48 or 72 hours post-transfection. This assay revealed that Hand1 T107;S109D-EGFP was dispersed throughout the nucleoplasm in discrete foci at all time points (Figure 5.3). This result suggests that Hand1 phosphorylation at residues T107 and S109 is sufficient for its release from the nucleolus during Rcho-1 differentiation.

We next counted cells to investigate whether the observed differences in the subcellular localisations of these two mutant Hand1-EGFP fusion proteins were statistically significant (Figure 5.4a,c). This data revealed that the number of Hand1-EGFP T107;S109A-transfected cells with nucleolar fluorescence at any time-point post-transfection was significantly higher than the number with nuclear-wide fluorescence at the same time point (also compare Figure 5.4a with Figure 4.2a for differences relating to wild-type Hand1-EGFP). In contrast, the Hand1-EGFP T107;S109D mutant was predominantly nucleoplasmic throughout the time course of the experiment and <5% of cells exhibited nucleolar fluorescence at any given time point (also compare Figure 5.4c with Figure 4.2a). Thus the observed differences in the sub-cellular locations of these two mutant Hand1-EGFP fusion proteins, with respect to wild-type Hand1-EGFP, were statistically significant.

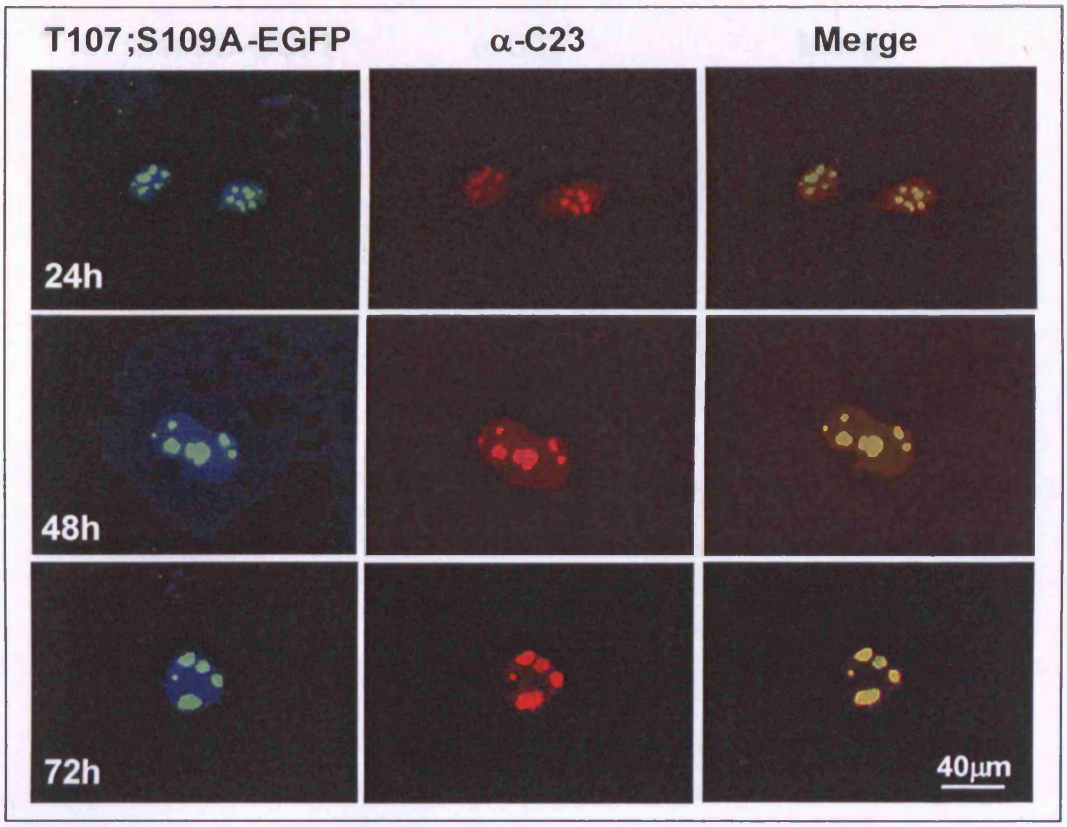

Figure 5.2. Mutation of Hand1 residues T107 and S109 to alanines creates a Hand1 mutant that cannot be released from the nucleolus.

A Hand1-EGFP T107;S109A mutant fusion protein remains nucleolar in transfected Rcho-1 cells over a 72 hour time-course post-transfection.

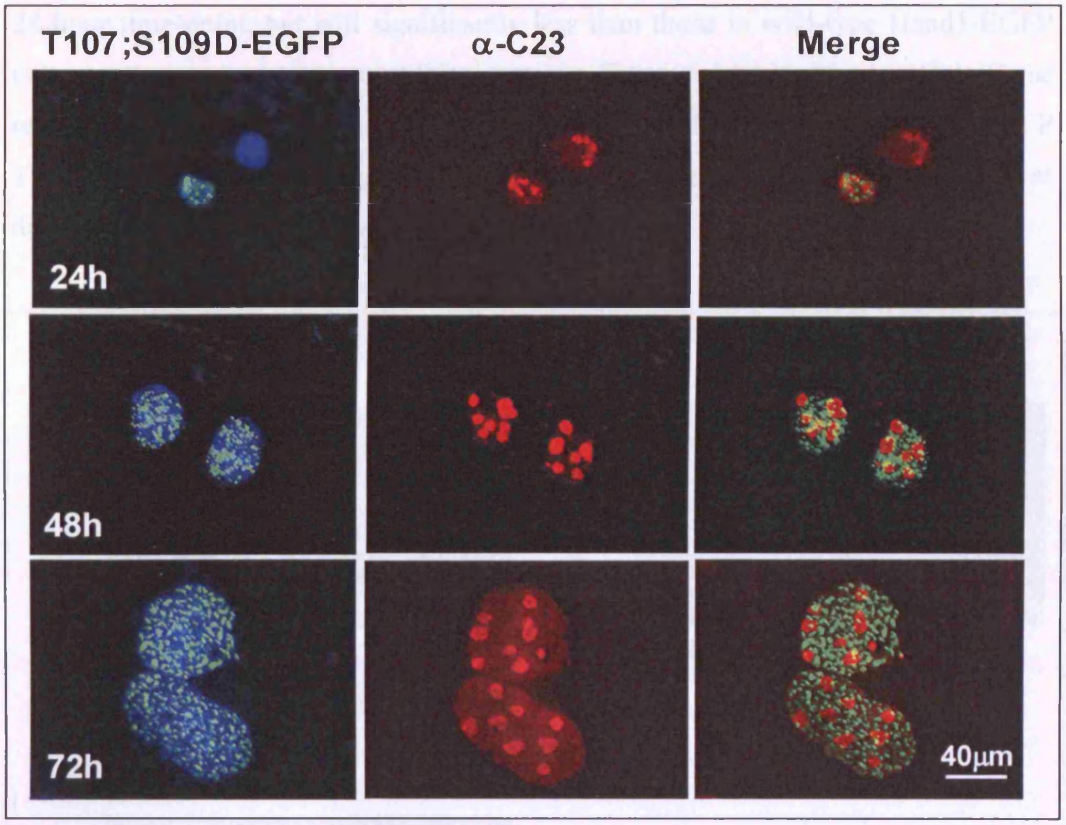

Figure 5.3. Mutation of Hand1 residues T107 and S109 to aspartic acids creates a Hand1 phosphorylation mimic that localises to nucleoplasmic foci.

Hand1-EGFP T107;S109D assumes a nuclear-wide punctate localisation in transfected Rcho-1 cells and this remains over a 72 hour time-course post-transfection.

Moreover the differences in the sub-cellular locations of the Hand1 mutant fusion proteins have a significant bearing on their ability, again relative to wild-type Hand1-EGFP, to induce TG cell differentiation (Figure 5.4b,d). The number of fluorescent TG cells in Hand1-EGFP T107;S109A-transfected populations, as assessed by up-regulation of *PL-1* and cytoskeletal complexity, was significantly less than the number in wild-type Hand1-EGFP-transfected populations at any given time point post-transfection (also compare Figure 5.4b with Figure 4.2b for differences relating to wild-type Hand1-EGFP). Moreover, the number of fluorescent TG cells in Hand1-EGFP T107;S109A-EGFP mutant populations did not significantly increase over the 72-hour time-course. In contrast, the numbers of fluorescent TG cells in Hand1-EGFP T107;S109D mutant populations at the 48- and 72-hours post-transfection were significantly greater than the number of fluorescent TG cells at the

24 hour time-point, but still significantly less than those in wild-type Hand1-EGFP cultures at any given time-point (also compare Figure 5.4d with Figure 4.2b). These results collectively reveal that the Hand1-EGFP T107;S109A and the Hand1-EGFP T107;S109D proteins are significantly less efficient than wild-type Hand1-EGFP at driving Rcho-1 differentiation.

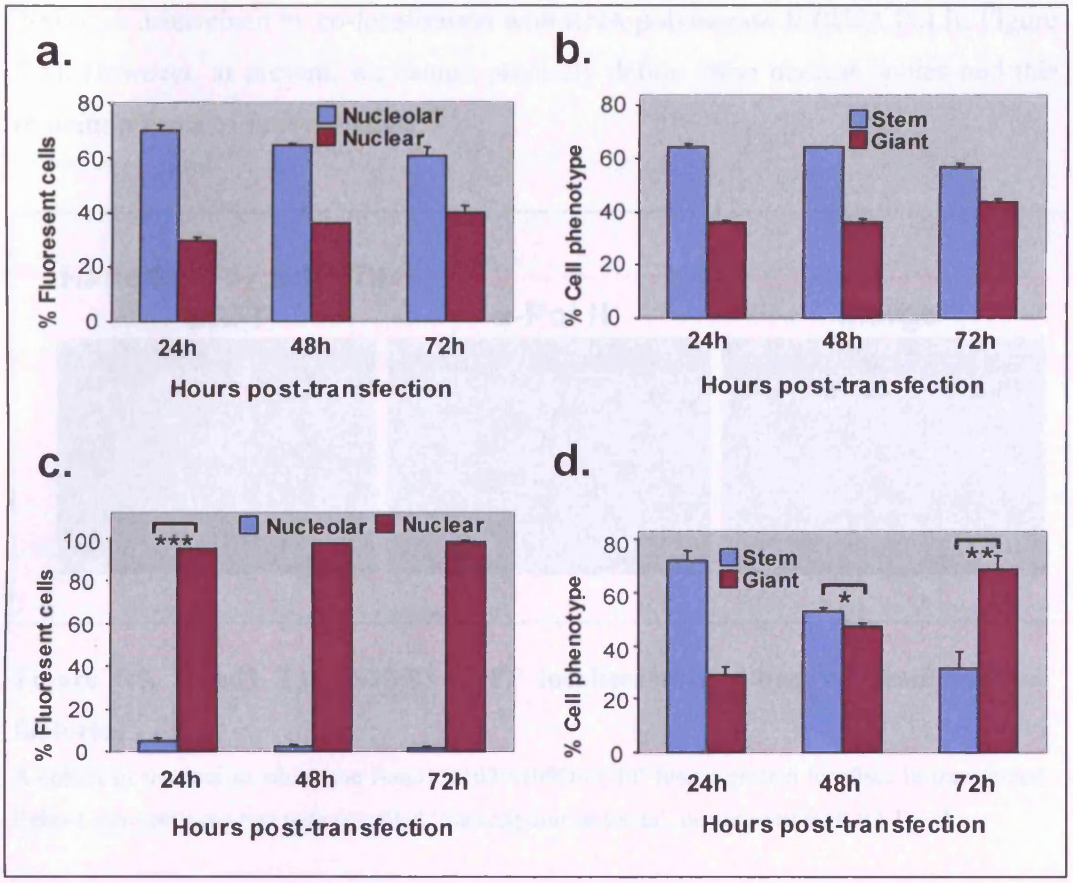

Figure 5.4. The subnuclear locations of the two Hand1 mutants are significantly different and correlate with their relative abilities to drive Rcho-1 differentiation.

Hand1 T107;S109A-EGFP localises predominantly to the nucleolus throughout the 72 hour time course of the experiment (**a**) and is unable to promote TG cell differentiation (**b**). In contrast Hand1 T107;S109D-EGFP is detectable throughout the nucleus at all time points during the experiment (**c**) and is able to promote TG differentiation to an extent similar to, but still significantly less than, wild-type Hand1-EGFP (**d**). Measurements are mean±S.E.M.; n=400. * indicates $p<0.05$; ** indicates $p<0.01$; *** indicates $p<0.001$.

We next carried out experiments with a view to identify the nuclear-wide foci to which the Hand1 T107;S109D-EGFP fusion protein localises. These bodies neither co-localise with Cajal bodies (as assessed by immunostaining with an anti-Coilin antibody; data not shown) nor centromeres (using an anti-CENPB antibody; data not shown). A cohort of these bodies do, however, co-localise with regions of active gene transcription, so called 'transcription factories' (Iborra *et al.*, 1996; Osbourne *et al*, 2004), as determined by co-localisation with RNA polymerase II (RNA Pol II; Figure 5.5). However, at present, we cannot precisely define these nuclear bodies and this remains an area of future studies.

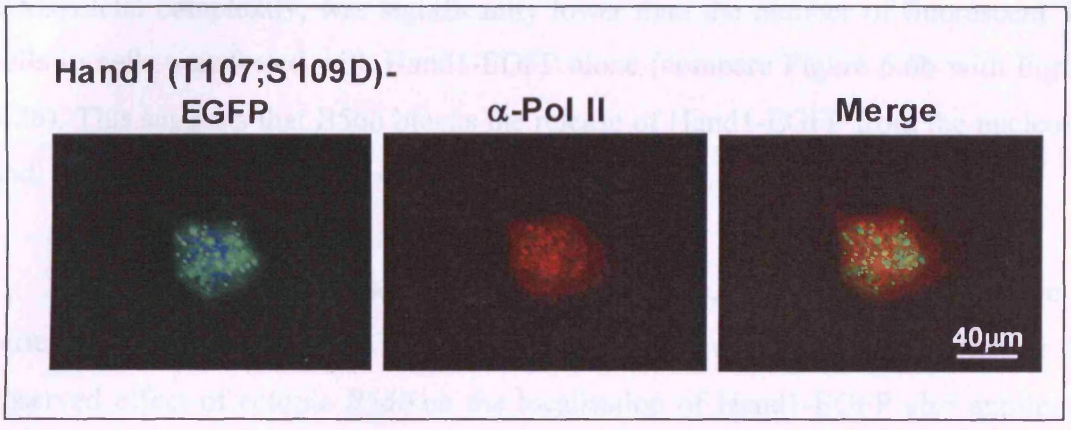

Figure 5.5. Hand1 T107;S109D-EGFP localises to a subset of 'transcription factories'.

A cohort of the foci to which the Hand1 T107;S109D-EGFP fusion protein localises in transfected Rcho-1 stem cells overlap with so-called 'transcription factories', demarcated by RNA Pol II .

5.2.3. B56δ antagonises Hand1-EGFP nucleolar release and is 'eliminated' during Rcho-1 differentiation

In light of our results implicating phosphorylation in the release of nucleolar Hand1, it is interesting that a protein phosphatase 2A (PP2A) complex site-specifically dephosphorylates Hand1 at the T107 and S109 residues in Rcho-1 stem cells (Firulli *et al.*, 2003). The PP2A complex responsible for this contains the regulatory (B, substrate-recognising) subunit B56δ and appropriately *B56δ* expression is down-regulated during Rcho-1 differentiation. Thus, we next

investigated whether B56δ is involved in the regulation of Hand1 activity via nucleolar sequestration.

To this end, we over-expressed a construct encoding *B56δ* in Rcho-1 stem cells co-transfected with Hand1-EGFP under non-differentiating conditions. Compared with Rcho-1 stem cells transfected with Hand1-EGFP alone, significantly more of these cells exhibited nucleolar EGFP fluorescence 72 hours post-transfection (compare Figure 5.6a with Figure 4.2a). Moreover, the number of fluorescent TG cells in co-transfected cultures, as assessed by up-regulation of *PL-1* and changes in cytoskeletal complexity, was significantly lower than the number of fluorescent TG cells in cells transfected with Hand1-EGFP alone (compare Figure 5.6b with Figure 4.2b). This suggests that B56δ blocks the release of Hand1-EGFP from the nucleolus and, in so doing, inhibits Rcho-1 TG cell differentiation.

We next over-expressed *B56δ* in Rcho-1 cells, 24 hours after a change in serum conditions to induce TG cell differentiation, in order to investigate whether the observed effect of ectopic *B56δ* on the localisation of Hand1-EGFP also applies to endogenous Hand1. This was observed to inhibit the differentiation of these cells into TG cells (Figure 5.7) as the number of Rcho-1 TG cells in transfected cultures was significantly lower than in untransfected cultures. Importantly, *B56δ* over-expression was associated with a significant block to the nucleolar release of endogenous Hand1. The percentage of control cells with nucleolar-endogenous Hand1 was 43.9±1.87 (mean±S.E.M.; n=210) compared with the percentage of *B56δ*-overexpressing cells with nucleolar-endogenous Hand1 72 hours after transfection, which was 69.2±2.56 (mean±S.E.M.; n=250) ($p=<0.001$). These results suggest that B56δ blocks the release of endogenous Hand1 from the nucleolus and this inhibits Rcho-1 differentiation.

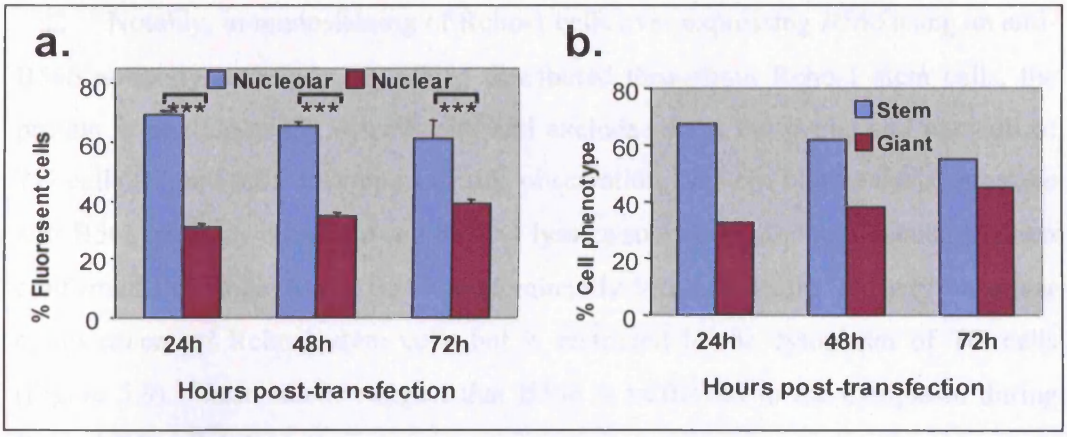

Figure 5.6. B56δ inhibits the nucleolar release of Hand1-EGFP and its promotion of Rcho-1 TG cell differentiation.

Co-expression of B56δ with Hand1-EGFP prevents release of the fluorescent fusion protein from the nucleolus (**a**), relative to when Hand1-EGFP is expressed alone (Figure 4.2a). Ectopic expression of B56δ blocks Hand1-EGFP-induced TG cell differentiation (**b**), relative to when Hand1-EGFP when expressed alone (Figure 4.2b). Measurements are mean±S.E.M.; n=330; * indicates $p<0.05$; ** indicates $p<0.01$; *** indicates $p<0.001$.

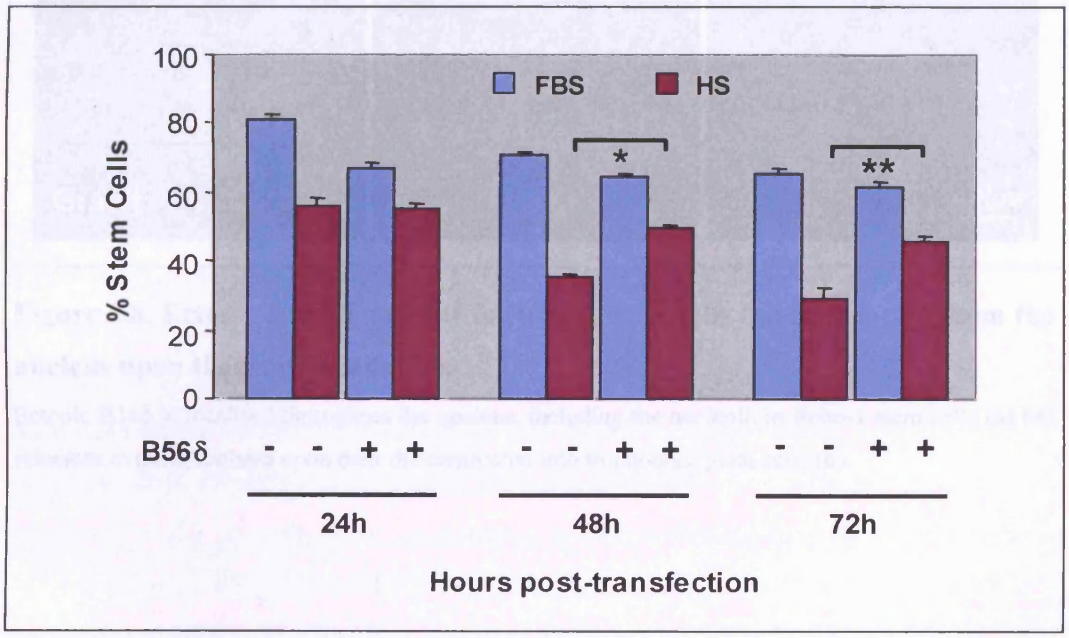

Figure 5.7. B56δ inhibits Rcho-1 TG cell differentiation induced by a change in serum conditions.

Ectopic expression of *B56δ* in Rcho-1 stem cells, 24 hours after serum replacement to induce differentiation, inhibits TG cell differentiation. Measurements are mean±S.E.M.; n=350; * indicates $p<0.05$; ** indicates $p<0.01$; *** indicates $p<0.001$.

Notably, immunostaining of Rcho-1 cells over-expressing *B56δ* using an anti-B56δ antibody revealed that, whilst distributed throughout Rcho-1 stem cells, the protein is predominantly cytoplasmic and excluded from the nuclei and nucleoli of TG cells (Figure 5.8). In support of this observation, western blot analysis using the anti-B56δ antibody on whole-cell Rcho-1 lysates subtracted for the nucleolar fraction confirmed that endogenous B56δ predominantly localises to the nuclear/ nucleolar compartment of Rcho-1 stem cells but is restricted to the cytoplasm of TG cells (Figure 5.9). These results suggest that B56δ is trafficked to the cytoplasm during Rcho-1 TG cell differentiation.

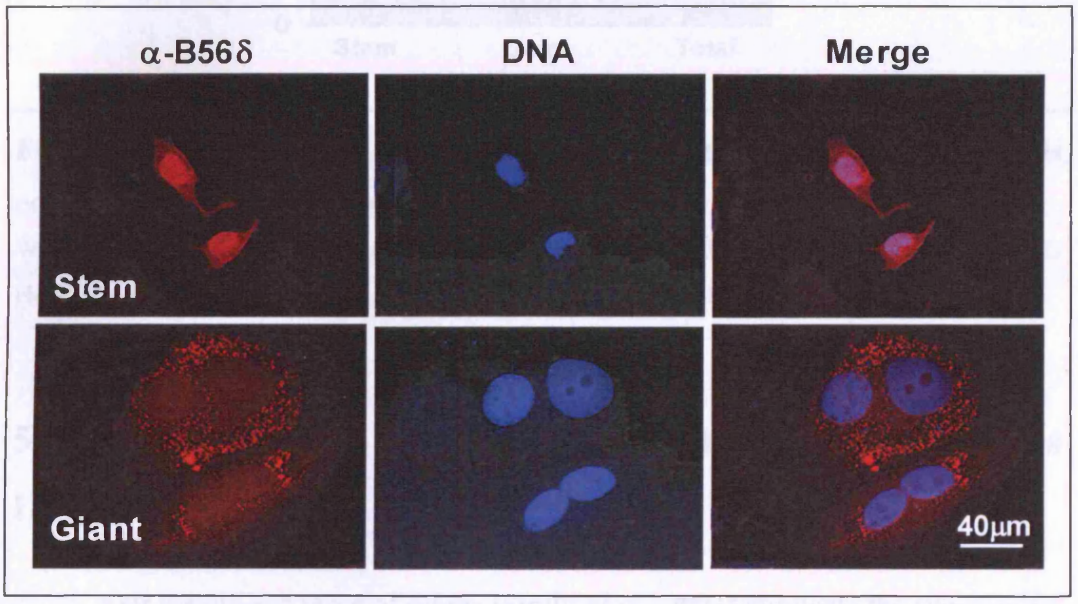

Figure 5.8. Ectopic B56δ is nuclear in Rcho-1 stem cells but is exported from the nucleus upon their differentiation.

Ectopic B56δ is localised throughout the nucleus, including the nucleoli, in Rcho-1 stem cells (**a**) but relocates to the cytoplasm upon their differentiation into trophoblast giant cells (**b**).

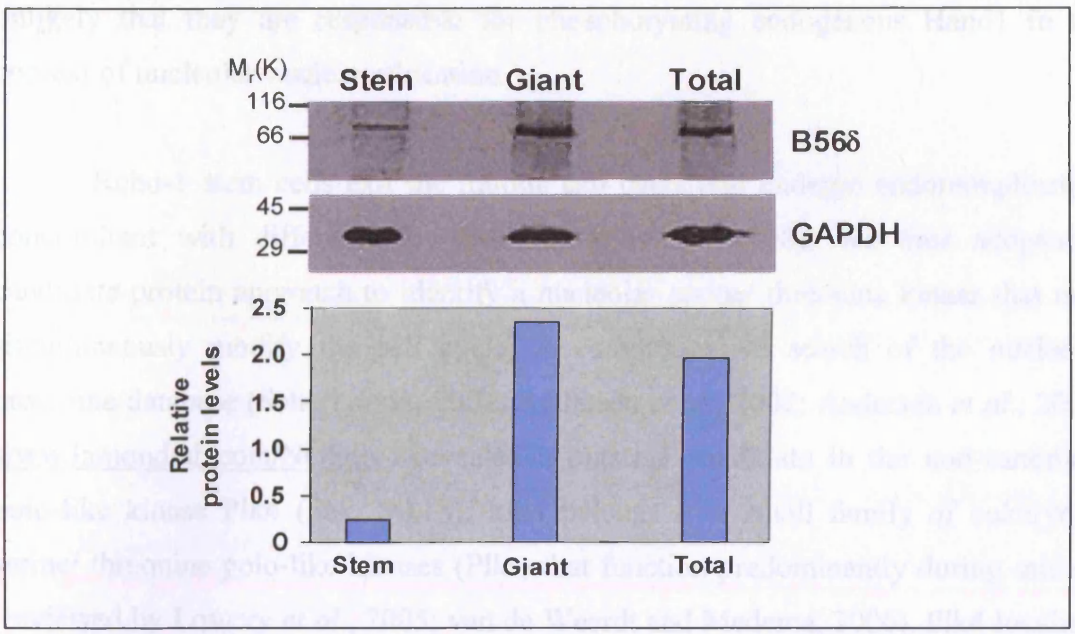

Figure 5.9. Relocation of endogenous B56δ during Rcho-1 differentiation is confirmed by western blot analysis.

Western blot analysis on whole-cell Rcho-1 lysates, subtracted for the nucleolar fraction, reveals elevated non-nucleolar, but decreased nucleolar, B56δ during Rcho-1 TG cell differentiation.

5.2.4. Plk4 is the nucleolar kinase that phosphorylates Hand1

Our results and those of others (Firulli *et al.*, 2003) implicate the site-specific phosphorylation of Hand1 as essential for its nucleolar release, subsequent heterodimer formation with E-factors and trans-activational activity in the nucleus. This cascade of events likely underlies the onset of Rcho-1 TG cell differentiation. Thus the next question we wished to address was the identity of the nucleolar kinase responsible for phospho-Hand1 nucleolar release. Previously, studies in HEK293 cells implicated protein kinase C and, particularly, protein kinase A (PKC and PKA), as the kinases that phosphorylate Hand1 at T107 and S109 during this process (Firulli *et al.*, 2003). However, since neither of these ubiquitous kinases localise to the nucleolus (reviewed by Jaken, 1996; Griffioen and Thevelein, 2002), and are absent from the mammalian nucleolar proteome, despite their ubiquitous cell type expression (Scherl *et al.*, 2002; Andersen *et al.*, 2002; Andersen *et al.*, 2005), it is

unlikely that they are responsible for phosphoryating endogenous Hand1 in the context of nucleolar-nuclear relocation.

Rcho-1 stem cells exit the mitotic cell cycle and undergo endoreduplication concomitant with differentiation (MacAuley *et al.*, 1998). We thus adopted a candidate-protein approach to identify a nucleolar serine/ threonine kinase that may simultaneously modify the cell cycle. A comprehensive search of the nucleolar proteome database (Scherl *et al.*, 2002; Andersen *et al.*, 2002; Andersen *et al.*, 2005; www.lamondlab.com/NOPdb/) revealed a putative candidate in the non-canonical polo-like kinase Plk4 (Sak, Stk18). Plk4 belongs to a small family of eukaryotic serine/ threonine polo-like kinases (Plks) that function predominantly during mitosis (reviewed by Lowery *et al.*, 2005; van de Weerdt and Medema, 2006). Plk4 localises to the nucleolus specifically at phase G2, the cell cycle stage at which both TS cells and Rcho-1 stem cells are thought to initiate endocycling upon their commitment to differentiate (MacAuley *et al.*, 1998). Moreover, Plk4 is involved in the anaphase-promoting complex/ cyclosome- (APC/C)-dependent destruction of the mitotic cyclin B1 and exit from mitosis in the post-gastrulation embryo (Hudson *et al.*, 2001). This is very relevant to our study as under certain conditions the APC/C destroys mitotic cyclins to promote mitotic cell cycle exit and the initiation of endoreduplication. For example, APC/C substrate-determining Cdh1 orthologues in angiosperm plants (Ccs52A) and *Drosophila* (Fizzy-related, Fzr) are respectively required for down-regulating mitotic cyclins to switch the mitotic cell cycle at phase G2 to the endocycle during seed (Cebolla *et al.*, 1999) and salivary gland (Sigrist and Lehner, 1997) development. Furthermore, mutations that interfere with the activity of the mitotic cyclin B-Cdk1 complex induce an endoreduplication phenotype in both fission yeast (Hayles *et al.*, 1994) and budding yeast (Azzam *et al.*, 2004). Indeed APC/C targets, including Cyclin B1, Cdk1 and Aurora A, persist beyond the appropriate cell cycle checkpoint in cells of a *Plk4*-null mouse (Hudson *et al.*, 2001).

Semi-quantitative RT-PCR using mRNA prepared from Rcho-1 stem cells and cells at different stages of their differentiation into TG cells revealed that *Plk4* is up-regulated during this process. This elevation was most marked a few hours after serum modification, and was subsequently maintained at high levels during a time-course of TG cell differentiation over eight-day time-course (Figure 5.10).

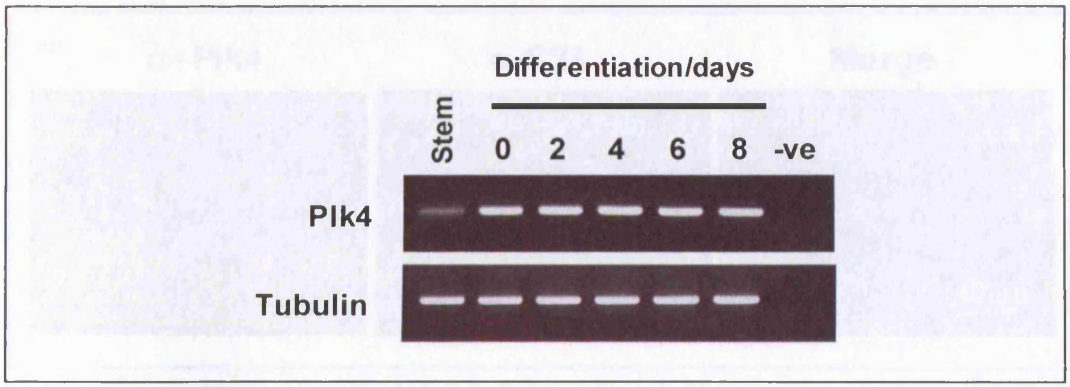

Figure 5.10. *Plk4* is up-regulated at the onset of Rcho-1 differentiation.

Semi-quantitative RT-PCR analysis reveals that *Plk4* is up-regulated at the onset of Rcho-1 differentiation induced by 10% horse serum (from the stem cell stage to 'day 0'; 3 hours' exposure to HS) and maintained at high levels during subsequent differentiation.

We subsequently sought to investigate the subcellular localisation of Plk4 in Rcho-1 stem cells. A GFP-Plk4 fusion protein localised to multiple nucleoli with additional peri-nuclear fluorescence in Rcho-1 stem cells synchronised at the G2/M checkpoint by nocodazole treatment (Figure 5.11). Furthermore, immunostaining with an anti-Plk4 antibody showed that endogenous Plk4 also localised to Rcho-1 stem cell nucleoli synchronised at the G2/M checkpoint using nocodazole (Figure 5.12). Interestingly, endogenous Plk4 occupied only a single nucleolus in each Rcho-1 stem cell, the significance of which is presently unclear.

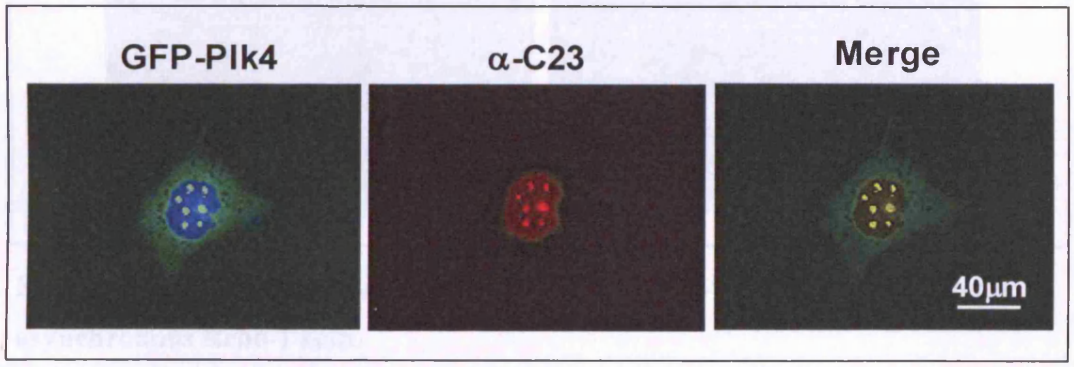

Figure 5.11. A GFP-Plk4 fusion protein is nucleolar in Rcho-1 stem cells synchronised at the G2/M phase checkpoint.

A GFP-Plk4 fusion protein localises to multiple nucleoli with additional peri-nuclear fluorescence in Rcho-1 stem cells synchronised at the G2/M phase checkpoint following nocodozole treatment.

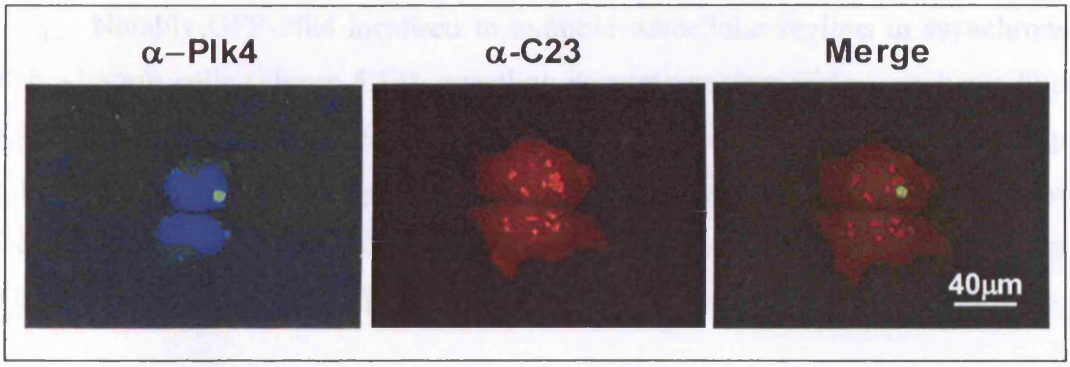

Figure 5.12. Endogenous Plk4 localises to a single nucleolus in Rcho-1 stem cells synchronised at the G2/M phase checkpoint.

Endogenous Plk4 localises to a single nucleolus in Rcho-1 stem cells synchronised at the G2/M phase checkpoint following nocodozole treatment.

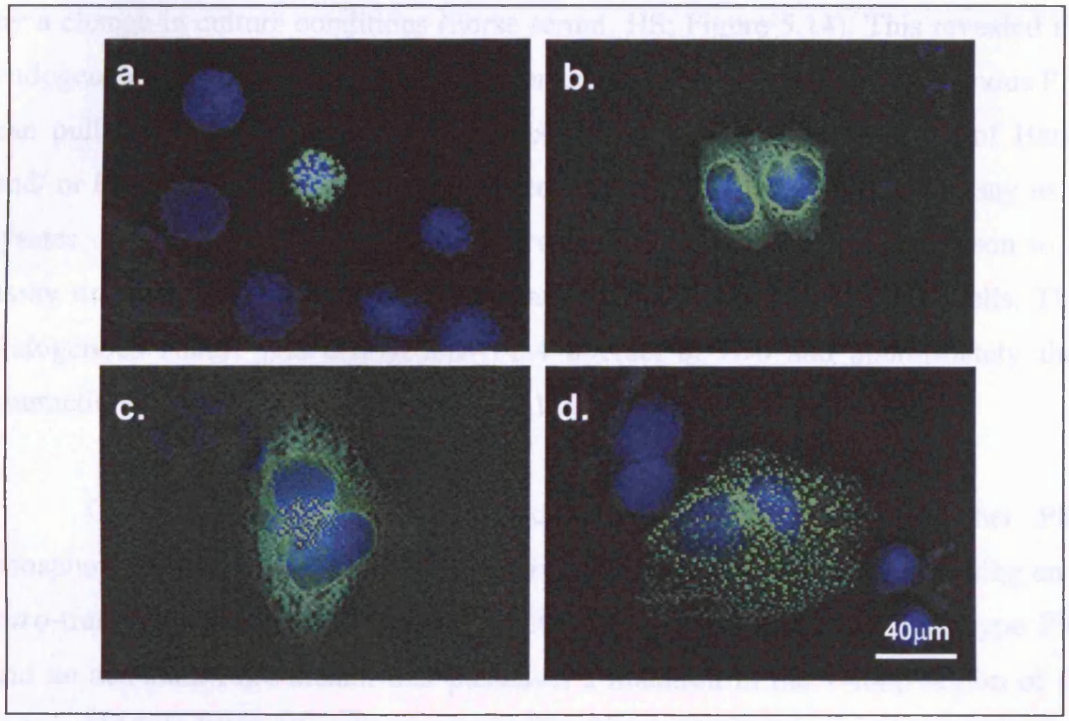

Figure 5.13. The sub-cellular localisation of GFP-Plk4 differs markedly in asynchronous Rcho-1 cells.

GFP-Plk4 localises to multiple subcellular regions in addition to the G2/M phase nucleolus, localizing throughout the nucleus in a punctuate, nuclear-wide pattern (**a**), to the peri-nucleus (**b**) along the cleavage furrow (**c**) and throughout the cytoplasm (**d**) depending on the cell cycle stage.

Notably GFP-Plk4 localised to multiple subcellular regions in asynchronous Rcho-1 stem cells (Figure 5.13), revealing punctate nuclear-wide (anaphase; Figure 5.13a), peri-nuclear (interphase; Figure 5.13b), cleavage furrow (telophase; Figure 5.13c) and cytoplasmic (prophase; Figure 5.13d) fluorescence depending on stage of the cell cycle. Thus the subcellular location of Plk4 in Rcho-1 cells mirrors that in 3T3 fibroblasts, where these localisations were first reported (Hudson *et al.*, 2001).

In light of these results, we then proceeded to investigate whether Plk4 phosphorylates Hand1 during Rcho-1 TG cell differentiation. Initially, we investigated whether Plk4 and Hand1 interact *in vivo*. To this end, we performed co-immunoprecipitation analysis using lysates of either untreated and asynchronous Rcho-1 stem cells (control, Co) or Rcho-1 cells induced to differentiate for one hour by a change in culture conditions (horse serum, HS; Figure 5.14). This revealed that endogenous Hand1 can pull-down endogenous Plk4 and conversely endogenous Plk4 can pull-down endogenous Hand1. Moreover, the relative concentration of Hand1 and/ or Plk4 immunoprecipitate was greater in a co-immunoprecipitation assay using lysates of Rcho-1 cells induced to differentiate for one hour, in comparison to an assay using control lysates of untreated and asynchronous Rcho-1 stem cells. Thus endogenous Hand1 and endogenous Plk4 interact *in vivo* and appropriately their interaction is enhanced by inducing Rcho-1 cells to differentiate.

Given Plk4 interacts with Hand1, we next investigated whether Plk4 phosphorylates Hand1. To do this, we carried out an *in vitro* kinase assay using an *in vitro*-translated Hand1-GST substrate protein and *in vivo*-translated wild-type Plk4 and an activated Plk4 mutant that possesses a mutation in the T-loop region of the kinase (T170D-Plk4) (Swallow *et al.*, 2005; Figure 5.15; Figure 5.23). This assay revealed that Plk4 is able to specifically phosphorylate Hand1 to greater than 1 mol $Pimol^{-1}$ substrate and at levels comparable to its established substrate α-Casein (Swallow *et al.*, 2005). Notably Plk4 could neither phosphorylate the T107;S109A nor the T107;S109D mutant EGFP fusion proteins in the same assay (data not shown). These results suggest that Plk4 acts in a site-specific manner at the predicted T107 and S109 residues in helix 1 and may act as a Hand1 kinase in a relevant physiological setting.

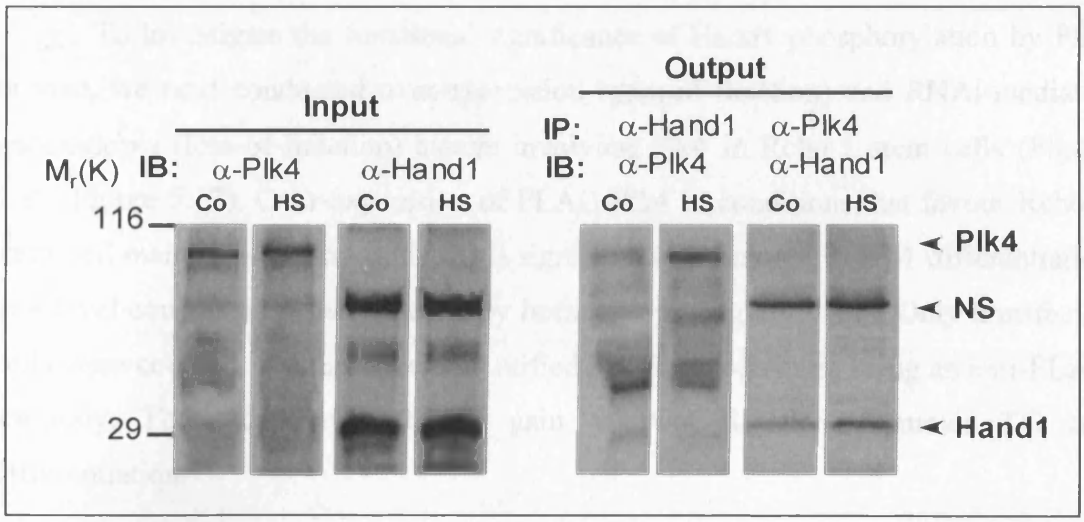

Figure 5.14. Endogenous Hand1 interacts with endogenous Plk4 *in vivo*.

Co-immunoprecipitation of endogenous Hand1 with endogenous Plk4, or vice versa, in either untransfected Rcho-1 stem control cells (**Co**), or Rcho-1 stem cells promoted to differentiate with 10% HS for one hour (**HS**) reveals that the two factors interact *in vivo*. Note the stronger interaction in the HS-treated cells, consistent with a commitment towards a TG cell fate. **NS**: non-specific band.

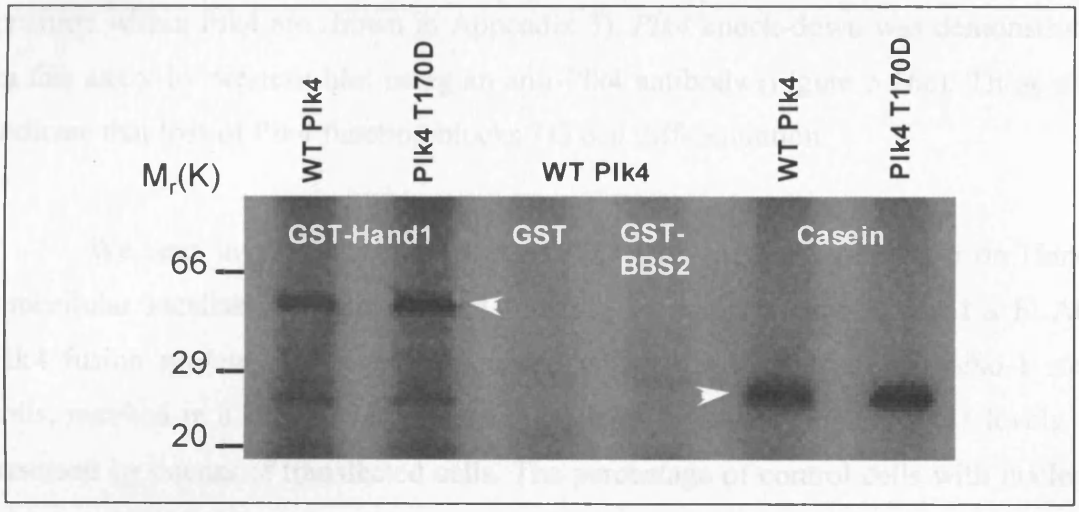

Figure 5.15. Plk4 phosphorylates Hand1 *in vitro*.

A GST-Hand1 fusion protein is specifically phosphorylated *in vitro* by both wild-type Plk4 and the activated mutant T170D-Plk4 (Swallow *et al.*, 2005) and at levels comparable to the Plk4 positive control substrate α-Casein. Plk4 can neither phosphorylate GST alone nor the negative control protein BBS2. **WT**: wild-type.

To investigate the functional significance of Hand1 phosphorylation by Plk4 *in vivo*, we next conducted over-expression (gain-of-function) and RNAi-mediated knock-down (loss-of-function) assays involving Plk4 in Rcho-1 stem cells (Figure 5.16, Figure 5.17). Over-expression of FLAG-Plk4 in conditions that favour Rcho-1 stem cell maintenance (shown as FBS) significantly promoted Rcho-1 differentiation to a level equivalent to that induced by horse serum (Figure 5.16a). Only transfected cells were counted, and these were identified by immunostaining using an anti-FLAG antibody. These data suggest that gain of Plk4 function promotes TG cell differentiation.

Conversely, RNAi-mediated knock-down of endogenous *Plk4*, using two independent RNAi sequences (*Plk4shRNAi1* and *Plk4shRNAi2*), significantly blocked the differentiation of Rcho-1 stem cells cultured under differentiation-inducing conditions (shown as HS; Figure 5.16b; sequence of RNAi oligonucleotides and position within Plk4 are shown in Appendix 3). *Plk4* knock-down was demonstrated in this assay by western blot using an anti-Plk4 antibody (Figure 5.16c). These data indicate that loss of Plk4 function blocks TG cell differentiation.

We next investigated the effect of *Plk4* gain- or loss-of-function on Hand1 subcellular localisation. Gain in Plk4 function by the over-expression of a FLAG-Plk4 fusion protein, which was associated with reduced numbers of Rcho-1 stem cells, resulted in a significant increase in nuclear-wide-endogenous Hand1 levels, as assessed by counts of transfected cells. The percentage of control cells with nuclear-wide-endogenous Hand1 localisation was 28.6±2.08 (mean±S.E.M.; n=210), whilst the percentage of Plk4-over-expressing cells with nuclear-wide-endogenous Hand1 localisation was 54.1±2.78 72 hours after transfection (mean±S.E.M.; n=250) ($p=<0.001$). These data suggest that gain of Plk4 function promotes nucleolar release of endogenous Hand1 in Rcho-1 stem cells.

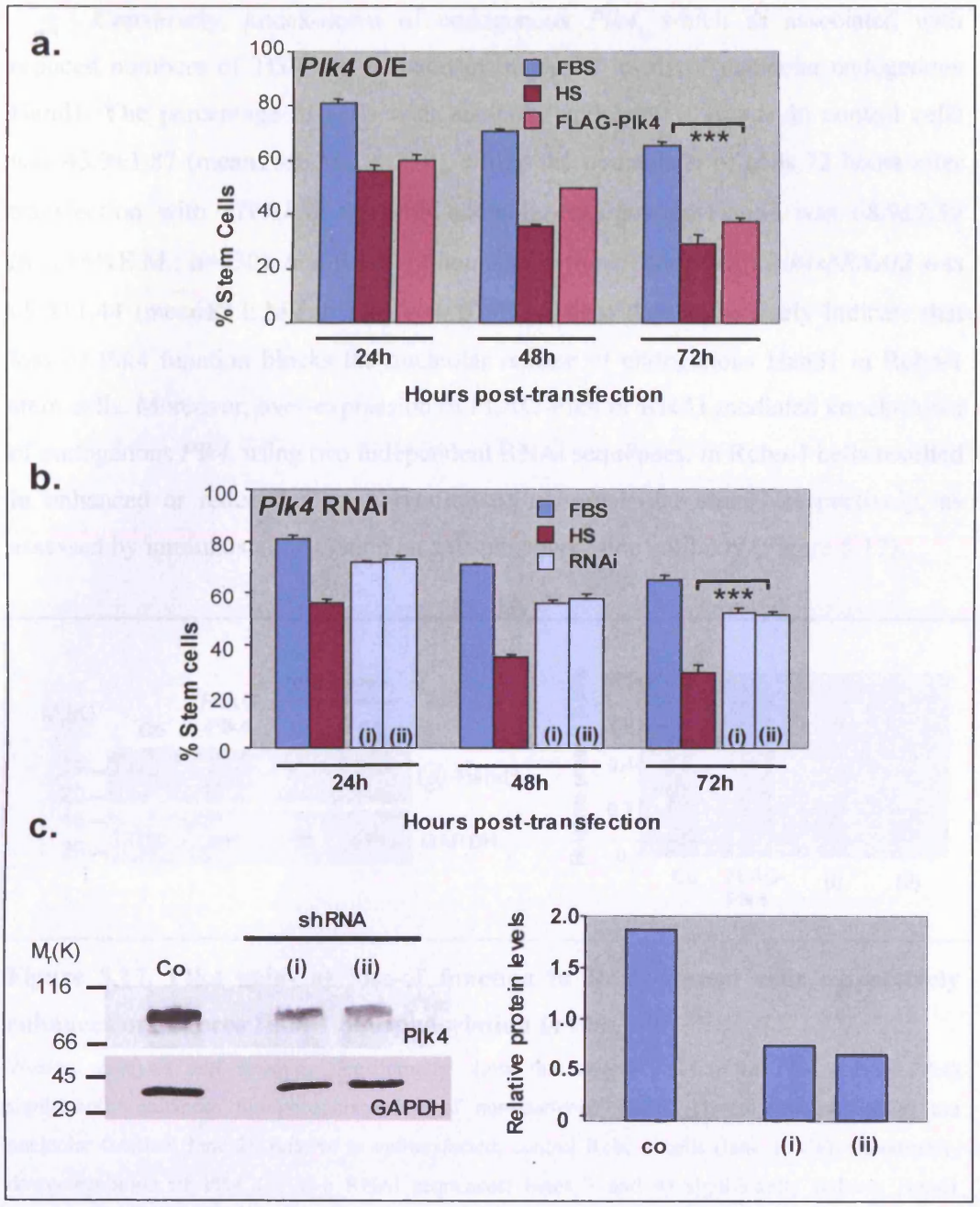

Figure 5.16. Gain- or loss-of function of Plk4 in Rcho-1 stem cells respectively enhances or inhibits TG cell differentiation.

Over-expression of Plk4 (FLAG-Plk4) in Rcho-1 cells cultured in non-differentiating conditions (shown as FBS) significantly promotes TG cell differentiation (**a**). Knock-down of endogenous Plk4 in Rcho-1 stem cells cultured in differentiation-inducing conditions (shown as HS), using two independent RNAi sequences (*Plk4shRNAi1* (i) and *Plk4shRNAi2* (ii)), significantly blocks TG cell differentiation (**b**). *Plk4* knock-down was demonstrated by western blot analysis using an anti-Plk4 antibody and then comparing Plk4 levels between un-transfected (control, Co) and transfected cells by scanning densitometry (**c**). Measurements: n=360; *** indicates $p<0.001$. **o/e**: over-expression.

Conversely, knock-down of endogenous *Plk4*, which as associated with reduced numbers of TG cells, resulted in increased levels of nucleolar-endogenous Hand1. The percentage of cells with nucleolar-endogenous Hand1 in control cells was 43.9±1.87 (mean±S.E.M.; n=210), whilst the percentage of cells 72 hours after transfection with *Plk4shRNAi1* with nucleolar-endogenous Hand1 was 68.9±2.39 (mean±S.E.M.; n=230), and those 72 hours after transfection with *Plk4shRNAi2* was 69.8±1.44 (mean±S.E.M.; n=230) (p=<0.001). These data collectively indicate that loss of Plk4 function blocks the nucleolar release of endogenous Hand1 in Rcho-1 stem cells. Moreover, over-expression of FLAG-Plk4 or RNAi-mediated knock-down of endogenous *Plk4*, using two independent RNAi sequences, in Rcho-1 cells resulted in enhanced or reduced phosphorylation of non-nucleolar Hand1 respectively, as assessed by immunostaining using an anti-phosphoserine antibody (Figure 5.17).

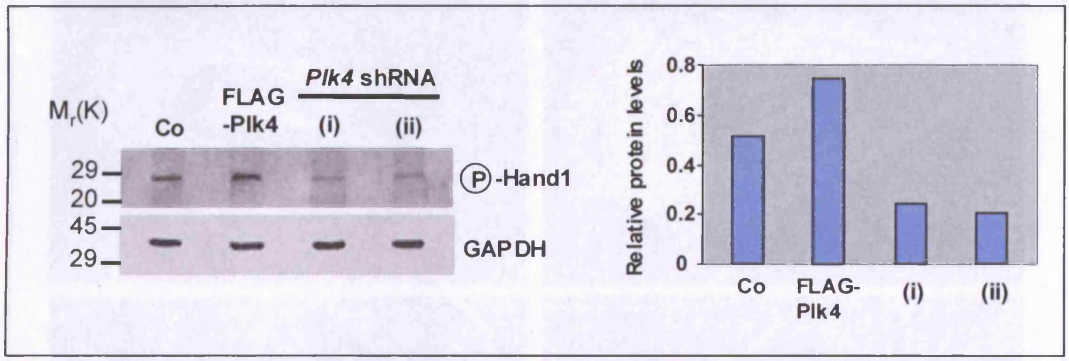

Figure 5.17. Plk4 gain- or loss-of function in Rcho-1 stem cells respectively enhances or reduces Hand1 phosphorylation *in vivo*.

Western analysis and scanning densitometry show that over-expression of Plk4 (FLAG-Plk4) significantly enhances the phosphorylation of non-nucleolar Hand1 (lysates subtracted for the nucleolar fraction; lane 2), relative to untransfected, control Rcho-1 cells (lane 1; **Co**). Conversely, down-regulation of Plk4 (by two RNAi sequences; lanes 3 and 4) significantly reduces Hand1 phosphorylation.

The results described so far suggest that the nucleolar phosphorylation of Hand1 by Plk4 underlies Hand1 nucleolar release as a pre-requisite for TG cell differentiation in the Rcho-1 cell line. However this data was derived from an *in vitro* cell-based model so we subsequently sought to investigate whether it occurred in an *in vivo* setting. To this end, we obtained *Plk4*-null embryos from the laboratory of

James Dennis and Carol Swallow (SLRI, Toronto, Canada). *Plk4*-heterozygous and *Plk4*-null E7.5 embryos were genotyped using primers and nested PCR techniques previously described (Hudson *et al.*, 2001; data not shown) and the lack of Plk4 protein in *Plk4*-null embryos was confirmed by immunostaining for anti-Plk4 (data not shown). Genotyped *Plk4*-null embryos were then investigated in terms of trophoblast differentiation and mis-localisation of Hand1 *in vivo* (Figure 5.18 – Figure 5.21). Compared with heterozygous control embryos, E7.5 *Plk4*-null concepti were smaller (Figure 5.18a,b) and have a markedly enlarged ectoplacental cone (EPC) (Figure 5.18c,d). This was consistent with an expansion in the diploid source of trophoblast 'stem cells' and reduced TG cell differentiation.

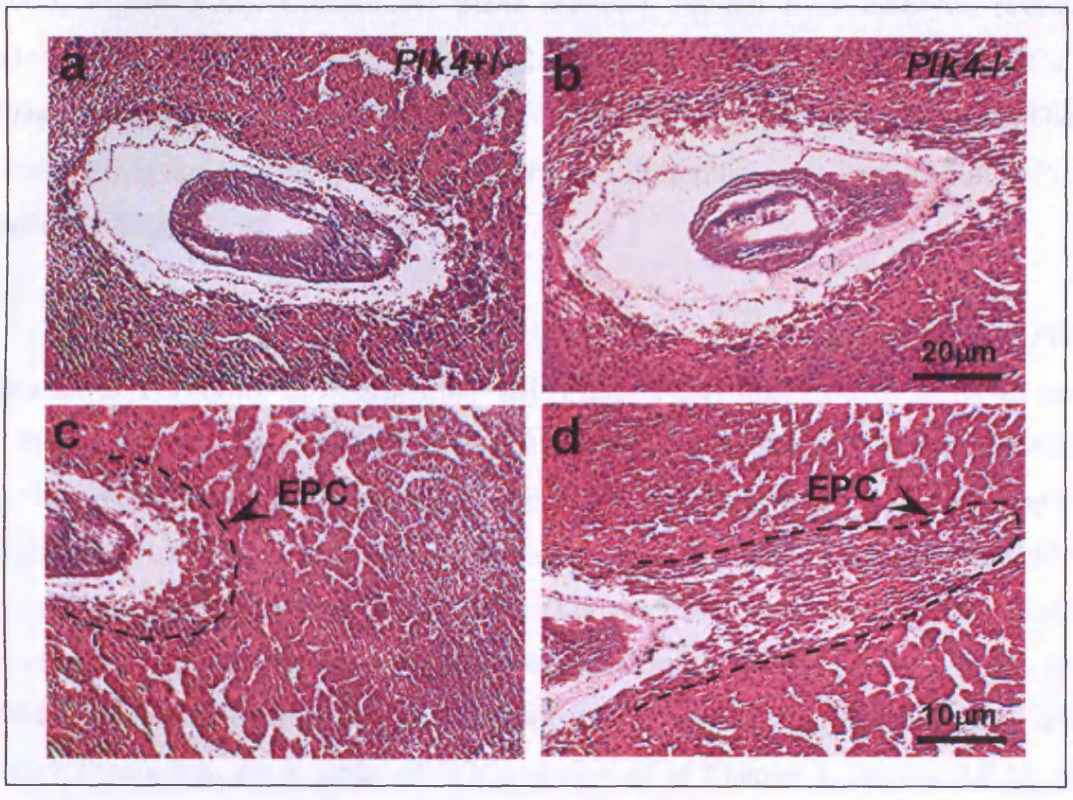

Figure 5.18. *Plk4*-null embryos are smaller and have an enlarged ectoplacental cone and reduced SGC number compared to *Plk4*-heterozygotes.

Histological sections through *Plk4*-heterozygous and -homozygous mutants at E7.5 reveal that *Plk4*-null embryos are smaller than their heterozygous littermates (compare (**a**) with (**b**)) and have a significantly expanded ectoplacental cone (EPC) of diploid trophoblast cells (compare (**c**) with (**d**)). The *Plk4*-homozygous mutant visceral yolk sac (**b**) also appears rough and disorganised in appearance.

DNA staining of histological sections revealed that the differentiation of primary trophoblast giant cells (PGC), namely those that arise directly from trophectoderm at the blastula stage, was normal in *Plk4*-null mutants (Figure 5.19a,c,e). However, the secondary trophoblast giant cell (SGC) population, which arises from the outer layer of the EPC, was significantly reduced with associated failed migration through the overlying maternal decidua (Figure 5.19b,d,f). PGC and SGC populations were distinguished by relative positions in relation to the maternal decidua (reviewed in Chapter 1, section 1.2.1) and by immunostaining for prolactin-like protein A (PLP-A), which is expressed exclusively in a peri-nuclear pattern in SGCs and Rcho-1 TG cells, but not in PGCs (Hamlin *et al.*, 1994; Ma and Linzer, 2000; Figure 5.22). Comparable plane sections through E7.5 embryos revealed 63±9.6 (mean±S.E.M.) SGCs in controls versus 21±5.2 (mean±S.E.M.) SGCs in *Plk4*-null embryos. Six replica sections for each genotype were analysed. These observations suggest that SGC, but not PGC, differentiation is impaired in a *Plk4*-deficient background.

The subcellular localisation of Hand1 was then investigated in the *Plk4*-heterozygous (Figure 5.20) and *Plk4*-null (Figure 5.21) backgrounds using an anti-Hand1 antibody. This revealed that Hand1 was nuclear-wide in the majority of SGCs in the control *Plk4* heterozygotes (Figure 5.20). However, in the expanded diploid trophoblast of *Plk4*-mutants, Hand1 remained predominantly nucleolar, coincident with a rare commitment to a SGC fate (Figure 5.21). Collectively, these studies confirmed inappropriate *in vivo* subcellular localisation of endogenous Hand1 in a *Plk4* loss-of-function background. This supports our *in vitro* analyses in Rcho-1 cells, which themselves are a model of SGCs (reviewed in Chapter 1, section 1.6.1), and strongly suggests that Plk4-dependent phosphorylation of Hand1 underlies its nucleolar release.

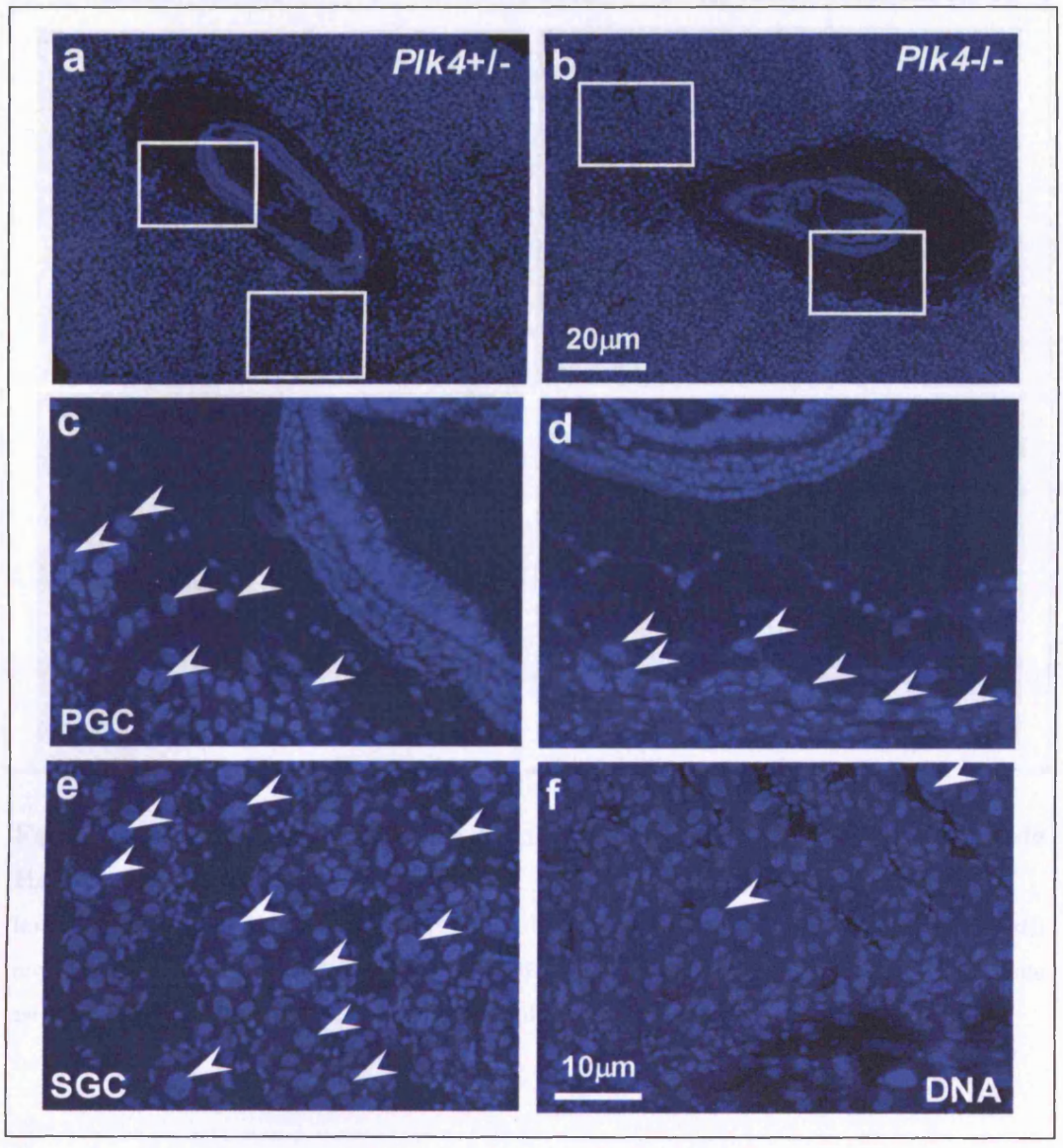

Figure 5.19. PGC differentiation, but not SGC differentiation, is normal in *Plk4*-null embryos.

DNA staining of sections (the boxes in (**a**) are magnified in (**c**) and (**e**), and the boxes in (**b**) are magnified in (**d**) and (**f**)) reveals that *Plk4*-homozygous mutants have equivalent levels of PGCs (**c**, **d**) but significantly reduced SGCs (**e**, **f**) compared with their *Plk4*-heterozygous littermates. White arrowheads identify PGCs in (**c**) and (**d**) and SGCs in (**e**) and (**f**).

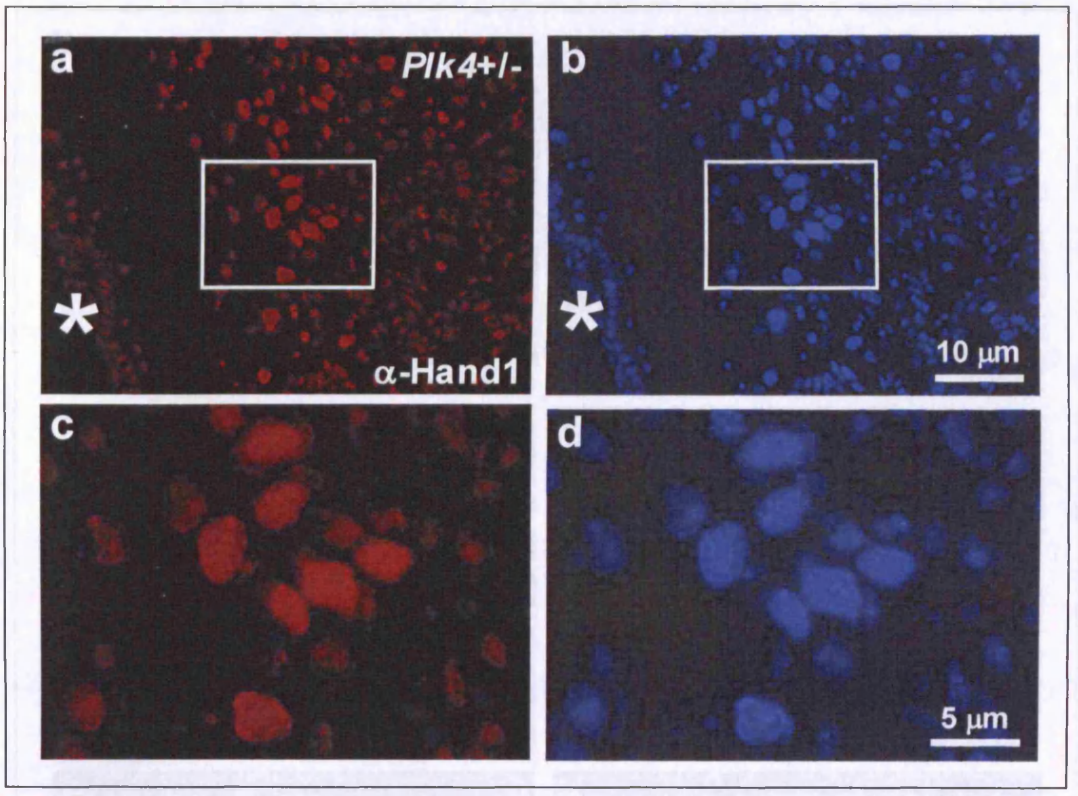

Figure 5.20. *Plk4*-heterozygous SGCs form normally and have nuclear-wide Hand1.

Immunostaining for Hand1 (the box in (**a**) is magnified in (**c**), and the box in (**b**) is magnified in (**d**)) reveals nuclear-wide localisation of Hand1 in SGCs in *Plk4*-heterozygous control embryos. White asterisks in (**a**) and (**b**) reveal the relative position of the most rostral part of the embryo in section.

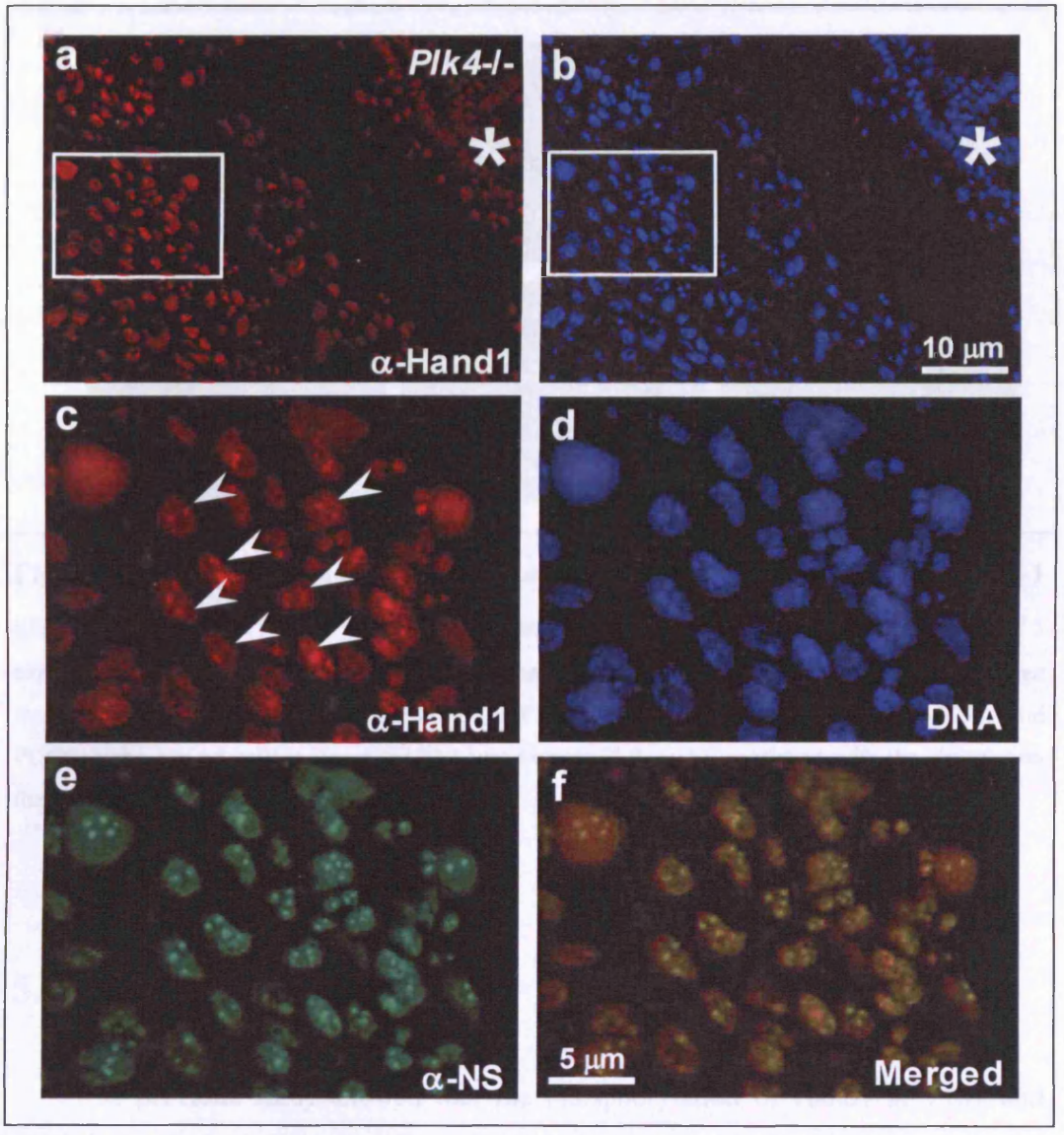

Figure 5.21. *Plk4*-null trophoblast remains undifferentiated and exhibits nucleolar-restricted Hand1.

Immunostaining for Hand1 (the box in (**a**) is magnified in (**c**) and (**e**), and the box in (**b**) is magnified in (**d**) and (**f**)) reveals nucleolar restriction of Hand1 in the expanded diploid trophoblast population of the *Plk4*-null embryos (**a**, **c**). This was confirmed by counterstaining for the nucleolar-specific maker Nucleostemin (NS; **e**, **f**). White asterisks in (**a**) and (**b**) reveal the relative position of the most rostral part of the embryo in section. White arrowheads in (**c**) highlight mutant cells with exclusively nucleolar Hand1.

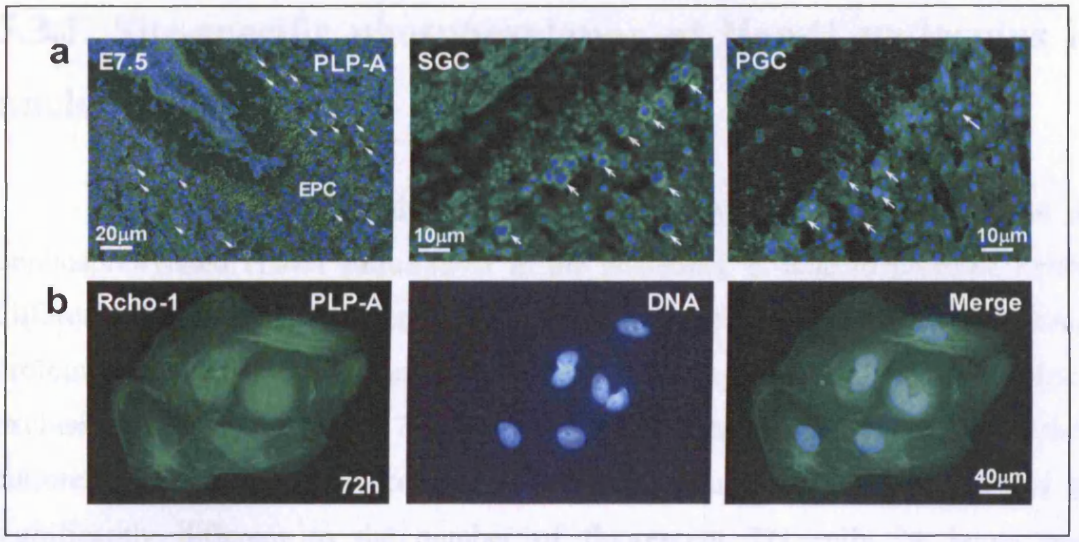

Figure 5.22. PLP-A is a specific marker of secondary giant cells and Rcho-1 giant cells. Secondary giant cells (SGCs) emerging from the ectoplacental cone (EPC) at E7.5 express PLP-A, as determined by immunofluorescence, whereas primary giant cells (PGCs), derived from the polar trophectoderm, are negative for PLP-A (**a**; white arrowheads highlight SGCs and PGCs). Rcho-1 giant cells cultured for 72 hours express PLP-A (**b**), consistent with the observation that they represent a model for SGCs.

5.3. DISCUSSION

A previous study showed that the phosphorylation of Hand1 at T107 and S109 during Rcho-1 TG cell differentiation enhances the affinity of the transcription factor for its E-factor binding partners and thus its biological activity (Firulli et al., 2003). In this chapter, we reveal that this phosphorylation event also underlies its nucleolar release at the onset of Rcho-1 differentiation. Moreover, we have revealed that the polo-like kinase Plk4 is responsible for Hand1 phosphorylation in this context. *Plk4*-null embryos appropriately have impaired SGC differentiation and this is underpinned by a failure of Hand1 nucleolar release. Additionally, nuclear export of B56δ during Rcho-1 differentiation counteracts PP2A-mediated Hand1 dephosphorylation and aids the increase in Hand1 phosphorylation. Taken together, our results show that Plk4-mediated Hand1 phosphorylation drives its nucleolar-nuclear release as a pre-requisite for TG cell differentiation during placentation.

5.3.1. Site-specific phosphorylation of Hand1 underpins its nucleolar release

Our results uniquely show that only nuclear-wide phospho-Hand1, but not unphosphorylated Hand1 sequestered in the nucleolus, is able to promote Rcho-1 differentiation. Firstly, we demonstrated that a Hand1 T107;S109A-EGFP fusion protein, which cannot be phosphorylated at these two residues, remained almost exclusively nucleolar during a 72-hour time-course of Rcho-1 differentiation. In these cultures, the number of fluorescent TG cells 72 hours post-transfection was not significantly different to the number of fluorescent TG cells 24 hours post-transfection. These observations suggest that the change in charge conferred by phosphorylation of these two helix 1 residues is necessary for promoting Hand1 nucleolar release. The few TG cells observed in the Hand1 T107;S109A-EGFP mutant cultures 72 hours post-transfection were likely attributable to endogenous wild-type Hand1 activity.

In contrast, substitution of both T107 and S109 for aspartic acid residues yielded the opposite result. The Hand1 T107;S109D-EGFP mutant fusion protein adopted a nuclear-wide distribution immediately after its expression, due to either a failure of nucleolar sequestration or retention. It is of note that aspartate substitutions serve as substitutes of phosphorylation, mimicking the change in charge that phosphorylation confers. For example, mutation of a serine residue to an aspartate in helix 1 of c-Myc renders the bHLH transcription factor constitutively active (Huang *et al.*, 2004b). Thus the Hand1 T107;S109D-EGFP mutant fusion protein acts as a useful positive control in this study. It suggests that the change in protein charge conferred by phosphorylation of these two helix 1 residues is sufficient for Hand1 nucleolar release. The fact that this mutant is not as potent as wild-type Hand1 in driving TG cell differentiation is in agreement with previous observations that this mutant has a reduced affinity for nucleoplasmic E-factors and a predisposition to homodimerise (Firulli *et al.*, 2003). In conclusion, the phosphorylation of Hand1 at T107 and/ or S109 is required for its release from the nucleolus in Rcho-1 stem cells at the onset of TG cell differentiation. It will be interesting in this regard to analyse the trophoblast phenotype of *Hand1 T107;S109A* and *Hand1 T107;S109D* knock-in

mice, which are currently being generated (A. Firulli, personal communication).

Interestingly, the Hand1 T107;S109D mutant fusion protein localised to discrete, as-yet unidentified nucleoplasmic foci. Why wild-type Hand1-EGFP does not occupy such foci is curious. Perhaps its association with these unidentified bodies occurs at a very early stage of differentiation or is only transient, whilst the Hand1 phosphorylation mimic constitutively resides within these foci. Preliminary data excluded co-localisation of these foci with centrosomes or Cajal bodies by immunostaining for markers specific for these organelles. However, a degree of co-localisation of the Hand1 phosphorylation mimic was demonstrated with so-called transcription factories (Iborra *et al.*, 1996; Osbourne *et al.*, 2004), specific nuclear sites of gene activation and nascent RNA synthesis. Immunostaining for RNA polymerase II, a marker for such foci, demonstrated a weak overlap with Hand1 T107;S109D. Since there was not a complete overlap in localisation of the T107;S109D mutant with transcription factories, it was hypothesised that this fusion protein may also in part become a component of site-specific multi-protein complexes involved in chromatin remodelling and gene expression. Indeed, during terminal differentiation of C2C12 myoblasts the nucleolar ZPF106 protein is released and localises to very similar nucleoplasmic foci that coincide with the TSPYL protein, a putative chromatin-remodelling factor (Grasberger and Bell, 2005). Interestingly, another of the Hand1 interactors identified in the Y2H screen was the SWI/SNF-related matrix-associated actin-dependent regulator of chromatin subfamily E member 1 (Smarce1; Appendix 8). This is involved in transcriptional activation and repression of select genes by chromatin remodeling (Belandia *et al.*, 2002). Thus activated, nucleoplasmic Hand1 may localise to these site-specific chromatin-remodelling complexes to regulate genes required for TG cell differentiation. In conclusion, despite some overlap with transcription factories and a strong possibility of co-localisation with a subset of chromatin remodeling complexes, the identity of the nuclear-wide foci to which the Hand1 T107;S109D mutant localises are currently unknown.

5.3.2. Nuclear export of B56δ complements Hand1 nucleolar release

The regulatory subunit B56δ of protein phosphatase 2A (PP2A) targets Hand1 for dephosphorylation at T107 and S109 (Firulli *et al.*, 2003). Appropriately, this previous study also showed that *B56δ* is down-regulated during Rcho-1 differentiation. As final confirmation that Hand1 nucleolar release is reliant on site-specific phosphorylation, we over-expressed *B56δ* in Rcho-1 stem cells co-transfected with Hand1-EGFP. This resulted in both a significant failure of the fluorescent fusion protein to exit the nucleolus and a significant reduction of TG cell differentiation compared to Rcho-1 stem cells transfected with Hand1-EGFP alone. Moreover, ectopic expression of B56δ in Rcho-1 stem cells cultured in differentiation-inducing conditions antagonised their differentiation as compared with untransfected Rcho-1 stem cells cultured under the same conditions. Importantly, this B56δ-induced block to differentiation was associated with a failure of endogenous Hand1 to exit the nucleolus.

We also demonstrated that the PP2A B56δ subunit is distributed throughout Rcho-1 stem cells but is predominantly cytoplasmic and excluded from the nuclei and nucleoli of TG cells. This observation is consistent with a relevant role for B56δ in Rcho-1 stem cell maintenance. As part of a PP2A complex, B56δ is possibly present in and/ or around the nucleoli of Rcho-1 stem cells. Here it may target any Hand1 that has been inappropriately phosphorylated and released from the nucleolus prior to cell commitment to differentiation. After the onset of TG cell differentiation, exclusion of B56δ from the nucleus, in combination with the down-regulation of the *B56δ* gene (Firulli *et al.*, 2003), may prevent $PP2A^{B56\delta}$ site-specifically dephosphorylating Hand1 in the nucleoplasm. Nuclear exclusion of B56δ is reminiscent of the cytoplasmic sequestration and negative regulation of the myogenic and Mash2 bHLH factors by I-mfa (Chen *et al.*, 1996; Kraut *et al.*, 1998) and of the p50 subunit of NF-κB by IκB (Beg *et al.*, 1992). In conclusion, the down-regulation (Firulli *et al.*, 2003) and nuclear export (data presented in this study) of B56δ prevents $PP2A^{B56\delta}$-mediated dephosphorylation of Hand1 during Rcho-1 differentiation.

5.3.3. Plk4 is the kinase responsible for nucleolar Hand1 phosphorylation

The data presented in this chapter are consistent with a requirement for the polo-like kinase Plk4 in the phosphorylation of nucleolar Hand1 as a pre-requisite for its release into the nucleus and concomitant TG cell differentiation. Appropriately, *Plk4* mRNA levels increase during this process, immediately after serum withdrawal. This is consistent with our interpretation that the kinase triggers the onset of endoreduplication at the point of Rcho-1 stem cell commitment to differentiate. *Plk4* mRNA levels are known to be cell cycle regulated, being low in G1 phase but reaching a peak at the G2/M transition (Swallow *et al.*, 2005). However, our observations in TG cells are in contrast with the findings of previous studies that have been unable to detect *Plk4* expression in other distinct quiescent and differentiated cells (Fode *et al.*, 1994). However, the differences in *Plk4* expression in TG cells versus other cell types may reflect the unique requirement for TS cells to enter the endocycle in order to differentiate into TG cells.

Despite the transient interaction between kinases and their substrates, we were able to demonstrate interaction and reaction between endogenous Hand1 and Plk4 *in vitro*. Moreover, over-expression and RNAi-mediated knock-down of *Plk4* had appropriate effects on Hand1 phosphorylation and sub-cellular localisation, as well as Rcho-1 stem cell fate. This confirms that Plk4 gain- or loss-of-function has effects on TG cell differentiation via the modulation of Hand1 subcellular localisation. It is interesting in this regard that transient over-expression of *Plk4* has previously been shown to suppress mitotic cell cycling and promote multi-nucleation (Fode *et al.*, 1994; Fode *et al.*, 1996). A non-canonical target consensus phosphorylation motif for Plk4 has only recently been determined via *in vitro* kinase assays on peptide spots arrays (Z-[Ile/Leu/Val]-Ser/Thr-Y-Y-X-Z/Pro; Leung *et al.*, 2007). In this degenerate consensus sequence, Y is a large, hydrophobic residue, Z is a charged residue, whose charge specifically depends on the context of the surrounding sequence, and residues in brackets are unfavoured. However, Plk4 cannot phosphorylate several peptides containing this theoretically-optimal motif, suggesting the existence of other sequences outside of the core motif that influence the reaction. Thus the consensus

phosphorylation motif of Plk4 is highly context-dependent. In peptides that have a net positive charge, Plk4 favours basic residues in the -2 and +4 positions. Conversely, in peptides with a net negative charge, Plk4 favours acidic residues in the -2 and +4 positions (Leung *et al.*, 2007). This may explain why the region of Hand1 containing the T107 and S109 residues does not strictly match this consensus sequence. Notably the study by Leung and co-workers also showed that Plk4 can phosphorylate peptides when they are free in solution, and that it cannot phosphorylate GST alone and requires a high substrate yield for *in vitro* kinase assays. These observations are in agreement with our findings.

Plk4-null mouse embryos arrest at E7.5 and are embryonic lethal at E8.0 due to widespread apoptosis caused by inappropriate anaphase arrest (Hudson *et al.*, 2001). However, the mutant extra-embryonic tissues were not analysed in detail (Hudson *et al.*, 2001). Consequently, our study is the first to investigate the phenotype of *Plk4*-null embryos in terms of trophoblast differentiation *in vivo*. We revealed that embryos deficient for *Plk4* have a markedly-enlarged ectoplacental cone (EPC) compared with *Plk4*-heterozygous controls. This is consistent with an expansion of the diploid source of trophoblast cells and reduced SGC differentiation from the outer layer of the EPC. Our data reveal that the inability of Hand1 to exit the nucleolus in *Plk4*-null diploid trophoblast underlies the enlarged EPC of these concepti, namely because the diploid TG cell precursors cannot exit the mitotic cell cycle and so continue to proliferate. At first, this finding does not appear to agree with the initial analyses of *Plk4*-null embryos, namely the defects in mitotic progression and thus impaired cell proliferation. However, the fact that *Plk4*-null embryos proceed through many cell divisions before arresting at E7.5 was proposed to be either due to a persistence of maternal Plk4 mRNA or protein, functional redundancy with another polo-like kinase or due to unique features of the mitotic exit network during early embryogenesis (Hudson *et al.*, 2001; Swallow *et al.*, 2005). These factors may also underlie the proliferation of diploid trophoblast until embryonic arrest at E7.5. That is, the larger EPC of *Plk4*-null concepti reflects not hyper-proliferation of diploid trophoblast, but rather a lack of SGC differentiation.

The observation of reduced SGC differentiation in *Plk4*-null embryos is also consistent with the phenotype previously described for *Hand1*-null embryos. *Hand1*-

null embryos develop until around E7.5 and begin to gastrulate and establish an implantation chamber through PGC migration. However, they have significantly reduced numbers of SGCs (Riley *et al.*, 1998). Despite the lack of SGCs being a common feature of both *Hand1*-null and *Plk4*-null concepti, *Plk4*-null mutants do not exactly phenocopy *Hand1*-null mutants. This is consistent with the fact that not all of Hand1 function during early embryogenesis is mediated through Plk4 and vice versa. Indeed, whilst Plk4 is required for mitotic cell cycle exit in rodent trophoblast, Hand1 is required for the proliferation and maintenance of diploid trophoblast in the EPC, by an as-yet unknown mechanism (Riley *et al.*, 1998). This may be dependent on its binding E-factors, which are present in SGC precursors but are down-regulated during TG cell differentiation (Scott *et al.*, 2000). In fact, in the absence of Hand1, the EPC is reduced to approximately 20% of its normal size due to reduced trophoblast cell number (Riley *et al.*, 1998). How these findings can be reconciled with the more recent finding that *Hand1*-null TS cells do not have proliferation defects in culture (Hemberger *et al.*, 2004) is currently unclear. Thus the crucial finding in the context of this study is that, in both genetic backgrounds, commitment of diploid trophoblast precursors to a SGC fate is impaired.

Importantly, whilst Hand1 was nuclear-wide in a significant number of SGCs in control embryos, the transcription factor remained predominantly nucleolar in the expanded diploid trophoblast of *Plk4*-null mutants. This was coincident with a restricted and rare commitment to a SGC fate in the mutant placentae and is consistent with our *in vitro* studies. Thus, the observed effects of *Plk4* knock-down in Rcho-1 cells, namely a block to TG cell differentiation and retention of nucleolar Hand1, mimics the *in vivo* situation following *Plk4* loss-of-function. It is important to acknowledge that some SGCs arise in *Plk4*-null concepti, and furthermore endogenous Hand1 was detected outside of the nucleolus in some of these cells. This is not hugely surprising, as other factors are known to drive TG cell differentiation (Chapter 1, Table 1.2b), and these would likely be able to still do so in the absence of Plk4. Moreover, Hand1 is phosphorylated at other residues in addition to T107 and S109 during TG cell differentiation (for example, the basic domain residue serine-98; Firulli *et al.*, 2003). Although we did not investigate whether Plk4 phosphorylates this residue and others, we acknowledge that other nucleolar kinases in addition to Plk4 target Hand1 for phosphorylation during this differentiation process and may

contribute to its nucleolar release.

Our data suggest a differential requirement for Plk4 and nuclear-localised Hand1 during the differentiation of PGCs and SGCs. DNA staining of histological sections revealed that the differentiation of PGCs, which arise directly from the trophectoderm at the blastocyst stage, was normal in *Plk4*-null mutants. Despite their morphological similarity, the mechanisms underlying the differentiation of PGCs and SGCs are different. This is supported by the fact that the glycoprotein rnCGM1 and certain hormones, such as PL-II and PLP-A, are confined to SGCs (Rebstock *et al.*, 1993; Ma and Linzer, 2000; reviewed in Chapter 1, section 1.2.4.2). Indeed Hand1, or at least zygotic Hand1, does not appear to be required for primary TG cell differentiation as *Hand1*-null blastocysts form trophectoderm and hatch and outgrow *in vitro* (Cross *et al.*, 1995; Riley *et al.*, 1998). Thus, by inference, Plk4-mediated nucleolar release of pre-existing Hand1 is not required for PGC differentiation. This differential effect on SGC versus PGC differentiation in *Plk4*-deficient embryos is in agreement with the *in vitro* studies, in that Rcho-1 differentiation is thought to most closely resemble SGC differentiation (Hamlin *et al.*, 1994). This is an observation supported by our demonstration of the expression of the SGC-specific marker PLP-A (prolactin-like protein A) in Rcho-1 TG cells, in agreement with previous studies (Hamlin *et al.*, 1994; Ma and Linzer, 2000). It is also worth mentioning that Hand1 is required for the normal differentiation of all four subtypes of SGCs in the recent study by Simmons and colleagues, which importantly includes the so-called 'parietal SGCs' that form the interface with the maternal decidua (Simmons *et al.*, 2007).

The cellular functions of Plk4 include regulating centriole duplication during prophase and spindle organisation during cytokenesis (Bettencourt-Dias *et al.*, 2005; Habedanck *et al.*, 2005; Kleylein-Sohn *et al.*, 2007). Down-regulation of *Plk4* is also thought to play a part in the DNA damage response at the G2/M checkpoint by promoting p53-dependent apoptosis, which possibly relies on an observed interaction between Plk4 and p53 (Li *et al.*, 2005; Swallow *et al.*, 2005). Plk4 is the most divergent member of the polo-like kinase family and, unlike other Plk members, does not exhibit functional redundancy (Swallow *et al.*, 2005; Figure 5.23a). The basis of this lack of conservation may be underpinned by the fact that Plk4 possesses only one so-called polo-box (pb), a protein-protein interaction domain that is thought to

localise the enzyme to subcellular structures, whilst all other Plks possess two (Leung *et al.*, 2002; Swallow *et al.*, 2005; Figure 5.23b). The single polo box of Plk4 is moreover thought to interact with an upstream Plk4-specific 'cryptic' polo-box, which forms a novel intra-molecular dimer that may play a part in the unique localisation of Plk4, amongst Plk family members, to the nucleolus (Hudson *et al.*, 2001; Leung *et al.*, 2002; Figure 5.23b).

Our findings provide insight into the functional basis for Plk4 nucleolar localisation during G2 phase in TS cells. Plk4 localises to the nucleolus specifically at phase G2, the cell cycle stage at which Rcho-1 cells are thought to initiate endocycling upon their commitment to differentiate (MacAuley *et al.*, 1998). We also provide evidence that Plk4 localises to a single nucleolus in each Rcho-1 stem cell. This raises the possibility that each nucleolus has a discrete identity in terms of protein content and putative function(s). Our *in vivo* data show that Plk4 phosphorylates nucleolar Hand1 during G2 as a prerequisite for Hand1 nucleolar release and the onset of endoreduplication and concomitant TG cell differentiation. The consequence of this is that Plk4 restricts the potency of TS cells by promoting mitotic cell cycle exit and the onset of endoreduplication with concomitant TG cell differentiation. This is the first role proposed for Plk4 in the nucleolus. Of relevance for our study, Plk4 is known to contribute to the activation of the anaphase-promoting complex/ cyclosome- (APC/C) ubiquitin ligase. This targets mitotic cyclins for proteasomal destruction as a pre-requisite for endocycle entry (Hudson *et al.*, 2001). Thus our data show that Plk4 plays a part in promoting mitotic cell cycle exit and entry into the endocycle, at least in rodent trophoblast. This is in addition to its role in promoting exit from mitosis during normal mitotic cell cycling.

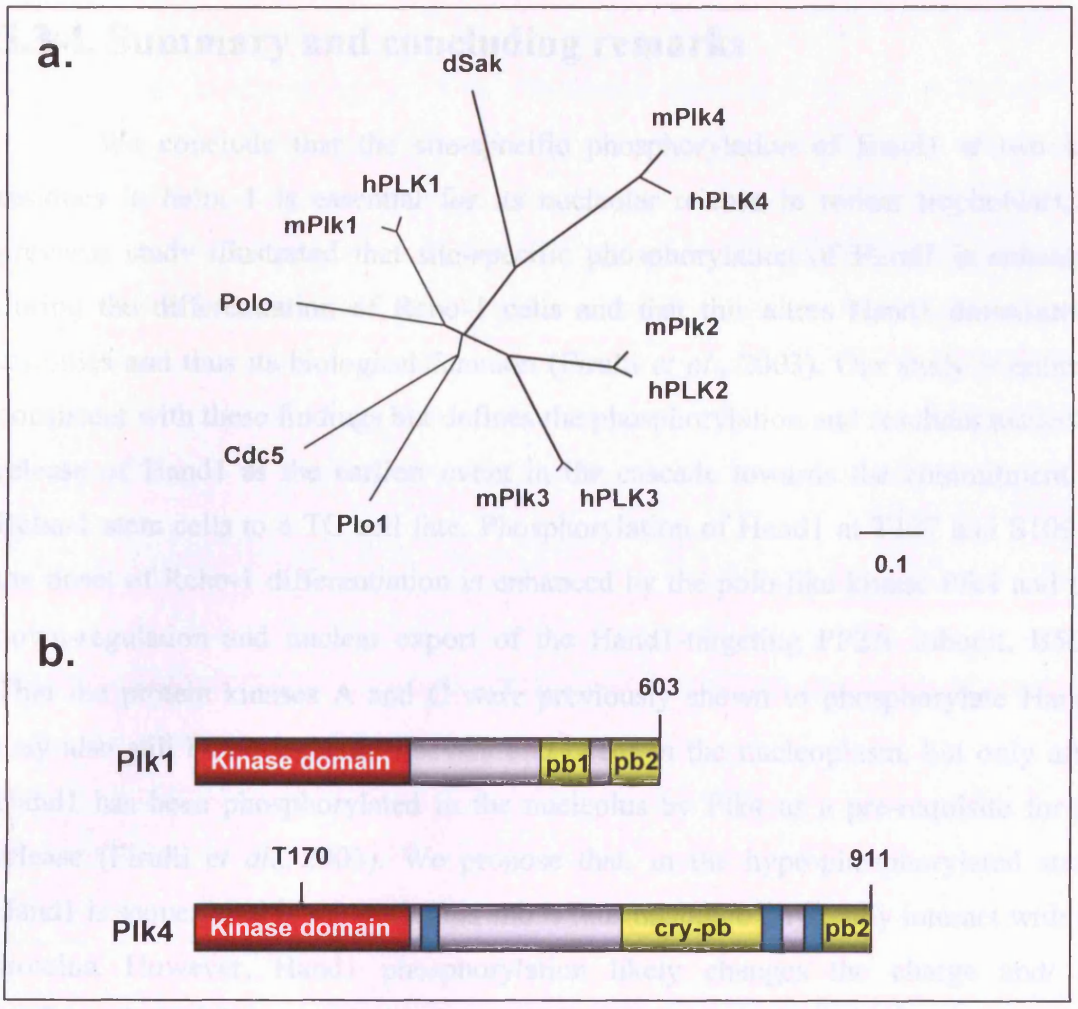

Figure 5.23. Comparison of the basic structure of murine Plk4 with that of Plk1 (a) and the evolutionary divergence of Plk4 from other members of the Plk family (b).

In (**a**), phylogenic relationship of polo-like kinases was determined by the CLUSTALX program, and the scale represents 0.1 amino acid replacement per site. In (**b**), the position of the threonine-170 residue, whose mutation to an aspartic acid generates a gain-of-function Plk4 allele (Swallow *et al.*, 2005), is shown. **pb**: polo box, **cry-pb**: cryptic polo-box, **blue boxes**: PEST destruction motifs., **d**: *Drosophila*, **m**: mouse, **h**: human. Adapted from Hudson *et al.*, 2001.

5.3.4. Summary and concluding remarks

We conclude that the site-specific phosphorylation of Hand1 at two key residues in helix 1 is essential for its nucleolar release in rodent trophoblast. A previous study illustrated that site-specific phosphorylation of Hand1 is enhanced during the differentiation of Rcho-1 cells and that this alters Hand1 dimerisation affinities and thus its biological function (Firulli *et al.*, 2003). Our study is entirely consistent with these findings but defines the phosphorylation and resultant nucleolar release of Hand1 as the earliest event in the cascade towards the commitment of Rcho-1 stem cells to a TG cell fate. Phosphorylation of Hand1 at T107 and S109 at the onset of Rcho-1 differentiation is enhanced by the polo-like kinase Plk4 and the down-regulation and nuclear export of the Hand1-targeting PP2A subunit, B56δ. That the protein kinases A and C were previously shown to phosphorylate Hand1 may also still be biologically-relevant and occur in the nucleoplasm, but only after Hand1 has been phosphorylated in the nucleolus by Plk4 as a pre-requisite for its release (Firulli *et al.*, 2003). We propose that, in the hypo-phosphorylated state, Hand1 is sequestered in the nucleolus and is thus unable to physically interact with E-proteins. However, Hand1 phosphorylation likely changes the charge and/ or conformation of the transcription factor and so abrogates its affinity for its nucleolar repressor, HICp40. This is particularly likely in view of the finding that the HLH domain of Hand1, within which region T107 and S109 reside, is known to bind several other proteins, possibly including HICp40. Nuclear-wide Hand1 is then able to heterodimerise with E-proteins and thus activate its target genes and/ or trigger mitotic cell cycle exit, an event which commits Rcho-1 stem cells towards a differentiated TG cell fate.

The processes that underlie the nucleolar-nucleoplasmic/ cytoplasmic shuttling of mammalian factors are largely unknown, but several studies, mainly in budding yeast, have shown that phosphorylation is responsible for such trafficking (Table 5.1). In this study we present the first example of phosphorylation underpinning the release of a nucleolar factor during interphase in a mammalian cell. Site-specific phosphorylation of nucleolar Hand1 by Plk4 identifies not only the first physiological substrate for this non-canonical polo-like kinase but also underpins the

functional release of Hand1 into the nucleoplasm. In the context of this study, the alteration of protein charge or steric hindrance introduced by phosphorylation or other post-translational modifications likely abrogates the interaction between the sequestered factor and its ribosomal-machinery-bound nucleolar anchor, namely HICp40, to permit its escape from the nucleolus. Otherwise, Hand1 phosphorylation may promote its interaction with a nuclear anchor or perhaps activate a putative nucleolar export signal. By whichever mechanism, this covalent modification may thus act as a 'molecular switch', implying that nucleoplasmic-nucleolar shuttling can be regulated and is responsive to extracellular stimuli via intracellular signalling pathways.

In conclusion, the findings presented in this chapter reveal a novel mode of Hand1 regulation during TG cell differentiation. This provides insight into the molecular mechanism underlying rodent trophoblast invasion and placentation. In the following chapter, we discuss the wider implications of these findings, the unanswered questions that remain and the aims of ongoing studies.

Chapter 6

General discussion

6.1. Nucleolar release of Hand1 acts as a molecular switch to determine trophoblast stem cell fate

The interaction of Hand1 with other factors is important for controlling its activity (Firulli *et al.*, 2000). Given the promiscuous dimerisation properties of Hand1 with both class A and class B bHLH factors (Chapter 1, Table 1.1), we hypothesised that the transcription factor may functionally interact with non-bHLH factors and that these co-factors may regulate Hand1 activity.

In our current study, we demonstrated that the activity of Hand1 is regulated by the rodent orthologue of the human I-mfa domain-containing protein (HICp40). HICp40-dependent nucleolar sequestration negatively-regulates Hand1 activity in a faithful model of TS cells, the Rcho-1 cell line (reviewed in Chapter 1, section 1.6). Specifically, the nucleolar localisation of Hand1 is associated with its transcriptional inactivity and TS cell renewal. Rcho-1 TS cells can be induced to undergo TG cell differentiation by modifying the culture conditions, namely by replacing fetal bovine serum with horse serum. We found that Hand1 disperses throughout Rcho-1 stem cell nuclei coincident with their differentiation into TG cells. As confirmation of this, HICp40 gain- and loss-of function assays modulate Rcho-1 TG cell differentiation by affecting Hand1 subcellular localisation. Thus the release of Hand1 from the nucleolus is necessary and sufficient for TG cell differentiation and this mechanism may underlie the first differentiation event during embryogenesis.

A previous study showed that Hand1 is phosphorylated at two residues in helix I during TG cell differentiation (Firulli *et al.*, 2003). This enhances the affinity of Hand1 for its bHLH binding partners as a crucial step in the TG cell differentiation program. We demonstrated that an increase in Hand1 phosphorylation at these two residues underpins its nucleolar release at the onset of TG cell differentiation. Crucially, our findings are entirely consistent with the earlier study (Firulli *et al.*, 2003), but place the phosphorylation and nucleolar release of Hand1 as the earliest event during TG cell differentiation. We speculate that this post-translational modification modifies the charge and/ or conformation of Hand1, so diminishing its affinity for nucleolar HICp40 and thus triggering its nucleolar release.

We then investigated which nucleolar kinase phosphorylates Hand1. This was shown to be Plk4 (Sak), a non-canonical member of the serine/ threonine polo-like kinase family whose members commonly modify the subcellular localisation of their substrates (Toyoshima-Morimoto *et al.*, 2001; 2002; Kim *et al.*, 2005). Haploinsufficiency for *Plk4* results in mitotic infidelity, chromosomal instability and carcinogenesis, particularly old age-onset liver tumourigenesis (Ko *et al.*, 2005). The basis of this is likely to be the crucial role for Plk4 in centriole duplication and spindle organisation during mitosis (Bettencourt-Dias *et al.*, 2005; Habedanck *et al.*, 2005; Kleylein-Sohn *et al.*, 2007). Indeed, *PLK4* expression is aberrant in some colorectal cancers and hepatomas (MacMillan *et al.*, 2001; Ko *et al.*, 2005). *Plk4*-null mice are embryonic lethal at E9.5-E10.0 due to widespread apoptosis caused by inappropriate anaphase arrest (Hudson *et al.*, 2001). However, the trophoblast lineage was not analysed in this study.

Plk4 is unique in the mammalian Plk family in that it localises to the nucleolus during the second gap phase (G2) of the mitotic cell cycle (Hudson *et al.*, 2001). Interestingly this is the stage at which TG cell differentiation is thought to be initiated (MacAuley *et al.*, 1998). Therefore, Plk4 is in the right place at the right time to activate Hand1 and so initiate endoreduplication. Our current study demonstrated that Plk4 can interact and react with Hand1 *in vitro* and *in vivo*. Moreover gain- and loss-of-function *Plk4* assays modify Hand1 subcellular localisation with appropriate effects on TG cell differentiation. Importantly, Hand1 is unable to exit the nucleoli of *Plk4*-null diploid trophoblast and this is associated with their impaired ability to undergo SGC differentiation.

Of note, the site-specific phosphorylation of Hand1 by Plk4 is complemented by the 'elimination' of a Hand1 phosphatase. During TG cell differentiation the Hand1-targeting regulatory subunit B56δ of protein phosphatase 2A (PP2A) is both exported from the nucleus (data presented in this study) and down-regulated (Firulli *et al.*, 2003). Thus a positive-feedback loop is likely to ensue, whereby the elimination of $PP2A^{B56\delta}$ from the nuclear compartment allows phosphorylated Hand1 to persist. Phosphorylated Hand1 is in turn able to accomplish its nuclear functions and this further drives the process of TG cell differentiation (Figure 6.1).

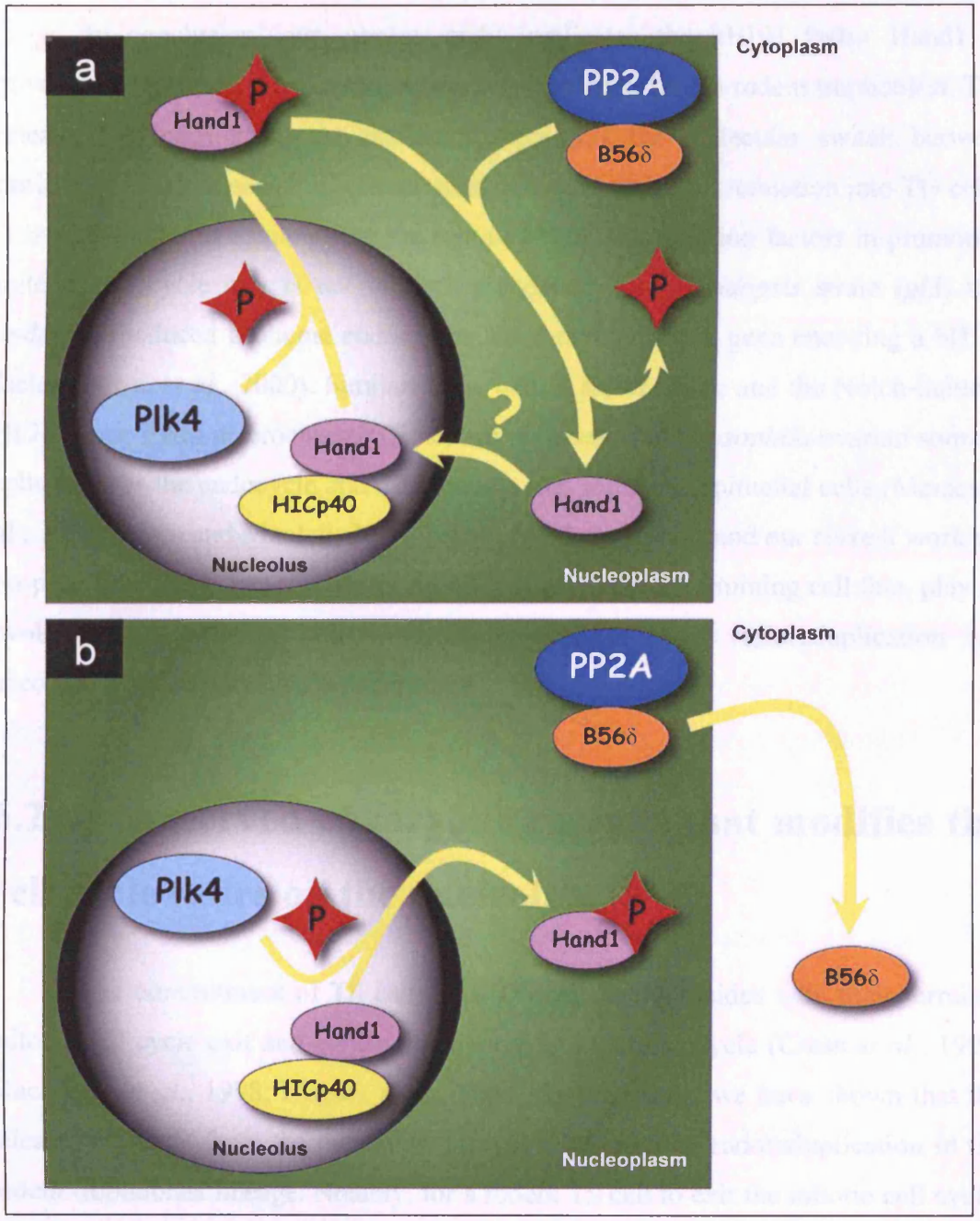

Figure 6.1. The molecular mechanism underlying mitotic cell cycle exit in rodent trophoblast.

During TS cell renewal, pre-existing Hand1 is sequestered in an inactive state in the nucleolus by the rat orthologue of HICp40. Should nucleolar Hand1 be inappropriately phosphorylated by Plk4 and released, nuclear $PP2A^{B56\delta}$ targets it for dephosphorylation and nucleolar re-entry. It is unknown whether Hand1 nucleolar sequestration is active or passive (**a**). A change in serum conditions results in the phosphorylation of nucleolar Hand1 by Plk4 during phase G2 of the final mitotic cell cycle. Concurrently, B56δ is exported to the cytoplasm and down-regulated. These events enhance the phosphorylation of Hand1, resulting in its nucleolar release (**b**). **P**: phosphoserine/ phosphothreonine.

In conclusion, our current study implicates the bHLH factor Hand1 in governing the onset of endoreduplication and thus cell fate in rodent trophoblast. The release of Hand1 from the nucleolus represents the molecular switch between proliferative self-renewal of Rcho-1 stem cells and their differentiation into TG cells. It is also worth mentioning that the role of bHLH transcription factors in promoting mitotic cell cycle exit is not without precedent. An *Arabidopsis* strain (*gl3*) that undergoes reduced trichome endocycles has a mutation in a gene encoding a bHLH factor (Payne *et al.*, 2000). Similarly, the bHLH factor dMyc and the Notch-induced HLH factor Extra macrochaetae (Emc) are necessary for *Drosophila* ovarian somatic cells to enter the endocycle and differentiate into follicular epithelial cells (Maines *et al.*, 2004; Adam and Montell, 2004). In light of these studies and our current work we propose that bHLH factors, which are often involved in determining cell fate, play an evolutionarily-conserved role in promoting the onset of endoreduplication and accompanying terminal differentiation.

6.2. A conserved eukaryotic cascade that modifies the cell cycle relies on the nucleolus

The commitment of TS cells to a TG cell fate coincides with their terminal mitotic cell cycle exit and concomitant entry into the endocycle (Cross *et al.*, 1995; MacAuley *et al.*, 1998; Hughes *et al.*, 2004). In this study, we have shown that the release of Hand1 from the nucleolus underlies the onset of endoreduplication in the rodent trophoblast lineage. Notably, for a rodent TS cell to exit the mitotic cell cycle, mitotic cyclins must also be ubiquitinated for proteasomal degradation by the anaphase-promoting complex/ cyclosome (APC/C) (MacAuley *et al.*, 1998). Otherwise their activity must be inactivated (Palazon *et al.*, 1998). The APC/C complex is also required for exit from mitosis during the mitotic cell cycle, which in turn is dependent again on its targeting of mitotic cyclins for degradation (reviewed by Cerutti and Simanis, 2000).

APC/C substrate specificity is governed by its interaction with WD-repeat family proteins including budding yeast Cdc20 (*Drosophila* Fizzy, human $p55^{CDC}$)

and Cdh1 (*Drosophila* Fizzy-related (Fzr), human hCDH1) (Sigrist and Lehner, 1997; Lorca *et al.*, 1998; Kramer *et al.*, 2000). APC/C^{Cdc20} appears during metaphase and is required for the destruction of the Separase inhibitor Securin as a crucial step towards sister chromatid separation and the trigger for anaphase entry. In contrast, APC/C^{Cdh1} predominates in late anaphase and promotes mitotic exit by targeting mitotic cyclins and other mitotic inducers for proteasomal degradation (reviewed by Sullivan and Morgan, 2007).

That the APC/C^{Cdh1} targets mitotic cyclins for proteasomal degradation to trigger mitotic exit is very relevant in light of the findings of our study. APC/C substrate-determining yeast Cdh1 orthologues in *Arabidopsis* (Ccs52A) and *Drosophila* (Fzr) are respectively required for down-regulating mitotic cyclins to switch the mitotic cell cycle at phase G2 to the endocycle during seed (Cebolla *et al.*, 1999) and salivary gland (Sigrist and Lehner, 1997) development. Furthermore, mutations that reduce mitotic Cyclin B-Cdk1 activity induce an endoreduplication phenotype in both fission (Hayles *et al.*, 1994) and budding (Azzam *et al.*, 2004) yeast. Thus in terms of mitotic cell cycle exit in TS cells, the release of Hand1 from the nucleolus underlies the onset of the endocycle. How Hand1 achieves this is as yet unknown, but possible mechanisms are discussed later in this chapter (section 6.3.2).

6.2.1. Release of a factor sequestered in the nucleolus underlies mitotic (cell cycle) exit and genomic hyper-amplification

In this study, we show that the release of a nucleolar factor, Hand1, underpins the onset of endoreduplication and concomitant TG cell differentiation in the Rcho-1 trophoblast stem cell line. Interestingly, studies in *S. cerevisiae* have also identified an APC/C^{Cdh1} activator that is sequestered in the pre-mitotic nucleolus, the phosphatase Cdc14 (Shou *et al.*, 1999; 2002; Visintin *et al.*, 1999; 2003; Yoshida and Toh-e, 2002). During interphase and early mitosis, Cdc14 is bound in an inactive state to the nucleolar, multi-functional regulator of nucleolar silencing and telophase (RENT) complex (reviewed by Cockell and Gasser, 1999). This complex comprises several nucleolar proteins including Cfi1 (Net1), Nan1 and Sir2. However, at the

onset of anaphase, Cdc14 is released from the nucleolus to dephosphorylate its nuclear targets (reviewed by Cockell and Gasser, 1999). These include a cyclin-dependent kinase inhibitor (Sic1), which is stabilised by dephosphorylation, and a Sic1 transcription factor (Swi5), whose dephosphorylation induces its nuclear entry. Another of its targets is the APC/C substrate-determining subunit Cdh1, whose dephosphorylation promotes its nuclear export and integration into an APC/C^{Cdh1} complex that ubiquitinates and marks mitotic cyclins for proteasomal degradation (Jaquenoud *et al.*, 2002; Bembenek *et al.*, 2005; reviewed by Morgan and Sullivan, 2007). Collectively, these events underlie exit from mitosis in budding yeast and the onset of the next mitotic cell cycle.

Cdc14 inactivation by nucleolar sequestration during interphase also serves a second cellular function in budding yeast. This negative regulatory mechanism prevents inappropriate Cdc14-dependent dephosphorylation and inactivation of DNA replication factors during S-phase (Bloom and Cross, 2007). In this regard, it is interesting that Hand1 is sequestered in the nucleolus in an inactive state until cells begin to hyper-amplify the genome during endoreduplication (data presented in this study). In conclusion, the nucleolar sequestration of a cell fate determinant, Cdc14 in budding yeast or Hand1 in rodent trophoblast, is a key cellular event that regulates exit from mitosis and genomic replication.

6.2.2. A polo-like kinase is recruited to the nucleolus to phosphorylate and release a factor involved in mitotic (cell cycle) exit

The mechanistic similarities between the budding yeast mitotic exit network and the entry of TS cells into the endocycle extend beyond the analogous function of the APC/C. We have shown that nucleolar release of Hand1 is dependent on its phosphorylation by the polo-like kinase, Plk4. Interestingly, the sole polo-like kinase in budding yeast, Cdc5, phosphorylates Cdc14 to initiate its nucleolar release (Shou *et al.*, 1999; Shou *et al.*, 2002; Visintin *et al.*, 1999; Visintin *et al.*, 2003; Yoshida and Toh-e, 2002).

Cdc5 phosphorylates Cdc14 at the end of the Cdc fourteen early anaphase release (FEAR) network, a poorly-understood cascade that releases a small amount of Cdc14 from the nucleolus (Stegmeier *et al.*, 2002). Cdc5 also phosphorylates Cdc14, amongst other targets, during the mitotic exit network (MEN). This cascade is initiated by the first wave of nucleolar-released Cdc14, which triggers a G protein- (Tem1-) initiated signalling cascade and the dephosphorylation of the Cdc15 kinase (Shou *et al.*, 2002). Ultimately, this results in a positive-feedback loop that releases Cdc14 from the nucleolus in bulk (Jaspersen *et al.*, 1998; Shou *et al.*, 1999; 2002; Visintin *et al.*, 1999; 2003; Yoshida and Toh-e, 2002).

Plk4 is a component of the analogous mammalian mitotic exit network that relies on the same premise of APC/C^{Cdh1}-dependent destruction of mitotic cyclins (Hudson *et al.*, 2001). Although *Plk4*-null embryos exhibit high levels of cyclin B and Cdk1, indicative of defective APC/C^{Cdh1} activation, it is unclear whether Plk4 directly phosphorylates and activates components of the APC/C^{Cdh1}. It is notable, however, that the sole polo-like kinase in fission yeast (Plo1; May *et al.*, 1998), and the related mammalian Plk family member, Plk1 (Kotani *et al.*, 1998; Feng *et al.*, 2001; Golan *et al.*, 2002; Moshe *et al.*, 2004), modulate APC/C activity by phosphorylating its subunits, inhibitors and even its proteasome effector.

Alternatively, the process may be analogous to the MEN in budding yeast in that Plk4 could activate an as-yet unidentified phosphatase that then dephosphorylates and activates an APC/C component. Indeed, one human CDC14 isoform, CDC14A, is centrosomal and dephosphorylates and activates the human CDH1 component of the APC/C as a pre-requisite for exit from mitosis (Bembenek and Yu, 2001). Another human CDC14 isoform, CDC14B, is nucleolar during interphase, but its function has been more elusive (Kaiser *et al.*, 2002; Mailand *et al.*, 2002). It will in this regard be interesting to see whether Plk4 can phosphorylate CDC14B in the G2 phase nucleolus and furthermore investigate the functional basis of such an event. However, it is worth mentioning that the *S. pombe* homologue of Cdc14 (Flp1p/ Clp1p) is not required for mitotic exit, but is instead involved in septum formation and cytokinesis (Cueille *et al.*, 2001; Trautmann *et al.*, 2001). Thus it would not be surprising to find that the mechanism governing mitotic cell cycle exit in rodent trophoblast does not involve CDC14 isoforms.

Notably other aspects of Cdc5 and Plk4 regulation are also conserved between yeast and mammals. For example, both Cdc5 and Plk4 are rapidly ubiquitinated for proteasomal degradation as part of a negative feedback loop during G1 by the APC/C, which they in part activated at the end of the previous mitotic cell cycle (Fode *et al.*, 1996; Shirayama *et al.*, 1998). In the case of Plk4, a low protein half-life is conferred by three so-called PEST sequences at its C-terminus (Fode *et al.*, 1996; Yamashita *et al.*, 2001; Figure 5.23b). In conclusion, whilst both Cdc5 and Plk4 are required at anaphase for exit from mitosis, we have shown in this study that Plk4 can additionally initiate endoreduplication during phase G2 under certain conditions. It achieves this by phosphorylating nucleolar Hand1, whose release into the nucleoplasm underlies the transition from the mitotic cell cycle to the endocycle.

6.2.3. A PP2A complex antagonises the nucleolar release of a factor involved in mitotic exit

The down-regulation (Firulli *et al.*, 2003) and nuclear export (data presented in this study) of the regulatory (B, substrate-recognising) subunit B56δ of the protein phosphatase 2A (PP2A) serine/ threonine phosphatase contributes to Rcho-1 TG cell differentiation. This exclusion of $PP2A^{B56\delta}$ from the nucleolus and nucleus likely facilitates Plk4-dependent Hand1 phosphorylation at the onset of TG cell differentiation. This is yet another conserved aspect of the cascade governing cell cycle regulation between yeast and mammals: the PP2A B-subunit Cdc55 plays a critical role in blocking the onset of the budding yeast MEN (Queralt *et al.*, 2006).

Budding yeast Net1, the nucleolar anchor for Cdc14, is kept hypo-phosphorylated prior to anaphase by a PP2A complex containing Cdc55 (Queralt *et al.*, 2006). This has the effect of suppressing ectopic Cdc14 nucleolar release and thus inappropriate mitotic exit outside of anaphase. At anaphase the sister chromatid-separating protease Separase, released at the onset of anaphase from its Securin inhibitor, interacts with and inactivates $PP2A^{Cdc55}$ (Queralt *et al.*, 2006). Thus, a PP2A complex containing Cdc55 (budding yeast) or B56δ (rat trophoblast; Firulli *et al.*, 2003; data presented in this study) antagonises exit from mitosis until the onset of anaphase or exit from the mitotic cell cycle until the onset of endoreduplication

respectively. However, the PP2A complexes achieve this effect by different means. $PP2A^{Cdc55}$ dephosphorylates the nucleolar sequesteror of Cdc14, Net1 (Queralt *et al.*, 2006), whereas $PP2A^{B56\delta}$ maintains the sequestered factor, Hand1, in a dephosphorylated state during TS cell renewal (data presented in this study).

6.2.4. Speculative extrapolations of our model

In conclusion, there are numerous similarities between a mechanism governing mitotic exit in budding yeast and mitotic cell cycle exit in rodent trophoblast. In light of these, it is possible that other aspects of the *S. cerevisiae* FEAR and MEN pathways also serve to modulate the onset of TG cell differentiation. Cdc55 is degraded by Separase at the onset of anaphase in budding yeast and this allows Cdc5-dependent phosphorylation of Cdc14 to persist (Queralt *et al.*, 2006). In this regard, it will be interesting to investigate whether mammalian Separase is partly responsible for B56δ 'elimination' at the onset of TG cell differentiation. Additionally, at anaphase, Cdc5 is also thought to phosphorylate the nucleolar sequesteror of Cdc14, Net1 (Yoshida and Toh-e, 2002). $PP2A^{Cdc55}$ conversely keeps Net1 hypo-phosphorylated prior to anaphase (Queralt *et al.*, 2006). Thus it is possible that Plk4 and $PP2A^{B56\delta}$ similarly modulate the phosphorylation of the Hand1 sequesteror, HICp40. Indeed another kinase, the pTEFb component Cdk9, phosphorylates HICp40 at conserved sites in its I-mfa domain (Wang *et al.*, 2007). Related to this, it would be interesting to investigate whether, like other bHLH proteins, Hand1 recruits the pTEFb complex to its target gene transcripts for the purpose of transcriptional elongation (Simone *et al.*, 2002). Should this be the case, the observed inhibitory effect of HICp40 on the pTEFb complex (Young *et al.*, 2003), possibly via nucleolar sequestration, may represent another mode by which HICp40 negatively-regulates Hand1 transcriptional activity. Further investigation is required to confirm these hypotheses.

6.3. Unanswered questions

There are, however, some aspects of our model that remain unclear and require further investigation. For example, the bHLH or non-bHLH transcription factor partners to which nucleolar-released Hand1 binds in TG cells remain to be definitively determined. A few studies have suggested that the bHLH factors Stra13 and/ or Hrt1-3, and the HMG-box factor Sox15, bind Hand1 during TG cell differentiation and that this makes Hand1 transcriptionally-competent (Firulli *et al.*, 2000; Hughes *et al.*, 2004; Yamada *et al.*, 2006). However, no *in vivo* evidence was provided by these studies. Another study suggested that Hand1 may act as a homodimer to drive the process of TG cell differentiation *in vivo* (Hu *et al.*, 2006). The identity of the pro-endoreduplicative signals and how they affect Plk4 and $PP2A^{B56\delta}$ activity upstream of Hand1 are also currently unknown. Finally, at present, we can only speculate as to how the nucleolar release of Hand1 triggers mitotic cell cycle exit. The following section discusses some of the putative underlying cellular and molecular mechanisms which could shed light on these key questions.

6.3.1. What precedes the release of Hand1 from the nucleolus?

The nucleolar release of Hand1 is by no means at the pinnacle of the cascade that promotes TG cell differentiation. However, precisely how the transition from the normal mitotic cycle to endocycle is regulated remains poorly understood, particularly in the rodent trophoblast lineage. In *Drosophila*, one study identified an insulin receptor/ phospho-inositol-3-kinase-reliant link between the abundance of dietary amino acids and mitotic cell cycle exit (Britton and Edgar, 1998; Britton *et al.*, 2002). There also appears to be a relationship between the onset of endoreduplication in *Drosophila* and oxygen concentration, dependent on cyclin D/Cdk4 (Frei and Edgar, 2004). This is interesting in light of the results of previous studies and ours that report that low oxygen concentration blocks aspects of invasive trophoblast differentiation (Gultice *et al.*, 2006; Lash *et al.*, 2007; Takeda *et al.*, 2007). However, whether such mechanisms induce rodent TS cells entry into the endocycle is currently unknown.

In light of our recent work we can assume that as-yet unidentified factors in horse serum (HS), or alternatively a lack of inhibitory factors present in fetal bovine serum (FBS), are responsible for driving TS cells into the endocycle. These extracellular factors are likely to initiate an intracellular signalling cascade that modulates Hand1 phosphorylation, via the adjustment of Plk4 and/ or B56δ levels, subcellular localisation and/ or activity. Such a mechanism would not be without precedent: a previous study showed that Fgf2 binds to Casein kinase II, and that this event promotes nucleolar serine/ threonine phosphorylation of Nucleolin (Bonnet *et al.*, 1996). More recently, the GTP-dependent shuttling of Nucleostemin between the nucleolar and nucleoplasmic compartments has been proposed to link extracellular signalling cascades to protein subcellular localisation (Tsai and McKay, 2002). Indeed, nucleoli are known to respond to changes in cellular growth rate and metabolic activity, suggesting that they constantly receive and respond to signalling events. At the onset of endoreduplication, *Plk4* expression increases (data presented in this study) whilst that of *B56δ* is down-regulated (Firulli *et al.*, 2003). This occurs in parallel with the export of the B56δ protein from the nucleus. Further investigation is therefore needed to identify the factors that regulate the transcription of these two genes in rodent trophoblast.

In proliferating diploid trophoblast, Plk4 plays a part in regulating centriole duplication during prophase and spindle organisation during cytokenesis (Bettencourt-Dias *et al.*, 2005; Habedanck *et al.*, 2005; Kleylein-Sohn *et al.*, 2007) and localises to the nucleoli at every G2 phase (Hudson *et al.*, 2001). However, it is clear from our data that Plk4 does not react with nucleolar Hand1 during each mitotic cell cycle in proliferating TS cells. How, then, is the nucleolar Plk4-Hand1 reaction confined to diploid trophoblast about to undergo TG cell differentiation? One possibility is that the $PP2A^{B56\delta}$ complex, present in TS cell nuclei, antagonistically counteracts Plk4-dependent Hand1 phosphorylation. Only when the TS cell is triggered to differentiate is B56δ protein exported to the cytoplasm and *B56δ* down-regulated, which allows phosphorylated Hand1 to persist in the nucleus. However, this cyclic phosphorylation-dephosphorylation mechanism strikes us as inefficient. Other mechanisms may thus restrict the reaction of Plk4 with Hand1 to an appropriate time.

Another possibility is that levels of Plk4 protein need to cross a critical threshold to phosphorylate nucleolar Hand1. Crucially, this level would be higher than that required for its other cellular functions. This hypothesis is supported by our observation of *Plk4* up-regulation at the onset of TG cell differentiation. Nevertheless, this up-regulation of *Plk4* is coincident with the nucleolar release of Hand1, which suggests that other mechanisms must also play a part. Perhaps in order to phosphorylate Hand1, Plk4 must bind a nucleolar co-activator, itself activated by a change in serum conditions. Yet another possibility is that Plk4 only recognises Hand1 after the transcription factor has first been phosphorylated by a nucleolar 'priming kinase'. This would be reminiscent of the mechanism of action of its related mammalian family member, Plk1 (Elia *et al.*, 2003). The polo-box domain (PBD) of Plk1, which comprises both of its polo-boxes and some flanking sequence, can only dock onto its substrates after their modification by enzymes including Cdks, MAP kinases and other mitotic kinases (reviewed by Lowery *et al.*, 2003). This mechanism of action may also apply to the *S. pombe* polo-like kinase Plo1 (Grallert and Hagan, 2002). Further investigation would be required to investigate whether kinase(s) act upstream of Plk4 on Hand1.

Alternatively it is possible that the signalling cascades upstream of nucleolar and non-nucleolar Plk4 may be independent. This was recently suggested by others (Tanenbaum and Medemao, 2007) and would entail the activation of nucleolar Plk4, but not non-nucleolar Plk4, in response to a change in serum conditions. Finally, we have assumed that Hand1 phosphorylation reduces its affinity for HICp40 and that this underlies its nucleolar release. An alternative possibility is that, in proliferating TS cells, HICp40 conceals the Hand1 phosphorylation sites targeted by Plk4. HICp40 modification in response to a change in serum conditions may subsequently expose these residues to the kinase.

6.3.2. What follows the release of Hand1 from the nucleolus?

Perhaps the principal question still remaining is just how the nucleolar release of Hand1 triggers mitotic cell cycle exit. The most obvious hypothesis is that nuclear-wide Hand1 commits TS cells to differentiation via transcriptional effects. However, very few target genes and protein-protein interactions have been identified for Hand1 in trophoblast. Furthermore, where interactions have been identified, such as occurs between Hand1 and the HMG-box transcription factor Sox15 (Yamada *et al.*, 2006), the functional significance remains unclear.

A pre-requisite for endoreduplication in all organisms is the down-regulation of genes whose products promote entry into mitosis (Grafi and Larkins, 1995; Sauer et al., 1995; MacAuley et al., 1998). Indeed, an inappropriate endocycle can be induced in diploid cells simply by inhibiting mitotic cyclin activity (Sigrist and Lehner, 1997). Conversely, ectopic expression of mitotic cyclins shunts endocycling plant cells into a mitotic cell cycle (Schnittger *et al.*, 2002). Hand1 can function as a transcriptional repressor but no evidence to date implicates it in the down-regulation of mitotic activators in trophoblast. It is interesting, however, that *Plk4*-null embryos exhibit high levels of cyclin B and Cdk1 (Hudson *et al.*, 2001), indicative of a loss of APC/C function. It is possible, then, that Plk4 may directly phosphorylate components, regulators or downstream effectors of the APC/C. Indeed, this is a function attributed to Plo1, the sole polo-like kinase in *S. pombe* (May *et al.*, 2002), and the highly-related mammalian polo-like kinase Plk1 (Kotani *et al.*, 1998; Feng *et al.*, 2001; Golan *et al.*, 2002; Moshe *et al.*, 2004). Otherwise nuclear-wide Hand1, or the products of its target genes, may block mitotic cyclin synthesis or activity. Indeed Hand1 is released during G2, just prior to what would normally be the start of mitosis and which is coincident with mitotic cyclin synthesis (MacAuley *et al.*, 1998).

A role for Hand1 in cell cycle control has been suggested previously, on the basis of the down-regulation of the transcription factor in gastric and pancreatic cancers (Kaneda *et al.*, 2002; Hagihara *et al.*, 2004). Two studies focusing on the cardiac lineage have implicated Hand1 in the regulation of genes encoding cell cycle

modifiers, including *cyclin D1* (Smart *et al.*, 2002; Risebro *et al.*, 2006). It is plausible, therefore, that the dramatic switch upon TG cell differentiation from *cyclin D3* to *D1* expression (MacAuley *et al.*, 1998; Palazon *et al.*, 1998), and the up-regulation of two associated cyclin-dependent kinase inhibitors (Bates *et al.*, 1998; Hattori *et al.*, 2000), may be instigated by Hand1. Notably Smart and co-workers identified *Wnt2* as a putative target gene of Hand1, albeit in a cardiac cell model (Smart *et al.*, 2002). Notably, deletion of the *Wnt2* gene in mice is associated with defective placentation characterised by ectopic TG cells (Monkley *et al.*, 1996). This suggests that Wnt2 is involved in blocking TG cell differentiation and moreover implicates Hand1 in its repression in trophoblast.

In the current study, we reveal that a constitutively-nucleoplasmic Hand1 phosphorylation mimic (Hand1 T107;S109D) localises to discrete subnuclear foci. These may represent a subset of so-called 'transcription factories', based on co-localisation of RNA polymerase II. These sites, which may be transiently occupied by wild-type Hand1, are hotspots of gene activation in the nucleus (Osbourne *et al.*, 2004). Additionally these subnuclear bodies resemble chromatin-remodelling complexes, which are involved in altering DNA-nucleosome topology, to which other transcription factors localise upon their release from the nucleolus (Grasberger and Bell, 2005). Chromatin-remodelling complexes have additionally been shown to bind and sequester the mitotic cyclins whose inactivation is necessary for mitotic cell cycle exit (Kellogg *et al.*, 1995). Interestingly, another of the Hand1 interactors identified in the Y2H screen was the SWI/SNF-related matrix-associated actin-dependent regulator of chromatin subfamily E member 1 (Smarce1; Appendix 8). This is involved in transcriptional activation and repression of select genes by chromatin remodeling (Belandia *et al.*, 2002). Further investigation is required to corroborate this interaction and to investigate whether it has functional significance in rodent TG cell differentiation.

Does nuclear-wide Hand1 alternatively promote mitotic cell cycle exit more directly, in a mechanism independent of transcription? One way in which Hand1 could achieve this is by promoting TS cells to endoreduplicate by default. Hand1 has been shown to promote TG cell differentiation by competing for the E-factor binding partners and promoters of Mash2, a bHLH factor required for TS cell maintenance

(Guillemot *et al.*, 1994; Scott *et al.*, 2000). However the role of Hand1 in promoting TG cell differentiation is not restricted to inhibiting Mash2-dependent transcription (Scott *et al.*, 2000). Moreover, Rcho-1 TS cells proliferate independently of Mash2 (Cross *et al.*, 1995).

Another possibility is that nuclear-wide Hand1, or the products of putative Hand1 target genes, interfere with fibroblast growth factor (Fgf)-dependent signalling. Fgfs, in particular Fgf4, have been shown previously to play a part in TS cell maintenance (Tanaka *et al.*, 1998; Zhong *et al.*, 2006). Such a role for Hand1 has been suggested previously, in view of the fact that ectopic Hand1 expression in TS cells can override Fgf4-dependent mitotic cell cycling and force endocycle entry (Hughes *et al.*, 2004). However, the mechanistic basis for this was not investigated. In this regard, it is also interesting that another of the Hand1 interactors identified in our Y2H screen was the receptor for Fgf4-dependent signaling in trophoblast stem cells (Fgf receptor-2 (Fgfr2); Appendix 8; Auman *et al.*, 1998). However, further investigation is needed to corroborate this interaction and assess its functional significance.

Retinoic acid (RA)-dependent signalling also promotes TG cell differentiation (Yan *et al.*, 2001), possibly via the transcription factors Stra2 (AP-2γ) and Stra13, which themselves drive TG cell differentiation (Auman *et al.*, 2002; Hughes *et al.*, 2004). However an involvement of Hand1 in this pathway has yet to be determined. It is also interesting that Notch-dependent signalling has been implicated in the transition from the mitotic cell cycle to the endocycle, at least in *Drosophila* follicular epithelial cells (Deng *et al.*, 2001; Schaeffer *et al.*, 2004; Sun and Deng, 2005). In one study Notch-dependent signalling was shown to down-regulate the homeodomain gene *Cut*, whose product is a negative regulator of the APC/C activator Fzr (Sun and Deng, 2005). Hand1 can bind Mastermind-like 2 (Maml2), a placenta-expressed trans-activator of the Notch signalling pathway (P. Riley, unpublished data). However, whether this interaction occurs in rodent trophoblast with functional significance is unknown.

An alternative possibility is that Hand1 modifies the function of the APC/C. A modified APC/C may target Snail and Geminin, factors that inhibit the onset of endoreduplication in diploid trophoblast (Nakayama *et al.*, 1998; Gonzalez *et al.*, 2006), for proteasomal degradation. Thus in *Plk4*-null trophoblast Hand1 would be unable to achieve this because it remains sequestered in the nucleolus. It is interesting in this regard that several of the Hand1 interactors identified in our Y2H screen are E3 ubiquitin ligases or proteins with RING-finger domains, which are motifs that mediate the transfer of ubiquitin from conjugating enzymes to substrates to be degraded. Whether a relationship exists between Hand1 and APC/C activity is unknown, however, and would require further investigation. The possible events downstream of the release of Hand1 from the nucleolus during TG cell differentiation are listed in Figure 6.2.

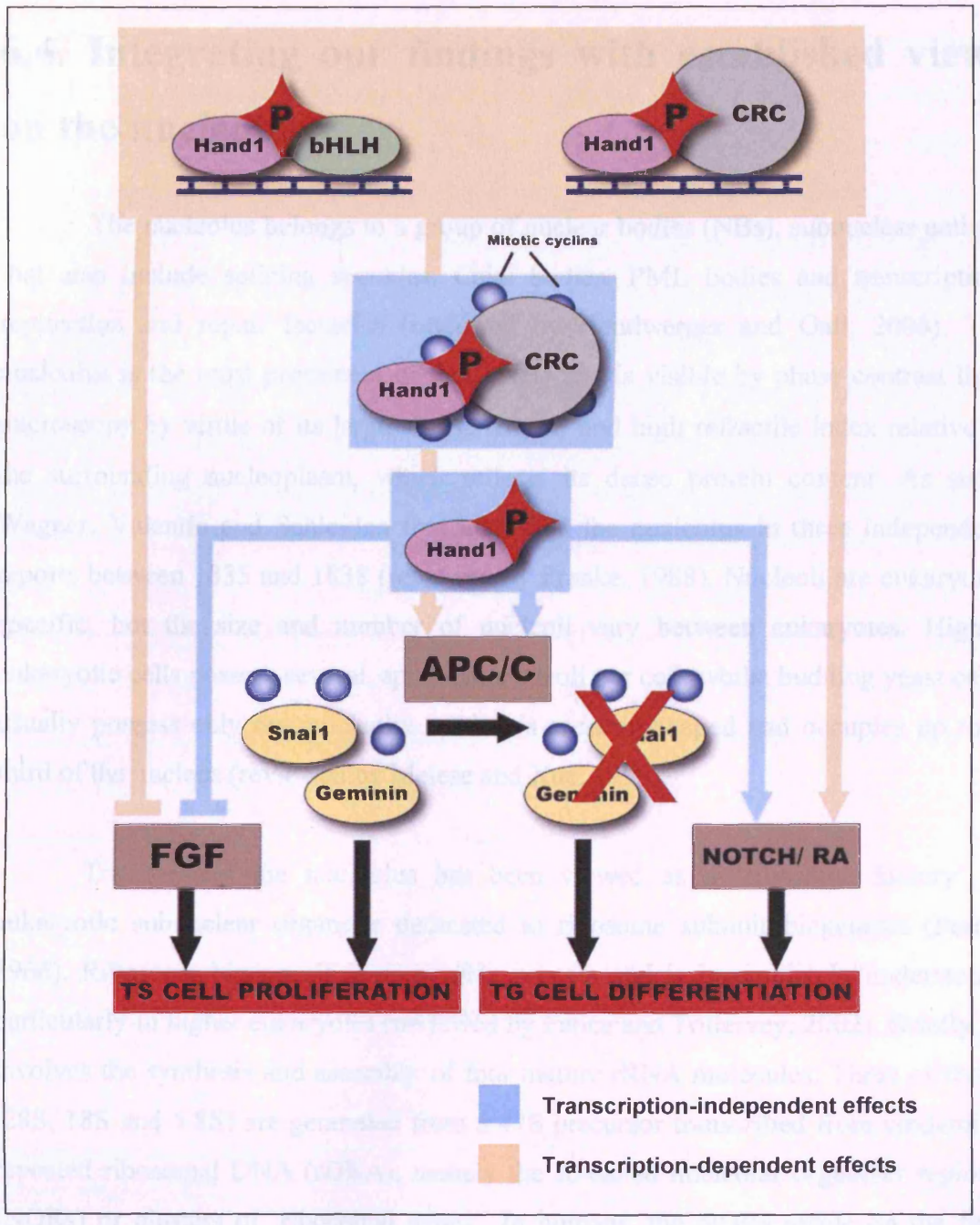

Figure 6.2. How does nuclear Hand1 promote mitotic cell cycle exit and the onset of endoreduplication in trophoblast stem cells?

Hand1 may promote endoreduplication in a transcription-dependent or transcription-independent fashion. This may antagonise Fgf-dependent signalling pathways, which sustain TS cell proliferation, or may promote RA- and Notch-dependent signalling pathways, which promote TG cell differentiation. Otherwise APC/C activity may be modified to target mitotic cyclins and endoreduplication inhibitors for destruction.

CRC: chromatin remodelling complex, **APC/C**: anaphase-promoting complex/ cyclosome, **FGF**: fibroblast growth factor, **RA**: retinoic acid, **P**: phosphoserine/ phosphothreonine.

6.4. Integrating our findings with established views on the nucleolus

The nucleolus belongs to a group of nuclear bodies (NBs), subnuclear entities that also include splicing speckles, Cajal bodies, PML bodies and transcription, replication and repair factories (reviewed by Handwerger and Gall, 2006). The nucleolus is the most prominent of these NBs and is visible by phase contrast light microscopy by virtue of its large size (5-10μm) and high refractile index relative to the surrounding nucleoplasm, which reflects its dense protein content. As such, Wagner, Valentin and Schleiden first identified the nucleolus in three independent reports between 1835 and 1838 (reviewed by Franke, 1988). Nucleoli are eukaryote-specific, but the size and number of nucleoli vary between eukaryotes. Higher eukaryotic cells possess several, spherical nucleoli per cell, whilst budding yeast cells usually possess only one nucleolus, which is crescent-shaped and occupies up to a third of the nucleus (reviewed by Melese and Xue, 1995).

Traditionally the nucleolus has been viewed as a 'ribosome factory', a eukaryotic subnuclear organelle dedicated to ribosome subunit biogenesis (Perry, 1966). Ribosome biogenesis is a complex process and is incompletely understood, particularly in higher eukaryotes (reviewed by Fatica and Tollervey, 2002). Briefly, it involves the synthesis and assembly of four mature rRNA molecules. Three of these (28S, 18S and 5.8S) are generated from a 47S precursor transcribed from tandemly-repeated ribosomal DNA (rDNA), namely the so-called nucleolar organizer regions (NORs) or clusters of 'ribosomal genes'. In humans, the NORs reside on the five acrocentric chromosomes and nucleoli form around these loci. The organelle contains both RNA polymerase I, responsible for the transcription of rDNA into pre-rRNA (the 47S precursor). They also contain the machinery for subsequent pre-rRNA processing, for example the small nucleolar ribonucleoproteins (snoRNPs). Finally, protein components that are later complexed with the mature rRNA species to form the 40S and 60S ribosome subunits are also concentrated in the nucleolus. These subunits ultimately leave the nucleolus and nucleus and bind to cytoplasmic mRNA to form a functional (80S) ribosome.

More recently, several studies have characterised the ultrastructure (reviewed in this chapter, section 6.4.1), biogenesis (section 6.4.2) and roles beyond ribosomal biogenesis (section 6.4.3) of the nucleolus. Additionally, motifs found in nucleolar proteins have been arranged into phylogenies and this has given an insight into its evolutionary history (Staub *et al.*, 2004). Although nucleoli are eukaryote-specific, many of their constituent proteins, particularly those related to ribosome biogenesis, are of prokaryotic, particularly archaebacterial, origin. An interesting observation is that most of the higher eukaryote-specific nucleolar protein domains are involved in protein-protein interaction, protein folding (chaperone) and chromatin remodelling. This suggests an increasing tendency during evolution towards compaction of material, perhaps to ensure efficient ribosome biogenesis and/ or to tightly sequester factors away from the rest of the cell. The nucleolus likely arose because it provided a selective advantage in terms of an enhanced efficiency of ribosomal biogenesis and thus proliferation rate. However, once evolved, cells probably exploited the presence of the nucleolus to incorporate additional functions. We show, for example, that the role of the nucleolus as a sequestration centre for proteins involved in cell cycle regulation is conserved between evolutionarily-distinct eukaryotes (discussed previously in this chapter (section 6.2)).

6.4.1. Theories of nucleolar ultrastructure

The amniote nucleolus is subdivided into three components (reviewed by Scheer and Hock, 1999; Dundr and Misteli, 2001; Raska *et al.*, 2006; Sirri *et al.*, 2008). The transcription of rDNA occurs at the border between the fibrillar centers (FC), which are rich in RNA Pol I subunits and surround the NORs, and the dense fibrillar component (DFC), which surrounds the FC and is characterised by an abundance of Fibrillarin. Although the number and size of the FC foci vary, a typical nucleolus contains about thirty, each accommodating about four rRNA genes (reviewed by Dundr and Misteli, 2001). Subsequent pre-rRNA processing occurs in the DFC, which is rich in snoRNPs, and then processed rRNA molecules are transported to the granular component (GC), for association with ribosomal proteins. The GC is the largest intra-nucleolar domain and is rich in B23. Thus the process of ribosomal biogenesis is vectorial. It occurs in discrete stages as the rRNA transcripts

move outwards through the concentric layers surrounding the ribosomal genes (Thiry *et al.*, 2000). There is, however, considerable diversity in the arrangement of the three nucleolar components between species. For example, only amniotes possess the FC, the nucleoli of lower eukaryotes such as *Drosophila* and yeast instead being bipartite (reviewed by Thiry and Lafontaine, 2005). Plant cell nucleoli also have a fourth nucleolar structure, the nucleolar vacuole or cavity, whose role is unknown (reviewed by Shaw and Brown, 2004). Additionally, the plant DFC and FC are integrated into a unique nucleolar structure called the nucleonema (Sato *et al.*, 2005).

The GC, the largest and most permeable nucleolar sub-domain, has been described as a 'non-ribosomal landscape' (Handwerger *et al.*, 2005; Politz *et al.*, 2005). This region lacks rDNA and ribosome biogenesis machinery and as such is unlikely to play any major role in ribosome biogenesis. The GC may therefore represent the 'sequestration centre', whose existence is strongly supported by the findings of our work and other studies. Indeed, the nucleolar proteins $p19^{ARF}$ and Nucleostemin specifically occupy this sub-domain (Lindstrom *et al.*, 2001; Politz *et al.*, 2005). Interestingly, we showed that Hand1 appears to co-localise with NS in this region (Figure 5.22), but further investigation using subnucleolar fractionation techniques would be required to definitively localise Hand1 to this domain. Notably, Politz and colleagues also noted that the GC is heterogeneous at a molecular level (Politz *et al.*, 2005). It is further subdivided into compartments, within which a certain factor or group of factors may be enriched.

Our results reveal that endogenous Plk4 resides in only a single Hand1-positive nucleolus in each Rcho-1 stem cell, being absent from the others. This appears to be a unique finding as, to our knowledge, no literature to date has reported such a protein sub-nucleolar localisation. This raises the possibility that different nucleoli within the same nucleus may possess different proteomes, which is implicit of heterogeneity between nucleoli within the same cell. Indeed, mammalian nuclei can possess nucleoli with considerable heterogeneity in size and morphology (reviewed by Hernandez-Verdun, 2006), which is implicit of differences in composition. If confirmed, such an observation impacts on the current theories regarding nucleolar biogenesis and structure. Nevertheless, we cannot rule out antibody-specific artifacts giving rise to these observations, especially in light of the

fact that an over-expressed GFP-Plk4 fusion protein localised to multiple nucleoli per cell.

6.4.2. The dynamic nucleolus theory

The formation of the nucleolus and the maintenance of its architecture are thought to be dependent on ribosomal biogenesis (reviewed by Scheer and Hock, 1999; Dundr and Misteli, 2001; Raska *et al.*, 2006). Early studies showed that ectopic rDNA transcription is sufficient for the genesis of a nucleolus in budding yeast and *Drosophila* cells (Karpen *et al.*, 1988; Oakes *et al.*, 1998). In humans, nucleolar size can be used to gauge the rapidity of cell proliferation in tumour cells (Derenzini *et al.*, 2000). Moreover, inhibition of ribosomal biogenesis, via the inactivation of RNA Pol I using actinomycin-D (Act-D), inactivation of upstream-binding factor (Ubf) using anti-Ubf antibodies, or upon infection by certain viruses, leads to a loss of nucleolar integrity and its breakdown (Dundr *et al.*, 1996; Rubbi and Milner, 2003; reviewed by Hiscox, 2007). These data have led to the now widely-believed theory that the nucleolus is self-organised, that is, 'the nucleolus is an organelle formed by the act of building a ribosome' (Melese and Xue, 1995). By this mechanism, nucleoli form passively as a result of local accumulation of factors around the rDNA genes.

However, a more recent study has uncoupled the maintenance of nucleolar morphology from RNA Pol I-driven transcription in *Xenopus* (Gonda *et al.*, 2003). In this study, two proteins (FRGY2a and FRGY2b) were shown to reversibly disassemble the nucleolus *in vitro* and *in vivo*, independently of transcriptional inhibition. It is interesting, also, that inhibition of proteasome activity can affect nucleolar morphology independently of RNA Pol I activity (Mattsson *et al.*, 2001). Furthermore, as discussed in the next section, the fact that several proteins accumulate in nucleoli after inhibition of RNA Pol I-dependent transcription suggests that neither resident nucleolar proteins, nor nucleolar structure, are dependent upon rDNA transcription.

In addition to the formation of the nucleolus, the maintenance of nucleolar architecture is also dependent on ongoing ribosomal biogenesis. As such, nucleoli

disassemble at the onset of mitosis, when rDNA transcription and pre-rRNA processing terminate (reviewed by Dundr and Misteli, 2000; Dundr *et al.*, 2000; Hernandez-Verdun *et al.*, 2002; Leung *et al.*, 2004). This is likely due to the phosphorylation and inactivation of components of the rDNA-transcription machinery by the increasing levels of Cyclin B1-Cdk1 during prophase (Sirri *et al.*, 2002). Although some components of the rDNA-transcription machinery remain attached to the NORs during mitosis, most nucleolar proteins, particularly those involved in pre-rRNA processing, are released from the NORs and disperse throughout the cell (Leung *et al.*, 2004). By metaphase these have either bound the peri-chromosomal region (PR) (Gautier *et al.*, 1992), or have clustered into cytoplasmic aggregates, so-called nucleolus-derived foci (NDF) (Dundr *et al.*, 1996; Dundr and Olson, 1998). Proteins may adopt the former localisation to maintain the integrity of chromosomes during mitotic segregation, or otherwise ensure an equal protein distribution between daughter cells.

RNA polymerase I transcription reinitiates at late telophase when Cyclin B1-Cdk1 activity reduces, and this, in combination with chromosomal decondensation, induces PR- and NDF-associated proteins to travel to the NORs (Dousset *et al.*, 2001). Here they form pre-nucleolar bodies (PNBs), which ultimately coalesce during early G1 phase into nucleoli in a step-wise process in which the FC and DFC form before the GC (Bell *et al.*, 1992; Jimenez-Garcia *et al.*, 1994; Savino *et al.*, 2001; reviewed by Dimario, 2004; Angelier, 2005; reviewed by Boisvert *et al.*, 2007). Notably, only higher eukaryotic nucleoli undergo these cycles of disassembly and reassembly prior to and after mitosis. Yeast nucleoli remain intact during cell division and rDNA transcription continues during yeast mitosis (Oakes *et al.*, 1998; reviewed by Fatica and Tollervey, 2002; Tschochner and Hurt, 2003). This is interesting in light of the fact that the mechanism governing mitotic exit in budding yeast is not conserved in higher eukaryotes (Kaiser *et al.*, 2002; Mailand *et al.*, 2002).

Several proteins have also been demonstrated via time-lapse video-microscopy with photo-bleaching (FLIP and FRAP) experiments to be in a state of continuous flux between the nucleolus and nucleoplasm during interphase (Phair and Misteli, 2000). The residence times of most nucleolar proteins are thought to be on the order of tens of seconds; thus a micrograph image of the nucleolus is just a

'snapshot of multiple nucleolar components in rapid motion' (reviewed by Olson and Dundr, 2005). These observations support the previously-described 'hit and run' model, namely that proteins enter the nucleolus by passive diffusion rather than by active targeting, and only those proteins with a high affinity for nucleolar components are retained. These observations have important implications for our model, namely that this rapid nucleolar-nucleoplasmic diffusion may also apply to Hand1.

On first consideration, these observations would suggest that mitotic Hand1 would trigger precocious TG cell differentiation. However this is clearly not the case, possibly because mitotic Hand1 is kept inactive in NDFs or at peri-chromosomal loci. Nevertheless, to date, only nucleolar proteins involved in ribosomal biogenesis have been localised to NDFs or to the PR during mitosis. It is interesting in this regard that we have demonstrated that the trans-activational activity of Hand1 is negatively-regulated by cytoplasmic HICp32. Although the functional basis and biological relevance of this interaction is not known, HICp32 may act in the same fashion as non-nucleolar I-mfa to inhibit Hand1 activity. That is, it may sequester mitotic Hand1 in the cytoplasm, away from its nuclear target genes, and/ or interfere with its DNA-binding activity (Chen *et al.*, 1996; Kraut *et al.*, 1998). Alternatively, of course, the Hand1-HICp40 interaction may remain intact during mitosis. In this case, non-nucleolar HICp40 may continue to block Hand1 activity by an as-yet uncharacterised mechanism. It should also be noted that the commitment of Rcho-1 stem cells to a TG cell fate is induced by Hand1 nucleolar release, specifically during G2. In this regard, mitotic Hand1 release from the nucleolus does not coincide with the pre-mitotic cellular conditions (at prophase) required to induce mitotic cell cycle exit. Nevertheless, these previous studies would explain why some Rcho-1 stem cells exhibit non-nucleolar Hand1, namely because they are mitotic.

6.4.3. The pluri-functional nucleolus theory

Traditionally the nucleolus has been thought of as a 'ribosome factory', a eukaryotic subnuclear organelle dedicated to ribosome subunit biogenesis. Recently, however, it has become clear that the nucleolus is actually more 'plurifunctional' than once thought, particularly in higher eukaryotes (reviewed by Pederson, 1998; Table

6.1). Yet further functions for the nucleolus have been inferred by the physical association and protein trafficking between nucleoli and other nuclear bodies such as splicing speckles, paraspeckles and Cajal (coiled) bodies (Sleeman *et al.*, 1998; Fox *et al.*, 2002; Leung and Lamond, 2002).

Table 6.1. The putative, wide-ranging roles of the nucleolus.

Role	Reference(s)
Translation and/ or export of certain mRNAs	Schneiter *et al.*, 1995. Ideue *et al.*, 2004.
Processing of tRNA precursors	Bertrand *et al.*, 1998. Pederson and Politz, 2000. Thompson *et al.*, 2003.
Control of ageing	Sinclair and Guarante, 1997. Johnson *et al.*, 1998.
Regulation of RNA editing	Desterro *et al.*, 2003. Sansam *et al.*, 2003.
Regulation of the meiotic pachytene checkpoint	San-Segundo and Roeder, 1999.
Biogenesis of ribonucleoprotein machines (signal recognition particle (SRP), spliceosomal U5 and U6 snoRNAs, and telomerase)	Jacobson and Pederson, 1998. Politz *et al.*, 2000. Jady and Kiss, 2001. Wong *et al.*, 2002.
Small interfering RNA (siRNA) pathways	Pontes *et al.*, 2006.

One major role for the nucleolus is as a cellular 'stress sensor' (reviewed by Olson, 2004), which is not surprising given the link between cell proliferation rate and ribosome biogenesis. The organelle importantly contributes to the control of apoptosis. This was first suggested by the DNA damage-dependent nucleolar-nucleoplasmic shuttling of the pro-apoptotic factors Dedd, Ing1 and Daxx (Stegh *et al.*, 1998; Scott *et al.*, 2001; Lin and Shih, 2002). The nucleolus has also been implicated in the cellular p53-dependent (Tao and Levine, 1999; Weber *et al.*, 1999; Tsai and McKay, 2002) and -independent (Mayer *et al.*, 2005) responses to DNA damage and other stresses. Notably, several nucleolar proteins are released into the nucleoplasm in response to DNA damage. These are thought to interact with

nucleoplasmic p53 to inhibit its proteasomal degradation, so stabilising the tumour-suppressor (Tao and Levine, 1999; Weber *et al.*, 1999; Colombo *et al.*, 2002; Daniely *et al.*, 2002; Kurki *et al.*, 2004). In this respect, chemical or immunological disruption of the nucleolus is sufficient to stabilise p53, even in the absence of DNA damage (Rubbi and Milner, 2003). The ability of the nucleolus to act as a 'stress sensor' is in part dependent on its compartmentalisation of proteins away from the rest of the cell (Table 6.2).

By the end of 2001, 121 human proteins had been localised to the nucleolus. In most cases, these were individually shown to adopt a nucleolar localisation by way of antibody staining and fluorescent tagging. Owing to their high density, nucleoli can be isolated from disrupted nuclei by centrifugation through a sucrose gradient. In this regard, large-scale nucleolar protein identification, by mass spectrometry, has been carried out and the human nucleolar proteome has recently been published (Scherl *et al.*, 2002; Andersen *et al.*, 2002; Andersen *et al.*, 2005; reviewed by Leung *et al.*, 2003). These proteomic analyses have provided a more detailed insight into the composition of the organelle.

The first two published proteomic analyses of nucleoli purified from HeLa (human cervical carcinoma) cells identified 271 proteins (Andersen *et al.*, 2002) and 210 proteins (Scherl *et al.*, 2002), where the combination of these results revealed a collection of approximately 350 different nucleolar proteins. Recently another study increased this number and also analysed the composition of HeLa cell nucleoli under differing metabolic conditions, for example chemical-induced inhibition of RNA Pol I transcription or proteasome-dependent proteolysis (Andersen *et al.*, 2005; Figure 6.3). This particular study allowed the examination of the behaviour and dynamics of certain sets of proteins. One interesting observation was that, whilst some proteins exit the nucleolus in response to metabolic inhibition, some actually accumulate in the organelle (Fox *et al.*, 2002; Andersen *et al.*, 2005). Thus there appears to be no unique, complete proteome for the nucleolus, but rather different proteomes that are dependent on the metabolic state of the cell. This is in agreement with our observations relating to the release of Hand1 from the nucleolus to the nucleoplasm during TG cell differentiation.

Currently, the nucleolar proteome database (NOPdb), listed at www.lamondlab.com/NOPdb/, comprises more than 700 proteins (Leung *et al.*, 2006). This represents about 2.5% of the predicted human proteome, and also details the quantitative changes in protein levels for 498 of these proteins after transcription is inhibited by treating cells with actinomycin-D. Of note, the *Arabidopsis thaliana* proteome has also been recently characterised (Pendle *et al.*, 2005). Approximately 70% of the 217 identified proteins were homologues of human nucleolar proteins. It is also of note that, whilst the budding yeast nucleolar proteome has not been definitely characterised, one study carried out large-scale protein localisation studies using GFP fusion proteins to illustrate the nucleolar localisation of numerous proteins (Huh *et al.*, 2003). Andersen and colleagues later compared the findings of this study with those of the human nucleolar proteome and showed that approximately 90% of the yeast nucleolar proteins with human homologues are also nucleolar in HeLa cells (Andersen *et al.*, 2005). These studies suggest that the contents of the nucleolus have been highly conserved throughout eukaryotic evolution.

Despite it becoming increasingly clear that the nucleolus is more plurifunctional than once thought, the findings of the nucleolar proteome analyses were still relatively surprising. An unexpectedly high percentage (88%) of the proteins identified in the original human nucleolar proteome screen were not previously thought to exist in this organelle. Furthermore, about 30% of proteins co-purified with isolated human nucleoli are of unknown function, being encoded by novel ORFs (Scherl *et al.*, 2002; Andersen *et al.*, 2002; Andersen *et al.*, 2005; reviewed by Leung *et al.*, 2003; Figure 6.3). A couple of studies have attempted to assign a function to these factors following literature searches and bioinformatics but with limited success (Coute *et al.*, 2006; Hinsby *et al.*, 2006). These two studies suggested potential functions for about 150 previously-uncharacterised human proteins, of which only 30% were projected to function in ribosomal biogenesis.

Further insight into the roles of the novel proteins that reside in the nucleolus was gained by an analysis of the domains they possess (Andersen *et al.*, 2002; Scherl *et al.*, 2002). The most abundant motifs in the nucleolar proteome, which include RRMs (RNA-recognition motifs), DEAD/DEAH (Asp-Glu-Ala-Asp/His)-box helicase domains and WD- (Trp-Asp)-repeat motifs (reviewed by Leung *et al.*, 2003),

are present in neither HICp40 nor in Hand1, however. Certain amino acid residues are also over- or under-represented in nucleolar proteins, in comparison with the total cell proteome. Charged amino acids (e.g. glutamate, aspartate, lysine and arginine) are favoured in nucleolar proteins compared to total cellular proteins. This is in accordance with the fact that several nucleolar-localised proteins possess basic NoLS motifs. In contrast, neutral residues (e.g. proline and cysteine), are disfavoured. This residue bias is true for both HICp40 and Hand1. Furthermore the protein phosphatase-1 (PP1)-binding motif, (Lys/Arg)-Val-X-Phe, and the tetra-peptides FGGR and RGGF are enriched in nucleolar proteins, compared with either total-cellular or nuclear-specific proteins (reviewed by Leung *et al.*, 2003). However, neither HICp40 nor Hand1 possess these tetrapeptides.

The unexpected protein content of the HeLa nucleolus is in agreement with our finding of Hand1 in the nucleolus of rodent diploid trophoblast cells, a protein with no known role in the traditional functions of the organelle. It is, however, unlikely that all proteins that localise to the nucleoli were identified in the nucleolar proteome analyses (Scherl *et al.*, 2002; Andersen *et al.*, 2002; Andersen *et al.*, 2005). Nucleolar samples for analysis were not obtained from cells exposed to certain metabolic conditions and, moreover, these cells were unsynchronised. Since several proteins undergo bi-directional shuttling between the nucleolus and nucleoplasm, depending on the cell cycle stage or in response to certain stimuli, many factors were also likely of a too low a concentration to be detected in these analyses. More importantly in light of the findings of our study, only nucleoli purified from HeLa cells were analysed. Thus tissue-specific factors, for example trophoblast-expressed Hand1, would not have been present. These are thus excluded from the current nucleolar proteome list and this was acknowledged by the authors (Andersen *et al.*, 2002). This is supported by the absence of other tissue-specific proteins in the published nucleolar proteome, which are nonetheless known to associate with the organelle, for example, the testes determinant Maestro (Smith *et al.*, 2003).

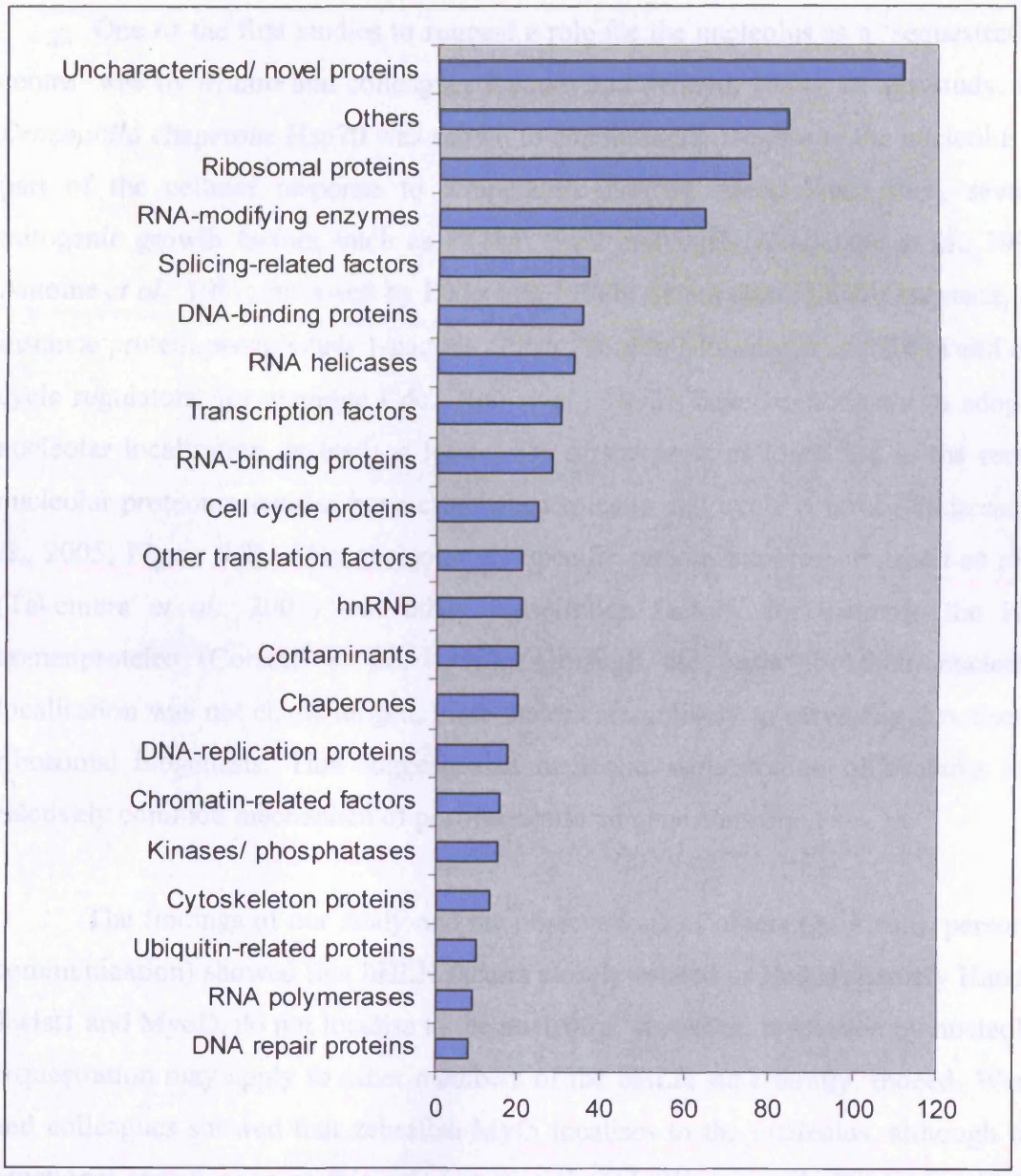

Figure 6.3. The findings of recent human nucleolar proteome analyses.

Adapted from www.lamondlab.com/NOPdb/NPDdatabase.htm. (January 2008). **hnRNP**: heterogeneous nuclear ribonucleoprotein.

One of the first studies to suggest a role for the nucleolus as a 'sequestration centre' was by Munro and colleagues (Munro and Pelham, 1984). In this study, the *Drosophila* chaperone Hsp70 was shown to conditionally localise to the nucleolus as part of the cellular response to temperature-induced stress. Since then, several mitogenic growth factors, such as PTHrP, Fgf2 and Fgf3 (Henderson *et al.*, 1995; Antoine *et al.*, 1997; reviewed by Pederson, 1998b; Sheng *et al.*, 2004), enzymes, for instance protein phosphatase 1-gamma (PP1γ; Trinkle-Mulcahy *et al.*, 2001) and cell cycle regulators, for example Cdc2 (Ino *et al.*, 1993), have been shown to adopt a nucleolar localisation. Indeed, at least 3.5% of the proteins identified in the recent nucleolar proteome screens have established roles in cell cycle control (Andersen et al., 2005; Figure 6.3). Also nucleolar are specific tumour suppressors, such as pRB (Takemura *et al.*, 2002) and other transcription factors, for example the Hox homeoproteins (Corsetti *et al.*, 1995). Although the basis for their nucleolar localisation was not characterised, these factors are unlikely to serve any function in ribosomal biogenesis. This suggests that nucleolar sequestration of proteins is a relatively common mechanism of post-translational gene control.

The findings of our study and the observations of others (A. Firulli, personal communication) showed that bHLH factors closely-related to Hand1, namely Hand2, Twist1 and MyoD, do not localise to the nucleolus. However, regulation by nucleolar sequestration may apply to other members of the bHLH superfamily. Indeed, Wang and colleagues showed that zebrafish Myf5 localises to the nucleolus, although the functional significance of this was not investigated (Wang *et al.*, 2005). It will be interesting to investigate whether this mechanism regulates not only bHLH transcription factors but also a wider range of factors involved in modulating transcription, some of which have been identified in the nucleolar proteome (Figure 6.3). Examples of protein regulation utilising nucleolar sequestration are described in Table 6.2.

Table 6.2. Well-characterised examples of proteins whose sequestration in the nucleolus regulates their activity.

Sequestered factor(s)	Nucleolar sequesteror(s)	Basis for nucleolar sequestration	References
Cdc14 (*S. cerevisiae*)	Net1	Cdc14 is nucleolar during interphase and early mitosis. At anaphase onset Cdc14 enters the nucleoplasm to dephosphorylate its targets and trigger mitotic exit.	Visintin *et al.*, 1999; 2003. Shou *et al.*, 2001; 2002. Yoshida and Toh-e, 2002.
Rnr2, Rnr4 (*S. cerevisiae*)	Wtm1	Rnr2 and Rnr4, subunits of ribonucleotide reductase (Rnr), are only released from the nucleolus to bind the cytoplasmic third subunit, Rnr1, at the advent of S-phase.	Lee and Elledge, 2006.
Mdm2 (Mouse)	Pml, $p19^{ARF}$	The ubiquitin ligase Mdm2 is nucleoplasmic in resting cells and targets p53 for proteolysis. Upon DNA damage, Mdm2 is recruited to the nucleolus to permit p53 stabilisation.	Tao and Levine, 1999. Weber *et al.*, 1999. Bernardi *et al.*, 2004.
HIF-1α (Mouse)	$p19^{ARF}$	In normoxic cells the α-subunit of HIF-1 is sequestered in the nucleolus. Upon hypoxic stress it is released to bind its β-subunit binding partner to form HIF-1.	Fatyol and Szalay, 2001.
VHL (Human)	Unknown	The ubiquitin ligase VHL is nucleoplasmic in resting cells and targets the alpha subunit of hypoxia-inducible factor-1 (HIF-1α) for proteolysis. However under hypoxic conditions, VHL is sequestered in the nucleolus and HIF-1 is stabilised.	Mekhail *et al.*, 2004.
Hsp70 (Mouse)	Unknown	Hsp70, an inhibitory chaperone of Hsf1, is nucleoplasmic in resting cells and prevents Hsf1 from binding Hsf2. Upon heat shock, Hsp70 is recruited to the nucleolus to allow Hsf1-Hsf2 interaction, stress granule formation and the heat shock response.	Alastalo *et al.*, 2003.
RelA (Mouse)	$p19^{ARF}$, B23, Nfbp	DNA damage recruits RelA, a component of NFκB, to the nucleolus. This prevents its binding cytoplasmic p50 to form NFκB and results in apoptosis. In response to mitogenic cytokines, RelA is released from nucleoli to form NFκB and this promotes cell proliferation.	Stark and Dunlop, 2005.
Telomerase (Human)	Nucleolin	Telomerase is sequestered in an inactive state in the nucleolus during most of the cell cycle, but is released at the onset of telomere replication in late S-phase. Interestingly, the nucleolar localisation of telomerase is neither detected in transformed cells nor in cells that have experienced DNA damage.	Wong *et al.*, 2002. Khurts *et al.*, 2004.

Once considered a simple ribosome biosynthesis factory, the eukaryotic nucleolus is now recognised as a major orchestrator of numerous cellular functions (reviewed by Pederson, 1998; Boisvert *et al.*, 2007). This is supported by the surprisingly wide range of factors recently discovered in the nucleolus by proteomic analysis (Andersen *et al.*, 2002; Scherl *et al.*, 2002; Andersen *et al.*, 2005). Our study supports previous studies that implicate the organelle as a molecular 'safe' or 'sink' that temporarily stores factors in an inactive state until a specific cell cycle stage or the occurrence of a certain metabolic state. Compartmentalisation of proteins within the cytoplasm (Beg *et al.*, 1992; Chen *et al.*, 1996; Kraut *et al.*, 1998), or within PML bodies (Goodson *et al.*, 2001) has also been reported. The nuclear lamina has also emerged as a major site for the sequestration of transcription factors, including c-Fos, Oct-1 and pRb, whose release into the nucleoplasm from the nuclear periphery coincides with an up-regulation of their target genes (Imai *et al.*, 1997; Johnson *et al.*, 2004; Ivorra *et al.*, 2006).

However, despite these studies, the nucleolus stands out as likely being the organelle most suited for use as a sequestration centre for transcription factors. This organelle is the largest in the nuclear matrix, is highly-permeable and furthermore lacks a membrane (reviewed by Dundr and Misteli, 2001; Handwerger *et al.*, 2005). These features would permit the storage of a stockpile of pre-existing protein that could be released, in response to cellular cues at a specific cell cycle stage or at a certain developmental time-point, without the need for transcriptional up-regulation or even nuclear import. That nucleoli are usually located at or near the nuclear envelope in higher eukaryotes, or otherwise connected to the nuclear envelope by a so-called 'nucleolar canal'; reviewed by Hernandez-Verdun, 2006b), suggests that nucleolar sequestration may also regulate the activity of cytoplasmic proteins. In conclusion, our current study represent the most compelling evidence to-date that the nucleolus can act in this fashion as a subnuclear 'sequestration centre' in the physiological setting of cell fate determination.

Several studies have reported a flux of cell fate determinants between the nucleolus and nucleoplasm. In many cases the subcellular localisation of these factors correlates with the status of the cell, namely whether it continues to proliferate or commits to differentiate (Galcheva-Gargova *et al.*, 1998; Gao and

Scott, 2002; Tsai and McKay, 2002; Kuroda *et al.*, 2004). For example, the nucleolar Rbm19 RNA-binding factor is expressed throughout the undifferentiated murine embryonic gut tube but restricted in the adult to stem cells residing in the duodenal crypts of Lieberkühn. This assumes a cell-wide distribution to promote intestinal epithelial differentiation (Lorenzen *et al.*, 2005). Another example concerns the bHLH-Zip transcription factor c-Myc, which has been localised to the nucleolus in several studies (Schlosser *et al.*, 2003; Datta et al., 2004; Arabi *et al.*, 2005; Sanders and Gruppuso, 2005). This is only released from $p19^{ARF}$-dependent nucleolar anchorage to reach its nucleoplasmic heterodimerisation partner Max if quiescent adult hepatocytes are induced to re-enter the cell cycle during liver regeneration after partial hepatectomy (Sanders and Gruppuso, 2005). Similarly the testis-specific transcription factor ZPF106 is released from the nucleolus during terminal differentiation of C2C12 myoblasts as levels of its sequesteror TSG118 diminish (Grasberger and Bell, 2005). Translocation from the nucleolus to the nucleoplasm of CTCF is also accompanied by differentiation of human myeloid cells and rat neuroblasts into neurones (Torrano *et al.*, 2006). Finally, Nucleostemin, a putative p53 regulator that resides in the nucleolus of several stem cell types, is similarly down-regulated and/ or released into the nucleoplasm during their terminal differentiation (Tsai and Mackay, 2002).

Despite these examples, we are nevertheless the first to report that the nucleolar sequestration and release of a protein can control the commitment of stem cells by effects *outside* of the nucleolus. That is, the change in subcellular localisation of many of the aforementioned nucleolar cell fate determinants affects the process of ribosome biogenesis with ultimate effects on cell fate. For example, nucleolar CTCF silences rDNA transcription (Torrano *et al.*, 2006) and nucleolar $p19^{ARF}$ targets the rRNA processing factor B23 for degradation through ubiquitination (Itahana *et al.*, 2003; Sugimoto *et al.*, 2003; Bertwistle *et al.*, 2004). In both cases, this coincides with cell cycle arrest, entry into the quiescent state and concomitant differentiation. Conversely, c-Myc promotes cell proliferation by facilitating rDNA transcription and rRNA processing (Schlosser *et al.*, 2003; Arabi *et al.*, 2005). Furthermore, even proteins whose localisation in the nucleolus has been attributed to their negative regulation by nucleolar sequestration have secondary, traditionally-nucleolar roles. For example, Cdc14 contributes to the

organisation of nucleolar chromatin and aids nucleolar segregation at mitosis (de Almeida *et al.*, 1999). Similarly, Pch2, whose sequestration in the nucleolus is thought to play a role in the meiotic pachytene checkpoint, represses rDNA recombination (San-Segundo and Roeder, 1999). Additionally, the growth factor Fgf2 regulates ribosomal biogenesis (Sheng *et al.*, 2005). We believe, however, that Hand1 is unlikely to have a role in ribosome biogenesis. Hand1 is tissue-specific and the components required for ribosomal biogenesis are thought to be uniform across cell types (reviewed by Fatica and Tollervey, 2002; Tschochner and Hurt, 2003). Thus, Hand1 nucleolar residence is likely solely explained by its negative regulation by HICp40. Its nucleolar localisation is thus the strongest evidence yet that the organelle can, in some cases, act solely as a subnuclear 'sequestration centre'.

6.5. Extrapolating our findings to human placentation

So what are the implications of our findings for the understanding of human placentation? Unfortunately it is unlikely that the role we propose for Hand1 in determining rodent TS cell fate is conserved in humans. As discussed in Chapter 1 (section 1.2), the placenta is evolutionarily a young organ. As such, the process of decidual invasion and the molecular mechanisms underlying it are in many cases very different between mammalian species (reviewed by Georgiades *et al.*, 2002 and Malassine *et al.*, 2003). Moreover, HAND1 is not thought to be essential for the differentiation of the human counterpart of rodent TG cells, the extravillous trophoblast (EVT) (Knofler *et al.*, 1998; Janatpour *et al.*, 1999; Loregger *et al.*, 2003; Meinhardt *et al.*, 2005). Strikingly, human EVT cells, the equivalent invasive trophoblast subtype to rodent TG cells, do not undergo endoreduplication. This notably represents circumstantial evidence that murine Hand1 is required for mitotic cell cycle exit at the onset of TG cell differentiation. Finally, many examples of protein regulation dependent on nucleolar sequestration are poorly conserved, even between mammals (Zhang and Xiong, 1999).

Our results do, however, confirm the findings of previous studies in

demonstrating that hypoxia has a negative effect on Rcho-1 TG cell differentiation (Gultice *et al.*, 2006; Lash *et al.*, 2007; Takeda *et al.*, 2007). This has implications for the understanding of the molecular basis of pre-eclampsia. Pre-eclampsia occurs in up to 10% of all human pregnancies and is characterised by inadequate invasion of trophoblast into the maternal decidua (reviewed by Redman and Sargeant, 2005; Sibai *et al.*, 2005; reviewed in Chapter 1, section 1.2.2.4). Our data, in combination with the work of others, strongly support the hypothesis that hypoxia inhibits the activation of critical factor(s) involved in the differentiation of invasive rodent trophoblast (Gultice *et al.*, 2006; Lash *et al.*, 2006; Takeda *et al.*, 2007). This may include Hand1, but appears to be independent of its nucleolar release. In any case, our data support the idea that pathologically-prolonged hypoxic conditions during placentation could give rise to pre-eclampsia or other defects.

6.6. Ongoing and future studies

It remains to be determined whether the nucleolar sequestration of Hand1 by HICp40 and its release upon Plk4-dependent phosphorylation regulates its biological activity in other key lineages in which a requirement for Hand1 function has been demonstrated, most notably the developing heart. Investigating how the cardiac function of Hand1 is controlled has proven difficult *in vivo*, due to early embryonic lethality following *Hand1* loss-of-function. Furthermore, few cardiac cell lines exist, precluding *in vitro* analysis of Hand1 function. In this section we address ongoing studies in the cardiomyocyte lineage to determine whether nucleolar sequestration and/ or release of Hand1 is a more widespread mechanism of regulating its activity during embryogenesis.

6.6.1. Ongoing and future *in vitro* studies

As described in Chapter 3 (section 3.2.2), Hand1-EGFP localises to the nucleoli of H9c2 cells, a rat ventricular cardiomyocyte cell line. This suggests that the underlying molecular mechanisms responsible for Hand1 nucleolar anchorage are retained in at least one cardiac cell model. However, this cell line is terminally-

differentiated and so the potential of its use *in vitro* to assess the functional significance of Hand1 nucleolar sequestration during cardiomyocyte differentiation is limited. We have, in this regard, also observed Hand1-EGFP nucleolar localisation in subtypes of embryonic carcinoma (EC) and embryonic stem (ES) cell lines, cells that can be induced to differentiate into derivatives of all three primary germ layers, including cardiomyocytes (Figure 6.4).

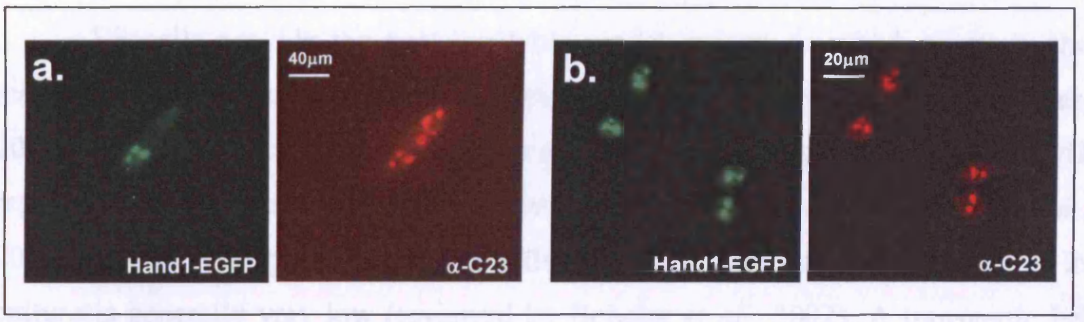

Figure 6.4. Hand1-EGFP localises to the nucleoli of embryonic carcinoma (EC) and embryonic stem (ES) cell lines.

Hand1-EGFP localises to the nucleoli of P19-CL6 cells, an EC cell line whose differentiation is modestly skewed towards the cardiomyocyte lineage (Habara-Ohkubo, 1996; **a**). Hand1-EGFP also localises to the nucleoli of an ES cell line that endogenously expresses *EGFP* upon their differentiation into *Nkx2.5*-expressing cardiomyocytes (Wu *et al.*, 2006; **b**).

Studies suggest that the process of ES cell differentiation into EBs *in vitro* faithfully models the molecular changes that accompany fetal cardiomyocyte differentiation in the developing heart *in vivo* (Maltsev *et al.*, 1993; Doevendans *et al.*, 2000). Despite this, a study in the HM1 ES cell line suggests that cardiomyocytes that differentiate *in vitro* are not mature cardiomyocytes, but instead, in terms of electrophysiological characteristics and gene expression, more closely resemble those of the early primary myocardium of the embryonic heart tube (Fijnvandraat *et al.*, 2003). Despite the results of this study, it is likely that different ES cell lines exhibit variation in behaviour and gene expression patterns. ES cells in culture are derived from the inner cell mass (ICM) of developing blastocysts. When maintained in an undifferentiated state by culturing in the presence of leukemia inhibitory factor (LIF), they are able to undergo proliferative self-renewal. However, by removing LIF from the culture medium, ES cells in

suspension spontaneously differentiate into embryoid bodies (EBs), three-dimensional floating cell aggregates. EBs comprise many different specialised cell types derived from the three germ layers of the developing embryo, namely the endoderm, ectoderm and mesoderm. Importantly for our study, EBs can contain beating cardiomyocytes, located between an epithelial layer and a basal layer of mesenchymal cells (Risebro *et al.*, 2006).

ES cells provide the best available model system in which to study the molecular basis of cardiomyocyte differentiation *in vitro* (reviewed by Boheler, 2002). Indeed, they have previously been employed to interrogate aspects of Hand1 regulation and function in *vivo* (Riley *et al.*, 2000; Smart *et al.*, 2002; Risebro *et al.*, 2006). However, the percentage of ES cells that differentiate into cardiomyocytes in culture is generally very low (reviewed by Boheler *et al.*, 2002). A transgenic ES cell line, generously provided by Sean Wu, was in this regard chosen for further study. Wu and colleagues introduced a 2.1kb enhancer fragment of the early cardiac differentiation marker *Nkx2.5*, as well as 500bp of *Nkx2.5* basal promoter, upstream of the *EGFP* cDNA into CJ7 ES cells (Wu *et al.*, 2006). Using this transgenic ES cell line, differentiated cardiomyocytes, which express *Nkx2.5*, can therefore be distinguished and isolated by virtue of EGFP fluorescence (Movie 6.1, Appendix 10).

Initially, we sought to investigate at which time-point the Hand1 protein became detectable during the differentiation of these transgenic ES cells into cardiomyocytes. In agreement with previous studies (Riley *et al.*, 2000; Risebro *et al.*, 2006), western blot analysis using an anti-Hand1 antibody revealed that Hand1 was absent in ES cells (data not shown) and was low in cells differentiated for 4 days (Figure 6.5). Hand1 protein levels had increased by 6 days after the onset of differentiation and persisted at high levels until day 10. After this period, the amount of Hand1 protein reduced (Figure 6.5). Consistent with these observations, we could neither detect Hand1 via immunostaining in stem cells nor in cells differentiated for 4 days (data not shown).

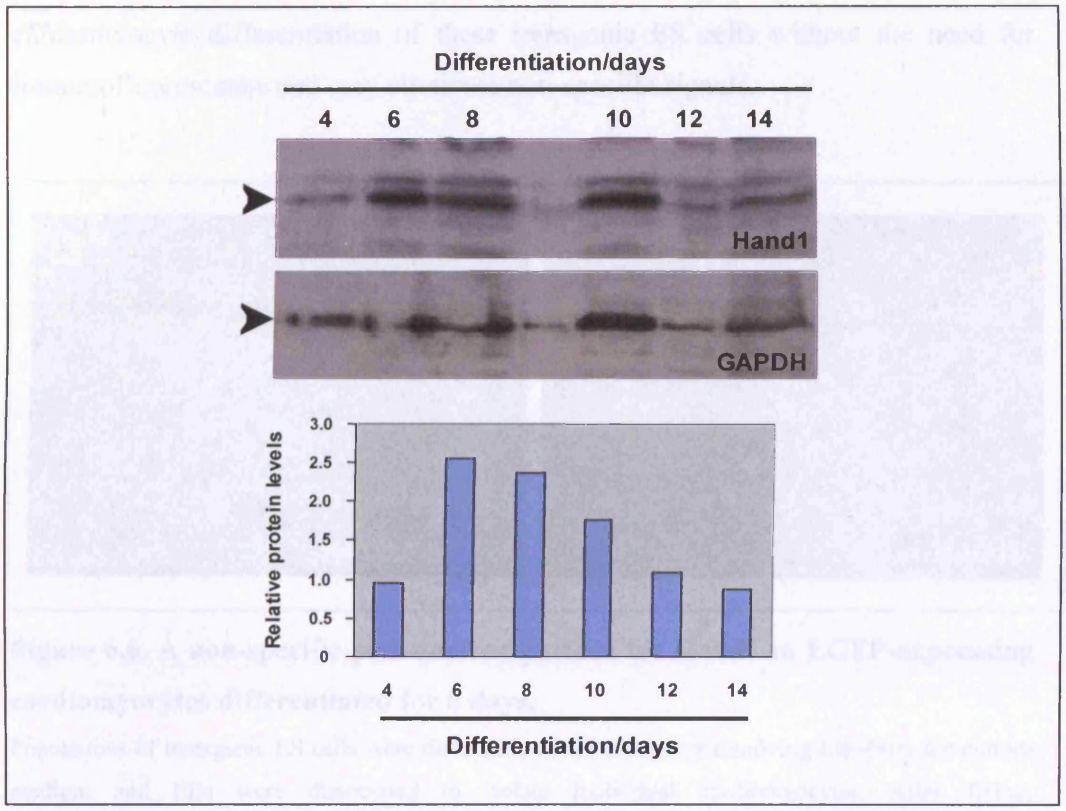

Figure 6.5. Hand1 is endogenously expressed in transgenic *in vitro*-differentiated cardiomyocytes.

Western blot analysis using an anti-Hand1 antibody and whole-cell transgenic ES cell lysates shows that, during a time-course of differentiation over 14 days, Hand1 appears in *EGFP*-expressing cardiomyocytes at the day 4-6 period (post-LIF removal) and persists until day 10, after which period its levels decline.

We then carried out immunostaining of cardiomyocytes, dissociated from EBs differentiated for 6 and 8 days, namely the time-points at which Hand1 levels are maximal. However, this has so far given spurious results. A peri-nuclear signal, seemingly for endogenous Hand1, was observed in fluorescent cardiomyocytes (Figure 6.6). Although this pattern was seen in some Rcho-1 TG cells (Chapter 4, Figure 4.5a), suggesting its reliability, cells in these cultures that lacked detectable EGFP expression also exhibited this pattern. Since these cells were unlikely to be Hand1-positive cardiomyocytes, this signal is likely non-specific. This result was independent of fixation method, antibody concentration and source. Currently, we are attempting to perform *in situ* hybridisation analyses with the anti-Hand1 antibody. This will allow us to analyse the subcellular localisation of Hand1 during

cardiomyocyte differentiation of these transgenic ES cells without the need for immunofluorescence and may eliminate non-specific signals.

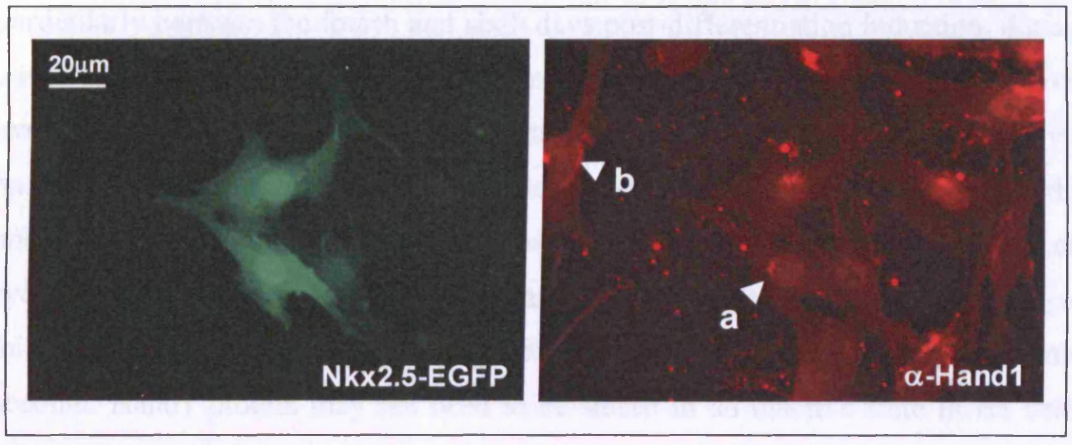

Figure 6.6. A non-specific peri-nuclear pattern for Hand1 in EGFP-expressing cardiomyocytes differentiated for 8 days.

Populations of transgenic ES cells were differentiated for 8 days by removing LIF from the culture medium and EBs were dissociated to isolate individual cardiomyocytes. After fixing, immunostaining with an anti-Hand1 antibody revealed a peri-nuclear pattern in cells with (**a**), but also in cells without (**b**), EGFP fluorescence.

In light of our inability to detect a specific signal for Hand1 by immunostaining EGFP-expressing cardiomyocytes, we harvested EBs differentiated over a 12 day time-course and performed western blot analysis on whole-cell lysates subtracted for the nucleolar fraction. Although FACS sorting was considered in order to isolate fluorescent cardiomyocytes, Hand1 expression is likely restricted to only those ES-derived cells that differentiate along the cardiomyocyte lineage. Thus whole EBs were harvested for use in this assay. In contrast to the results we obtained using Rcho-1 cell lysates subtracted for the nucleolar fraction (Chapter 4, Figure 4.6), the relative amounts of Hand1 we observed in the non-nucleolar ES cell lysates at each time-point mirrors those observed in the whole-cell ES cell lysates at each time-point in Figure 6.5 (data not shown). This suggests that following an up-regulation in Hand1 at approximately day 6 post-differentiation induction, Hand1 is immediately, or very soon after becomes, nuclear-wide.

This result suggests that Hand1 may be released almost immediately after its nucleolar sequestration during cardiomyocyte differentiation. Ongoing studies seek to investigate this by analysing a more detailed time-course of differentiation, particularly between the fourth and sixth days post-differentiation induction, during which period we observe the most dramatic increase in Hand1 levels. However, overall, the results described in this chapter suggest that Hand1 is not regulated via nucleolar sequestration during cardiomyocyte differentiation *in vitro*. Unlike the onset of differentiation of TG cells, which is marked by immediate mitotic cell cycle exit and endocycle entry, cardiomyocyte differentiation is not thought to initiate so abruptly and is a more gradual multi-step process. Taking this into account, Hand1 protein may not need to be stored in an inactive state in ES cells with a view to being instantaneously activated at a specific developmental time-point. Thus *Hand1* up-regulation may be sufficient to regulate Hand1 activity during cardiomyocyte differentiation *in vitro*. In any case, we are currently modifying the transgenic ES cells used in the assays described in this chapter to stably express a Hand1-dsRed fusion protein. This will enable us to analyse changes in the subcellular location of Hand1 during ES cell differentiation into EGFP-expressing cardiomyocytes.

6.6.2. Ongoing and future *in vivo* studies

As illustrated in Chapter 3 (Figure 3.7), whole-mount *in situ* hybridisation using a probe for full-length *HICp40* demonstrated that the murine orthologue is expressed in the left ventricle and outflow tract. These are regions of the developing heart in which *Hand1* is endogenously co-expressed, as reviewed in Chapter 1 (section 1.3.2.2). Thus HICp40 is expressed in the right place and at the right time to negatively-regulate Hand1 activity by nucleolar sequestration during murine cardiac morphogenesis.

In light of the *MICp40* expression pattern, it would be interesting to generate a mouse model lacking *MICp40* expression in cardiac tissues. This has been considered, and would be carried out by electroporating a construct with similarity to the RNAi vector used in this study, namely based on the described H1

polymerase III shRNAi (Kunath *et al.*, 2003). In this vector, the 5T termination sequence, preceding the relevant RNAi hairpin sequence, is flanked by loxP sequences. Using this approach, it would not be necessary to target the endogenous locus; the construct would be present but inactive in all cells, but RNAi knock-down of *HICp40* would only occur upon cre-recombination of the 5T termination sequence. Furthermore, an *EGFP* reporter gene has been incorporated between the *loxP* sequences, which would mark cells transfected with the conditional vector. Initially the construct would be extensively tested *in vitro*, namely by inducing cre-recombination in stably-transfected cells and assessing EGFP expression. Floxed *MICp40* shRNA mice would be crossed with two knock-in strains of cardiac-specific *cre recombinase*-expressing mice already in house, namely *Mlc2v*-creKI mice (provided by Ken Chien) and *Nkx2.5*-creKI mice (provided by Robert Schwartz). Hearts of embryos derived from such matings would then be analysed between E8.0-E10.5 and cardiomyocytes immunostained to assess the subcellular localisation of Hand1.

On the basis of our findings in the trophoblast lineage, and assuming MICp40 plays a similar role in negatively-regulating Hand1 activity during cardiac morphogenesis, conditional *MICp40*-null mice would be predicted to exhibit a gain-of-function Hand1 cardiac phenotype. This would likely result in OFT extension and LV abnormalities, as recently reported in a mouse over-expressing *Hand1* in its 'native' (endogenously-expressed) tissues (Risebro *et al.*, 2006). Interestingly, the study by Risebro and co-workers implicated Hand1 in governing the balance between cardiac precursor cell (CPC) proliferation and differentiation. Specifically, whilst down-regulation of Hand1 during normal cardiac morphogenesis permits CPC cell cycle exit and differentiation, CPCs over-expressing Hand1 are hyper-proliferative, which results in distal OFT hyperplasia and thus extension (Risebro *et al.*, 2006; reviewed in Chapter 1, section 1.3.2.2). In view of the function for Hand1 in governing TS cell fate, it may be the case that excess Hand1 protein in these CPCs is responsible for their hyper-proliferation and the mechanism for this may be retention of Hand1 in the nucleolus. This hypothesis is supported by the fact that Hand1, presumably nucleolar, is required for proliferation of diploid trophoblast in the EPC (Riley *et al.*, 1998). To address this question we have prepared cryosections of *Hand1*-overexpressing E9.5 mouse hearts. We hope to conduct

immunostaining and/ or *in situ* hybridisation analysis to investigate the subcellular localisation of Hand1 in cells of the presumptive OFT and LV, and analyse whether the relative proportions of nucleolar versus nuclear-wide Hand1 differ with respect to wild-type hearts at the same developmental stage.

In light of the findings of this study in the rodent trophoblast lineage, a non-conditional *MICp40*-null mouse model would be equally interesting. On first consideration, and in light of the role we demonstrate for the rat orthologue of HICp40 in rodent trophoblast, we would predict that this mouse would phenocopy certain aspects of the *Mash2*-deficient mouse (Guillemot *et al.*, 1994). As discussed in Chapter 1 (section 1.2.4.2), Mash2 plays a complementary role to Hand1 during trophoblast differentiation in that it maintains TS cell diploidy through an as-yet uncharacterised mechanism. *Mash2*-null mice are appropriately embryonic lethal at E7.0 as a consequence of precocious TG cell differentiation (Guillemot *et al.*, 1994). This phenotype would be predicted to apply also to a loss-of-function *MICp40* (that is, gain-of-function Hand1) mouse. In the absence of its nucleolar sequesteror, Hand1, which promotes TG cell differentiation, would likely be ectopically nuclear-wide and could thus promote mitotic cell cycle exit. That said, a simple lack of Hand1 nucleolar sequestration may not precede its normal, nuclear function. One possible reason for this is that Plk4-dependent phosphorylation of Hand1, which not only promotes Hand1 nucleolar release but also enhances the affinity of Hand1 for its nuclear E-factor binding partners (Firulli *et al.*, 2003), only occurs during a narrow developmental window during placentation.

In conclusion, further work is needed to investigate whether nucleolar sequestration modulates the activity of Hand1 in the cardiomyocyte lineage. Although our preliminary data suggest that nucleolar sequestration is unlikely to control Hand1 activity during cardiomyocyte differentiation *in vitro*, further experiments will be needed to rule this out *in vivo*. Additional studies are also required to investigate whether Hand1 activity is regulated by nucleolar sequestration in other lineages in which it is expressed during development, namely the developing limb, gut and autonomic nervous system. It is entirely possible, however, that Hand1 regulation via nucleolar sequestration is a tissue-specific mechanism and restricted exclusively to the rodent trophoblast lineage.

REFERENCES

1. Achen, M.G., Gad, J.M., Stacker, S.A., Wilks, A.F. (1997). Placenta growth factor and vascular endothelial growth factor are co-expressed during early embryonic development. Growth Factors. *15*, 69-80.
2. Adam, J.C. and Montell, D.J. (2004). A role for extra macrochaetae downstream of Notch in follicle cell differentiation. Development *131*, 5971-5980.
3. Adamson, S.L., Lu,Y., Whiteley, K.J., Holmyard, D., Hemberger, M., Pfarrer, C., Cross, J.C. (2002). Interactions between trophoblast cells and the maternal and fetal circulation in the mouse placenta. Dev. Biol. *250*, 358-73.
4. Adelman, D.M., Gertsenstein, M., Nagy, A., Simon, M.C., Maltepe, E. (2000). Placental cell fates are regulated in vivo by HIF-mediated hypoxia responses. Genes. Dev. *14*, 3191-203.
5. Afonso, S., Romagnano, L., Babiarz, B. (1997). The expression and function of cystatin C and cathepsin B and cathepsin L during mouse embryo implantation and placentation. Development *124*, 3415-25.
6. Alastalo, T.P., Hellesuo, M., Sandqvist, A., Hietakangas, V., Kallio, M., Sistonen, L. (2003). Formation of nuclear stress granules involves HSF2 and coincides with the nucleolar localisation of Hsp70. J Cell Sci *116*, 3557-70.
7. al-Lamki RS, Skepper JN, Burton GJ. (1999). Are human placental bed giant cells merely aggregates of small mononuclear trophoblast cells? An ultrastructural and immunocytochemical study. Hum Reprod *14*, 496-504.
8. Andersen, J.S., Lam, Y.W., Leung, A.K., Ong, S.E., Lyon, C.E., Lamond, A.I., Mann, M. (2005). Nucleolar proteome dynamics. Nature *433*, 77-83.
9. Andersen, J.S., Lyon, C.E., Fox, A.H., Leung, A.K., Lam, Y.W., Steen, H., Mann, M., Lamond, A.I. (2002). Directed proteomic analysis of the human nucleolus. Curr Biol *12*, 1-11.
10. Angelier N. (2005). Tracking the interactions of rRNA processing proteins during nucleolar assembly in living cells. Mol. Biol. Cell 16, 2862-2871.
11. Angelo, S., Lohr, J., Lee, K.H., Ticho, B.S., Breitbart, R.E., Hill, S., Yost, H.J., Srivastava, D. (2000). Conservation of sequence and expression of Xenopus and zebrafish dHAND during cardiac, branchial arch and lateral mesoderm development. Mech Dev *95*, 231-7.
12. Anson-Cartwright, L., Dawson, K., Holmyard, D., Fisher, S.J., Lazzarini, R.A., Cross, J.C. (2000). The glial cells missing-1 protein is essential for branching morphogenesis in the chorioallantoic placenta. Nat Genet *25*, 311-4.
13. Antoine, M., Reimers, K., Dickson, C., Kiefer, P. (1997). Fibroblast growth factor 3, a protein with dual subcellular localisation, is targeted to the nucleus and nucleolus by the concerted action of two nuclear localisation signals and a nucleolar retention signal. J Biol Chem *272*, 29475-81.
14. Arabi, A., Wu, S., Ridderstrale, K., Bierhoff, H., Shiue, C., Fatyol, K., Fahlen, S., Hydbring, P., Soderberg, O., Grummt, I., Larsson, L.G., Wright, A.P. (2005). c-Myc associates with ribosomal DNA and activates RNA polymerase I transcription. Nat Cell Biol *7*, 303-10.
15. Arber, S., Hunter, J.J., Ross, J. Jr., Hongo, M., Sansig, G., Borg, J., Perriard, J.C., Chien, K.R., Caroni, P. (1997). MLP-deficient mice exhibit a disruption of cardiac cytoarchitectural organisation, dilated cardiomyopathy, and heart failure. Cell *88*, 393-403.

16. Arman, E., Haffner-Krausz, R., Chen, Y., Heath, J.K., Lonai, P. (1998). Targeted disruption of fibroblast growth factor (FGF) receptor 2 suggests a role for FGF signalling in pregastrulation mammalian development. Proc Natl Acad Sci USA *95*, 5082-7.
17. Atchley, W.R., Fitch, W.M. (1997). A natural classification of the basic helix-loop-helix class of transcription factors. Proc Natl Acad Sci USA *94*, 5172-6.
18. Auman, H.J., Nottoli, T., Lakiza, O., Winger, Q., Donaldson, S., Williams, T. (2002). Transcription factor AP-2gamma is essential in the extra-embryonic lineages for early postimplantation development. Development *129*, 2733-2747.
19. Azzam, R., Chen, S.L., Shou, W., Mah, A.S., Alexandru, G., Nasmyth, K., Annan, R.S., Carr, S.A., Deshaies, R.J. (2004). Phosphorylation by cyclin B-Cdk underlies release of mitotic exit activator Cdc14 from the nucleolus. Science *305*, 516-519.
20. Bamberger, A.M., Bamberger, C.M., Aupers, S., Milde-Langosch, K., Loning, T., Makrigiannakis, A. (2004). Expression pattern of the activating protein-1 family of transcription factors in the human placenta. Mol Hum Reprod *10*: 223-8.
21. Barbosa, A.C., Funato, N., Chapman, S., McKee, M.D., Richardson, J.A., Olson, E.N., Yanagisawa, H. (2007). Hand transcription factors cooperatively regulate development of the distal midline mesenchyme. Dev Biol *310*, 154-68.
22. Bartram, U., Molin, D.G., Wisse, L.J., Mohamad, A., Sanford, L.P., Doetschman, T., Speer, C.P., Poelmann, R.E., Gittenberger-de Groot, A.C. (2001). Double-outlet right ventricle and overriding tricuspid valve reflect disturbances of looping, myocardialisation, endocardial cushion differentiation, and apoptosis in TGF-beta(2)-knockout mice. Circulation *103*, 2745-52.
23. Bates, S., Ryan, K.M., Phillips, A.C., Vousden, K.H. (1998). Cell cycle arrest and DNA endoreduplication following $p21^{Waf1/Cip1}$ expression. Oncogene *17*, 1691-1703.
24. Beg, A.A., Ruben, S.M., Scheinman, R.I., Haskill, S., Rosen, C.A., Baldwin, A.S. Jr. (1992). I kappa B interacts with the nuclear localisation sequences of the subunits of NF-kappa B: a mechanism for cytoplasmic retention. Genes Dev *6*, 1899-913.
25. Belandia B, Orford RL, Hurst HC, Parker MG. (2002). Targeting of SWI/SNF chromatin remodelling complexes to estrogen-responsive genes. EMBO J. *21*, 4094-103.
26. Bell, P., Dabauvalle, M.C., Scheer, U. (1992) In vitro assembly of prenucleolar bodies in Xenopus egg extract. J Cell Biol *118*, 1297-1304.
27. Bembenek J, Kang J, Kurischko C, Li B, Raab JR, Belanger KD, Luca FC, Yu H. (2005). Crm1-mediated nuclear export of Cdc14 is required for the completion of cytokinesis in budding yeast. Cell Cycle. *4*, 961-71.
28. Bembenek J, Yu H. (2001). Regulation of the anaphase-promoting complex by the dual specificity phosphatase human Cdc14a. J Biol Chem. *276*, 48237-42.
29. Benezra, R. (1994). An intermolecular disulfide bond stabilizes E2A homodimers and is required for DNA binding at physiological temperatures. Cell *79*, 1057-67.
30. Bernardi, R., Scaglioni, P.P., Bergmann, S., Horn, H.F., Vousden, K.H., Pandolfi, P.P. (2004). PML regulates p53 stability by sequestering Mdm2 to the nucleolus. Nat Cell Biol *6*, 665-72.
31. Bertrand, E., Houser-Scott, F., Kendall, A., Singer, R.H., Engelke, D.R.

(1998). Nucleolar localisation of early tRNA processing. Genes Dev *12*, 2463-8.

32. Bertwistle, D., Sugimoto, M., Sherr, C.J. (2004). Physical and functional interactions of the Arf tumour suprressor protein with nucleophosmin/ B23. Mol Cell Biol 24, 985-996.
33. Bettencourt-Dias, M., Rodrigues-Martins, A., Carpenter, L., Riparbelli, M., Lehmann, L., Gatt, M.K., Carmo, N., Balloux, F., Callaini, G., Glover, D.M. (2005). SAK/PLK4 is required for centriole duplication and flagella development. Curr Biol *15*, 2199-207.
34. Biben, C., Harvey, R.P. (1997). Homeodomain factor Nkx2-5 controls left/right asymmetric expression of bHLH gene eHand during murine heart development. Genes Dev *11*, 1357-69.
35. Bloom, J., Cross, F.R. (2007). Novel role for Cdc14 sequestration: Cdc14 dephosphorylates factors that promote DNA replication. Mol Cell Biol *27*, 842-53.
36. Boheler, K.R., Czyz, J., Tweedie, D., Yang, H.T., Anisimov, S.V., Wobus, A.M. (2002). Differentiation of pluripotent embryonic stem cells into cardiomyocytes. *91*, 189-201.
37. Boisvert, F.M., van Koningsbruggen, S., Navascues, J., Lamond, A.I. (2007). The multifunctional nucleolus. Nat Rev *8*, 574-585.
38. Bonnet, H.O., Filhol, I., Truchet, P., Brethenou, C., Cochet, F., Almaric, F., Bouche, G. (1996). Fibroblast groeth factor-2 binds to the regulatory beta-subunit of CK2 and directly stimulates CK2 activity toward nucleolin. J Biol Chem 271, 24781-24787.
39. Boudjelal, M., Taneja, R., Matsubara, S., Bouillet, P., Dolle, P., Chambon, P. (1997). Overexpression of Stra13, a novel retinoic acid-inducible gene of the basic helix-loop-helix family, inhibits mesodermal and promotes neuronal differentiation of P19 cells. Genes Dev *11*, 2052-65.
40. Bounpheng, M.A., Morrish, T.A., Dodds, S.G., Christy, B.A. (2000). Negative regulation of selected bHLH proteins by eHAND. Exp Cell Res *257*, 320-31.
41. Bourgeois, C.A., Hubert, J. (1988). Spatial relationship between the nucleolus and the nuclear envelope: structural aspects and functional significance. Int Rev Cytol *111*, 1-52.
42. Britton JS, Edgar BA. (1998). Environmental control of the cell cycle in Drosophila: nutrition activates mitotic and endoreplicative cells by distinct mechanisms. Development *125*, 2149-2158.
43. Britton, J.S., Lockwood, W.K., Li, L., Cohen, S.M., Edgar, B.A. (2002). Drosophila's insulin/PI3-kinase pathway coordinates cellular metabolism with nutritional conditions. Dev Cell *2*, 239-249.
44. Brown, L., Baer, R. (1994). HEN1 encodes a 20-kilodalton phosphoprotein that binds an extended E-box motif as a homodimer. Mol Cell Biol *14*, 1245-55.
45. Bruneau, B.G., Bao, Z.Z., Fatkin, D., Xavier-Neto, J., Georgakopoulos, D., Maguire, C.T., Berul, C.I., Kass, D.A., Kuroski-de Bold, M.L., de Bold, A.J., Conner, D.A., Rosenthal, N., Cepko, C.L., Seidman, C.E., Seidman, J.G. (2001). Cardiomyopathy in Irx4-deficient mice is preceded by abnormal ventricular gene expression. Mol Cell Biol *21*, 1730-6.
46. Busk, P.K., Hinrichsen, R., Bartkova, J., Hansen, A.H., Christoffersen, T.E., Bartek, J., Haunso, S. (2005). Cyclin D2 induces proliferation of cardiac myocytes and represses hypertrophy. Exp Cell Res *304*, 149-61.
47. Cai, C.L., Liang, X., Shi, Y., Chu, P.H., Pfaff, S.L., Chen, J., Evans, S. (2003).

Isl1 identifies a cardiac progenitor population that proliferates prior to differentiation and contributes a majority of cells to the heart. Dev Cell *5*, 877-89.

48. Caniggia, I., Mostachfi, H., Winter, J., Gassmann, M., Lye, S.J., Kuliszewski, M., Post, M. (2000). Hypoxia-inducible factor-1 mediates the biological effects of oxygen on human trophoblast differentiation through TGFbeta(3) J Clin Invest *105*, 577-87.
49. Caniggia, I., Mostachfi, H., Winter, J., Gassmann, M., Lye, S.J., Kuliszewski, M., Post, M. (2000). Hypoxia-inducible factor-1 mediates the biological effects of oxygen on human trophoblast differentiation through TGFbeta(3). J Clin Invest *105*, 577-87.
50. Cano, A., Perez-Moreno, M.A., Rodrigo, I., Locascio, A., Blanco, M.J., del Barrio, M.G., Portillo, F., Nieto, M.A. (2000). The transcription factor snail controls epithelial-mesenchymal transitions by repressing E-cadherin expression. Nat Cell Biol *2*, 76-83.
51. Carmeliet, P., Ferreira, V., Breier, G., Pollefeyt, S., Kieckens, L., Gertsenstein, M., Fahrig, M., Vandenhoeck, A., Harpal, K., Eberhardt, C., Declercq, C., Pawling, J., Moons, L., Collen, D., Risau, W., Nagy, A. (1996). Abnormal blood vessel development and lethality in embryos lacking a single VEGF allele. Nature *380*, 435-9.
52. Carmo-Fonseca, M., Mendes-Soares, L., Campos, I. (2000). To be or not to be in the nucleolus. Nat Cell Biol *2*, 107-112.
53. Carney, E.W., Prideaux, V., Lye, S.J., Rossant, J. (1993). Progressive expression of trophoblast-specific genes during formation of mouse trophoblast giant cells in vitro. Mol Reprod Dev. *34*, 357-68.
54. Cebolla, A., Vinardell, J.M., Kiss, E., Oláh, B., Roudier, F., Kondorosi, A., Kondorosi, E (1999). The mitotic inhibitor ccs52 is required for endoreduplication and ploidy-dependent cell enlargement in plants. EMBO J *18*, 4476-4484.
55. Cerutti, L., Simanis, V. (2000). Controlling the end of the cell cycle. Curr Opin Genet Dev *10*, 65-9.
56. Cueille N, Salimova E, Esteban V, Blanco M, Moreno S, Bueno A, Simanis V. (2001). Flp1, a fission yeast orthologue of the s. cerevisiae CDC14 gene, is not required for cyclin degradation or rum1p stabilisation at the end of mitosis. J Cell Sci *114*, 2649-64.
57. Charite, J., McFadden, D.G., Merlo, G., Levi, G., Clouthier, D.E., Yanagisawa, M., Richardson, J.A., Olson, E.N. (2001). Role of Dlx6 in regulation of an endothelin-1-dependent, dHAND branchial arch enhancer. Genes Dev *15*, 3039-49.
58. Charite, J., McFadden, D.G., Olson, E.N. (2000). The bHLH transcription factor dHAND controls Sonic hedgehog expression and establishment of the zone of polarizing activity during limb development. Development *127*, 2461-70.
59. Chen, C.M., Kraut, N., Groudine, M., Weintraub, H. (1996). I-mf, a novel myogenic repressor, interacts with members of the MyoD family. Cell *86*, 731-741.
60. Chen, J.N., Fishman, M.C. (2000). Genetics of heart development. Trends Genet. *16*, 383-8.
61. Chiaramello, A., Neuman, K., Palm, K., Metsis, M., Neuman, T. (1995). Helix-loop-helix transcription factors mediate activation and repression of the

p75LNGFR gene. Mol Cell Biol *15*, 6036-44.
62. Christoffels, V.M., Habets, P.E., Franco, D., Campione, M., de Jong, F., Lamers, W.H., Bao, Z.Z., Palmer, S., Biben, C., Harvey, R.P., Moorman, A.F. (2000). Chamber formation and morphogenesis in the developing mammalian heart. Dev Biol *223*,266-78.
63. Cockell, M.M., Gasser, S.M. (1999). The nucleolus: nucleolar space for RENT. Curr Biol *9*, 575-6.
64. Colgin, M.A., Nyborg, J.K. (1998). The human T-cell leukemia virus type 1 oncoprotein Tax inhibits the transcriptional activity of c-Myb through competition for the CREB binding protein. J Virol *72*, 9396-9.
65. Collop, A.H., Broomfield, J.A., Chandraratna, R.A., Yong, Z., Deimling, S.J., Kolker, S.J., Weeks, D.L., Drysdale, T.A. (2006). Retinoic acid signalling is essential for formation of the heart tube in Xenopus. Dev Biol *291*, 96-109.
66. Colombo E, Marine JC, Danovi D, Falini B, Pelicci PG. (2002). Nucleophosmin regulates the stability and transcriptional activity of p53. Nat Cell Biol *4*, 529-533.
67. Corsetti, M.T., Levi, G., Lancia, F., Sanseverino, L., Ferrini, S., Boncinelli, E., Corte, G. (1995). Nucleolar localisation of three Hox homeoproteins. J Cell Sci *108*, 187-93.
68. Coute, Y., Burgess, J.A., Diaz, J.J., Chichester, C., Lisacek, F., Greco, A., Sanchez, J.C. (2006). Deciphering the human nucleolar proteome. Mass Spectrom Rev *25*, 215-34.
69. Cowden-Dahl, K.D., Fryer, B.H., Mack, F.A., Compernolle, V., Maltepe, E., Adelman, D.M., Carmeliet, P., Simon, M.C. (2005). Hypoxia-inducible factors 1alpha and 2alpha regulate trophoblast differentiation. Mol Cell Biol *25*, 10479-91.
70. Cross, J.C. (2000). Genetic insights into trophoblast differentiation and placental morphogenesis. Cell Dev Biol *11*, 105-113.
71. Cross, J.C., Anson-Cartwright, L., Scott, I.C. (2002). Transcription factors underlying the development and endocrine functions of the placenta. Recent Prog Horm Res *57*, 221-34.
72. Cross, J.C., Flannery, M.L., Blanar, M.A., Steingrimsson, E., Jenkins, N.A., Copeland, N.G., Rutter, W.J., Werb, Z. (1995). Hxt encodes a basic helix-loop-helix transcription factor that regulates trophoblast cell development. Development *121*, 2513-2523.
73. Cross, S.M., Sanchez, C.A., Morgan, C.A., Schimke, M.K., Ramel, S., Idzerda, R.L., Raskind, W.H., Reid, B.J. (1995). A p53-dependent mouse spindle checkpoint. Science *267*, 1353-6.
74. Cserjesi, P., Brown, D., Lyons, G.E., Olson, E.N. (1995). Expression of the novel basic helix-loop-helix gene eHAND in neural crest derivatives and extraembryonic membranes during mouse development. Dev Biol. *170*, 664-78.
75. Cui, W., Ning, J., Naik, U.P., Duncan, M.K. (2004). OptiRNAi, an RNAi design tool. Com. Meth. Prog. Biomed. *75*, 67-73.
76. Dai, Y.S., Cserjesi, P., Markham, B.E., Molkentin, J.D. (2002). The transcription factors GATA4 and dHAND physically interact to synergistically activate cardiac gene expression through a p300-dependent mechanism. J Biol Chem *277*, 24390-8.
77. Damsky, C.H., Librach, C., Lim, K.H., Fitzgerald, M.L., McMaster, M.T., Janatpour, M., Zhou, Y., Logan, S.K., Fisher, S.J. (1994). Integrin switching

regulates normal trophoblast invasion. Development *120*, 3657-66.
78. Daniely, Y., Dimitrova, D.D., Borowiec, J.A. (2002). Stress-dependent nucleolin mobilisation mediated by p53-nucleolin complex formation. Mol Cell Biol *22*, 6014-22.
79. Datta, A., Nag, A., Pan, W., Hay, N., Gartel, A.L., Colamonici, O., Mori, Y., Raychaudhuri, P. (2004). Myc-ARF (alternate reading frame) interaction inhibits the functions of Myc. J Biol Chem *279*, 36698-36707.
80. D'Autréaux, F., Morikawa, Y., Cserjesi, P., Gershon, M.D. (2007). Hand2 is necessary for terminal differentiation of enteric neurons from crest-derived precursors but not for their migration into the gut or for formation of glia. Development *134*, 2237-49.
81. Davidson B, Levine M. (2003). Evolutionary origins of the vertebrate heart: Specification of the cardiac lineage in Ciona intestinalis. Proc Natl Acad Sci USA *100*, 11469-73.
82. Davis, R.L., Cheng, P.F., Lassar, A.B., Weintraub, H. (1990). The MyoD DNA binding domain contains a recognition code for muscle-specific gene activation. Cell *60*, 733-46.
83. de Almeida, A., Raccurt, I., Peyrol, S., Charbonneau, M. (1999). The Saccharomyces cerevisiae Cdc14 phosphatase is implicated in the structural organisation of the nucleolus. Biol Cell *91*, 649-63.
84. Deng, W.M., Althauser, C., Ruohola-Baker, H. (2001). Notch-Delta signalling induces a transition from mitotic cell cycle to endocycle in Drosophila follicle cells. Development *128*, 4737-4736.
85. Derenzini, M., Trere, D., Pession, A., Govoni, M., Sirri, V., Chieco, P. (2000). Nucleolar size indicates the rapidity of cell proliferation in cancer tissues. J Pathol *191*, 181-6.
86. Desterro, J.M., Keegan, L.P., Lafarga, M., Berciano, M.T., O'Connell, M., Carmo-Fonseca, M. (2003). Dynamic association of RNA-editing enzymes with the nucleolus. J Cell Sci *116*, 1805-18.
87. Dimario, P.J. (2004). Cell and molecular biology of nucleolar assembly and disassembly. Int Rev Cytol *239*, 99-178.
88. Doevendans, P.A., Kubalak, S.W., An, R.H., Becker, D.K., Chien, K.R., Kass, R.S. (2000). Differentiation of cardiomyocytes in floating embryoid bodies is comparable to fetal cardiomyocytes. J Mol Cell Cardiol *32*, 839-51.
89. Donnison, M., Beaton, A., Davey, H.W., Broadhurst, R., L'Huillier, P., Pfeffer, P.L. (2005). Loss of the extraembryonic ectoderm in Elf5 mutants leads to defects in embryonic patterning. Development *132*, 2299-308.
90. Dousset, T., Wang, C., Verheggen, C., Chen, D., Hernandez-Verdun, D., Huang, S. (2000). Initiation of nucleolar assembly is independent of RNA polymerase I transcription. Mol Biol Cell. *11*, 2705-17.
91. Dundr, M., Leno, G.H., Lewis, N., Rekosh, D., Hammarskjoid, M.L., Olson, M.O. (1996). Location of the HIV-1 Rev protein during mitosis: inactivation of the nuclear export signal alters the pathway for postmitotic re-entry into nucleoli. J Cell Sci *109*, 2239-2251.
92. Dundr, M., Misteli, T. (2001). Functional architecture in the cell nucleus. Biochem J *356*, 297-310.
93. Dundr, M., Misteli, T., Olson, M.O. (2000). The dynamics of postmitotic reassembly of the nucleolus. J Cell Biol *150*, 433-46.
94. Dundr, M., Olson, M.O. (1998). Partially processed pre-rRNA is preserved in association with processing components in nucleolus-derived foci during

mitosis. Mol Biol Cell *9*, 2407-22.
95. Dunwoodie, S.L., Rodriguez, T.A., Beddington, R.S. (1998). Msg1 and Mrg1, founding members of a gene family, show distinct patterns of gene expression during mouse embryogenesis. Mech Dev *72*, 27-40.
96. Eisenberg, L.M., Markwald, R.R. (1995). Molecular regulation of atrioventricular valvuloseptal morphogenesis. Circ Res *77*, 1-6.
97. Elam, C., Hesson, L., Vos, M.D., Eckfeld, K., Ellis, C.A., Bell, A., Krex, D., Birrer, M.J., Latif, F., Clark, G.J. (2005). RRP22 is a farnesylated, nucleolar, Ras-related protein with tumor suppressor potential. Cancer Res *65*, 3117-25.
98. El-Hashash, A.H., Esbrit, P., Kimber, S.J. (2005). PTHrP promotes murine secondary trophoblast giant cell differentiation through induction of endocycle, upregulation of giant-cell-promoting transcription factors and suppression of other trophoblast cell types. Differentiation *73*, 154-74.
99. El-Hashash, A.H., Kimber, S.J. (2006). PTHrP induces changes in cell cytoskeleton and E-cadherin and regulates Eph/Ephrin kinases and RhoGTPases in murine secondary trophoblast cells. Dev Biol *290*, 13-31.
100. Elia, A.E., Cantley, L.C. and Yaffe, M.B. (2003). Proteomic screen finds pSer/pThr-binding domain localizing Plk1 to mitotic substrates. Science *299*, 1228-1231.
101. Endl, E., Gerdes, J. (2000). Posttranslational modifications of the KI-67 protein coincide with two major checkpoints during mitosis. J Cell Physiol *182*, 371-80.
102. Faria, T.N., Soares, M.J. (1991). Trophoblast cell differentiation: establishment, characterisation, and modulation of a rat trophoblast cell line expressing members of the placental prolactin family. Endocrinology *129*, 2895-906.
103. Fatica, A., Tollervey, D. (2002). Making ribosomes. Curr Opin Cell Biol *14*, 313-8.
104. Fatyol, K., Szalay, A.A. (2001). The p14ARF tumor suppressor protein facilitates nucleolar sequestration of hypoxia-inducible factor-1alpha (HIF-1alpha) and inhibits HIF-1-mediated transcription. J Biol Chem *276*, 28421-9.
105. Feng, Y., Longo, D.L., Ferris, D.K. (2001). Polo-like kinase interacts with proteasomes and regulates their activity. Cell Growth Differ *12*, 29-37.
106. Fernandez-Teran, M., Piedra, M.E., Rodriguez-Rey, J.C., Talamillo, A., Ros, M.A. (2003). Expression and regulation of eHAND during limb development. Dev Dyn *226*, 690-701.
107. Fijnvandraat, A.C., van Ginneken, A.C., Schumacher, C.A., Boheler, K.R, Deprez, R.H., Christoffels, V.M., Moorman, A.F. (2003). Cardiomyocytes purified from differentiated embryonic stem cells exhibit characteristics of early chamber myocardium. J Mol Cell Cardiol *35*, 1461-72.
108. Finch, R.A., Chang, D.C., Chan, P.K. (1995). GTP gamma S restores nucleophosmin (NPM) localisation to nucleoli of GTP-depleted HeLa cells. Mol Cell Biochem *146*, 171-8.
109. Firulli, A.B. (2003). A HANDful of questions: the molecular biology of the heart and neural crest derivatives (HAND)-subclass of basic helix-loop-helix transcription factors. Gene *17*, 27-40.
110. Firulli, A.B., McFadden, D.G., Lin, Q., Srivastava, D., Olson, E.N. (1998). Heart and extra-embryonic mesodermal defects in mouse embryos lacking the bHLH transcription factor Hand1. Nat Genet *18*, 266-70.
111. Firulli, B.A., Hadzic, D.B., McDaid, J.R., Firulli, A.B. (2000). The basic helix-

loop-helix transcription factors dHAND and eHAND exhibit dimerisation characteristics that suggest complex regulation of function. J Biol Chem *275*, 33567-33573.

112. Firulli, B.A., Howard, M.J., McDaid, J.R., McIlreavey, L., Dionne, K.M., Centonze, V.E., Cserjesi, P., Virshup, D.M., Firulli. A.B. (2003). PKA, PKC, and the protein phosphatase 2A influence HAND factor function: a mechanism for tissue-specific transcriptional regulation. Mol Cell *12*, 1225-37.
113. Firulli, B.A., Krawchuk, D., Centonze, V.E., Vargesson, N., Virshup, D.M., Conway, S.J., Cserjesi, P., Laufer, E., Firulli, A.B. (2005). Altered Twist1 and Hand2 dimerisation is associated with Saethre-Chotzen syndrome and limb abnormalities. Nat Genet *37*, 373-381.
114. Fisher, A.L., Ohsako, S., Caudy, M. (1996). The WRPW motif of the hairy-related basic helix-loop-helix repressor proteins acts as a 4-amino-acid transcription repression and protein-protein interaction domain. Mol Cell Biol *16*, 2670-7.
115. Fishman, M.C., Olson, E.N. (1997). Parsing the heart: genetic modules for organ assembly. Cell *91*, 153-6.
116. Fode, C., Binkert, C., Dennis, J.W. (1996). Constitutive expression of murine Sak-a suppresses cell growth and induces multinucleation. Mol Cell Biol *16*, 4665-72.
117. Fode, C., Motro, B., Yousefi, S., Heffernan, M., Dennis, J.W. (1994). Sak, a murine protein-serine/threonine kinase that is related to the Drosophila polo kinase and involved in cell proliferation. Proc Natl Acad Sci USA *91*, 6388-92.
118. Fox, A.H., Lam, Y.W., Leung, A.K., Lyon, C.E., Andersen, J., Mann, M., Lamond, A.I. (2002). Paraspeckles: a novel nuclear domain. Curr Biol. *12*, 13-25.
119. Franke, W.W. (1988). Matthias Jacob Schleiden and the definition of the cell nucleus. Eur. J. Cell Biol. *47*, 145-156.
120. Frei, C., Edgar, B.A. (2004). Drosophila cyclin D/Cdk4 requires Hif-1 prolyl hydroxylase to drive cell growth. Dev Cell *6*, 241-251.
121. Fryer, B.H., Simon, M.C. Hypoxia, HIF and the placenta. Cell Cycle (2006). *5*, 495-498.
122. Fuse, N., Hirose, S., Hayashi, S. (1994). Diploidy of Drosophila imaginal cells is maintained by a transcriptional repressor encoded by escargot. Genes Dev *8*, 2270-81.
123. Galcheva-Gargova, Z., Gangwani, L., Konstantinov, K.N., Mikrut, M., Theroux, S.J., Enoch, T., Davis, R.J. (1998). The cytoplasmic zinc finger protein ZPR1 accumulates in the nucleolus of proliferating cells. Mol Biol Cell *9*, 2963-2971.
124. Gao, S., Scott, R.E. (2002). P2P-R protein overexpression restricts mitotic progression at prometaphase and promotes mitotic apoptosis. J Cell Physiol *193*, 199-207.
125. Gardner, R.L., Beddington, R.S. (1988). Multi-lineage 'stem' cells in the mammalian embryo. J Cell Sci Suppl *10*, 11-27.
126. Garrell, J., Campuzano, S. (1991). The helix-loop-helix domain: a common motif for bristles, muscles and sex. Bioessays *13*, 493-8.
127. Gautier, T., Robert-Nicoud, M., Guilly, M.N., Hernandez-Verdun, D. (1992). Relocation of nucleolar proteins around chromosomes at mitosis. A study by confocal laser scanning microscopy. J Cell Sci *102*, 729-737.
128. Genbacev, O., Zhou, Y., Ludlow, J.W., Fisher, S.J. (1997). Regulation of

human placental development by oxygen tension. Science 1997 *277*, 1669-72.
129. Geng, Y., Yu, Q., Sicinska, E., Das, M., Schneider, J.E., Bhattacharya, S., Rideout, W.M., Bronson, R.T., Gardner, H., Sicinski, P. (2003). Cyclin E ablation in the mouse. Cell *114*, 431-43.
130. Georgiades, P., Ferguson-Smith, A.C., Burton, G.J. (2002). Comparative developmental anatomy of the murine and human definitive placentae. Placenta. *23*, 3-19.
131. Golan, A., Yudkovsky, Y., Hershko, A. (2002). The cyclin-ubiquitin ligase activity of cyclosome/APC is jointly activated by protein kinases Cdk1-cyclin B and Plk. J Biol Chem *277*, 15552-15557.
132. Gonda, K., Fowler, J., Katoku-Kikyo, N., Haroldson, J., Wudel, J., Kikyo, N. (2003). Reversible disassembly of somatic nucleoli by the germ cell proteins FRGY2a and FRGY2b. Nat Cell Biol *5*, 205-10.
133. Gonzalez, M.A., Tachibana, K.E., Adams, D.J., van der Weyden, L., Hemberger, M., Coleman, N., Bradley, A., Laskey, R.A. (2006). Geminin is essential to prevent endoreduplication and to form pluripotent cells during mammalian development. Genes Dev *20*, 1880-1884.
134. Goodson, M.L., Hong, Y., Rogers, R., Matunis, M.J., Park-Sarge, O.K., Sarge, K.D. (2001). Sumo-1 modification regulates the DNA binding activity of heat shock transcription factor 2, a promyelocytic leukemia nuclear body associated transcription factor. J Biol Chem *276*, 18513-8.
135. Goyal, P., Pandey, D., Siess, W. (2006). Phosphorylation-dependent regulation of unique nuclear and nucleolar localisation signals of LIM kinase 2 in endothelial cells. J Biol Chem *281*, 25223-30.
136. Grafi, G., Larkins, B.A. (1995). Endoreduplication in maize endosperm: involvement of M phase-promoting factor inhibition and induction of S phase-related kinases. Science *269*, 1262-1264.
137. Grallert, A., Hagan, I.M. (2002). Schizosaccharomyces pombe NIMA-related kinase, Fin1, regulates spindle formation and an affinity of Polo for the SPB. EMBO J. *21*, 3096-107.
138. Grasberger, H., Bell, G.I. (2005). Subcellular recruitment by TSG118 and TSPYL implicates a role for zinc finger protein 106 in a novel developmental pathway. Int J Biochem Cell Biol *37*, 1421-1437.
139. Griffioen, G., Thevelein, J.M. (2002). Molecular mechanisms controlling the localisation of protein kinase A. Curr Genet *41*, 199-207.
140. Grimes HL, Chan TO, Zweidler-McKay PA, Tong B, Tsichlis PN. (1996). The Gfi-1 proto-oncoprotein contains a novel transcriptional repressor domain, SNAG, and inhibits G1 arrest induced by interleukin-2 withdrawal. Mol Cell Biol *16*, 6263-72.
141. Grummer, R., Hellmann, P., Traub, O., Soares, M.J., el-Sabban, M.E., Winterhager, E. (1996). Regulation of connexin31 gene expression upon retinoic acid treatment in rat choriocarcinoma cells. Exp Cell Res *227*, 23-32.
142. Guillemot, F., Nagy, A., Auerbach, A., Rossant, J., Joyner, A.L. (1994). Essential role of Mash-2 in extraembryonic development. Nature *371*, 333-336.
143. Gultice, A.D., Selesniemi, K.L., Brown, T.L. (2006). Hypoxia inhibits differentiation of lineage-specific Rcho-1 trophoblast giant cells. Biol Reprod *74*, 1041-50.
144. Guzman-Ayala, M., Ben-Haim, N., Beck, S., Constam, D.B. (2004). Nodal protein processing and fibroblast growth factor 4 synergize to maintain a trophoblast stem cell microenvironment. Proc Natl Acad Sci USA. *101*, 15656-

60.
145. Habara-Ohkubo, A. (1996). Differentiation of beating cardiac muscle cells from a derivative of P19 embryonal carcinoma cells. Cell Struct Funct *21*, 101-10.
146. Habedanck, R., Stierhof, Y.D., Wilkinson, C.J., Nigg, E.A. (2005). The Polo kinase Plk4 functions in centriole duplication. Nat Cell Biol *7*, 1140-1146.
147. Hagihara, A., Miyamoto, K., Furuta, J., Hiraoka, N., Wakazono, K., Seki, S., Fukushima, S., Tsao, M.S., Sugimura, T., Ushijima, T. (2004). Identification of 27 5' CpG islands aberrantly methylated and 13 genes silenced in human pancreatic cancers. Oncogene. *23*, 8705-10.
148. Hamamori, Y., Sartorelli, V., Ogryzko, V., Puri, P.L., Wu, H.Y., Wang, J.Y., Nakatani, Y., Kedes, L. (1999). Regulation of histone acetyltransferases p300 and PCAF by the bHLH protein twist and adenoviral oncoprotein E1A. Cell *96*, 405-13.
149. Hamlin, G.P., Lu, X.J., Roby, K.F., Soares, M.J. (1994). Recapitulation of the pathway for trophoblast giant cell differentiation in vitro: stage-specific expression of members of the prolactin gene family. Endocrinology *134*, 2390-2396.
150. Hamlin, G.P., Soares, M.J. (1995). Regulation of deoxyribonucleic acid synthesis in proliferating and differentiating trophoblast cells: involvement of transferrin, transforming growth factor-beta, and tyrosine kinases *136*, 322-31.
151. Han Z, Yi P, Li X, Olson EN. (2006). Hand, an evolutionarily conserved bHLH transcription factor required for Drosophila cardiogenesis and hematopoiesis. Development *133*, 1175-1182.
152. Han, K., Manley, J.L. (1993). Transcriptional repression by the Drosophila even-skipped protein: definition of a minimal repression domain. Genes Dev *7*, 491-503.
153. Han, Z., Olson, E.N. (2005). Hand is a direct target of Tinman and GATA factors during Drosophila cardiogenesis and hematopoiesis. Development *132*, 3525-36.
154. Handwerger, K.E., Cordero, J.A., Gall, J.G. (2005). Cajal bodies, nucleoli, and speckles in the Xenopus oocyte nucleus have a low-density, sponge-like structure. Mol. Biol. Cell *16*, 202-211.
155. Handwerger, K.E., Gall, J.G. (2006). Subnuclear organelles: new insights into form and function. Trends Cell Biol *16*, 19-26.
156. Hannon, G.J. (2002). RNA interference. Nature *418*, 244-251.
157. Harvey, R.P. (1999). Seeking a regulatory roadmap for heart morphogenesis. Semin Cell Dev Biol *10*, 99-107.
158. Hassanein, M., Korant, B.D., Lu, G., Mason, R.W. (2007). Expression of cathepsin P mRNA, protein and activity in the rat choriocarcinoma cell line, Rcho-1, during giant cell transformation. Placenta *28*, 912-9.
159. Hatse, S., Naesens, L., De Clercq, E., Balzarini, J. (1998). Potent differentiation-inducing properties of the antiretroviral agent 9-(2-phosphonylmethoxyethyl) adenine (PMEA) in the rat choriocarcinoma (RCHO) tumor cell model. Biochem Pharmacol *56*, 851-9.
160. Hattori, N., Davies, T.C., Anson-Cartwright, L., Cross, J.C. (2000). Periodic expression of the cyclin-dependent kinase inhibitor $p57^{Kip2}$ in trophoblast giant cells defines a G2-like gap phase of the endocycle. Mol Biol Cell *11*, 1037-1045.
161. Hayashi M, Sakata M, Takeda T, Yamamoto T, Okamoto Y, Sawada K,

Kimura A, Minekawa R, Tahara M, Tasaka K, Murata Y. (2004). Induction of glucose transporter 1 expression through hypoxia-inducible factor 1alpha under hypoxic conditions in trophoblast-derived cells. J Endocrinol *183*, 145-154.

162. Hayashi, S., Hirose, S., Metcalfe, T., Shirras, A.D. (1993). Control of imaginal cell development by the escargot gene of Drosophila. Development *118*, 105-15.
163. Hayles, J., Fisher, D., Woollard, A., Nurse, P. (1994). Temporal order of S phase and mitosis in fission yeast is determined by the state of the p34cdc2-mitotic B cyclin complex. Cell *78*, 813-822.
164. Heine, M.A., Rankin, M.L., DiMario, P.J. (1993). The Gly/Arg-rich (GAR) domain of Xenopus nucleolin facilitates in vitro nucleic acid binding and in vivo nucleolar localisation. Mol Biol Cell *4*, 1189-204.
165. Hemberger, M., Cross, J.C. (2001). Genes governing placental development. Trends Endocrinol Metabol *12*, 162-168.
166. Hemberger, M., Hughes, M., Cross, J.C. (2004). Trophoblast stem cells differentiate in vitro into invasive trophoblast giant cells. Dev Biol *271*, 362-371.
167. Henderson, J.E., Amizuka, N., Warshawsky, H., Biasotto, D., Lanske, B.M., Goltzman, D., Karaplis, A.C. (1995). Nucleolar localisation of parathyroid hormone-related peptide enhances survival of chondrocytes under conditions that promote apoptotic cell death. Mol Cell Biol *15*, 4064-75.
168. Hernandez-Verdun, D. (2006). Nucleolus: from structure to dynamics. Histochem Cell Biol *125*, 127-137.
169. Hernandez-Verdun, D. (2006). The nucleolus: a model for the organisation of nuclear functions. Histochem Cell Biol *126*, 135-148.
170. Hernandez-Verdun, D., Roussel, P., Gebrane-Younes, J. Emerging concepts of nucleolar assembly. J Cell Sci (2002) *112*, 2265-2270.
171. Hill, A.A., Riley, P.R. (2004). Differential regulation of Hand1 homodimer and Hand1-E12 heterodimer activity by the cofactor FHL2. Mol Cell Biol *24*, 9835-9847.
172. Hinsby, A.M., Kiemer, L., Karlberg, E.O., Lage, K., Fausbøll, A., Juncker, A.S., Andersen, J.S., Mann, M., Brunak, S. (2006). A wiring of the human nucleolus. Mol Cell *22*, 285-95.
173. Hiscox, J.A. (2007). RNA viruses: hijacking the dynamic nucleolus. Nature Reviews Microbiol *5*, 119-128.
174. Hoffman, J.I. (1995). Incidence of congenital heart disease: II. Prenatal incidence. Pediatr Cardiol *16*, 155-65.
175. Hollenberg, S.M., Sternglanz, R., Cheng, P.F., Weintraub, H. (1995). Identification of a new family of tissue-specific basic helix-loop-helix proteins with a two-hybrid system. Mol Cell Biol *15*, 3813-3822.
176. Hough, S.R., Clements, I., Welch, P.J., Wiederholt, K.A. (2006). Differentiation of mouse embryonic stem cells after RNA interference-mediated silencing of OCT4 and Nanog. Stem Cells *24*, 1467-75.
177. Hove, J.R., Köster, R.W., Forouhar, A.S., Acevedo-Bolton, G., Fraser, S.E., Gharib, M. (2003). Intracardiac fluid forces are an essential epigenetic factor for embryonic cardiogenesis. Nature *421*, 172-7.
178. Howard, M., Foster, D.N., Cserjesi, P. (1999). Expression of HAND gene products may be sufficient for the differentiation of avian neural crest-derived cells into catecholaminergic neurons in culture. Dev Biol *215*, 62-77.
179. Hu, D., Scott, I.C., Geary, C., Zhao, X., Cross, J.C. (2006). The Hand1

transcription factor functions as a homodimer during mouse development. Dev Biol *295*, 368-380.
180. Huang Z, Traugh JA, Bishop JM. (2004). Negative control of the Myc protein by the stress-responsive kinase Pak2. Mol Cell Biol. *24*, 1582-94.
181. Huang, F., Wagner, M., Siddiqui, M.A. (2004). Ablation of the CLP-1 gene leads to down-regulation of the HAND1 gene and abnormality of the left ventricle of the heart and fetal death. Mech Dev *121*, 559-72.
182. Hudson, J.W., Kozarova, A., Cheung, P., Macmillan, J.C., Swallow, C.J., Cross, J.C., Dennis, J.W. (2001). Late mitotic failure in mice lacking Sak, a polo-like kinase. Curr Biol *11*, 441-446.
183. Hughes, M., Dobric, N., Scott, I.C., Su, L., Starovic, M., St-Pierre, B., Egan, S.E., Kingdom, J.C., Cross, J.C. (2004). The Hand1, Stra13 and Gcm1 transcription factors override FGF signalling to promote terminal differentiation of trophoblast stem cells. Dev Biol *271*, 26-37.
184. Huh, W.K., Falvo, J.V., Gerke, L.C., Carroll, A.S., Howson, R.W., Weissman, J.S., O'Shea, E.K. (2003). Global analysis of protein localisation in budding yeast. Nature *425*, 686-91.
185. Iborra, F.J., Pombo, A., McManus, J., Jackson, D.A., Cook, P.R. (1996). The topology of transcription by immobilised polymerases. Exp Cell Res *229*, 167-73.
186. Ideue, T., Azad, A.K., Yoshida, J., Matsusaka, T., Yanagida, M., Ohshima, Y., Tani, T. (2004). The nucleolus is involved in mRNA export from the nucleus in fission yeast. J Cell Sci *117*, 2887-95.
187. Imai, S., Nishibayashi, S., Takao, K., Tomifuji, M., Fujino, T., Hasegawa, M., Takano, T. (1997). Dissociation of Oct-1 from the nuclear peripheral structure induces the cellular aging-associated collagenase gene expression. Mol Biol Cell *8*, 2407-19.
188. Ino, H., Mochizuki, T., Yanaihara, N., Chiba, T. (1993). p34cdc2 homologue is located in nucleoli of the nervous and endocrine systems. Brain Res *614*, 131-6.
189. Ishibashi, M., Sasai, Y., Nakanishi, S., Kageyama, R. (1993). Molecular characterisation of HES-2, a mammalian helix-loop-helix factor structurally related to Drosophila hairy and Enhancer of split. Eur J Biochem *215*, 645-52.
190. Isobe, A., Takeda, T., Sakata, M., Yamamoto, T., Minekawa, R., Hayashi, M., Auernhammer, C.J., Tasaka, K., Murata, Y. (2006). STAT3-mediated constitutive expression of SOCS3 in an undifferentiated rat trophoblast-like cell line. Placenta *27*, 912-8.
191. Itahana, K., Bhat, K.P., Jin, A., Itahana, Y., Hawke, D., Kobayashi, R., Zhang, Y. (2003). Tumor suppressor ARF degrades B23, a nucleolar protein involved in ribosome biogenesis and cell proliferation. Mol Cell *12*, 1151-64.
192. Ivanova, A.V., Ivanov, S.V., Danilkovitch-Miagkova, A., Lerman, M.I. (2001). Regulation of STRA13 by the von Hippel-Lindau tumor suppressor protein, hypoxia, and the UBC9/ubiquitin proteasome degradation pathway. J Biol Chem *276*, 15306-15.
193. Ivey, K., Tyson, B., Ukidwe, P., McFadden, D.G., Levi, G., Olson, E.N., Srivastava, D., Wilkie, T.M. (2003). Galphaq and Galpha11 proteins mediate endothelin-1 signalling in neural crest-derived pharyngeal arch mesenchyme. Dev Biol *255*, 230-7.
194. Ivorra, C., Kubicek, M., Gonzalez, J.M., Sanz-Gonzalez, S.M., Alvarez-Barrientos, A., O'Connor, J.E., Burke, B., Andres, V. (2006). A mechanism of

AP-1 suppression through interaction of c-Fos with lamin A/C. Genes Dev. *20*, 307-20.

195. Jackson, M.R., Carney, E.W., Lye, S.J., Ritchie, J.W. (1994). Localisation of two angiogenic growth factors (PDECGF and VEGF) in human placentae throughout gestation. Placenta *15*, 341-53.
196. Jacobson, M.R., Pederson, T. (1998). Localisation of SRP RNA in the nucleolus of mammalian cells. Proc Natl Acad Sci USA *95*, 7981-6.
197. Jady, B.E., Kiss, T. (2001). A small nucleolar guide RNA functions both in 2'-O-ribose methylation and pseudouridylation of the U5 spliceosomal RNA. EMBO J *20*, 541-51.
198. Jaken, S. (1996). Protein kinase C isozymes and substrates. Curr Opin Cell Biol *8*, 168-73.
199. Janatpour MJ, Utset MF, Cross JC, Rossant J, Dong J, Israel MA, Fisher SJ. (1999). A repertoire of differentially expressed transcription factors that offers insight into mechanisms of human cytotrophoblast differentiation. Dev Genet *25*, 146-57.
200. Janatpour, M.J., McMaster, M.T., Genbacev, O., Zhou, Y., Dong, J., Cross, J.C., Israel, M.A., Fisher, S.J. (2000). Id-2 regulates critical aspects of human cytotrophoblast differentiation, invasion and migration. Development *127*, 549-58.
201. Jaquenoud M, van Drogen F, Peter M. (2002). Cell cycle-dependent nuclear export of Cdh1p may contribute to the inactivation of APC/C(Cdh1). EMBO J. *21*, 6515-26.
202. Jaspersen SL, Charles JF, Tinker-Kulberg RL, Morgan DO. A late mitotic regulatory network controlling cyclin destruction in Saccharomyces cerevisiae. Mol Biol Cell *9*, 2803-17.
203. Jen, Y., Manova, K., Benezra, R. (1997). Each member of the Id gene family exhibits a unique expression pattern in mouse gastrulation and neurogenesis. Dev Dyn *208*, 92-106.
204. Jimenez-Garcia, L.F., Segura-Valdez, M.D.L., Ochs, R.L., Rothblum, L., Hannan, I., Spector, D.L. (1994). Nucleologenesis: U3 snRNA-containing prenucleolar bodies move to sites of active pre-rRNA transcrtipion after mitosis. Mol. Biol. Cell *5*, 955-966.
205. Johnson, B.R., Nitta, R.T., Frock, R.L., Mounkes, L., Barbie, D.A., Stewart, C.L., Harlow, E., Kennedy, B.K. (2004). A-type lamins regulate retinoblastoma protein function by promoting subnuclear localisation and preventing proteasomal degradation. Proc Natl Acad Sci USA. *101*, 9677-82.
206. Johnson, F.B., Marciniak, R. A., Guarente, L. (1998). Telomeres, the nucleolus and aging. Curr Opin Cell Biol *10*, 332-338.
207. Kaiser, B.K., Zimmerman, Z.A., Charbonneau, H., Jackson, P.K. (2002). Disruption of centrosome structure, chromosome segregation, and cytokinesis by misexpression of human Cdc14A phosphatase. Mol Biol Cell *13*, 2289-2300.
208. Kamei T., Jones, S.R., Chapman, B.M., McGonigle, K.L., Dai, G., Soares, M.J. (2002). The phosphatidylinositol 3-kinase/Akt signalling pathway modulates the endocrine differentiation of trophoblast cells. Mol Endocrinol *16*, 1469-81.
209. Kamei, T., Hamlin, G.P., Chapman, B.M., Burkhardt, A.L., Bolen, J.B., Soares, M.J. (1997). Signalling pathways controlling trophoblast cell differentiation: Src family protein tyrosine kinases in the rat. Biol Reprod *57*, 1302-11.

210. Kanai-Azuma, M., Kanai Y., Matsuda, H., Kurohmaru, M., Tachi, C., Yazaki, K., Hayashi, Y. (1997). Nerve growth factor promotes giant-cell transformation of mouse trophoblast cells in vitro. Biochem Biophys Res Commun *231*, 309-15.
211. Kaneda, A., Kaminishi, M., Yanagihara, K., Sugimura, T., Ushijima, T. (2002). Identification of silencing of nine genes in human gastric cancers. Cancer Res *62*, 6645-6650.
212. Karpen, G.H., Schaefer, J.E., Laird, C.D. (1988). A Drosophila rRNA gene located in euchromatin is active in transcription and nucleolus formation. Genes Dev *2*, 1745-63.
213. Kellogg, D.R., Kikuchi, A., Fujii-Nakata, T., Turck, C.W., Murray, A.W. (1995). Members of the NAP/SET family of proteins interact specifically with B-type cyclins. J Cell Biol *130*, 661-673.
214. Kelly, R.G., Buckingham, M.E. (2002). The anterior heart-forming field: voyage to the arterial pole of the heart. Trends Genet *18*, 210-6.
215. Khurts, S., Masutomi, K., Delgermaa, L., Arai, K., Oishi, N., Mizuno, H., Hayashi, N., Hahn, W.C., Murakami, S. (2004). Nucleolin interacts with telomerase. J Biol Chem *279*, 51508-15.
216. Kim, S.A., Yoon, J.H., Lee, S.H., Ahn, S.G. (2005). Polo-like kinase 1 phosphorylates heat shock transcription factor 1 and mediates its nuclear translocation during heat stress. J Biol Chem *280*, 12653-12657.
217. Kirby, M.L., Waldo, K.L. (1995). Neural crest and cardiovascular patterning. Circ Res *77*, 211-5.
218. Klaffky, E., Williams, R., Yao, C.C., Ziober, B., Kramer, R., Sutherland, A. (2001). Trophoblast-specific expression and function of the integrin alpha 7 subunit in the peri-implantation mouse embryo. Dev Biol *239*, 161-75.
219. Kleylein-Sohn, J., Westendorf, J., Le Clech, M., Habedanck, R., Stierhof, Y.D., Nigg, E.A. (2007). Plk4-induced centriole biogenesis in human cells. Dev Cell *13*, 190-202.
220. Knofler, M., Meinhardt, G., Bauer, S., Loregger, T., Vasicek, R., Bloor, D.J., Kimber, S.J., Husslein, P. (2002). Human Hand1 basic helix-loop-helix (bHLH) protein: extra-embryonic expression pattern, interaction partners and identification of its transcriptional repressor domains. Biochem J *361*, 641-51.
221. Knofler, M., Meinhardt, G., Vasicek, R., Husslein, P., Egarter, C. (1998). Molecular cloning of the human Hand1 gene/cDNA and its tissue-restricted expression in cytotrophoblastic cells and heart. Gene *224*, 77-86.
222. Ko, M.A., Rosario, C.O., Hudson, J.W., Kulkarni, S., Pollett, A., Dennis, J.W., Swallow, C.J. (2005). Plk4 haploinsufficiency causes mitotic infidelity and carcinogenesis. Nat Genet *37*, 883-888.
223. Kohn, M.J., Bronson, R.T., Harlow, E., Dyson, N.J., Yamasaki, L. (2003). Dp1 is required for extra-embryonic development. Development *130*, 1295-305.
224. Kolsch, V., Paululat, A. (2002). The highly conserved cardiogenic bHLH factor Hand is specifically expressed in circular visceral muscle progenitor cells and in all cell types of the dorsal vessel during Drosophila embryogenesis. Dev Genes Evol *212*, 473-85.
225. Komatsu, D., Abe, T., Sano, Y., Shimazaki, K., Tomita, M., Kanayama, N., Takahashi, K. (2007). Increase of the trophoblast giant cells with prolactin-releasing peptide (PrRP) receptor expression in p53-null mice. Mol Reprod Dev *74*, 1089-94.
226. Kong, Y., Shelton, J.M., Rothermel, B., Li, X., Richardson, J.A., Bassel-Duby,

R., Williams, R.S. (2001). Cardiac-specific LIM protein FHL2 modifies the hypertrophic response to beta-adrenergic stimulation Circulation. *103*, 2731-8.

227. Kotani, S., Tugendreich, S., Fujii, M., Jorgensen, P.M., Watanabe, N., Hoog, C., Hieter, P., Todokoro, K. (1998). PKA and MPF-activated polo-like kinase regulate anaphase-promoting complex activity and mitosis progression. Mol Cell *1*, 371-380.
228. Kozak, K.R., Abbott, B., Hankinson, O. (1997). ARNT-deficient mice and placental differentiation. Dev Biol *191*, 297-305.
229. Kramer, E.R., Scheuringer, N., Podtelejnikov, A.V., Mann, M., Peters, J.M. (2000). Mitotic regulation of the APC activator proteins CDC20 and CDH1. Mol Biol Cell *11*, 1555-69.
230. Kraut, N., Snider, L., Chen, C.M., Tapscott, S.J., Groudine, M. (1998). Requirement of the mouse I-mfa gene for placental development and skeletal patterning. EMBO J *17*, 6276-6288.
231. Kuhn, A., Vente, A., Doree, M., Grummt, I. (1998). Mitotic phosphorylation of the TBP-containing factor SL1 represses ribosomal gene transcription. J Mol Biol *284*, 1-5.
232. Kunath, T., Gish, G., Lickert, H., Jones, N., Pawson, T., Rossant, J. (2003). Transgenic RNA interference in ES cell-derived embryos recapitulates a genetic null phenotype. Nat Biotechnol. *21*, 559-61.
233. Kurki, S., Peltonen, K., Latonen, L., Kiviharju, T.M., Ojala, P.M., Meek, D., Laiho, M. (2004). Nucleolar protein NPM interacts with HDM2 and protects tumor suppressor protein p53 from HDM2-mediated degradation. Cancer Cell *5*, 465-75.
234. Kuroda, T.S., Maita, H., Tabata, T., Taira, T., Kitaura, H., Ariga, H., Iguchi-Ariga, S.M. (2004). A novel nucleolar protein, PAPA-1, induces growth arrest as a result of cell cycle arrest at the G1 phase. Gene *340*, 83-98.
235. Kusano, S., Raab-Traub, N. (2002). I-mfa domain proteins interact with Axin and affect its regulation of the Wnt and c-Jun N-terminal kinase signalling pathways. Mol Cell Biol *22*, 6393-6405.
236. Lam MH, Thomas RJ, Martin TJ, Gillespie MT, Jans DA. (2000). Nuclear and nucleolar localisation of parathyroid hormone-related protein. Immunol Cell Biol *78*, 395-402.
237. Lash, G.E., Hornbuckle, J., Brunt, A., Kirkley, M., Searle, R.F., Robson, S.C., Bulmer, J.N. (2007). Effect of low oxygen concentrations on trophoblast-like cell line invasion. Placenta *28*, 390-8.
238. Lee, Y.D., Elledge, S.J. (2006). Control of ribonucleotide reductase localisation through an anchoring mechanism involving Wtm1. Genes Dev *20*, 334-44.
239. Lemercier, C., To, R.Q., Carrasco, R.A., Konieczny, S.F. (1998). The basic helix-loop-helix transcription factor Mist1 functions as a transcriptional repressor of myoD. EMBO J *17*, 1412-22.
240. Lenormand, J.L., Benayoun, B., Guillier, M., Vandromme, M., Leibovitch, M.P., Leibovitchm S.A. (1997). Mos activates myogenic differentiation by promoting heterodimerisation of MyoD and E12 proteins. Mol Cell Biol *17*, 584-93.
241. Leung, A.K., Andersen, J.S., Mann, M., Lamond, A.I. (2003). Bioinformatic analysis of the nucleolus. Biochem J *376*, 553-69.
242. Leung, A.K., Gerlich, D., Miller, G., Lyon, C., Lam, Y.W., Lleres, D., Daigle, N., Zomerdijk, J., Ellenberg, J., Lamond, A.I. (2004). Quantitative kinetic

analysis of nucleolar breakdown and reassembly during mitosis in live human cells. J. Cell Biol. *166*, 787-800.

243. Leung, A.K., Lamond, A.I. (2002). In vivo analysis of NHPX reveals a novel nucleolar localisation pathway involving a transient accumulation in splicing speckles. J Cell Biol *157*, 615-29.
244. Leung, A.K., Trinkle-Mulcahy, L., Lam, Y.W., Andersen, J.S., Mann, M., Lamond, A.I. (2006). NOPdb: Nucleolar Proteome Database. Nucleic Acids Res *34*, 218-20.
245. Leung, G.C., Ho, C.S., Blasutig, I.M., Murphy, J.M., Sicheri, F. (2007). Determination of the Plk4/Sak consensus phosphorylation motif using peptide spots arrays. FEBS Lett *581*, 77-83.
246. Leung, G.C., Hudson, J.W., Kozarova, A., Davidson, A., Dennis, J.W., Sicheri, F. (2002). The Sak polo-box comprises a structural domain sufficient for mitotic subcellular localisation. Nat Struct Biol *9*, 719-24.
247. Lewis, A.L., Xia, Y., Datta, S.K., McMillin, J., Kellems, R.E. (1999). Combinatorial interactions regulate cardiac expression of the murine adenylosuccinate synthetase 1 gene. J Biol Chem *274*, 14188-97.
248. Li, J., Tan, M., Li, L., Pamarthy, D., Lawrence, T.S., Sun, Y. (2005). SAK, a new polo-like kinase, is transcriptionally repressed by p53 and induces apoptosis upon RNAi silencing. Neoplasia *7*, 312-23.
249. Li, L., Heller-Harrison, R., Czech, M., Olson, E.N. (1992). Cyclic AMP-dependent protein kinase inhibits the activity of myogenic helix-loop-helix proteins. Mol Cell Biol *12*, 4478-85.
250. Librach CL, Werb Z, Fitzgerald ML, Chiu K, Corwin NM, Esteves RA, Grobelny D, Galardy R, Damsky CH, Fisher SJ. (1991). 92-kD type IV collagenase mediates invasion of human cytotrophoblasts. J Cell Biol. *113*, 437-49.
251. Licht, J.D., Grossel, M.J., Figge, J., Hansen, U.M. (1990). Drosophila Kruppel protein is a transcriptional repressor. Nature *346*, 76-9.
252. Lin, D.Y., Shih, H.M. (2002). Essential role of the 58-kDa microspherule protein in the modulation of Daxx-dependent transcriptional repression as revealed by nucleolar sequestration. J Biol Chem *277*, 25446-56.
253. Linask, K.K., Yu, X., Chen, Y., Han, M.D. (2002). Directionality of heart looping: effects of Pitx2c misexpression on flectin asymmetry and midline structures. Dev Biol *246*, 407-17.
254. Lindstrom, M.S., Klangby, U., Inoue, R., Pisa, P., Wiman, K.G., Asker, C.E. (2000). Immunolocalisation of human p14(ARF) to the granular component of the interphase nucleolus. Exp Cell Res *256*, 400-10.
255. Lints TJ, Parsons LM, Hartley L, Lyons I, Harvey RP. (1993). Nkx-2.5: a novel murine homeobox gene expressed in early heart progenitor cells and their myogenic descendants Development *119*, 419-31.
256. Lints, T.J., Parsons, L.M., Hartley, L., Lyons, I., Harvey, R.P. (1993). Nkx-2.5: a novel murine homeobox gene expressed in early heart progenitor cells and their myogenic descendants. Development *119*, 419-31.
257. Llanos, S., Clark, P.A., Rowe, J., Peters, G. (2001). Stabilisation of p53 by p14ARF without relocation of MDM2 to the nucleolus. Nat Cell Biol *3*, 445-52.
258. Lohrum, M.A., Ashcroft, M., Kubbutat, M.H., Vousden, K.H. (2000). Contribution of two independent MDM2-binding domains in p14(ARF) to p53 stabilisation. Curr Biol *10*, 539-42.

259. Lorca, T., Castro, A., Martinez, A.M., Vigneron, S., Morin, N., Sigrist, S., Lehner, C., Doree, M., Labbe, J.C. (1998). Fizzy is required for activation of the APC/cyclosome in Xenopus egg extracts. EMBO J *17*, 3565-75.
260. Loregger, T., Pollheimer, J., Knofler, M. (2003). Regulatory transcription factors controlling function and differentiation of human trophoblast--a review. Placenta *24*, 104-10.
261. Lorenzen, J.A., Bonacci, B.B., Palmer, R.E., Wells, C., Zhang, J., Haber, D.A., Goldstein, A.M., Mayer, A.N. (2005). Rbm19 is a nucleolar protein expressed in crypt/progenitor cells of the intestinal epithelium. Gene Expr Patterns *6*, 45-56.
262. Louvet, E., Junéra, H.R., Berthuy, I., Hernandez-Verdun, D. (2006). Compartmentation of the nucleolar processing proteins in the granular component is a CK2-driven process. Mol Biol Cell. *17*, 2537-46.
263. Lowery, D.M., Lim, D., Yaffe, M.B. (2005). Structure and function of Polo-like kinases. Oncogene *24*, 248-59.
264. Lowery, D.M., Mohammad, D.H., Elia, A.E., Yaffe, M.B. (2004). The Polo-box domain: a molecular integrator of mitotic kinase cascades and Polo-like kinase function. Cell Cycle *3*, 128-31.
265. Lundin, L.G. (1993). Evolution of the vertebrate genome as reflected in paralogous chromosomal regions in man and the house mouse. Genomics *16*, 1-19.
266. Luo, J., Sladek, R., Bader, J.A., Matthyssen, A., Rossant, J., Giguere, V. (1997). Placental abnormalities in mouse embryos lacking the orphan nuclear receptor ERR-beta. Nature *388*, 778-82.
267. Lyons I, Parsons LM, Hartley L, Li R, Andrews JE, Robb L, Harvey RP. (1995). Myogenic and morphogenetic defects in the heart tubes of murine embryos lacking the homeo box gene Nkx2-5. Genes Dev *9*, 1654-66.
268. Ma Q, Sommer L, Cserjesi P, Anderson DJ. (1997). Mash1 and neurogenin1 expression patterns define complementary domains of neuroepithelium in the developing CNS and are correlated with regions expressing notch ligands. J Neurosci *17*, 3644-52.
269. Ma, G.T., Linzer, D.I. (2000). GATA-2 restricts prolactin-like protein A expression to secondary trophoblast giant cells in the mouse. Biol Reprod *63*, 570-4.
270. Ma, G.T., Soloveva, V., Tzeng, S.J., Lowe, L.A., Pfendler, K.C., Iannaccone, P.M., Kuehn, M.R., Linzer, D.I. (2001). Nodal regulates trophoblast differentiation and placental development. Dev Biol *236*, 124-35.
271. MacAuley, A., Cross, J.C., Werb, Z. (1998). Reprogramming the cell cycle for endoreduplication in rodent trophoblast cells. Mol Biol Cell *9*, 795-807.
272. Macmillan, J.C., Hudson, J.W., Bull, S., Dennis, J.W., Swallow, C.J. (2001). Comparative expression of the mitotic regulators SAK and PLK in colorectal cancer. Ann Surg Oncol *8*, 729-40.
273. Maeda, Y., Hisatake, K., Kondo, T., Hanada, K., Song, C.Z., Nishimura, T., Muramatsu, M. (1992). Mouse rRNA gene transcription factor mUBF requires both HMG-box1 and an acidic tail for nucleolar accumulation: molecular analysis of the nucleolar targeting mechanism. EMBO J *11*, 3695-704.
274. Mailand, N., Lukas, C., Kaiser, B.K., Jackson, P.K., Bartek, J., Lukas, J. (2002). Deregulated human Cdc14A phosphatase disrupts centrosome separation and chromosome segregation. Nat Cell Biol *4*, 317-322.
275. Maines, J.Z., Stevens, L.M., Tong, X., Stein, D. (2004). Drosophila dMyc is

required for ovary cell growth and endoreduplication. Development *131*, 775-786.
276. Malassine, A., Frendo, J.L., Evain-Brion, D. (2003). A comparison of placental development and endocrine functions between the human and mouse model. Hum Reprod Update *9*, 531-539.
277. Maltsev, V.A., Rohwedel, J., Hescheler, J., Wobus, A.M. (1993). Embryonic stem cells differentiate in vitro into cardiomyocytes representing sinusnodal, atrial and ventricular cell types. Mech Dev *44*, 41-50.
278. Markus, M., Benezra, R. (1999). Two isoforms of protein disulfide isomerase alter the dimerisation status of E2A proteins by a redox mechanism. J Biol Chem *274*, 1040-9.
279. Massari, M.E., Murre, C. (2000). Helix-loop-helix proteins: regulators of transcription in eucaryotic organisms. Mol Cell Biol *20*, 429-40.
280. Mathies, L.D., Henderson, S.T., Kimble, J. (2003). The C. elegans Hand gene controls embryogenesis and early gonadogenesis. Development *130*, 2881-92.
281. Mattsson, K., Pokrovskaja, K., Kiss, C., Klein, G., Szekely, L. (2001). Proteins associated with the promyelocytic leukemia gene product (PML)-containing nuclear body move to the nucleolus upon inhibition of proteasome-dependent protein degradation. Proc Natl Acad Sci USA. *98*, 1012-7.
282. May KM, Reynolds N, Cullen CF, Yanagida M, Ohkura H. (2002). Polo boxes and Cut23 (Apc8) mediate an interaction between polo kinase and the anaphase-promoting complex for fission yeast mitosis. J Cell Biol *156*, 23-28.
283. Mayer, C., Bierhoff, H., Grummt, I. (2005). The nucleolus as a stress sensor: JNK2 inactivates the transcription factor TIF-IA and down-regulates rRNA synthesis. Genes Dev *19*, 933-41.
284. McFadden, D.G., Barbosa, A.C., Richardson, J.A., Schneider, M.D., Srivastava, D., Olson, E.N. (2005). The Hand1 and Hand2 transcription factors regulate expansion of the embryonic cardiac ventricles in a gene dosage-dependent manner. Development *132*, 189-201.
285. McFadden, D.G., Charite, J., Richardson, J.A., Srivastava, D., Firulli, A.B., Olson, E.N. (2000). A GATA-dependent right ventricular enhancer controls dHAND transcription in the developing heart. Development *127*, 5331-41.
286. McFadden, D.G., McAnally, J., Richardson, J.A., Charite, J., Olson, E.N. (2002). Misexpression of dHAND induces ectopic digits in the developing limb bud in the absence of direct DNA binding. Development *129*, 3077-88.
287. Mehta, D.V., Kim, Y.S., Dixon, D., Jetten, A.M. (2002). Characterisation of the expression of the retinoid-related, testis-associated receptor (RTR) in trophoblasts. Placenta. *23*, 281-7.
288. Meilhac, S.M., Esner, M., Kelly, R.G., Nicolas, J.F., Buckingham, M.E. (2004). The clonal origin of myocardial cells in different regions of the embryonic mouse heart. Dev Cell. 2004 May;6(5):685-98.
289. Meinhardt, G., Husslein, P., Knofler, M. (2005). Tissue-specific and ubiquitous basic helix-loop-helix transcription factors in human placental trophoblasts. Placenta *26*, 527-539.
290. Mekhail, K., Gunaratnam, L., Bonicalzi, M.E., Lee, S. (2004). HIF activation by pH-dependent nucleolar sequestration of VHL. Nat Cell Biol *6*, 642-7.
291. Melese, T., Xue, Z. (1995). The nucleolus: an organelle formed by the act of building a ribosome. Curr Opin Cell Biol *7*, 319-24.
292. Minekawa, R., Sakata, M., Okamoto, Y., Hayashi, M., Isobe, A., Takeda, T., Yamamoto, T., Koyama, M., Ohmichi, M., Tasaka, K., Imai, K., Okamoto, T.,

Murata, Y. (2007). Involvement of RelA-associated inhibitor in regulation of trophoblast differentiation via interaction with transcriptional factor specificity protein-1. Endocrinology. *148*, 5803-10.

293. Mitsui, K., Tokuzawa, Y., Itoh, H., Segawa, K., Murakami, M., Takahashi, K., Maruyama, M., Maeda, M., Yamanaka, S. (2003). The homeoprotein Nanog is required for maintenance of pluripotency in mouse epiblast and ES cells. Cell. *113*, 631-42.
294. Mizutani, T., Yamada, K., Yazawa, T., Okada, T., Minegishi, T., Miyamoto, K. (2001). Cloning and characterisation of gonadotropin-inducible ovarian transcription factors (GIOT1 and -2) that are novel members of the (Cys)(2)-(His)(2)-type zinc finger protein family. Mol Endocrinol *15*, 1693-705.
295. Mohun, T.J., Leong, L.M., Weninger, W.J., Sparrow, D.B. (2000). The morphology of heart development in Xenopus laevis. Dev Biol *218*, 74-88.
296. Monkley, S.J., Delaney, S.J., Pennisi, D.J., Christiansen, J.H., Wainwright, B.J. (1996). Targeted disruption of the Wnt2 gene results in placentation defects. Development *122*, 3343-53.
297. Morikawa, Y., Cserjesi, P. (2004). Extra-embryonic vasculature development is regulated by the transcription factor HAND1. Development *131*, 2195-204.
298. Morin, S., Pozzulo, G., Robitaille, L., Cross, J., Nemer, M. (2005). MEF2-dependent recruitment of the HAND1 transcription factor results in synergistic activation of target promoters. J Biol Chem *280*, 32272-8.
299. Morris Buus, R., Boockfor, F.R. (2004). Transferrin expression by placental trophoblastic cells. Placenta. *25*, 45-52.
300. Moshe, Y., Boulaire, J., Pagano, M., Hershko, A. (2004). Role of Polo-like kinase in the degradation of early mitotic inhibitor 1, a regulator of the anaphase promoting complex/cyclosome. Proc Natl Acad Sci USA *101*, 7937-7942.
301. Munro, S., Pelham, H.R. (1984). Use of peptide tagging to detect proteins expressed from cloned genes: deletion mapping functional domains of Drosophila hsp 70. EMBO J *3*, 3087-93.
302. Nadra, K., Anghel, S.I., Joye, E., Tan, N.S., Basu-Modak, S., Trono, D., Wahli, W., Desvergne, B. (2006). Differentiation of trophoblast giant cells and their metabolic functions are dependent on peroxisome proliferator-activated receptor beta/delta. Mol Cell Biol *26*, 3266-81.
303. Nakayama, H., Scott, I.C., Cross, J.C. (1998). The transition to endoreduplication in trophoblast giant cells is regulated by the mSNA zinc finger transcription factor. Dev Biol *199*, 150-163.
304. Natarajan, A., Yamagishi, H., Ahmad, F., Li, D., Roberts, R., Matsuoka, R., Hill, S., Srivastava, D. (2001). Human eHAND, but not dHAND, is down-regulated in cardiomyopathies. J Mol Cell Cardiol *33*, 1607-14.
305. Naya, F.J., Wu, C., Richardson, J.A., Overbeek, P., Olson, E.N. (1999). Transcriptional activity of MEF2 during mouse embryogenesis monitored with a MEF2-dependent transgene. Development *126*, 2045-52.
306. Negi, S.S., Olson, M.O. (2006). Effects of interphase and mitotic phosphorylation on the mobility and location of nucleolar protein B23. J Cell Sci *119*, 3676-3685.
307. Ng, Y.K., George, K.M., Engel, J.D., Linzer, D.I. (1994). GATA factor activity is required for the trophoblast-specific transcriptional regulation of the mouse placental lactogen I gene. Development *120*, 3257-66.
308. Nichols, J., Zevnik, B., Anastassiadis, K., Niwa, H., Klewe-Nebenius, D.,

Chambers, I., Scholer, H., Smith, A. (1998). Formation of pluripotent stem cells in the mammalian embryo depends on the POU transcription factor Oct4. Cell *95*, 379-91.

309. Nie, G., Li, Y., Salamonsen, L.A. (2005). Serine protease HtrA1 is developmentally regulated in trophoblast and uterine decidual cells during placental formation in the mouse. Dev Dyn *233*, 1102-9.
310. Nieder, G.L., Jennes, L. (1990). Production of mouse placental lactogen-I by trophoblast giant cells in utero and in vitro. Endocrinology *126*, 2809-14.
311. Novak, D., Quiggle, F., Matthews, J. (2004). Androgen secretion by Rcho-1 cells is independent of extracellular glutamate concentration. Placenta *25*, 548-52.
312. Oakes, M., Aris, J.P., Brockenbrough, J.S., Wai, H., Vu, L., Nomura, M. (1998). Mutational analysis of the structure and localisation of the nucleolus in the yeast Saccharomyces cerevisiae. J Cell Biol *143*, 23-34.
313. Oda, M., Sun, W., Hattori, N., Tanaka, S., Shiota, K. (2001). PAL31 expression in rat trophoblast giant cells. Biochem Biophys Res Commun. *287*, 721-6.
314. Olson, E.N., Srivastava, D. (1996). Molecular pathways controlling heart development. Science *272*, 671-6.
315. Olson, M.O. (2004). Sensing cellular stress: another new function for the nucleolus? Sci STKE *224*, 10.
316. Olson, M.O., Dundr, M. (2005). The moving parts of the nucleolus. Histochem Cell Biol *123*, 203-16.
317. Olson, M.O.J., Dundr, M., Szebeni, A. (2000). The nucleolus: an old factory with unexpected capabilities. Trends Cell Biol *10*, 189-196.
318. Osborne, C.S., Chakalova, L., Brown, K.E., Carter, D., Horton, A., Debrand, E., Goyenechea, B., Mitchell, J.A., Lopes, S., Reik, W., Fraser, P. (2004). Active genes dynamically colocalise to shared sites of ongoing transcription. Nat Genet *36*, 1065-1071.
319. Ozturk, A., Donald, L.J., Li, L., Duckworth, H.W., Duckworth, M.L. (2006). Proteomic identification of AP2 gamma as a rat placental lactogen II trophoblast cell-specific enhancer binding protein. Endocrinology *147*, 4319-29.
320. Palazon, L.S., Davies, T.J., Gardner, R.L. (1998). Translational inhibition of cyclin B1 and appearance of cyclin D1 very early in the differentiation of mouse trophoblast giant cells. Mol Hum Reprod *4*, 1013-1020.
321. Parast, M.M., Aeder, S., Sutherland, A.E. (2001). Trophoblast giant-cell differentiation involves changes in cytoskeleton and cell motility. Dev Biol *230*, 43-60.
322. Parast, M.M., Otey, C.A. (2000). Characterisation of palladin, a novel protein localised to stress fibers and cell adhesions. J Cell Biol *150*, 643-56.
323. Parisi, T., Beck, A.R., Rougier, N., McNeil, T., Lucian, L., Werb, Z., Amati, B. (2003). Cyclins E1 and E2 are required for endoreplication in placental trophoblast giant cells. EMBO J *22*, 4794-803.
324. Pasumarthi, K.B., Nakajima, H., Nakajima, H.O., Soonpaa, M.H., Field, L.J. (2005). Targeted expression of cyclin D2 results in cardiomyocyte DNA synthesis and infarct regression in transgenic mice. Circ Res. *96*, 110-8.
325. Payne, C.T., Zhang, F., Lloyd, A.M. (2000). GL3 encodes a bHLH protein that regulates trichome development in Arabidopsis through interaction with GL1 and TTG1. Genetics *159*, 1349-1362.

326. Pederson T. (1998). Growth factors in the nucleolus? Cell Biol *143*, 279-81.
327. Pederson, T. (1998). The plurifunctional nucleolus. Nucleic Acids Res *26*, 3871-3786.
328. Pederson, T., Politz, J.C. (2000). The nucleolus and the four ribonucleoproteins of translation. J Cell Biol *148*, 1091-5.
329. Peled, A., Schwartz, D., Elkind, N.B., Wolkowicz, R., Li, R., Rotter, V. (1996). The role of p53 in the induction of polyploidity of myelomonocytic leukemic M1/2 cells. Oncogene *13*, 1677-85.
330. Pendle, A.F., Clark, G.P., Boon, R., Lewandowska, D., Lam, Y.W., Andersen, J., Mann, M., Lamond, A.I., Brown, J.W., Shaw, P.J. (2005). Proteomic analysis of the Arabidopsis nucleolus suggests novel nucleolar functions. Mol Biol Cell *16*, 260-9.
331. Perry, R.P. (1966). Nucleolus: Structure and Function. Science. *153*, 214-219.
332. Peters, T.J., Albieri, A., Bevilacqua, E., Chapman, B.M., Crane, L.H., Hamlin, G.P., Seiki, M., Soares, M.J. (1999). Differentiation-dependent expression of gelatinase B/matrix metalloproteinase-9 in trophoblast cells. Cell Tissue Res *295*, 287-96.
333. Phair, R.D., Misteli, T. (2000). High mobility of proteins in the mammalian cell nucleus. Nature *404*, 604-9.
334. Politz, J.C., Polena, I., Trask, I., Bazett-Jones, D.P., Pederson, T. (2005). A nonribosomal landscape in the nucleolus revealed by the stem cell protein nucleostemin. Mol Biol Cell *16*, 3401-10.
335. Politz, J.C., Yarovoi, S., Kilroy, S.M., Gowda, K., Zwieb, C., Pederson, T. (2000). Signal recognition particle components in the nucleolus. Proc Natl Acad Sci USA. *97*, 55-60.
336. Pontes, O., Li, C.F., Nunes, P.C., Haag, J., Ream, T., Vitins, A., Jacobsen, S.E., Pikaard, C.S. (2006). The Arabidopsis chromatin-modifying nuclear siRNA pathway involves a nucleolar RNA processing center. Cell *126*, 79-92.
337. Queralt, E., Lehane, C., Novak, B., Uhlmann, F. (2006). Downregulation of PP2A(Cdc55) phosphatase by separase initiates mitotic exit in budding yeast. Cell *125*, 719-732.
338. Rao, M.R., Kumari, G., Balasundaram, D., Sankaranarayanan, R., Mahalingam, S. (2006). A novel lysine-rich domain and GTP binding motifs regulate the nucleolar retention of human guanine nucleotide binding protein, GNL3L. J Mol Biol *364*, 637-54.
339. Raska, I., Shaw, P.J., Cmarko, D. (2006). Structure and function of the nucleolus in the spotlight. Curr Opin Cell Biol *18*, 325-34.
340. Rebstock, S., Lucas, K., Weiss, M., Thompson, J., Zimmermann, W. (1993). Spatiotemporal expression of pregnancy-specific glycoprotein gene rnCGM1 in rat placenta. Dev Dyn *198*, 171-81.
341. Redman, C.W., Sargent, I.L. (2005). Latest advances in understanding preeclampsia. Science *308*, 1592-4.
342. Reimers, K., Antoine, M., Zapatka, M., Blecken, V., Dickson, C., Kiefer, P. (2001). NoBP, a nuclear fibroblast growth factor 3 binding protein, is cell cycle regulated and promotes cell growth. Mol Cell Biol *21*, 4996-5007.
343. Reuss, B., Hellmann, P., Dahl, E., Traub, O., Butterweck, A., Grummer, R., Winterhager, E. (1996). Connexins and E-cadherin are differentially expressed during trophoblast invasion and placenta differentiation in the rat. Dev Dyn *205*, 172-82.
344. Riley, P., Anson-Cartwright, L., Cross, J.C. (1998). The Hand1 bHLH

transcription factor is essential for placentation and cardiac morphogenesis. Nat Genet *18*, 271-5.
345. Riley, P.R., Gertsenstein, M., Dawson, K., Cross, J.C. (2000). Early exclusion of hand1-deficient cells from distinct regions of the left ventricular myocardium in chimeric mouse embryos. Dev Biol *227*, 156-168.
346. Rinkenberger J, Werb Z. (2000). The labyrinthine placenta. Nat Genet *25*, 248-50.
347. Risebro CA, Riley PR. (2006). Formation of the ventricles. ScientificWorldJournal *6*, 1862-80.
348. Risebro, C.A., Smart, N., Dupays, L., Breckenridge, R., Mohun, T.J., Riley, P.R. (2006). Hand1 regulates cardiomyocyte proliferation versus differentiation in the developing heart. Development *133*, 4595-606.
349. Roark M, Sturtevant MA, Emery J, Vaessin H, Grell E, Bier E. (1995). scratch, a pan-neural gene encoding a zinc finger protein related to snail, promotes neuronal development. Genes Dev *9*, 2384-98.
350. Rodesch, F., Simon, P., Donner, C., Jauniaux, E. (1992). Oxygen measurements in endometrial and trophoblastic tissues during early pregnancy. Obstet Gynecol *80*, 283-5.
351. Rodriguez, T.A., Sparrow, D.B., Scott, A.N., Withington, S.L., Preis, J.I., Michalicek, J., Clements, M., Tsang, T.E., Shioda, T., Beddington, R.S., Dunwoodie, S.L. (2004). Cited1 is required in trophoblasts for placental development and for embryo growth and survival.
352. Rossant, J., Cross, J.C. (2001). Placental development: lessons from mouse mutants. Nat Rev Genet *2*, 538-548.
353. Roth I, Corry DB, Locksley RM, Abrams JS, Litton MJ, Fisher SJ. (1996). Human placental cytotrophoblasts produce the immunosuppressive cytokine interleukin 10. J Exp Med *184*, 539-48.
354. Rubbi, C.P., Milner, J. (2003). Disruption of the nucleolus mediates stabilisation of p53 in response to DNA damage and other stresses. EMBO J *22*, 6068-77.
355. Russ, A.P., Wattler, S., Colledge, W.H., Aparicio, S.A., Carlton, M.B., Pearce, J.J., Barton, S.C., Surani, M.A., Ryan, K., Nehls, M.C., Wilson, V., Evans, M.J. (2005). Eomesodermin is required for mouse trophoblast development and mesoderm formation. Nature *404*, 95-9.
356. Russell MW, Baker P, Izumo S. (1997). Cloning, chromosomal mapping, and expression of the human eHAND gene. Mamm Genome. *8*, 863-5.
357. Sahgal N, Canham LN, Konno T, Wolfe MW, Soares MJ. (2005). Modulation of trophoblast stem cell and giant cell phenotypes: analyses using the Rcho-1 cell model. Differentiation *73*, 452-62.
358. Sahgal, N., Canham, L.N., Canham, B., Soares, M.J. (2006). Rcho-1 trophoblast stem cells: a model system for studying trophoblast cell differentiation. Methods Mol Med *121*,159-178.
359. Sanders, J.A., Gruppuso, P.A. (2005). Nucleolar localisation of hepatic c-Myc: a potential mechanism for c-Myc regulation. Biochim Biophys Acta *1743*, 141-50.
360. Sansam, C.L., Wells, K.S., Emeson, R.B. (2003). Modulation of RNA editing by functional nucleolar sequestration of ADAR2. Proc Natl Acad Sci USA *100*, 14018-23.
361. San-Segundo, P.A., Roeder, G.S. (1999). Pch2 links chromatin silencing to meiotic checkpoint control. Cell *97*, 313-24.

362. Sato, S., Yano, H., Makimoto, Y., Kaneta, T., Sato, Y. (2005). Nucleolonema as a fundamental substructure of the nucleolus. J Plant Res *118*, 71-81.
363. Sato, T.N., Tozawa, Y., Deutsch, U., Wolburg-Buchholz, K., Fujiwara, Y., Gendron-Maguire, M., Gridley, T., Wolburg, H., Risau, W., Qin, Y. (1995). Distinct roles of the receptor tyrosine kinases Tie-1 and Tie-2 in blood vessel formation. Nature *376*, 70-4.
364. Sauer, K., Knoblich, J.A., Richardson, H., Lehner, C.F. (1995). Distinct modes of cyclin E/cdc2c kinase regulation and S-phase control in mitotic and endoreduplication cycles of Drosophila embryogenesis Genes Dev *5*, 1327-1339.
365. Savino, T.M., Gebrane-Younes, J., De Mey, J., Sibarita, J.B., Hernandez-Verdun, D. (2001). Nucleolar assembly of the rRNA processing machinery in living cells. J. Cell Biol. 153, 1097-1110.
366. Schaeffer, V., Althauser, C., Shcherbata, H.R., Deng, W.M., Ruohola-Baker, H. (2004). Notch-dependent Fizzy-related/Hec1/Cdh1 expression is required for the mitotic-to-endocycle transition in Drosophila follicle cells. Curr Biol *14*, 630-636.
367. Scheer, U., Hock, R. (1999). Structure and function of the nucleolus. Curr Opin Cell Biol *11*, 385-390.
368. Scherl, A., Coute, Y., Deon, C., Calle, A., Kindbeiter, K., Sanchez, J.C., Greco, A., Hochstrasser, D., Diaz, J.J. (2002). Functional proteomic analysis of human nucleolus. Mol Biol Cell *13*, 4100-4109.
369. Schlosser, I., Hölzel, M., Mürnseer, M., Burtscher, H., Weidle, U.H., Eick, D. (2003). A role for c-Myc in the regulation of ribosomal RNA processing. Nucleic Acids Res *31*, 6148-56.
370. Schmidt-Zachmann, M.S., Nigg, E.A. (1993). Protein localisation to the nucleolus: a search for targeting domains in nucleolin. J Cell Sci *105*, 799-806.
371. Schneiter, R., Kadowaki, T., Tartakoff, A.M. (1995). mRNA transport in yeast: time to reinvestigate the functions of the nucleolus. Mol Biol Cell *6*, 357-70.
372. Schnittger, A., Schobinger, U., Stierhof, Y.D., Hulskamp, M. (2002). Ectopic D-type cyclin expression induces mitotic cycles in endoreduplicating Arabidopsis trichomes. Curr Biol *12*, 415-420.
373. Schorpp-Kistner, M., Wang, Z.Q., Angel, P., Wagner, E.F. (1999). JunB is essential for mammalian placentation. EMBO J *18*, 934-48.
374. Schwab, M.S., Dreyer, C. (1997). Protein phosphorylation sites regulate the function of the bipartite NLS of nucleolin. Eur J Cell Biol *73*, 287-97.
375. Scott, I.C., Anson-Cartwright, L., Riley, P., Reda, D., Cross, J.C. (2000). The HAND1 basic helix-loop-helix transcription factor regulates trophoblast differentiation via multiple mechanisms. Mol Cell Biol *20*, 530-41.
376. Scott, M., Boisvert, F.M., Vieyra, D., Johnston, R.N., Bazett-Jones, D.P., Riabowol, K. (2001). UV induces nucleolar translocation of ING1 through two distinct nucleolar targeting sequences. Nucleic Acids Res *29*, 2052-8.
377. Shaw, P.J., Brown, J.W. (2004). Plant nuclear bodies. Curr Opin Plant Biol *7*, 614-20.
378. Sheng Z, Lewis JA, Chirico WJ. (2004). Nuclear and nucleolar localisation of 18-kDa fibroblast growth factor-2 is controlled by C-terminal signals J Biol Chem. *279*, 40153-60.
379. Sheng, Z., Liang, Y., Lin, C.Y., Comai, L., Chirico, W.J. (2005). Direct regulation of rRNA transcription by fibroblast growth factor 2. Mol Cell Biol *25*, 9419-9426.

380. Shi Y, Seto E, Chang LS, Shenk T. (1991). Transcriptional repression by YY1, a human GLI-Krüppel-related protein, and relief of repression by adenovirus E1A protein. Cell *67*, 377-88.
381. Shida, M.M., Ng, Y.K., Soares, M.J., Linzer, D.I. (1993). Trophoblast-specific transcription from the mouse placental lactogen-I gene promoter. Mol Endocrinol *7*, 181-8.
382. Shirayama, M., Zachariae, W., Ciosk, R., Nasmyth, K. (1998). The Polo-like kinase Cdc5p and the WD-repeat protein Cdc20p/fizzy are regulators and substrates of the anaphase promoting complex in Saccharomyces cerevisiae. EMBO J *17*, 1336-49.
383. Shou, W., Azzam, R., Chen, S.L., Huddleston, M.J., Baskerville, C., Charbonneau, H., Annan, R.S., Carr, S.A., Deshaies, R.J. (2002). Cdc5 influences phosphorylation of Net1 and disassembly of the RENT complex. BMC Mol Biol *17*, 3.
384. Shou, W., Seol, J.H., Shevchenko, A., Baskerville, C., Moazed, D., Chen, Z.W., Jang, J., Shevchenko, A., Charbonneau, H., Deshaies, R.J. (1999). Exit from mitosis is triggered by Tem1-dependent release of the protein phosphatase Cdc14 from nucleolar RENT complex. Cell *97*, 233-244.
385. Sibai B, Dekker G, Kupferminc M. (2005). Pre-eclampsia. Lancet *365*, 785-99.
386. Sigrist, S.J., Lehner, C.F. (1997). Drosophila fizzy-related down-regulates mitotic cyclins and is required for cell proliferation arrest and entry into endocycles. Cell *90*, 671-681.
387. Sigvardsson, M., O'Riordan, M., Grosschedl, R. (1997). EBF and E47 collaborate to induce expression of the endogenous immunoglobulin surrogate light chain genes. Immunity *7*, 25-36.
388. Simmons, D.G., Fortier, A.L., Cross, J.C. (2007). Diverse subtypes and developmental origins of trophoblast giant cells in the mouse placenta. Dev Biol *304*, 567-78.
389. Sinclair, D.A., Guarente, L. (1997). Extrachromosomal rDNA circles--a cause of aging in yeast. Cell *91*, 1033-42.
390. Sirri V, Urcuqui-Inchima S, Roussel P, Hernandez-Verdun D. (2008). Nucleolus: the fascinating nuclear body. Histochem Cell Biol *129*, 13-31.
391. Sirri, V., Hernandez-Verdun, D., Roussel, P. (2002). Cyclin-dependent kinases govern formation and maintenance of the nucleolus. J Cell Biol. 156, 969-981.
392. Sleeman, J., Lyon, C.E., Platani, M., Kreivi, J.P., Lamond, A.I. (1998). Dynamic interactions between splicing snRNPs, coiled bodies and nucleoli revealed using snRNP protein fusions to the green fluorescent protein. Exp Cell Res *243*, 290-304.
393. Smart, N., Hill, A.A., Cross, J.C., Riley, P.R. (2002). A differential screen for putative targets of the bHLH transcription factor Hand1 in cardiac morphogenesis. Mech Dev *119*, 65-71.
394. Smart, N., Risebro, C.A., Melville, A.A., Moses, K., Schwartz, R.J., Chien, K.R., Riley, P.R. (2007). Thymosin beta4 induces adult epicardial progenitor mobilisation and neovascularisation. Nature *445*, 177-82.
395. Smith L, Van Hateren N, Willan J, Romero R, Blanco G, Siggers P, Walsh J, Banerjee R, Denny P, Ponting C, Greenfield A. (2003). Candidate testis-determining gene, Maestro (Mro), encodes a novel HEAT repeat protein. Dev Dyn *227*, 600-607.
396. Snider, L., Tapscott, S.J. (2005). XIC is required for Siamois activity and dorsoanterior development. Mol Cell Biol *25*, 5061-5072.

397. Snider, L., Thirlwell, H., Miller, J.R., Moon, R.T., Groudine, M., Tapscott, S.J. (2001). Inhibition of Tcf3 binding by I-mfa domain proteins. Mol Cell Biol *21*, 1866-1873.
398. Solberg, H., Ploug, M., Høyer-Hansen, G., Nielsen, B.S., Lund, L.R. (2001). The murine receptor for urokinase-type plasminogen activator is primarily expressed in tissues actively undergoing remodelling. J Histochem Cytochem *49*, 237-46.
399. Soloveva, V., Linzer, D.I. (2004). Differentiation of placental trophoblast giant cells requires downregulation of p53 and Rb. Placenta *25*, 29-36.
400. Sparrow, D.B., Kotecha, S., Towers, N., Mohun, T.J. (1998). Xenopus eHAND: a marker for the developing cardiovascular system of the embryo that is regulated by bone morphogenetic proteins. Mech Dev *71*, 151-63.
401. Spicer DB, Rhee J, Cheung WL, Lassar AB. (1996). Inhibition of myogenic bHLH and MEF2 transcription factors by the bHLH protein Twist. Science *272*, 1476-80.
402. Srivastava D, Thomas T, Lin Q, Kirby ML, Brown D, Olson EN. (1997). Regulation of cardiac mesodermal and neural crest development by the bHLH transcription factor, dHAND. Nat Genet *16*, 154-60
403. Srivastava, D. (1999). HAND proteins: molecular mediators of cardiac development and congenital heart disease. Trends Cardiovasc Med *9*, 11-8.
404. Srivastava, D., Cserjesi, P., Olson, E.N. (1995). A subclass of bHLH proteins required for cardiac morphogenesis. Science *270*, 1995-9.
405. Srivastava, D., Thomas, T., Lin, Q., Kirby, M.L., Brown, D., Olson, E.N. (1997). Regulation of cardiac mesodermal and neural crest development by the bHLH transcription factor, dHAND. Nat Genet *16*, 154-60.
406. Stark, L.A., Dunlop, M.G. (2005). Nucleolar sequestration of RelA (p65) regulates NF-kappaB-driven transcription and apoptosis. Mol Cell Biol *25*, 5985-6004.
407. Staub, E., Fiziev, P., Rosenthal, A., Hinzmann, B. (2004). Insights into the evolution of the nucleolus by an analysis of its protein domain repertoire. Bioessays *26*, 567-81.
408. Stegh, A.H., Schickling, O., Ehret, A., Scaffidi, C., Peterhansel, C., Hofmann, T.G., Grummt, I., Krammer, P.H., Peter, M.E. (1998). DEDD, a novel death effector domain-containing protein, targeted to the nucleolus. EMBO J *17*, 5974-86.
409. Stegmeier, F., Visintin, R., Amon, A. (2002). Separase, polo kinase, the kinetochore protein Slk19, and Spo12 function in a network that controls Cdc14 localisation during early anaphase. Cell *108*, 207-20.
410. Steidl, C., Leimeister, C., Klamt, B., Maier, M., Nanda, I., Dixon, M., Clarke, R., Schmid, M., Gessler, M. (2000). Characterisation of the human and mouse HEY1, HEY2, and HEYL genes: cloning, mapping, and mutation screening of a new bHLH gene family. Genomics *66*, 195-203.
411. Stewart, C.L., Kaspar, P., Brunet, L.J., Bhatt, H., Gadi, I., Kontgen, F., Abbondanzo, S.J. (1992). Blastocyst implantation depends on maternal expression of leukaemia inhibitory factor. Nature *359*, 76-9.
412. Strumpf, D., Mao, C.A., Yamanaka, Y., Ralston, A., Chawengsaksophak, K., Beck, F., Rossant, J. (2005). Cdx2 is required for correct cell fate specification and differentiation of trophectoderm in the mouse blastocyst. Development *132*, 2093-102.
413. Sudakin, V., Ganoth, D., Dahan, A., Heller, H., Hershko, J., Luca, F.C.,

Ruderman, J.V., Hershko, A. (1995). The cyclosome, a large complex containing cyclin-selective ubiquitin ligase activity, targets cyclins for destruction at the end of mitosis. Mol Biol Cell *6*, 185-197.

414. Sugimoto, M., Kuo, M.L., Roussel, M.F., Sherr, C.J. (2003). Nucleolar Arf tumor suppressor inhibits ribosomal RNA processing. Mol Cell *11*, 415-24.
415. Sullivan, M., Morgan, D.O. (2007). Finishing mitosis, one step at a time. Nat Rev Mol Cell Biol *8*, 894-903.
416. Sun, J., Deng, W.M. (2005). Notch-dependent downregulation of the homeodomain gene cut is required for the mitotic cycle/endocycle switch and cell differentiation in Drosophila follicle cells. Development *132*, 4299-4308.
417. Sun, Y., Duckworth, M.L. (1999). Identification of a placental-specific enhancer in the rat placental lactogen II gene that contains binding sites for members of the Ets and AP-1 (activator protein 1) families of transcription factors. Mol Endocrinol *13*, 385-99.
418. Sutherland, A.E., Calarco, P.G., Damsky, C.H. (1993). Developmental regulation of integrin expression at the time of implantation in the mouse embryo. Development *119*, 1175-86.
419. Swallow, C.J., Ko, M.A., Siddiqui, N.U., Hudson, J.W., Dennis, J.W. (2005). Sak/Plk4 and mitotic fidelity. Oncogene *24*, 306-12.
420. Takahashi, K., Kobayashi, T., Kanayama, N. (2000). p57(Kip2) regulates the proper development of labyrinthine and spongiotrophoblasts. Mol Hum Reprod. *6*, 1019-25.
421. Takahashi, Y., Carpino, N., Cross, J.C., Torres, M., Parganas, E., Ihle, J.N. (2003). SOCS3: an essential regulator of LIF receptor signalling in trophoblast giant cell differentiation. EMBO J *22*, 372-84.
422. Takeda, T., Sakata, M., Isobe, A., Yamamoto, T., Nishimoto, F., Minekawa, R., Hayashi, M., Okamoto, Y., Desprez, P.Y., Tasaka, K., Murata, Y. (2007). Involvement of Sp-1 in the regulation of the Id-1 gene during trophoblast cell differentiation. Placenta *28*, 192-8.
423. Takeda, T., Sakata, M., Isobe, A., Yamamoto, T., Nishimoto, F., Minekawa, R., Okamoto, Y., Tasaka, K., Murata, Y. (2007). Hypoxia represses the differentiation of Rcho-1 rat trophoblast giant cells. Gynecol Obstet Invest *63*, 188-94.
424. Takemura, M., Ohoka, F., Perpelescu, M., Ogawa, M., Matsushita, H., Takaba, T., Akiyama, T., Umekawa, H., Furuichi, Y., Cook, P.R., Yoshida, S. (2002). Phosphorylation-dependent migration of retinoblastoma protein into the nucleolus triggered by binding to nucleophosmin/B23. Exp Cell Res *276*, 233-41.
425. Takeuchi, J.K., Ohgi, M., Koshiba-Takeuchi, K., Shiratori, H., Sakaki, I., Ogura, K., Saijoh, Y., Ogura, T. (2003). Tbx5 specifies the left/right ventricles and ventricular septum position during cardiogenesis. Development *130*, 5953-64.
426. Tanaka, M., Chen, Z., Bartunkova, S., Yamasaki, N., Izumo, S. (1999). The cardiac homeobox gene Csx/Nkx2.5 lies genetically upstream of multiple genes essential for heart development. Development *126*, 1269-80.
427. Tanaka, S., Kunath, T., Hadjantonakis, A.K., Nagy, A., Rossant, J. (1998). Promotion of trophoblast stem cell proliferation by FGF4. Science *82*, 2072-2075.
428. Tanenbaum, M.E., Medemao, R.H. (2007). Cell fate in the Hand of Plk4. Nat Cell Biol *9*, 1127-1129.

429. Tao, W., Levine, A.J. (1999). P19(ARF) stabilizes p53 by blocking nucleo-cytoplasmic shuttling of Mdm2. Proc Natl Acad Sci USA *96*, 6937-41.
430. Teshima, S., Shimosato, Y., Koide, T., Kuroki, M., Kikuchi, Y., Aizawa, M. (1983). Transplantable choriocarcinoma of rats induced by fetectomy and its biological activities. Gann *74*, 205-12.
431. Tevosian, S.G., Deconinck, A.E., Tanaka, M., Schinke, M., Litovsky, S.H., Izumo, S., Fujiwara, Y., Orkin, S.H. (2000). FOG-2, a cofactor for GATA transcription factors, is essential for heart morphogenesis and development of coronary vessels from epicardium. Cell *101*, 729-39.
432. Thattaliyath, B.D., Firulli, B.A., Firulli, A.B. (2002). The basic-helix-loop-helix transcription factor HAND2 directly regulates transcription of the atrial naturetic peptide gene. J Mol Cell Cardiol *34*, 1335-44.
433. Thattaliyath, B.D., Livi, C.B., Steinhelper, M.E., Toney, G.M., Firulli, A.B. (2002). HAND1 and HAND2 are expressed in the adult-rodent heart and are modulated during cardiac hypertrophy. Biochem Biophys Res Commun *297*, 870-5.
434. Thebault, S., Basbous, J., Gay, B., Devaux, C., Mesnard, J.M. (2001). Sequence requirement for the nucleolar localisation of human I-mfa domain-containing protein (HIC p40). Eur J Cell Biol *79*, 834-838.
435. Thebault, S., Gachon, F., Lemasson, I., Devaux, C., Mesnard, J.M. (2000). Molecular cloning of a novel human I-mfa domain-containing protein that differently regulates human T-cell leukaemia virus type I and HIV-1 expression. J Biol Chem *275*, 4848-4857.
436. Thebault, S., Mesnard, J.M. (2001). How the sequestration of a protein interferes with its mechanism of action: example of a new family of proteins characterised by a particular cysteine-rich carboxy-terminal domain involved in gene expression regulation. Curr Protein Pept Sci *2*, 155-67.
437. Thiry, M., Cheutin, T., O'Donohue, M.F., Kaplan, H., Ploton, D. (2000). Dynamics and three-dimensional localisation of ribosomal RNA within the nucleolus. RNA *6*, 1750-61.
438. Thiry, M., Lafontaine, D.L. (2005). Birth of a nucleolus: the evolution of nucleolar compartments. Trends Cell Biol *15*, 194-9.
439. Thomas T, Kurihara H, Yamagishi H, Kurihara Y, Yazaki Y, Olson EN, Srivastava D. (1998). A signalling cascade involving endothelin-1, dHAND and msx1 regulates development of neural-crest-derived branchial arch mesenchyme. Development *125*, 3005-3014.
440. Thomas, T., Yamagishi, H., Overbeek, P.A., Olson, E.N., Srivastava, D. (1998). The bHLH factors, dHAND and eHAND, specify pulmonary and systemic cardiac ventricles independent of left-right sidedness. Dev Biol *196*, 228-36.
441. Thompson, M., Haeusler, R.A., Good, P.D., Engelke, D.R. (2003). Nucleolar clustering of dispersed tRNA genes. Science *302*, 1399-401.
442. Thorogate, R., Torok, K. (2007). Role of Ca2+ activation and bilobal structure of calmodulin in nuclear and nucleolar localisation. Biochem J *402*, 71-80.
443. Togi, K., Kawamoto, T., Yamauchi, R., Yoshida, Y., Kita, T., Tanaka, M. (2004). Role of Hand1/eHAND in the dorso-ventral patterning and interventricular septum formation in the embryonic heart. Mol Cell Biol *24*, 4627-35.
444. Tompers, D.M., Foreman, R.K., Wang, Q., Kumanova, M., Labosky, P.A. (2005). Foxd3 is required in the trophoblast progenitor cell lineage of the

mouse embryo. Dev Biol *285*, 126-37.
445. Torrano, V., Navascues, J., Docquier, F., Zhang, R., Burke, L.J., Chernukhin, I., Farrar, D., Leon, J., Berciano, M.T., Renkawitz, R., Klenova, E., Lafarga, M., Delgado, M.D. (2006). Targeting of CTCF to the nucleolus inhibits nucleolar transcription through a poly(ADP-ribosyl)ation-dependent mechanism. J Cell Sci *119*, 1746-59.
446. Toyoshima-Morimoto, F., Taniguchi, E., Shinya, N., Iwamatsu, A., Nishida, E. (2001). Polo-like kinase 1 phosphorylates cyclin B1 and targets it to the nucleus during prophase. Nature *410*, 215-220.
447. Toyoshima-Morimoto, F., Taniguchi, E., Shinya, N., Iwamatsu, A., Nishida, E. (2002). Plk1 promotes nuclear translocation of human Cdc25C during prophase. EMBO Rep *3*, 341-348.
448. Trautmann S, Wolfe BA, Jorgensen P, Tyers M, Gould KL, McCollum D. (2001). Fission yeast Clp1p phosphatase regulates G2/M transition and coordination of cytokinesis with cell cycle progression. Curr Biol *11*, 931-40.
449. Tremblay, G.B., Kunath, T., Bergeron, D., Lapointe, L., Champigny, C., Bader, J.A., Rossant, J., Giguère, V. (2001). Diethylstilbestrol regulates trophoblast stem cell differentiation as a ligand of orphan nuclear receptor ERR beta. Genes Dev *15*, 833-8.
450. Trinkle-Mulcahy, L., Sleeman, J.E., Lamond, A.I. (2001). Dynamic targeting of protein phosphatase I within the nuclei of living mammalian cells. J. Cell Sci 114, 4219-4228.
451. Tsai, R.Y., McKay, R.D. (2002). A nucleolar mechanism controlling cell proliferation in stem cells and cancer cells. Genes Dev *16*, 2991-3003.
452. Tschochner, H., Hurt, E. (2003). Pre-ribosomes on the road from the nucleolus to the cytoplasm. Trends Cell Biol *12*, 255-263.
453. Tsuda, T., Philp, N., Zile, M.H., Linask, K.K. (1996). Left-right asymmetric localisation of flectin in the extracellular matrix during heart looping. Dev Biol *173*, 39-50.
454. van de Weerdt, B.C., Medema, R.H. (2006). Polo-like kinases: a team in control of the division. Cell Cycle *5*, 853-64.
455. van den Hoff MJ, Kruithof BP, Moorman AF. (2004). Making more heart muscle. Bioessays *26*, 248-61.
456. van Eenennaam, H., van der Heijden, A., Janssen, R.J., van Venrooij, W.J., Pruijn, G.J. (2001). Basic domains target protein subunits of the RNase MRP complex to the nucleolus independently of complex association. Mol Biol Cell *12*, 3680-9.
457. Varmuza, S., Prideaux, V., Kothary, R., Rossant, J. (1988). Polytene chromosomes in mouse trophoblast giant cells. Development *102*, 127-134.
458. Vasicek, R., Meinhardt, G., Haidweger, E., Rotheneder, H., Husslein, P., Knofler, M. (2003). Expression of the human Hand1 gene in trophoblastic cells is transcriptionally regulated by activating and repressing specificity protein (Sp)-elements. Gene *302*, 115-27.
459. Verstuyf, A., Fonteyn, E., Sobis, H., Vandeputte, M. (1992). A rat cytotrophoblast antigen defined by a monoclonal antibody. Am J Reprod Immunol *28*, 6-11.
460. Visintin, R., Hwang, E.S., Amon, A. (1999). Cfi1 prevents premature exit from mitosis by anchoring Cdc14 phosphatase in the nucleolus. Nature *398*, 818-823.
461. Visintin, R., Stegmeier, F., Amon, A. (2003). The role of the polo kinase Cdc5

in controlling Cdc14 localisation. Mol Biol Cell *14*, 4486-4498.
462. Voronov, D.A., Alford, P.W., Xu, G., Taber, L.A. (2004). The role of mechanical forces in dextral rotation during cardiac looping in the chick embryo. Dev Biol *272*, 339-50.
463. Waldo, K., Zdanowicz, M., Burch, J., Kumiski, D.H., Stadt, H.A., Godt, R.E., Creazzo, T.L., Kirby, M.L. (1999). A novel role for cardiac neural crest in heart development. J Clin Invest *103*, 1499-507.
464. Waldo, K.L., Hutson, M.R., Stadt, H.A., Zdanowicz, M., Zdanowicz, J., Kirby, M.L. (2005). Cardiac neural crest is necessary for normal addition of the myocardium to the arterial pole from the secondary heart field. Dev Biol *281*, 66-77.
465. Waldo, K.L., Kumiski, D.H., Wallis, K.T., Stadt, H.A., Hutson, M.R., Platt, D.H., Kirby, M.L. Conotruncal myocardium arises from a secondary heart field. Development *128*, 3179-88.
466. Wang, Q., Young, T.M., Mathews, M.B., Pe'ery, T. (2007). Developmental regulators containing the I-mfa domain interact with T cyclins and Tat and modulate transcription. J Mol Biol *367*, 630-646.
467. Wang, Y.H., Chen, Y.H., Lu, J.H., Tsai, H.J. (2005). A 23-amino acid motif spanning the basic domain targets zebrafish myogenic regulatory factor myf5 into nucleolus. DNA Cell Biol *24*, 651-60.
468. Weber, J.D., Taylor, L.J., Roussel, M.F., Sherr, C.J., Bar-Sagi, D. (1999). Nucleolar Arf sequesters Mdm2 and activates p53. Nat Cell Biol *1*, 20-6.
469. Weiler-Guettler, H., Aird, W.C., Rayburn, H., Husain, M., Rosenberg, R.D. (1996). Developmentally regulated gene expression of thrombomodulin in postimplantation mouse embryos. Development *122*, 2271-81.
470. Weintraub, H. (1993). The MyoD family and myogenesis: redundancy, networks, and thresholds. Cell *75*, 1241-4.
471. Westerman, B.A., Poutsma, A., Maruyama, K., Schrijnemakers, H.F., van Wijk, I.J., Oudejans, C.B. (2002). The proneural genes NEUROD1 and NEUROD2 are expressed during human trophoblast invasion. Mech Dev *113*, 85-90.
472. Wong, J.M., Kusdra, L., Collins, K. (2002). Subnuclear shuttling of human telomerase induced by transformation and DNA damage. Nat Cell Biol *4*, 731-6.
473. Wu, L., Sun, T., Kobayashi, K., Gao, P., Griffin, J.D. (2002). Identification of a family of mastermind-like transcriptional coactivators for mammalian Notch receptors. Mol Cell Biol. *22*, 7688-7700.
474. Wu SM, Fujiwara Y, Cibulsky SM, Clapham DE, Lien CL, Schultheiss TM, Orkin SH. (2006). Developmental origin of a bipotential myocardial and smooth muscle cell precursor in the mammalian heart. Cell *127*, 1137-50.
475. Wu, X., Howard, M.J. (2002). Transcripts encoding HAND genes are differentially expressed and regulated by BMP4 and GDNF in developing avian gut. Gene Expr 1*0*, 279-93.
476. Xu, C., Henry, P.A., Setya, A., Henry, M.F. (2003). In vivo analysis of nucleolar proteins modified by the yeast arginine methyltransferase Hmt1/Rmt1p. RNA *9*, 746-59.
477. Xu, Y., Knipp, G.T., Cook, T.J. (2005). Expression of CYP4A isoforms in developing rat placental tissue and rat trophoblastic cell models. Placenta *26*, 218-25.
478. Yamada, K., Kanda, H., Tanaka, S., Takamatsu, N., Shiba, T., Ito, M. (2005).

Sox15 enhances trophoblast giant cell differentiation induced by Hand1 in mouse placenta. Differentiation *74*, 212-221.

479. Yamamoto, H., Flannery, M.L., Kupriyanov, S., Pearce, J., McKercher, S.R., Henkel, G.W., Maki, R.A., Werb, Z., Oshima, R.G. (1998). Defective trophoblast function in mice with a targeted mutation of Ets2. Genes Dev. *12*, 1315-26.
480. Yamamoto, T., Roby, K.F., Kwok, S.C., Soares, M.J. (1994). Transcriptional activation of cytochrome P450 side chain cleavage enzyme expression during trophoblast cell differentiation. J Biol Chem *269*, 6517-23.
481. Yamashita, Y., Kajigaya, S., Yoshida, K., Ueno, S., Ota, J., Ohmine, K., Ueda, M., Miyazato, A., Ohya, K., Kitamura, T., Ozawa, K., Mano, H. (2001). Sak serine-threonine kinase acts as an effector of Tec tyrosine kinase. J Biol Chem *276*, 39012-20.
482. Yan, J., Tanaka, S., Oda, M., Makino, T., Ohgane, J., Shiota, K. (2001). Retinoic acid promotes differentiation of trophoblast stem cells to a giant cell fate. Dev Biol *235*, 422-432.
483. Yelon, D., Ticho, B., Halpern, M.E., Ruvinsky, I., Ho, R.K., Silver, L.M., Stainier, D.Y. (2000). The bHLH transcription factor hand2 plays parallel roles in zebrafish heart and pectoral fin development. Development *127*, 2573-82.
484. Yoshida, S., Toh-e, A. (2002). Budding yeast Cdc5 phosphorylates Net1 and assists Cdc14 release from the nucleolus. Biochem Biophys Res Commun *294*, 687-91.
485. Yotsumoto, S., Shimada, T., Cui, C.Y., Nakashima, H., Fujiwara, H., Ko, M.S. (1998). Expression of adrenomedullin, a hypotensive peptide, in the trophoblast giant cells at the embryo implantation site in mouse. Dev Biol. *203*, 264-75.
486. Young, T.M., Wang, Q., Pe'ery, T., Mathews, M.B. (2003). The human I-mfa domain-containing protein, HIC, interacts with cyclin T1 and modulates P-TEFb-dependent transcription. Mol Cell Biol *23*, 6373-6384.
487. Yutzey, K., Gannon, M., Bader, D. (1995). Diversification of cardiomyogenic cell lineages in vitro. Dev Biol *170*, 531-41.
488. Zaffran, S., Kelly, R.G., Meilhac, S.M., Buckingham, M.E., Brown, N.A. (2004). Right ventricular myocardium derives from the anterior heart field. Circ Res *95*, 261-8.
489. Zhang, Y., Xiong, Y. (1999). Mutations in human ARF exon 2 disrupt its nucleolar localisation and impair its ability to block nuclear export of MDM2 and p53. Mol Cell *3*, 579-591.
490. Zhong, W., Wang, Q.T., Sun, T., Wang, F., Liu, J., Leach, R., Johnson, A., Puscheck, E.E., Rappolee, D.A. (2006). FGF ligand family mRNA expression profile for mouse preimplantation embryos, early gestation human placenta, and mouse trophoblast stem cells. Mol Reprod Dev *73*, 540-550.
491. Zhou, J., Olson, E.N. (1994). Dimerisation through the helix-loop-helix motif enhances phosphorylation of the transcription activation domains of myogenin. Mol Cell Biol *14*, 6232-43.
492. Zhu Y, Pe'ery T, Peng J, Ramanathan Y, Marshall N, Marshall T, Amendt B, Mathews MB, Price DH. Transcription elongation factor P-TEFb is required for HIV-1 tat transactivation in vitro. (1997). Genes Dev *11*, 2622-32.
493. Zybina, T.G., Zybina, E.V. (2005). Polytene chromosomes in mouse trophoblast giant cells. Cell Biol Int *29*, 1071-1083.

APPENDICES

APPENDIX 1. Reagents

All reagents were of AnalaR grade and were obtained from *Sigma Aldrich* or *Gibco* (*Invitrogen*) unless otherwise stated. Solutions were made using Milli-Q-purified dH_20 and autoclaved where appropriate. The reagents are listed below.

1. Construction of plasmids

- **1% agarose gel**: 1g agarose, 1ml 10×TBE running buffer (25mM EDTA pH8.0 (186.1g EDTA, 20g NaOH, 1.0l dH_20)), 0.9M Tris/ HCl pH 8.0 (121.1g TRIZMA^{TM} base (Tris), 42ml c.HCl, 1.0l dH_20), 0.9mM Boric Acid), 9ml dH_20, 0.5μg/ml ethidium bromide.
- **10x TE**: 100mM Tris-HCl (pH 8.0), 10mM EDTA.
- **Ampicillin**: Ampicillin (200mg) was dissolved in 4ml dH_20 (final concentration 50mg/ml), filtered (using a 0.22μm Millipore filter (Waters, Harrow, Middx, U.K)) using a 5ml syringe, before being stored at -20°C.
- **Annealing Buffer**: 0.25mM TE pH8.0 (10mM Tris/ HCl pH 8.0, 1mM EDTA pH8.0), 100mM NaCl.
- **Gel loading solution**: 0.5% bromophenol blue, 0.5% xylene cyanol, 50% $Ficoll_{400}$.
- **Kanamycin**: Kanamycin (150mg) was dissolved in 10ml dH_20 (final concentration 15mg/ml) filtered (using a 0.22μm Millipore filter (Waters, Harrow, Middx, U.K)) using a 5ml syringe, before being stored at -20°C.
- **LB/ agar plates**: 15g bacto-agar (*Difco*) was added to 1 litre LB and this was autoclaved. After setting, the LB-Agar mix was heated in a microwave to melt, allowed to cool and supplemented with either 50μg/ml ampicillin or 15μg/ml kanamycin (1:1000), poured into bacteriological plates and allowed to set at room temperature. Plates were then stored at 4°C.
- **Luria broth (LB)**: 10g NaCl, 10g Bacto-Tryptone (*Difco*) and 5g Bacto-Yeast Extract (*Difco*) were dissolved in 1 litre dH_20 and this was autoclaved.
- ***Pfu* polymerase PCR reaction mixtures**: solution A (100mM dNTP mix,

15mM *Pfu* Buffer, 50% glycerol, 10pmol of each primer, 10ng template); solution B (20mM *Pfu* buffer, 10 units *Pfu* DNA polymerase).

- **TELT plasmid preparation solution A**: 500µl 50mM Tris pH 8.0, 400µl 4% Triton X-100, 5ml 2.5M LiCl, 1.25ml 62.5mM EDTA, 2.85ml dH_20.

2. Cell culture

- **0.1% gelatin**: 1g gelatin in 1.0l dH_20, autoclaved.
- **Cell culture β-galactosidase assay buffer**: 2xβ-gal assay buffer (0.2M sodium phosphate (pH 7.4), 2mM magnesium chloride, 0.1M β-mercaptoethanol, 1.5mg/ml ONPG).
- **H9c2/ MEF medium**: DMEM + GlutaMAX, 10% Foetal Bovine Serum, 1% (100mg/ml) Penicillin-Streptomycin Mix.
- **NIH-3T3 medium**: DMEM + GlutaMAX, 10% Bovine Calf Serum, 1% (100mg/ml) Penicillin-Streptomycin Mix.
- **NP-40 lysis buffer**: 25mM Tris-HCl (pH 8.0), 120mM NaCl, 0.5% NP-40, 4mM NaF, 100µM Na_3VO_4, 1mM PMSF, 100µg/ml aprotinin, 10µg/ml leupeptin.
- **P19-CL6 medium, maintains P19-CL6 stem cell proliferation**: MEM Alpha + GlutaMAX, 10% Foetal Bovine Serum, 1% (100mg/ml) Penicillin-Streptomycin Mix.
- **P19-CL6 medium, promotes P19-CL6 EC cell differentiation**: MEM Alpha + GlutaMAX, 10% Foetal Bovine Serum, 1% (100mg/ml) Penicillin-Streptomycin Mix, 1% dimethyl sulphoxide (DMSO).
- **Rcho-1 medium, maintains stem cell proliferation**: NCTC-135, 20% Foetal Bovine Serum, 1% (100mg/ml) Penicillin-Streptomycin Mix, 1% Sodium Pyruvate, 100µM β-mercaptoethanol solution.
- **Rcho-1 medium, promotes TG cell differentiation**: NCTC-135, 10% Horse Serum, 1% (100mg/ml) Penicillin-Streptomycin Mix, 1% Sodium Pyruvate, 100µM β-mercaptoethanol solution.
- **RIPA buffer**: 50mM Tris-HCl (pH7.6), 150mM NaCl, 1% NP-40, 0.5% DOC, 0.1% SDS, 0.01mM PMSF (in isopropanol), 1mM DTT, 1× protease inhibitors (added fresh).
- **Transgenic ES stem cell medium, maintains stem cell proliferation**:

DMEM + GlutaMAX, 15% ES-qualified FCS, 1% (100mg/ml) Penicillin-Streptomycin Mix, 1% non-essential amino acids, 1mM sodium pyruvate, 100μM β-mercaptoethanol solution, 10^3 units/ml ESGRO™ (*Chemicon*).

- **Transgenic ES stem cell medium, promotes differentiation**: DMEM + GlutaMAX, 15% ES-qualified FCS (*Chemicon*), 1% (100mg/ml) Penicillin-Streptomycin Mix, 1% non-essential amino acids, 1mM sodium pyruvate, 100μM β-mercaptoethanol solution.
- **Trophoblast stem cell medium**: RPMI1640 (pH 7.2), 20% Foetal Bovine Serum, 1% L-glutamine, 1% Sodium Pyruvate, 25ng/ml Fgf4 (*Peprotech*), 1μg/ml heparin, 1% (100mg/ml) Penicillin-Streptomycin Mix, 100μM β-mercaptoethanol.

3. Yeast two-hybrid assay

- **Yeast complete medium (1.0l)**: 20g bacto-peptone, 10g yeast extract, 50ml 40% glucose, 10ml 0.2% adenine.
- **Yeast lysis buffer**: 10mM Tris-HCl (pH 8.0), 2% Triton X-100, 1% SDS, 100mM NaCl, 1mM EDTA.
- **Yeast minimal medium (1.0l)**: 6.7g nitrogen base, 50ml 40%glucose, 10ml 0.2% adenine, 10ml 0.2% uracil, 3m 1% lysine.
- **Yeast plates**: appropriate medium containing 20g agar.

4. *In vitro*-translation and GST pull-down assay

- **Binding buffer**: 20mM Tris-HCl pH8.0, 100mM NaCl, 1mM EDTA, 0.5% NP-40, protease inhibitor cocktail (*Roche*; added fresh).

5. Whole mount *in situ* hybridisation

- **Hybridisation buffer**: 50% formaldehyde, 1.3× SSC (pH5.3 with citric acid), 5mM EDTA pH8.0, 50μg/ml yeast RNA, 0.002% Tween-20, 0.005% CHAPS, 100mg/ml heparin in dH_20.
- **NTMT**: 100mM Tris-HCl pH9.5, 100mM NaCl, 50mM $MgCl_2$, 0.05% Tween-20.

6. Luciferase assay

- **2×β-Gal assay buffer**: 0.2M Sodium Phosphate, 2mM Magnesium Chloride, 0.1M β-mercaptoethanol, 1.5mg/ml O-Nitrophenyl-β-D-galactopyranoside.
- **Luciferase cell culture lysis buffer**: 25mM Tris (pH7.8), 2mM DTT, 2mM 1,2-diaminocyclohexane-N,N,N',N'-tetraacetic acid, 10% glycerol, 1% Triton X-100.

7. RNA extraction and RT-PCR

Reagents were provided in the Micro-FastTrack^{TM} 2.0 kit from *Invitrogen.*

- **Binding buffer**: 500mM NaCl, 10mM Tris-HCl pH7.5 in dH_20.
- **Elution Buffer**: 10mM Tris-HCl pH7.5 in dH_20.
- **Micro-FastTrack^{TM} 2.0 Lysis Buffer**: 1ml Stock Buffer + 20μl Protein/ RNase degrader (proprietary mix of proteases; added fresh).
- **Stock buffer**: 200mM NaCl, 200mM Tris-HCl pH7.5, 1.5mM $MgCl_2$, 2% SDS.

8. Northern blot analysis

Reagents were provided in the NorthernMax^{TM} Formaldehyde based system kit from *Ambion.*

- **High stringency wash solution**: 0.1×SSC (20×: 3×NaCl, 0.3M sodium citrate pH7.0), 0.1% SDS.
- **Low stringency wash solution**: 1×SSC, 0.1% SDS.
- **MOPS gel running buffer (10×)**: 200mM MOPS (3-[N-Morpholino]propanesulphonic acid), 50mM sodium acetate, 10mM EDTA.

9. Western blot analysis

- **1×Running Buffer**: 25mM Tris-HCl, 192mM Glycine, 0.4% SDS
- **1×Transfer Buffer**: 25mM Tris-HCl, 192mM Glycine, 0.4% SDS, 20% Methanol.
- **10×TBS**: 250mM Tris-HCl pH 8.0, 50mM KCl, 25mM NaCl.
- **2×Laemelli Buffer for SDS-PAGE** (5% β-mercaptoethanol added fresh):

250mM Tris-HCl pH6.8, 4% SDS, 25% glycerol, 0.1% bromophenol blue

- **Blocking buffer**: 5% non-fat milk (*Marvel*) in TBS with 0.05%Tween-20.
- **Gel loading solution**: 250mM Tris-HCl pH 6.8, 4% SDS, 25% glycerol, 0.1% bromophenol blue, 5% β-mercaptoethanol (added fresh).
- **SDS-PAGE Resolving Gel** (10%; component volumes per 10ml gel): 3.33ml 30% acrylamide (*National Diagnostics*), 50µl 20% SDS, 3.75ml 1M Tris pH8.8, 2.82ml dH_20, 3.3µl Temed, 50µl 20% ammonium persulphate (Amps). Once the resolving gel was poured, a layer of dH_20-saturated isobutanol was placed on top to prevent air from blocking the polymerisation process.
- **SDS-PAGE Stacking Gel** (8%; component volumes per 5ml gel): 1.33ml 30% acrylamide, 25µl 20% SDS, 0.625ml 1M Tris pH6.8, 3ml dH_20, 5µl Temed, 25µl 20% ammonium persulphate (Amps)
- **Stripping buffer**: 70mM Tris-HCl pH 6.8, 2% SDS, 100mM β-mercaptoethanol
- **TBST**: 0.05% Tween-20 in 1×TBS.
- **Wash buffer**: 0.5% Tween-20 in 1×TBS

10. Immunoprecipitation

Reagents were provided in the α-FLAG M2 antibody kit from *Sigma*.

- **Lysis buffer**: 50mM Tris HCl (pH7.4), 150mM NaCl, 1mM EDTA, 1% Triton X, 0.1M PMSF,

11. *In vitro* phosphorylation (kinase) assay

- **Kinase Buffer**: 50mM Hepes pH7.5, 5mM $MgCl_2$, 1mM DTT

12. *Plk4*-null embryo analysis

- **10×PBS**: 1.37M NaCl, 27mM KCl, 43mM $Na_2HPO_4.7H_2O$, 14mM KH_2PO_4, treated with DEPC.
- **Eosin stain**: 0.2% eosin Y in 95% ethanol.
- **Mayer's Haematoxylin**: 50g potassium alum, 0.2g sodium iodate, 1.0g citric acid, 50.0g chloral hydrate, 1.0g haematoxylin, made to 1.0l with dH_20

13. Embryoid body dissociation

- **Enzyme medium**: Low calcium medium supplemented with 1mg/ml collagenase B (*Roche*) and 30μM $CaCl_2$
- **KB medium**: 85mM KCl, 30mM K_2HPO_4, 5mM $MgSO_4$, 1mM EGTA, 5mM sodium pyruvate, 5mM creatine, 20mM taurine, 20mM glucose, 2mM Na_2ATP in dH_20.
- **Low calcium medium**: 120mM NaCl, 5.4mM KCl, 5mM $MgSO_4$, 5mM sodium pyruvate, 20mM Taurine, 10mM Hepes/NaOH pH6.9 in dH_20.

APPENDIX 2. PCR Primers

The melting temperature (T_m) of an oligonucleotide primer can be determined from the equation T_m=2AT+4GC, where AT is the number of AT base pairs and GC the number of GC base pairs. The annealing temperature in a PCR is set at 5°C less than the T_m of the primers. All primers were ordered from *Sigma Aldrich* (www.Sigma-Aldrich.com), were received as lyophilised powder and were re-suspended in dH_20 to 10μg/μl and then to a working concentration of 0.1μg/μl.

- **Colony PCR (*HICshRNA1*)**: forward (5'-ATCCTTCAGCTGGTGAACT-3'); reverse (5'- ATTCGCGCTAGGTTGATTC -3').
- **Colony PCR (*HICshRNA2*)**: forward (5'-AGTCCAGCTTGTCTGTAAA-3'); reverse (5'- ATTCGCGCTAGGTTGATTC -3').
- **Colony PCR (*Plk4shRNA1*)**: forward (5'-ACAGAGATTTCCAGGACTA-3'); reverse (5'- ATTCGCGCTAGGTTGATTC -3').
- **Colony PCR (*Plk4shRNA1*)**: forward (5'-ATACTGGCGGAAAATATCA-3'); reverse (5'- ATTCGCGCTAGGTTGATTC -3').
- ***HICshRNA1***: 5'-AATCCTTCAGCTGGTGAACTT-3'.
- ***HICshRNA2***: 5'-CAGTCCAGCTTGTCTGTAAACA-3'.
- ***MICp32* IMAGE clone amplification**: forward (5'-TATGCGATCGATAGCTAGGA-3'); reverse (5'-GATAGCGCTAGGCGGATCG-3').
- ***MICp32* RT-PCR**: forward (5'-GAGCAGCAGTGCCCGGTCGA-3'); reverse (5'-CTGATGTCTGGAGTTGAGGC-3').

- ***MICp40* BAC amplification**: forward (5'-CGGGGTACCGCTTCCCTGGGGCATTCCT-3'); reverse (5'-CTTGGCATCCCCCCGTGGGCTGT-3').
- ***MICp40* RT-PCR**: forward (5'-GGAGTGGTCAGGCTGCCAGG-3'); reverse (5'-AGCGAGGGCTTCACCCGCGC-3').
- **Murine *Hand1* (wild-type and mutant) amplification for cloning**: forward (5'-CCGGAATTCTGTCCAACATGAACCTCGTGGGC-3'); reverse (5'-CGGGGTACCGTCTGGTTTAGCTCCAGCGCCCA-3').
- **Murine *Hand1* bHLH domain amplification for cloning**: forward (5'-CCGGAATTCTGTCCAACATGCGAAAAGGCTCA-3'); reverse (5'-CGGGGTACCGTTCCTTGGCCAGCACGTCCATC-3').
- **Murine *Hand1* histidine-rich stretch (and flanking sequence) amplification for cloning**: forward (5'-CCGGAATTCTGTCCAACATGAGCTACGCACAT-3'); reverse (5'-CGGGGTACCGTTGCGGCGGGTGTGAGTGGTGA-3').
- **Murine *Hand2* amplification for cloning**: forward (5'-CCGGAATTCTGTCCAACATGAGTCTGGTGGGG-3'); reverse (5'-CGGGGTACCCTGCTTGAGCTCCAGGGCCCAGA-3').
- **Murine *Plk4* RT-PCR**: forward (5'-GTTGGTTGGGCTACACAGCT-3'); reverse (5'-CTGATGGAAGATACTCCTGC-3').
- **Murine *Tubulin* RT-PCR**: forward (5'-TCACTGTGCCTGAACTTACC-3'); reverse (5'-GGAACATAGCCGTAAACTGC-3').
- ***Plk4*-null embryo genotyping round 1 (mutant)**: forward (5'-TTTAAAAGTGCCCGCTAGC-3'); reverse (5'-ATCGCTTCTTGACGAGTTC-3').
- ***Plk4*-null embryo genotyping round 1 (wild-type)**: forward (5'-GCCCCCACTAAGACGAC-3'); reverse (5'-AGCTGGGGCTCGACTAG-3').
- ***Plk4*-null embryo genotyping round 2 (mutant)**: forward (5'-TTTAAAAGTGCCCGCTAGC-3'); (5'-AAGCCTGGGGATGTACC-3').
- ***Plk4*-null embryo genotyping round 2 (wild-type)**: forward (5'-GCCCCCACTAAGACGAC-3'); reverse (5'-TGCTAGTAAATAATCCGACAGG-3').
- ***Plk4shRNA1***: 5'-AACAGAGATTTCCAGGACTAT-3'.
- ***Plk4shRNA2***: 5'-AATACTGGCGGAAAATATCAGT-3'.

APPENDIX 3. Position of RNAi sequences

The oligonucleotides designed for RNAi analysis (listed in Appendix 2) are shown below to illustrate the dsRNA, comprising a 9-nucleotide hairpin loop, that is expected to form *in vivo*. Also shown are the positions within HICp40 and Plk4 to which the RNAi oligonucleotides were designed. Please refer to Figures 3.1 and 5.23b for further information regarding HICp40 and Plk4 protein structure.

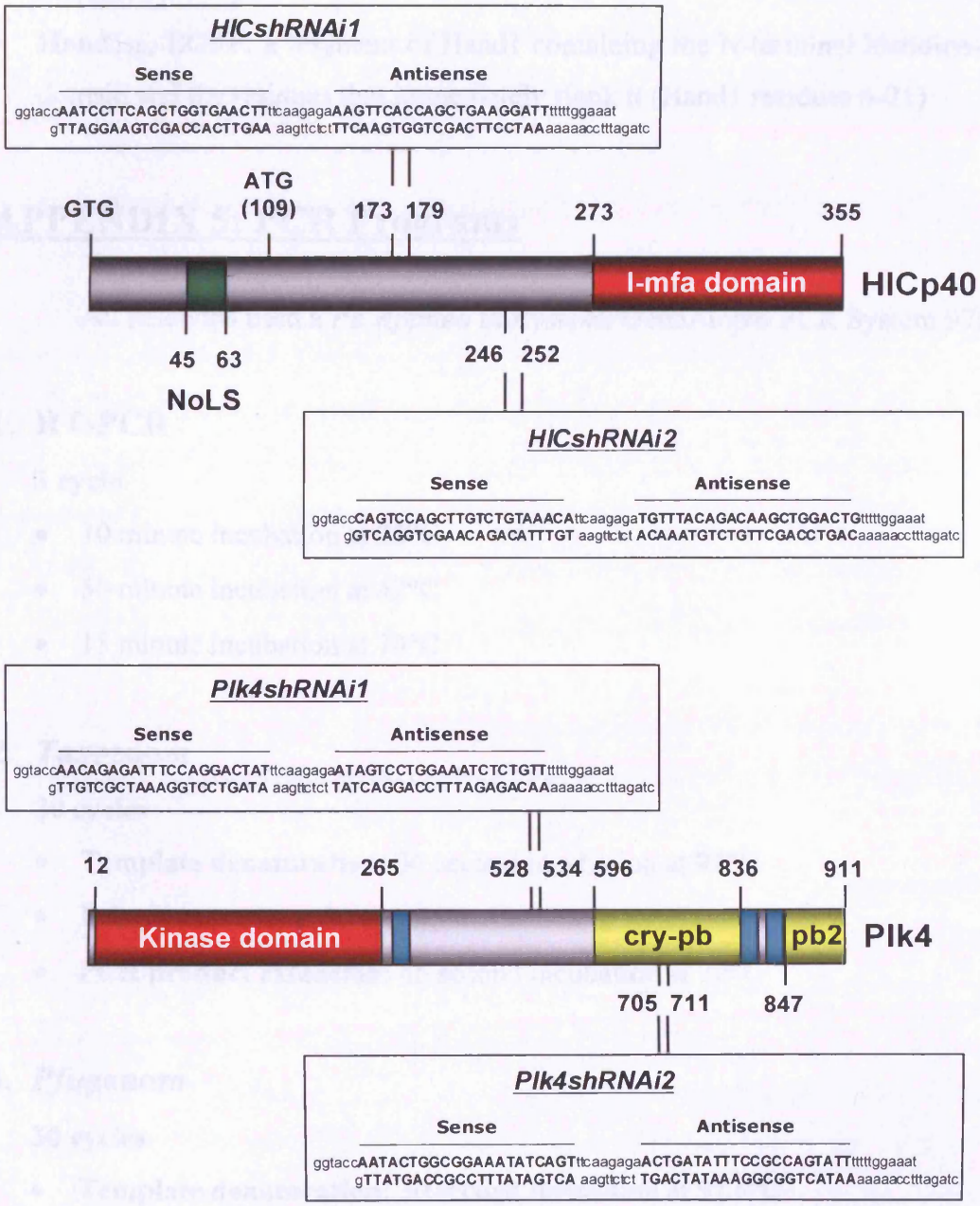

APPENDIX 4. Hand1 fragment constructs

The two Hand1 fragment constructs were constructed as described in Chapter 2 (section 2.1), and are as follows. Please refer to Figure 1.1b for further information regarding Hand1 protein structure.

- **$bHLH_{Hand1}$-EGFP**: the isolated bHLH domain of Hand1 fused to EGFP (Hand1 residues 93-147).
- **$Hand1_{His}$-EGFP**: a fragment of Hand1 containing the N-terminal histidine-rich domain and the residues that immediately flank it (Hand1 residues 6-21).

APPENDIX 5: PCR Programs

All reactions used a *PE Applied Biosystems* GeneAmp® PCR System 9700.

1. RT-PCR

1 cycle

- 10 minute incubation at 25°C
- 50 minute incubation at 42°C
- 15 minute incubation at 70°C

2. *Taq*genom

30 cycles

- **Template denaturation**: 30 second incubation at 94°C
- **Primer annealing**: 30 second incubation at 58°C
- **PCR product extension**: 45 second incubation at 72°C

3. *Pfu*genom

30 cycles

- **Template denaturation**: 30 second incubation at 97.5°C
- **Primer annealing**: 30 second incubation at 58°C
- **PCR product extension**: 45 second incubation at 72°C

APPENDIX 6. Antibodies

Primary antibodies are listed below with the employed respective fluorescent-tagged (for immunostaining) or horse radish peroxidase-conjugated (for immunoblotting) secondary antibody. Rhodamine-phalloidin (*Molecular Probes*) was used at a final concentration of 5 units (165nM).

- **α-B56δ** (*Strategene*): used at a concentration of 1/500 for immunostaining (mouse-TRITC (*Dako*) at a concentration of 1/50 used as the secondary antibody) and 1/2000 for immunoblotting (mouse-HRP (*Amersham*) at a concentration of 1/5000 used as the secondary antibody).
- **α-C23** (α-Nucleolin; *Santa Cruz*): used at a concentration of 1/100 for immunostaining (rabbit-TRITC (*Dako*) at a concentration of 1/50 used as the secondary antibody) and 1/100 for immunoblotting (rabbit-HRP (*Amersham*) at a concentration of 1/5000 used as the secondary antibody).
- **α-EGFP** (*Clontech*): used at a concentration of 1/1000 for immunoblotting (mouse-HRP (*Amersham*) at a concentration of 1/5000 used as the secondary antibody).
- **α-FLAG M2** (*Sigma*): used at a concentration of 1/700 for immunoblotting (mouse-HRP (*Amersham*) at a concentration of 1/5000 used as the secondary antibody).
- **α-GAPDH** (*Chemicon*): used at a concentration of 1/1000 for immunoblotting (mouse-HRP (*Amersham*) at a concentration of 1/5000 used as the secondary antibody).
- **α-Hand1** (*Abcam*): used at a concentration of 1/300 for immunostaining (rabbit-FITC (*Santa Cruz*) at a concentration of 1/100 used as the secondary antibody) and 1/500 for immunoblotting (rabbit-HRP (*Amersham*) at a concentration of 1/5000 used as the secondary antibody).
- **α-Hand1 C-terminus** (*Santa Cruz*): used at a concentration of 1/100 for immunostaining (goat-FITC (*Dako*) at a concentration of 1/50 used as the secondary antibody) and 1/200 for immunoblotting (goat-HRP (*Santa Cruz*) at a concentration of 1/5000 used as the secondary antibody).
- **α-HIC** (a kind gift from Jean-Paul Mesnard): used at a concentration of 1/500

for immunoblotting (mouse-HRP (*Amersham*) at a concentration of 1/5000 used as the secondary antibody).

- **α-HIF** (*Sigma*): used at a concentration of 1/250 for immunoblotting (mouse-HRP (*Amersham*) at a concentration of 1/5000 used as the secondary antibody).
- **α-HIS** (*Abcam*): used at a concentration of 1/1000 for immunoblotting (mouse-HRP (*Amersham*) at a concentration of 1/5000 used as the secondary antibody).
- **α-phosphoserine** (*Abcam*): used at a concentration of 1/150 for immunoblotting (mouse-HRP (*Amersham*) at a concentration of 1/5000 used as the secondary antibody).
- **α-PL1** (*Chemicon*): used at a concentration of 1/200 for immunostaining (rabbit-FITC (*Santa Cruz*) at a concentration of 1/100 used as the secondary antibody).
- **α-Plk4** (*Abcam*): used at a concentration of 1/200 for immunostaining (goat-FITC (*Dako*) at a concentration of 1/50 used as the secondary antibody) and 1/200 for immunoblotting (goat-HRP (*Santa Cruz*) at a concentration of 1/5000 used as the secondary antibody).
- **α-PLP-A** (*Chemicon*): used at a concentration of 1/200 for immunostaining (mouse-TRITC (*Dako*) at a concentration of 1/50 used as the secondary antibody).
- **α-PolII** (*Upstate*): used at a concentration of 1/100 for immunostaining (mouse-TRITC (*Dako*) at a concentration of 1/50 used as the secondary antibody).

APPENDIX 7. *In situ* hybridisation riboprobes

- **Hand1 (pcDNA3-Hand1)**: cDNA expression driven by T7 RNA polymerase, probe linearised with NotI.
- **HICp40 (pKS$^+$-HICp40)**: cDNA expression driven by T3 RNA polymerase, probe linearised with HindIII. Cross-reacts with MICp40.

APPENDIX 8. Y2H screen data

The table below lists details of clones with homology to known proteins that were identified in the Y2H screen. False positives are excluded.

Clone	Size (bp)	Protein
A10	411	Checkpoint with forkhead and RING finger domains protein (Chfr); RING finger protein 196 (Rfp196)
B12	536	Zinc finger protein 313 (Zfp313)
B15	570	Mastermind-like protein-2 (Maml2)
C23	397	Hypothetical RING finger domain-containing protein
D18	328	Fibrillarin-2 (Fib2)
E17	467	RING finger protein 26 (Rnf26)
G18	607	Bromodomain and PHD finger containing-protein 1 (Brpf1; Peregrin)
J24	547	SWI/SNF-related matrix-associated actin-dependent regulator of chromatin subfamily E member 1 (Smarce1)
J31	515	Nicotinamide nucleotide transhydrogenase (Nrn)
L1	438	Tubulin
L18	593	Exportin-T (tRNA exportin) (Xpot)
N27	613	Fibroblast growth factor receptor-2 (Fgfr2)
Q8	512	Thrombospondin-1 precursor (Thbs-1)
Q27	324	Human I-mfa domain-containing protein (HIC)
R19	307	Human I-mfa domain-containing protein (HIC)
S23	527	Alf1
S31	611	RING finger protein 31 (Zinc in-between RING finger ubiquitin A protein; Zibra)

APPENDIX 9. Quantitative data

The following tables list the quantitative data obtained during the course of this study.

a. Luciferase assay

Transfected constructs	Luciferase activity (RLU)				β-Gal activity				RLU/ β-Gal activity
	R1	R2	R3	Mean	R1	R2	R3	Mean	
Reporter alone	0.27	0.04	0.55	0.29	1.26	0.80	0.90	0.99	0.29
Hand1 + reporter	1.44	1.88	1.17	1.50	0.66	1.02	0.75	0.81	1.85
E12 + reporter	0.51	0.58	0.89	0.66	0.75	0.61	0.70	0.69	0.95
HICp40 + reporter	0.23	0.40	0.20	0.28	0.99	1.48	0.95	1.14	0.24
HICΔC + reporter	0.12	0.20	0.67	0.50	0.72	0.70	0.84	0.75	0.67
HICp32 + reporter	0.43	0.81	1.02	0.75	0.28	0.50	0.61	0.57	1.32
Hand1 + E12 + reporter	15.69	20.91	17.11	17.90	0.93	0.91	1.39	1.08	16.57
Hand1 + E12+ HICp40 + reporter	8.21	6.10	5.10	6.47	1.29	1.92	1.60	1.60	4.04
Hand1 + E12+ HICΔC + reporter	13.19	19.04	11.22	14.48	0.89	1.09	0.76	0.91	15.91
Hand1 + E12+ HICp32 + reporter	13.29	12.56	10.00	11.95	0.72	0.98	1.19	0.96	12.44

R1: reading 1; **R2**: reading 2; **R3**: reading 3; **RLU**: relative light units.

b. Hand1-EGFP immuno-localisation assays in NIH-3T3 and H9c2 cells

Cell population	Nucleolar Hand1-EGFP (%)	S.E.M.
NIH-3T3, Hand1-EGFP o/e	15.0	1.55
NIH-3T3, Hand1-EGFP & HICp40 o/e	85.4	1.24
H9c2, Hand1-EGFP o/e	98.6	2.70

o/e: over-expression.

c. Hand1-EGFP immuno-localisation assays in Rcho-1 cells

Cells were cultured in normoxic conditions in medium supplemented with fetal bovine serum (FBS) unless otherwise stated.

Cell population	Nucleolar Hand1-EGFP (%)			S.E.M.		
	24hr	48hr	72hr	24hr	48hr	72hr
Hand1-EGFP o/e	68.4	46.4	33.4	1.32	0.95	1.80
Hand1- EGFP T107;S109A o/e	70.2	64.2	60.5	1.79	0.95	3.17
Hand1-EGFP T107;S109D o/e	5.10	2.50	1.20	0.82	0.44	1.30
Hand1-EGFP & B56δ o/e	69.4	65.4	61.1	1.05	1.54	6.48

o/e: over-expression.

d. Endogenous Hand1 immuno-localisation assays in Rcho-1 cells

Cells were cultured in normoxic conditions in medium supplemented with fetal bovine serum (FBS) unless otherwise stated.

Cell population	Hand1-EGFP (%)	S.E.M.
Untransfected, HS	28.6 (Nu), 43.9 (No)	2.08 (Nu), 1.87 (No)
Untransfected, HS, HxC	44.6 (No)	2.01 (No)
Untransfected, HS, $CoCl_2$	45.6 (No)	1.51 (No)
B56δ o/e, HS	69.2 (No)	2.56 (No)
HICp40-EGFP o/e, HS	77.6 (No)	2.67 (No)
FLAG-Sak o/e	54.1 (Nu)	2.78 (Nu)
***HICshRNAi1* o/e**	47.1 (Nu)	1.93 (Nu)
***HICshRNAi2* o/e**	46.4 (Nu)	2.39 (Nu)
***Plk4shRNAi1* o/e**	68.9 (No)	2.39 (No)
***Plk4shRNAi2* o/e**	69.8 (No)	1.44 (No)

Nu: nuclear-wide; **No**: nucleolar; **o/e**: over-expression; **HS**: cultured in medium supplemented with horse serum; **$CoCl_2$**: cultured in medium supplemented with 250μM cobalt chloride; **HxC**: cultured in a hypoxic chamber.

e. Rcho-1 TG cell differentiation assays

Cells were cultured in normoxic conditions in medium supplemented with fetal bovine serum (FBS) unless otherwise stated. All cell counts have been corrected for the spontaneous differentiation rate of Rcho-1 stem cells (5.9±0.5% per 24 hours), which represents the percentage of Rcho-1 cells cultured in FBS-supplemented medium that initiate TG cell differentiation over a 24 hour period (Nakayama *et al.*, 1998; Scott *et al.*, 2000). All cell counts have also been corrected for an observed increase in differentiation rate due to the transfection with a construct encoding EGFP alone (10.3% per 24-hour period; mean±S.E.M.; n=250; $p<0.01$).

Cell population	Rcho-1 TS cells (%)			S.E.M.		
	24hr	48hr	72hr	24hr	48hr	72hr
Untransfected	81.2	70.9	65.2	1.32	0.95	1.8
Untransfected, HS	56.1	35.5	29.2	1.79	0.95	3.17
Untransfected, HS, HxC	-	-	40.1	-	-	1.60
Untransfected, HS, $CoCl_2$	-	-	38.0	-	-	2.16
Hand1-EGFP o/e	59.1	35.7	24.8	0.82	0.44	1.30
Hand1-EGFP o/e, HxC	61.4	34.5	25.0	1.40	2.30	1.08
Hand1-EGFP, o/e, $CoCl_2$	60.1	37.5	23.4	1.35	1.03	2.09
Hand1- EGFP T107;S109A o/e	64.4	64.1	56.5	1.05	0.45	1.59

Cell population	Rcho-1 TS cells (%)			S.E.M.		
	24hr	48hr	72hr	24hr	48hr	72hr
Hand1-EGFP T107;S109D o/e	71.8	52.7	31.4	3.77	1.54	6.48
B56δ o/e	67.2	64.8	61.4	1.17	0.44	1.22
B56δ o/e, HS	54.8	49.4	45.8	1.68	1.22	1.48
Hand1-EGFP (wt) & B56δ o/e	68.2	62.0	56.8	1.44	3.10	1.50
HICp40-EGFP o/e, HS	68.6	63.2	54.5	2.22	1.07	0.57
FLAG-Plk4 o/e	60.2	49.5	37.1	1.68	0.50	1.17
***HICshRNAi1* o/e**	58.0	40.5	39.8	0.71	1.21	1.93
***HICshRNAi2* o/e**	61.8	51.9	40.6	0.60	0.61	0.64
***Plk4shRNAi1* o/e, HS**	72.3	57.9	54.8	0.36	0.44	1.21
***Plk4shRNAi2* o/e, HS**	73.0	58.8	54.1	1.68	1.36	1.30

o/e: over-expression; **HS**: cultured in medium supplemented with horse serum; **$CoCl_2$**: cultured in medium supplemented with 250μM cobalt chloride; **HxC**: cultured in a hypoxic chamber.

APPENDIX 10. Time-lapse movies

QuickTime time-lapse movies (.mov format) are provided on the attached CD.

- **Movie 4.1.** Hand1-EGFP is released from the nucleolus over a 12-hour period as individual transfected Rcho-1 stem cells commit to differentiate, which is coincident with decreased motility and an expansion in size. Time-lapse was initiated 24 hours after transfection and images captured every 20 minutes over a period of 12 hours.
- **Movie 6.1.** After differentiation, *EGFP*-expressing transgenic ES cells produce embryoid bodies (EBs) containing contractile, fluorescent cardiomyocytes.

APPENDIX 11. Publications based on this work

a. Martindill, D.M.J., Risebro, C.A., Smart, N., Franco-Viseras, M. del Mar, Rosario, C.O., Swallow, C.J., Dennis, J.W., Riley, P.R. (2007). Nucleolar release of Hand1 acts as a molecular switch to determine cell fate. Nature Cell Biology *9*, 1131-1141.

b. Martindill, D.M.J., Riley, P.R. (2008). Cell cycle switch to endocycle: the nucleolus lends a Hand. Cell Cycle *7*, 17-23.

APPENDIX 12. External presentations of this work

Listed below are the external conferences and/ or institutions at which I, David Martindill, have presented this work.

a. British Society for Developmental Biology Annual General Meeting. The University of York, U.K. March 20th-23rd, 2006 (poster presentation).
b. 4th International Symposium on bHLH genes: development and diseases. The University of Kyoto, Japan. May 17th-18th 2007 (oral and poster presentation).
c. Presentation at the institution of our collaborator (Anthony Firulli). Herman B Wells Centre for Pediatric Research, University of Indiana, Indianapolis, USA. February 6th 2008 (oral presentation).